

BOEMRE TA&R PROGRAM ON SAFETY OIL AND GAS OPERATIONS IN THE US OCS
OCEAN CURRENT MONITORING FROM 500 – 1000 METERS

Report Number: C56323/6708/R0

Issue Date: 15 June 2011

**This report is not to be used for contractual or engineering purposes
unless described as 'Final' in the approval box below**

Prepared for:
BOEMRE
381 Elden Street, MS-4021
Herndon, VA 20170-4817



BOEMRE

Client Reference:
Safety of Oil and Gas Operations in
the US OCS (B-FY 2011)
Solitcituation No.: M10PS00185

0	Initial Issue	Shejun Fan Lie-Yauw Oey	Liam Harrington-Missin	Jan van Smirren	15 June 2011
Rev	Description	Prepared	Checked	Approved	Date

DOCUMENT ARRANGEMENT

CONTENTS

	Page
Executive summary	1
1. INTRODUCTION	2
1.1 Background and Program Objectives	2
1.2 Data and Output Descriptions	2
1.2.1 Numerical Model Data	2
1.2.2 Observation Data	4
1.3 Report Organization	5
1.4 Units and Conventions	5
1.5 Abbreviations	5
2. Northern Gulf of Mexico Sundivisions	6
2.1 Current Characteristics	6
2.2 Current Kinetic Energy Distribution	8
2.3 Zones Selection	12
3. Current DATA Database	14
3.1 NTL data Acquisition and Quality Control	14
3.1.1 Data Quality Control	17
3.2 Historical mooring data	18
3.3 PROFS model data	19
4. Subsurface ELEVATED Current Events	28
4.1 Subsurface Elevated Current Events Screening	28
4.2 Subsurface Elevated Current Events Interpretation	88
4.2.1 Submerged Speed Peaks with Inertial Period	89
4.2.2 Events Isolated in Time with No Clear Periodicity – Deep Jet Events	89
4.2.3 Events Isolated in Time with No Clear Periodicity –Shallow Jet Events	89
5. Current Profile Characterizations	95
5.1 Zone 1	95
5.1.1 Long Term Current Profile Characterizations	95
5.1.2 Short Term Current Profile Characterizations	95
5.2 Zone 2	95
5.2.1 Long Term Current Profile Characterizations	95
5.2.2 Short Term Current Profile Characterizations	96
5.3 Zone 3	96
5.3.1 Long Term Current Profile Characterizations	96
5.3.2 Short Term Current Profile Characterizations	96
5.4 Zone 4	97
5.4.1 Long Term Current Profile Characterizations	97
5.4.2 Short Term Current Profile Characterizations	97
6. REFERENCE	98

SUMMARY OF TABLES AND FIGURES

	Page
Figure 1-1 The northwest Atlantic Ocean model ($\Delta \approx 6\text{--}12 \text{ km}$ within the Gulf of Mexico) (NWAOM; the whole Gulf of Mexico shown) and the fine-grid resolution ($\Delta \approx 3\text{--}7 \text{ km}$) Gulf of Mexico and northwest Caribbean Sea region (west of the dashed line). Contours show isobaths in meters, and silhouettes at 55°W show steady transports specified for the Gulf Stream and returned flows.	3
Figure 1-2 NTL ADCP stations (blue dots), PROFS stations (black squares) and historical current mooring locations (red stars).	4
Table 1-1 Directional Sectors	5
Figure 2-1 Historical Category 4 and 5 Hurricanes in the Gulf of Mexico	6
Figure 2-2 Hurricane Measurement at Buoy 42040 and NTL Station 42868 ($28.164^\circ\text{N } 88.484^\circ\text{W}$)	7
Figure 2-3 Spatial frequency (%) for the location of LCE centers using a 27-year (1977 – 2003) database (From OCS Study MMS 2005-031)	8
Figure 2-4 Mean currents (u_m, v_m) as vectors superimposed on color images (and also in blue contours) of $(KE_m)^{1/2}$ at $z = -250, -500, -800$ and -1400m . Thin black contours show 200m, 2000m, 3000m and 3500m isobaths.	9
Figure 2-5 Color maps and contours of $Frq(x, spd)$ = frequency of occurrences of currents that are stronger than speed $Spd = 0.1 \text{ m/s}$, at $z = -250, -500, -800$ and -1100m . Note color scale is from 0 to 0.4 (=40%) and contour (blue) interval is = 0.05 (=5%). Thin black contours show 200m, 2000m, 3000m and 3500m isobaths.	10
Table 2-1 Localized regions of strong currents inferred from Figure 2-4.	11
Figure 2-6 Color maps and contours of $Frq(x, spd)$ = frequency of occurrences of currents that are stronger than speed $Spd = 0.2 \text{ m/s}$, at $z = -250, -500, -800$ and -1100m . Note color scale is from 0 to 0.2 (=20%) and contour (blue) interval is = 0.05 (=5%). Thin black contours show 200m, 2000m, 3000m and 3500m isobaths.	11
Figure 2-7 NTL ADCP stations (circled dots) and historical current mooring (+) locations. Red box is the region in Figure 2-4, Figure 2-5 and Figure 2-6. The red ellipses are proposed representative Zones.	12
Figure 3-1 NTL ADCP stations used in this study – zone 1	14
Table 3-1 BOEMRE NTL ADCP Stations used in this study – zone 1	14
Figure 3-2 NTL ADCP stations used in this study – zone 2	15
Table 3-2 BOEMRE NTL ADCP Stations used in this study – zone 2	15
Figure 3-3 NTL ADCP stations used in this study – zone 3	16
Table 3-3 BOEMRE NTL ADCP stations used in this study – zone 3	16
Figure 3-4 NTL ADCP stations used in this study – zone 4	17
Table 3-4 BOEMRE NTL ADCP stations used in this study – zone 4	17
Table 3-5 BOEMRE Historical Mooring Stations Used in This Study	18
Figure 3-5 BOEMRE Historical Mooring Stations Used in this Study	19
Figure 3-6 Sea surface elevation on 10 October 2007. The region is where daily data were generated for this project.	19
Table 3-6 PROFS Model Stations	20
Figure 3-7 SSH + currents at surface (top) and temperature and currents at $z=-10\text{m}$ below the surface for Hurricane Katrina on Aug/28/2005. Dashed region is where data were generated for this project.	26

Figure 3-8 SSH + currents at surface (top) and temperature and currents at z=-10m below the surface for Hurricane Katrina on Sep/23/2005. Dashed region is where data were generated for this project.	27
Figure 4-1 Current Speed Contour at NTL Station 42364 – May 2005	28
Figure 4-2 Current Speed Contour at NTL Station 42364 – June 2005	29
Figure 4-3 Current Speed Contour at NTL Station 42364 – July 2005	29
Figure 4-4 Current Speed Contour at NTL Station 42364 – August 2005	30
Figure 4-5 Current Speed Contour at NTL Station 42364 – November 2005	30
Figure 4-6 Current Speed Contour at NTL Station 42364 – December 2005	31
Figure 4-7 Current Speed Contour at NTL Station 42364 – January 2006	31
Figure 4-8 Current Speed Contour at NTL Station 42364 – February 2006	32
Figure 4-9 Current Speed Contour at NTL Station 42364 – March 2006	32
Figure 4-10 Current Speed Contour at NTL Station 42364 – April 2006	33
Figure 4-11 Current Speed Contour at NTL Station 42364 – May 2006	33
Figure 4-12 Current Speed Contour at NTL Station 42364 – December 2006	34
Figure 4-13 Current Speed Contour at NTL Station 42364 – January 2007	34
Figure 4-14 Current Speed Contour at NTL Station 42364 – February 2007	35
Figure 4-15 Current Speed Contour at NTL Station 42364 – March 2007	35
Figure 4-16 Current Speed Contour at NTL Station 42364 – April 2007	36
Figure 4-17 Current Speed Contour at NTL Station 42364 – May 2007	36
Figure 4-18 Current Speed Contour at NTL Station 42364 – June 2007	37
Figure 4-19 Current Speed Contour at NTL Station 42364 – July 2007	37
Figure 4-20 Current Speed Contour at NTL Station 42364 – Agust 2007	38
Figure 4-21 Current Speed Contour at NTL Station 42364 – September 2007	38
Figure 4-22 Current Speed Contour at NTL Station 42364 – October 2007	39
Figure 4-23 Current Speed Contour at NTL Station 42364 – November 2007	39
Figure 4-24 Current Speed Contour at NTL Station 42364 – December 2007	40
Figure 4-25 Current Speed Contour at NTL Station 42364 – Janurary 2008	40
Figure 4-26 Current Speed Contour at NTL Station 42364 – February 2008	41
Figure 4-27 Current Speed Contour at NTL Station 42364 – March 2008	41
Figure 4-28 Current Speed Contour at NTL Station 42364 – April 2008	42
Figure 4-29 Current Speed Contour at NTL Station 42364 – May 2008	42
Figure 4-30 Current Speed Contour at NTL Station 42364 – June 2008	43
Figure 4-31 Current Speed Contour at NTL Station 42364 – July 2008	43
Figure 4-32 Current Speed Contour at NTL Station 42364 – Agust 2008	44
Figure 4-33 Current Speed Contour at NTL Station 42364 – September 2008	44
Figure 4-34 Current Speed Contour at NTL Station 42364 – October 2008	45
Figure 4-35 Current Speed Contour at NTL Station 42364 – November 2008	45
Figure 4-36 Current Speed Contour at NTL Station 42364 – December 2008	46
Figure 4-37 Current Speed Contour at NTL Station 42364 – January 2009	46
Figure 4-38 Current Speed Contour at NTL Station 42364 – February 2009	47
Figure 4-39 Current Speed Contour at NTL Station 42364 – March 2009	47
Figure 4-40 Current Speed Contour at NTL Station 42364 – April 2009	48
Figure 4-41 Current Speed Contour at NTL Station 42364 – May 2009	48

Figure 4-42 Current Speed Contour at NTL Station 42364 – June 2009	49
Figure 4-43 Current Speed Contour at NTL Station 42364 – July 2009	49
Figure 4-44 Current Speed Contour at NTL Station 42364 – August 2009	50
Figure 4-45 Current Speed Contour at NTL Station 42364 – September 2009	50
Figure 4-46 Current Speed Contour at NTL Station 42364 – October 2009	51
Figure 4-47 Current Speed Contour at NTL Station 42364 – November 2009	51
Figure 4-48 Current Speed Contour at NTL Station 42364 – December 2009	52
Figure 4-49 Current Speed Contour at NTL Station 42364 – January 2010	52
Figure 4-50 Current Speed Contour at NTL Station 42364 – February 2010	53
Figure 4-51 Current Speed Contour at NTL Station 42364 – March 2010	53
Figure 4-52 Current Speed Contour at NTL Station 42364 – April 2010	54
Figure 4-53 Current Speed Contour at NTL Station 42364 – May 2010	54
Figure 4-54 Current Speed Contour at NTL Station 42364 – June 2010	55
Figure 4-55 Current Speed Contour at NTL Station 42364 – July 2010	55
Figure 4-56 Current Speed Contour at NTL Station 42364 – August 2010	56
Figure 4-57 Current Speed Contour at NTL Station 42370 – May 2005	56
Figure 4-58 Current Speed Contour at NTL Station 42370 – June 2005	57
Figure 4-59 Current Speed Contour at NTL Station 42370 – July 2005	57
Figure 4-60 Current Speed Contour at NTL Station 42370 – August 2005	58
Figure 4-61 Current Speed Contour at NTL Station 42370 – September 2005	58
Figure 4-62 Current Speed Contour at NTL Station 42370 – October 2005	59
Figure 4-63 Current Speed Contour at NTL Station 42370 – November 2005	59
Figure 4-64 Current Speed Contour at NTL Station 42370 – December 2005	60
Figure 4-65 Current Speed Contour at NTL Station 42370 – January 2006	60
Figure 4-66 Current Speed Contour at NTL Station 42370 – February 2006	61
Figure 4-67 Current Speed Contour at NTL Station 42370 – March 2006	61
Figure 4-68 Current Speed Contour at NTL Station 42370 – April 2006	62
Figure 4-69 Current Speed Contour at NTL Station 42370 – May 2006	62
Figure 4-70 Current Speed Contour at NTL Station 42370 – June 2006	63
Figure 4-71 Current Speed Contour at NTL Station 42370 – July 2006	63
Figure 4-72 Current Speed Contour at NTL Station 42370 – August 2006	64
Figure 4-73 Current Speed Contour at NTL Station 42370 – September 2006	64
Figure 4-74 Current Speed Contour at NTL Station 42370 – October 2006	65
Figure 4-75 Current Speed Contour at NTL Station 42370 – November 2006	65
Figure 4-76 Current Speed Contour at NTL Station 42370 – December 2006	66
Figure 4-77 Current Speed Contour at NTL Station 42370 – January 2007	66
Figure 4-78 Current Speed Contour at NTL Station 42370 – February 2007	67
Figure 4-79 Current Speed Contour at NTL Station 42370 – March 2007	67
Figure 4-80 Current Speed Contour at NTL Station 42370 – April 2007	68
Figure 4-81 Current Speed Contour at NTL Station 42370 – May 2007	68
Figure 4-82 Current Speed Contour at NTL Station 42370 – June 2007	69
Figure 4-83 Current Speed Contour at NTL Station 42370 – July 2007	69
Figure 4-84 Current Speed Contour at NTL Station 42370 – Agust 2007	70

Figure 4-85 Current Speed Contour at NTL Station 42370 – September 2007	70
Figure 4-86 Current Speed Contour at NTL Station 42370 – October 2007	71
Figure 4-87 Current Speed Contour at NTL Station 42370 – November 2007	71
Figure 4-88 Current Speed Contour at NTL Station 42370 – December 2007	72
Figure 4-89 Current Speed Contour at NTL Station 42370 – January 2008	72
Figure 4-90 Current Speed Contour at NTL Station 42370 – February 2008	73
Figure 4-91 Current Speed Contour at NTL Station 42370 – March 2008	73
Figure 4-92 Current Speed Contour at NTL Station 42370 – April 2008	74
Figure 4-93 Current Speed Contour at NTL Station 42370 – May 2008	74
Figure 4-94 Current Speed Contour at NTL Station 42370 – June 2008	75
Figure 4-95 Current Speed Contour at NTL Station 42370 – July 2008	75
Figure 4-96 Current Speed Contour at NTL Station 42370 – August 2008	76
Figure 4-97 Current Speed Contour at NTL Station 42370 – September 2008	76
Figure 4-98 Current Speed Contour at NTL Station 42370 – October 2008	77
Figure 4-99 Current Speed Contour at NTL Station 42370 – November 2008	77
Figure 4-100 Current Speed Contour at NTL Station 42370 – December 2008	78
Figure 4-101 Current Speed Contour at NTL Station 42370 – January 2009	78
Figure 4-102 Current Speed Contour at NTL Station 42370 – February 2009	79
Figure 4-103 Current Speed Contour at NTL Station 42370 – March 2009	79
Figure 4-104 Current Speed Contour at NTL Station 42370 – April 2009	80
Figure 4-105 Current Speed Contour at NTL Station 42370 – May 2009	80
Figure 4-106 Current Speed Contour at NTL Station 42370 – June 2009	81
Figure 4-107 Current Speed Contour at NTL Station 42370 – July 2009	81
Figure 4-108 Current Speed Contour at NTL Station 42370 – August 2009	82
Figure 4-109 Current Speed Contour at NTL Station 42370 – September 2009	82
Figure 4-110 Current Speed Contour at NTL Station 42370 – October 2009	83
Figure 4-111 Current Speed Contour at NTL Station 42370 – November 2009	83
Figure 4-112 Current Speed Contour at NTL Station 42370 – December 2009	84
Figure 4-113 Current Speed Contour at NTL Station 42370 – January 2010	84
Figure 4-114 Current Speed Contour at NTL Station 42370 – February 2010	85
Figure 4-115 Current Speed Contour at NTL Station 42370 – March 2010	85
Figure 4-116 Current Speed Contour at NTL Station 42370 – April 2010	86
Figure 4-117 Current Speed Contour at NTL Station 42370 – May 2010	86
Figure 4-118 Current Speed Contour at NTL Station 42370 – June 2010	87
Figure 4-119 Current Speed Contour at NTL Station 42370 – July 2010	87
Figure 4-120 Current Speed Contour at NTL Station 42370 – August 2010	88
Table 4-1 Selected Subsurface Elevated Current Events	88
Figure 4-121 Hurricane Katrina track, NDBC buoy 42040 and selected NTL ADCP measurement locations	88
Figure 4-122 Observed (left) and PROFS (right) horizontal current velocity at NTL Station 42868 during and following Hurricane Katrina. Upward is North. Speed unit is m/s.	90
Figure 4-123 Near surface (80m at station 42868) and subsurface (477m at station 42868) PROFS model current velocity. Speed unit is m/s.	91

Figure 4-124. Observed (left) and PROFS (right) horizontal current velocity at NTL Station 42364. Upward is North. Speed unit is m/s.	92
Figure 4-125 Near surface (45m at station 42364) and near bottom (894m at station 42364) PROFS horizontal current velocity. Speed unit is m/s. The solid line is Hurricane Dennis track.	92
Figure 4-126 Observed (left) and PROFS (right) horizontal current velocity at NTL Station 42873. Upward is North. Speed unit is m/s.	93
Figure 4-127 Near surface (42m at station 42873) and near bottom (846m at station 42873) PROFS horizontal current velocity. Speed unit is m/s. The solid line is Hurricane Dennis track.	93
Figure 4-128 Observed horizontal current velocity at NTL Station 42863 and 42868. Upward is North. Speed unit is m/s.	94
Figure 4-129 Satellite sea surface height and sea surface temperature. The black dots are the locations of NTL stations 42863 and 42868.	94

EXECUTIVE SUMMARY

The Bureau of Ocean Energy Management, Regulation and Enforcement (BOEMRE) of the U.S. Department of the Interior funded the study of ocean current monitoring from 500 – 1,000 meters in the deep water region of the Gulf of Mexico. The contract was awarded to MCS Kenny and Fugro GEOS on 21 September 2010, and the work was performed by scientists and engineers from MCS Kenny (Ayman Eltaher, Program Manager, Burak Ozturk, MCS Kenny Project Lead and Kartik Sharma, Senior Specialist) and Fugro (Shejun Fan, Fugro Project Lead, Lie-Yauw Oey, Scientist at Princeton University and Fugro Consultant and Liam Harrington-Missin, Senior Oceanographer). The study objectives are to a) assess the characteristics of Gulf of Mexico current forcing in the 500 to 1,000 meter range, b) identify the occurrence of elevated events and c) to use those data to assess the importance of such currents on the fatigue and design of risers, moorings and TLP tendons.

BOEMRE NTL ADCP data, historical mooring current data and three types of PROFS model data were used for this study.

Based on the analysis of current characteristics, ocean current kinetic energy distribution and observational data availability, four representative zones are identified. Zone 1 and 3 are areas dominated by Loop Current/Loop Current Eddie events and hurricane generated currents, zone 2 is an area with relatively strong currents found near the continental rise and slope in the northern Gulf especially where isobaths converge or narrow, and zone 4 is the new front area and corresponding to the high kinetic energy at 500m.

The long term and event current profile characterizations and subsurface elevated event screening were undertaken using all the BOEMRE NTL ADCP data available on the NDBC web site up to August 2010. A total of more than 7 million individual ensemble binary files were downloaded. Individual ensemble data were combined into a single RDI broadband binary file for each separate instrument and location within each NDBC station.

After brief review of the data, 13, 6, 17 and 8 (total 44) NTL ADCP stations were selected for further quality control and analysis for Zones 1, 2, 3 and 4, respectively.

The subsurface elevated current events screening study further confirmed the conclusions drawn by (Jeans and Fan, 2007) and Fan et al. (2007) that two modes of subsurface elevated current events exist in the Gulf of Mexico: (1) submerged speed peaks with inertial period and (2) events isolated in time with no clear periodicity. The latter can be divided further as shallow jet events (between 150m to 600m) and deep jet events (deeper than 600m). **Most of the events are within the top 500m, only a few weak deep (deeper than 500m) events have been identified.**

For each zone, long term and short terms full water column current profile characterizations (representative current profiles and associated probabilities) were derived from selected quality controlled NTL ADCP data, historical mooring data and PROFS model data. These current profiles and specific riser models for each type (Drilling, SCR, TTR, Hybrid Risers, and TLP Tendons) were used to assess the VIV damage.

1. INTRODUCTION

1.1 Background and Program Objectives

Safe and efficient exploration and development of deepwater offshore oil and gas fields require the development of a comprehensive knowledge of the local oceanographic current regime. The study of ocean current monitoring from 500 – 1,000 meters in the Gulf of Mexico was sponsored by the Bureau of Ocean Energy Management, Regulation and Enforcement (BOEMRE) of the U.S. Department of the Interior. The purpose of this study was three-fold:

- 1) Assess the characteristics of Gulf of Mexico current forcing in the 500 to 1,000 meter range and occurrence of elevated events;
- 2) To evaluate the significance of ocean currents in water depths between 500 and 1000 meters on the fatigue and design of risers, moorings and TLP tendons;
- 3) Based on findings, to form a recommendation on whether monitoring below 500 meters is justifiable in regards to fatigue analysis of riser or mooring systems.

This report describes the activities associated with the first purpose of the study. The tasks relevant to this report are:

- Identify representative Zones in the study area based on literature review and ocean current kinetic energy distribution from a 4-year PROFS model run;
- Identify data from historical and concurrent programs;
- Acquire these data;
- Perform quality assurance and quality control (QA/QC) processing on the assembled data and add to the database;
- Derive representative long term current profiles and associated probabilities for each Zone;
- Derive elevated events current profiles and associated probabilities for each Zones.

1.2 Data and Output Descriptions

1.2.1 Numerical Model Data

The Princeton Regional Ocean Forecasting System (PROFS) was developed over the last decade through various supports from BOEMRE. It is a numerical circulation model that provides high-resolution hindcast three-dimensional current data from 1993 to present in the Gulf of Mexico. The model has also been used in a research capacity to study processes and mechanisms. The realistic hindcast current data is used in BOEMRE's oil spill risk analysis program. It was (and is being) used to help provide long-term forecasts of the BP oil spill¹. PROFS provides a tool that helps to define the temporal and spatial distributions of the current events in different areas of the Gulf of Mexico. From these, the long term current distributions, current profile characterizations and extreme currents can be defined

PROFS is based on the Princeton Ocean Model² which uses an efficient scheme that projects satellite sea-surface height anomaly (SSHA) data from AVISO³ to the model density field (e.g. Yin and Oey, 2007). Sea-surface temperature (SST) is also assimilated but its effects are less than

¹ <http://www-aos.princeton.edu/WWWPUBLIC/PROFS> accessed 15-Jun-2011

² http://www-aos.princeton.edu/WWWPUBLIC/htdocs_pom/ accessed 15-Jun-2011

³ <http://www.aviso.oceanobs.com/> accessed 15-Jun-2011

SSHA. Six-hourly CCMP⁴ winds at $\frac{1}{4} \times \frac{1}{4}$ degree and daily river discharges⁵ from 51 US rivers (34 in the Gulf and 17 in the eastern coasts) are specified. Model domain covers most of the northwestern Atlantic Ocean (NWAQ) from 100°W–55°W and 5°N–50°N at approximately 5~10 km resolution in the Gulf of Mexico, and there are 25 vertical terrain-following (i.e. sigma) levels; this will be referred to as the NWAQ model (Figure 1-1).

An accurate fourth-order pressure-gradient scheme is used (Berntsen and Oey, 2010). The first sigma grid is $z = -1.05$ m below the surface in 1500 m of water. Monthly temperature and salinity climatologies from NODC's World Ocean Atlas⁶ are used to specify open boundary conditions at 55°W. To prevent long-term drift, temperatures and salinities below $z = -1000$ m are also relaxed to WOA climatologies with a long time scale of 600 days; this does not impede short-period mesoscale variability. A modified Mellor and Yamada's 2.5-level closure scheme that inputs breaking-wave turbulence energy at the surface is used (Craig and Banner, 1994; Mellor, 2002). This improves mixed layer depths and corrects unrealistically large speeds close to the surface sometimes found in the original scheme. The model has been used for research in the Gulf of Mexico where we have also extensively compared the results against observations both in the surface and subsurface (Oey and Lee, 2002; Ezer et al. 2003; Wang et al. 2003; Fan et al. 2004; Oey et al. 2005a,b, 2006, 2007, 2008, 2009; Lin et al. 2007; Yin and Oey, 2007; Oey, 2008; Wang and Oey, 2008; Mellor et al. 2008).

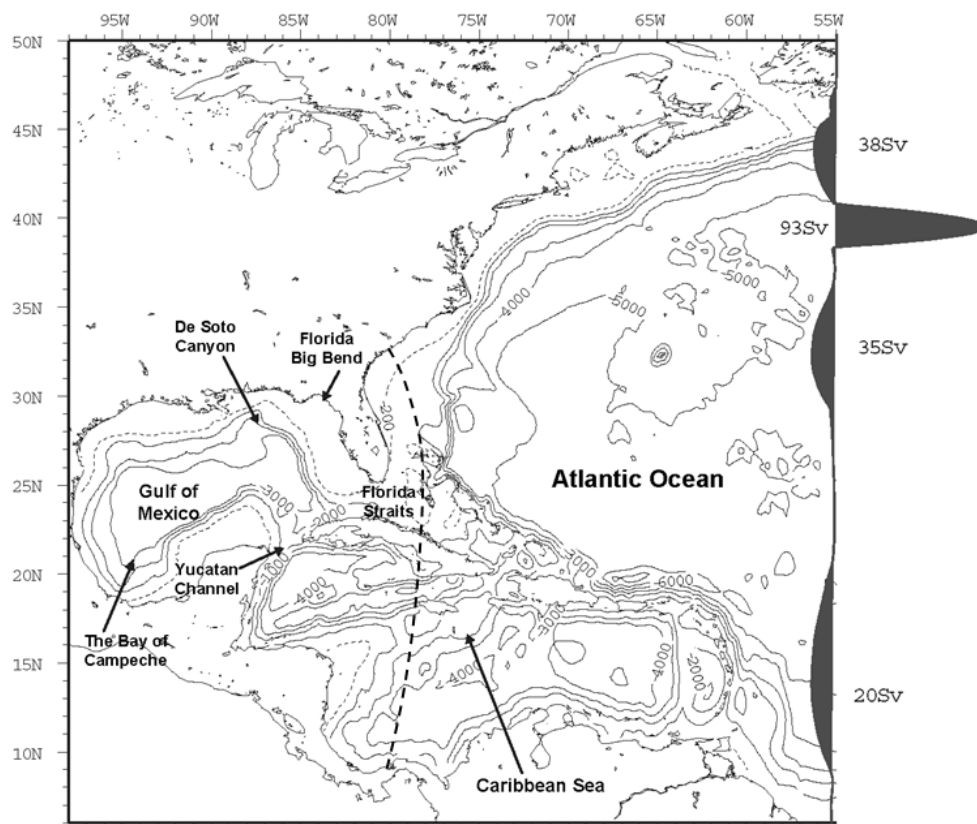


Figure 1-1 The northwest Atlantic Ocean model ($\Delta \approx 6\text{--}12$ km within the Gulf of Mexico) (NAOM; the whole region shown) and the fine-grid resolution ($\Delta \approx 3\text{--}7$ km) Gulf of Mexico and northwest Caribbean Sea region (west of the dashed line). Contours show isobaths in meters, and silhouettes at 55°W show steady transports specified for the Gulf Stream and returned flows.

⁴ http://podaac.jpl.nasa.gov/DATA_CATALOG/ccmpinfo.html accessed 15-Jun-2011

⁵ <http://waterdata.usgs.gov/nwis/rt> accessed 15-Jun-2011

⁶ http://www.nodc.noaa.gov/OC5/WOA05/pr_woa05.html accessed 15-Jun-2011

For this project, a domain west of ~78°W and from 6°N~33°N nested within the NWAO model at double the resolution (3~5 km horizontal grids and the same 25 sigma levels) were used. The nest encompasses the northwestern Caribbean Sea, the southern portion of the South Atlantic Bight east of Florida, and the entire Gulf of Mexico. The nest receives boundary conditions from the NWAO model (Oey and Zhang, 2004; Chang and Oey, 2010). Three dimensional current data were archived at hourly interval at selected stations for analyses (black squares in Figure 1-2). Daily data were also be archived for the entire Gulf of Mexico.

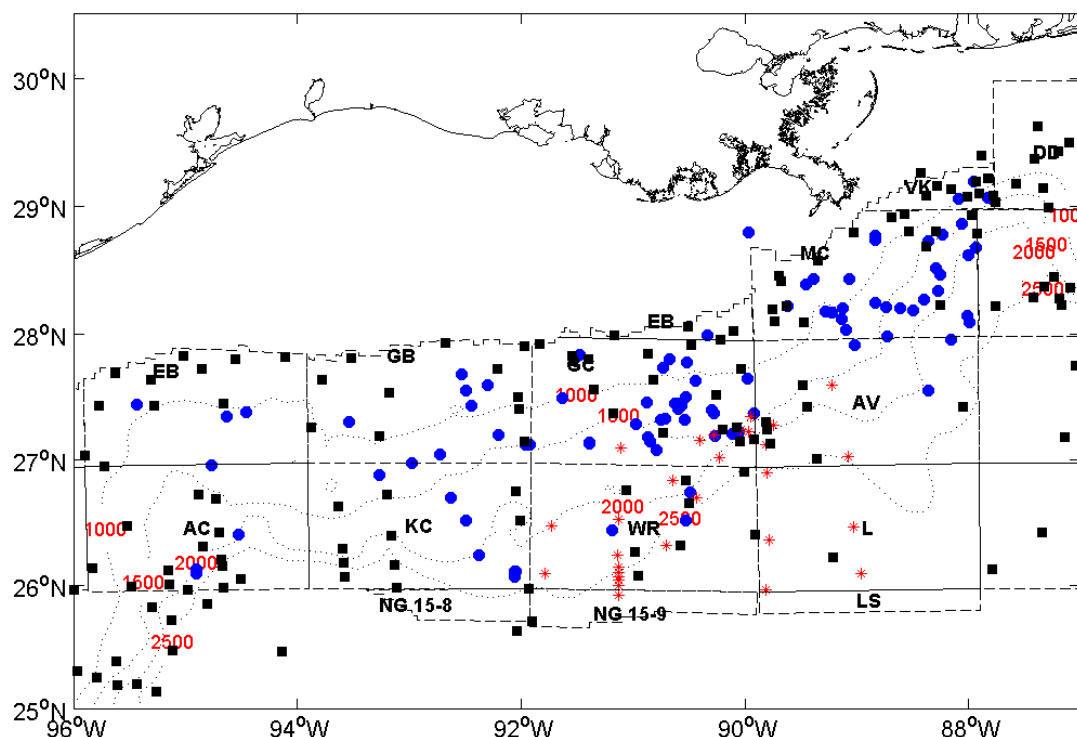


Figure 1-2 NTL ADCP stations (blue dots), PROFS stations (black squares) and historical current mooring locations (red stars).

1.2.2 Observation Data

In April 2005, BOEMRE issued a Notice to Lessees and Operators (NTL) regarding the reporting of ocean current data in the deep water of Gulf of Mexico. An extensive body of NTL current data has since been collected by the offshore oil and gas industry and made available via the National Data Buoy Center (NDBC) web site (http://www.ndbc.noaa.gov/maps/ADCP_WestGulf.shtml).

Based on a comprehensive reanalysis and synthesis of existing data (Nowlin et al 2001), a series of deepwater current studies were undertaken by BOEMRE. Notably are The Exploratory Study of Deepwater Currents in the Gulf of Mexico, the Survey of Deepwater Currents in the Northwestern Gulf of Mexico, the Survey of Deepwater Currents in the Eastern Gulf of Mexico, Dynamics of the Loop Current in U.S. Waters and other ongoing deepwater data collection.

The available NTL Acoustic Doppler Current Profile (ADCP) and historical BORMRE mooring data within selected zones were quality controlled and screened to assess the distribution of currents in the 500 to 1,000 meters layer. Profile shapes were characterized to identify background and significant events.

1.3 Report Organization

Section 2 of this report presents descriptions of the methodology used to divide the study area into 4 zones. Section 3 describes observational data collection, processing, QA/QC procedures, file formatting, and naming conventions. PROFS model data is also documented. Section 4 presents descriptions of the Subsurface elevated current events found in current meter observations. The long term and events current profile characterizations were presented in section 5.

1.4 Units and Conventions

The following list outlines the units and conventions adopted in this report.

- Current speed is expressed in meter per second (m/s).
- Current direction is expressed in degrees clockwise from true North and describes the directions towards which the current was flowing.

Table 1-1 Directional Sectors

DIRECTIONAL SECTOR	N	NE	E	SE	S	SW	W	NW
RANGE ($^{\circ}$ T)	337.5 -< 22.5	22.5 -< 67.5	67.5 -< 112.5	112.5 -< 157.5	157.5 -< 202.5	202.5 -< 247.5	247.5 -< 292.5	292.5 -< 337.5

1.5 Abbreviations

The following list outline the abbreviations adopted in this report.

- ADCP Acoustic Doppler Current Profiler
- AOML Atlantic Oceanographic and Meteorological Laboratory
- AVISO Archiving, Validation and Interpretation of Satellite Oceanographic data
- AVISOM AVISO SSH + the (present) model 10-year mean SSH
- BEnF Bred Ensemble Forecast
- BOEMRE Bureau of Ocean Energy Management, Regulation and Enforcement
- HRD Hurricane Research Division
- NCEP National Centers for Environmental Prediction
- NOAA National Oceanic and Atmospheric Administration
- OBS Observation(s)
- POM Princeton Ocean Model
- RMS Root Mean Square
- SSH Sea Surface Height
- SSHA Sea Surface Height Anomaly
- SST Sea Surface Temperature

2. NORTHERN GULF OF MEXICO SUNDIVISIONS

Due to the limited resources, we need to select representative subdivisions of the Gulf of Mexico so that the analysis on the limited riser or mooring systems can provide a realistic response of the impact of increased current monitoring depth on the riser or mooring system VIV fatigue damage.

The selection of representative study areas are based on current characteristics, ocean current kinetic energy distribution and observational data availability.

2.1 Current Characteristics

The Gulf of Mexico is a semi-enclosed sea. Observations and numerical studies have indicated that the current in the Gulf of Mexico has a basic two-layer structure. The circulation in the upper layer upper (surface to depths of 800~1200 m) is dominated by Loop Current (LC) and Loop Current Eddy (LCE), warm-core rings that episodically separate from the Loop. Strong Loop Current/Loop Current Eddy currents as high as 3m/s have been observed. The lower layer is dominated by deep eddies and Topographic Rossby Waves (TRWs). The deep eddies are generally vertically coherent (Welsh and Inoue, 2000) in the lower layer about 1000 m above seabed, and effective in producing cross-isobath motions, hence possibly TRWs, with a tendency for bottom intensification (Hamilton and Lugo-Fernandez, 2001, Oey, 2008). Deepwater currents in the Gulf of Mexico can be classified as the following four categories:

- Currents caused by energetic atmospheric events including inertial oscillations driven by hurricanes.
- Surface-intensified circulation features including the loop current and associated eddies.
- Deep barotropic currents including topographic Rossby waves and associated near bed flows.
- High-speed subsurface-intensified currents.

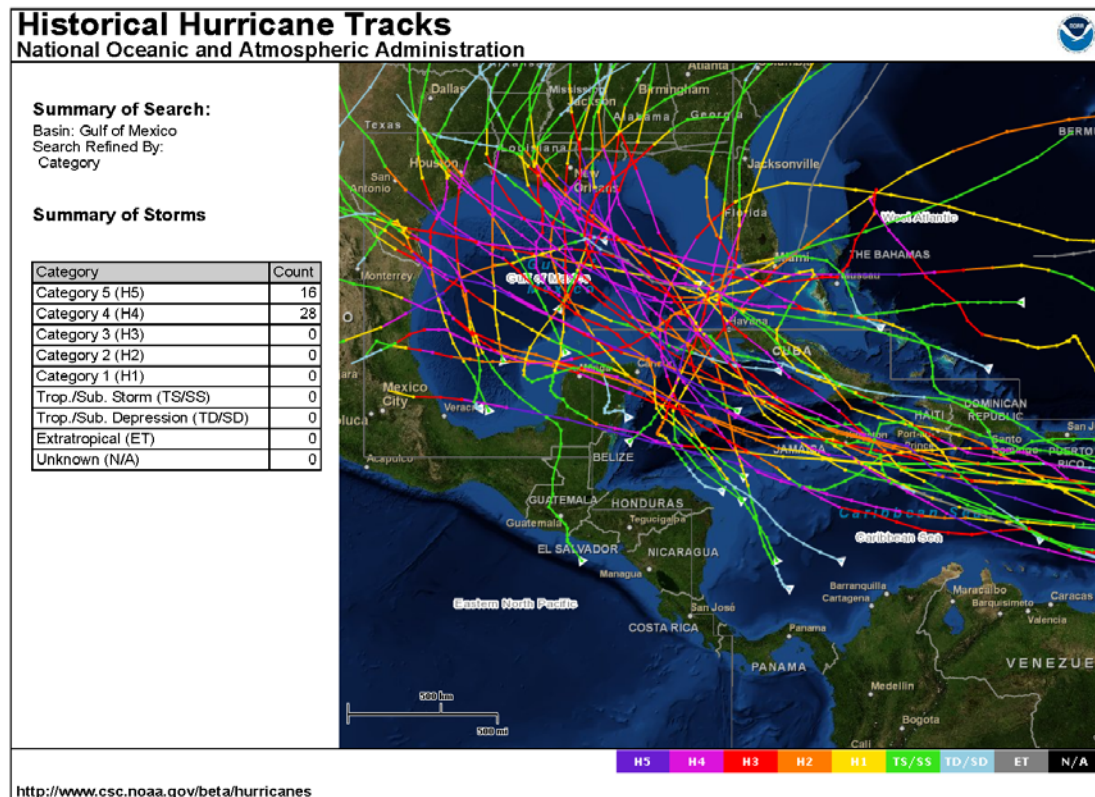


Figure 2-1 Historical Category 4 and 5 Hurricanes in the Gulf of Mexico

Figure 2-1 shows all category 4 and 5 historical hurricane tracks that in the Gulf of Mexico. The hurricanes are fairly uniformly distributed in the oil-producing regions of the northern Gulf of Mexico. A fast moving hurricane will excite large inertial currents. Inertial currents can penetrate into the deep portions of the existing strong anticyclonic LCEs. These deep penetrations and trapping of inertial energy occur days (up to ~ 10) after a hurricane has passed, and could have important implications to the riser systems.

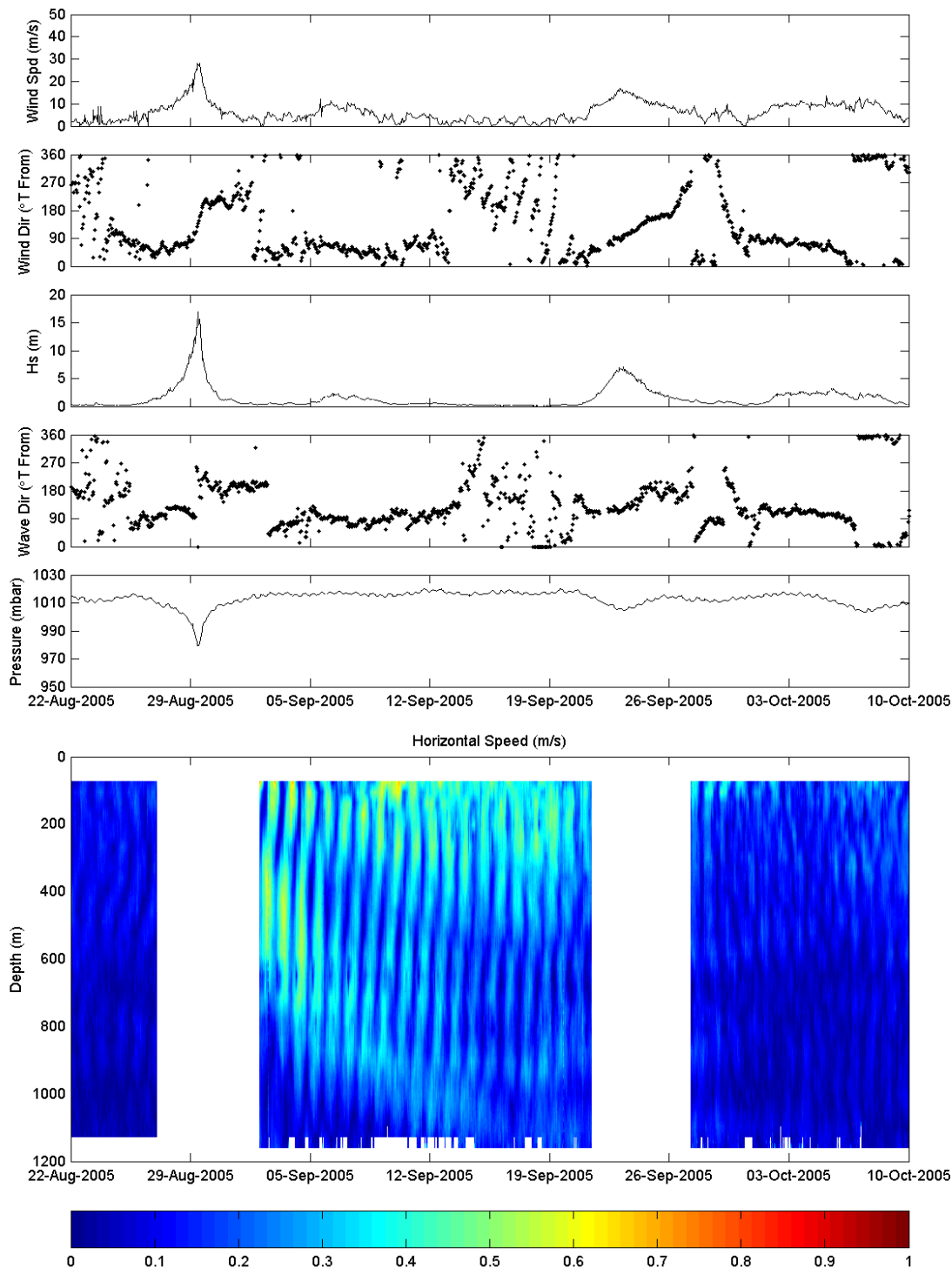


Figure 2-2 Hurricane Measurement at Buoy 42040 and NTL Station 42868 (28.164°N 88.484°W)

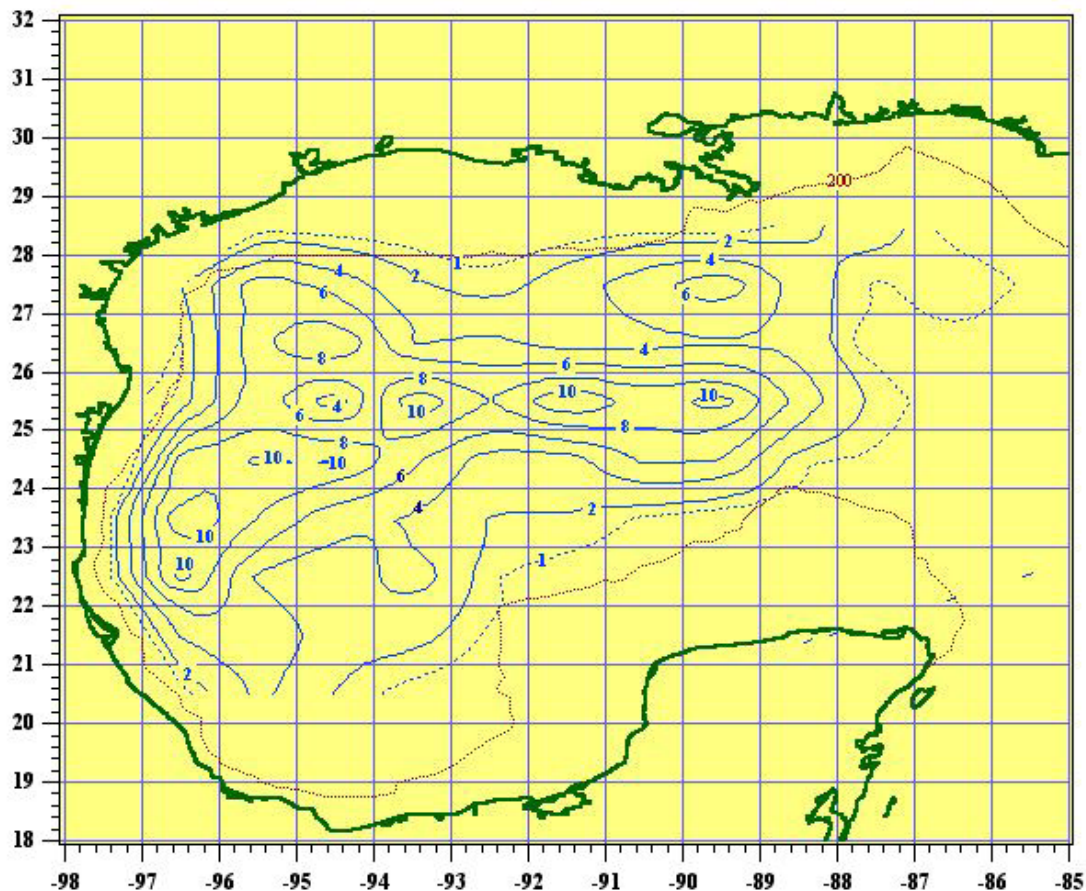


Figure 2-3 Spatial frequency (%) for the location of LCE centers using a 27-year (1977 – 2003) database (From OCS Study MMS 2005-031)

Figure 2-2 is measured wind/wave/pressure and current data during hurricane Katrina. The inertial energy penetrated as deep as 1000m thanks to the existence of eddy Vortex.

Figure 2-3 shows the spatial frequency for the location of LCE centers. Eddies can affect a site for weeks to months per year.

The lower layer is dominated by deep eddies and Topographic Rossby Waves (TRWs). Deep eddies are generally vertically coherent in the lower layer, about 1000 m above seabed, and effective in producing cross-isobath motions, hence possibly TRWs, with a tendency for bottom intensification. It is known that the relatively high lower-water-column current is nearly depth independent and exist over the slope and rise in the northern Gulf of Mexico (the Desoto Canyon slope and the Sigsbee Escarpment).

Parasitic cyclones and jets can be generated when a warm eddy impinging upon a continental slope.

2.2 Current Kinetic Energy Distribution

The ocean current kinetic energy distribution was studied using high-resolution Princeton Regional Ocean Forecasting System (PROFS) run.

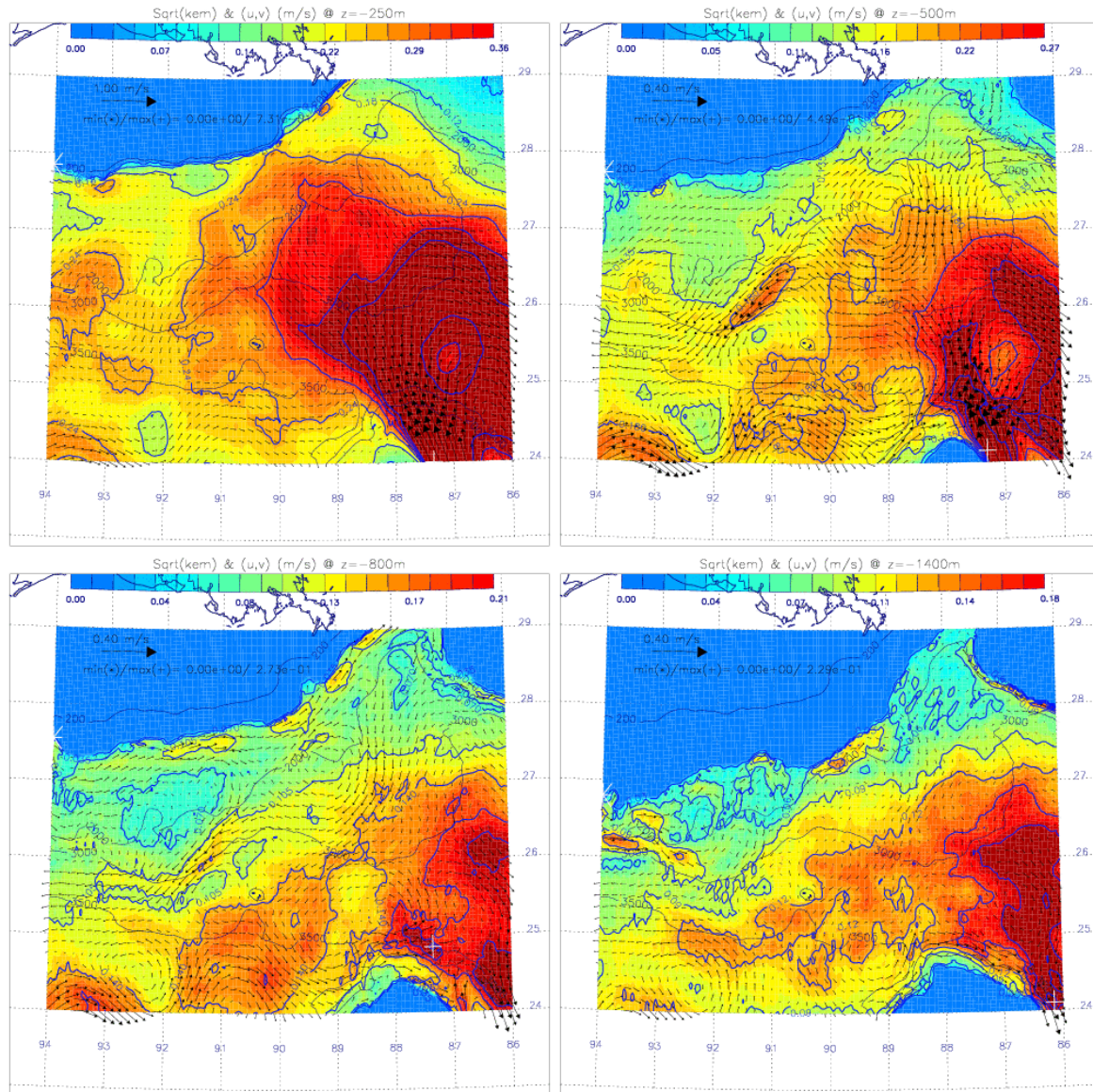


Figure 2-4 Mean currents (u_m, v_m) as vectors superimposed on color images (and also in blue contours) of $(KE_m)^{1/2}$ at $z = -250, -500, -800$ and -1400m . Thin black contours show 200m, 2000m, 3000m and 3500m isobaths.

The 4-year (December 2002 to December 2006) run outputs daily currents (and other fields) at the model's (original) terrain-following grid levels and curvilinear horizontal grids. These are then interpolated to a uniform $5\text{ km} \times 5\text{ km}$ grid over a smaller region from $94 - 86^\circ\text{W}$ and $24 - 29^\circ\text{N}$ and also to fixed z -levels: $0, -50, -100, \dots -500, -800, \dots -3600\text{m}$. This region includes most of the deepwater developments and BORMRE ADCP locations. The 4-year time-means and fluctuations from the time-means are then computed for each model variable, and various statistics are then derived. This study calculated the mean currents $(u_m, v_m) = \langle u, v \rangle$ where $\langle \cdot \rangle$ denotes time-averaging (i.e. 4 years), standard deviations $(KE_m)^{1/2} = \sqrt{\langle u^2 + v^2 \rangle}$ (i.e. speeds) of the total currents (i.e. mean + fluctuations), as well as the frequency of occurrences of currents that are stronger than a specified speed,

$\text{Frq}(\mathbf{x}, \text{spd})$, for $\text{spd} = 0.1, 0.2$ and 0.4 m/s , where $\mathbf{x} = (x, y, z)$ is the position vector. For example, near the surface for a point within the Loop Current, $\text{Frq}|0.4$ would be in the high values of

say 0.8 for $\text{spd} = 0.4 \text{ m/s}$ – i.e. current speeds are stronger than 0.4 m/s 80% of the time at that location. Accordingly, for a point at $z \approx -500 \text{ m}$ in 2000m depth of water just south of New Orleans in the northern Gulf, the $\text{Frq}|0.2$ might be low ≈ 0.05 for $\text{spd} = 0.2 \text{ m/s}$. For convenience, we will use the notation $\text{Frq}|\text{spd}$.

Figure 2-4 shows (u_m, v_m) vectors superimposed on color images of $(\text{KE}_m)^{1/2}$ at $z = -250, -500, -800$ and -1400 m .

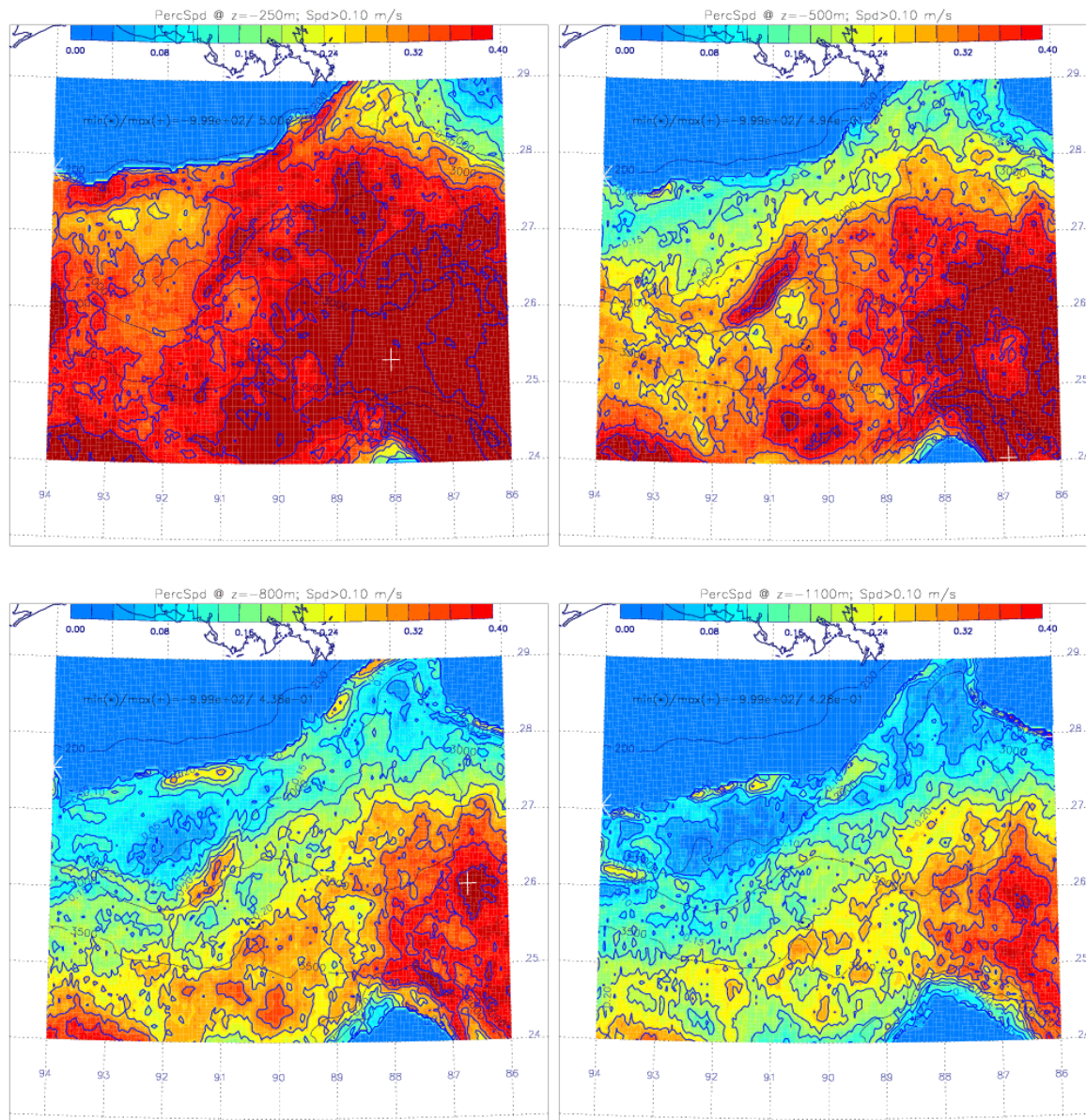


Figure 2-5 Color maps and contours of $\text{Frq}(x, \text{spd}) = \text{frequency of occurrences of currents that are stronger than speed } \text{Spd} = 0.1 \text{ m/s, at } z = -250, -500, -800 \text{ and } -1100 \text{ m. Note color scale is from 0 to 0.4 (=40%) and contour (blue) interval is = 0.05 (=5%). Thin black contours show 200m, 2000m, 3000m and 3500m isobaths.}$

At levels nearer the surface (e.g. $z = -250 \text{ m}$ in Figure 2-4), the mean currents (u_m, v_m) are dominated by the Loop Current and remnants of eddies that were shed from the Loop and that propagate westward. The strong-current region extends northwestward from the center of the Loop Current near $(90^\circ\text{W}, 24^\circ\text{N})$ to south of the Mississippi Delta near $(90^\circ\text{W}, 28^\circ\text{N})$, and also directly westward from the Loop. These surface features provide energy to deeper layers of the Gulf, focusing in particular along isobaths and over the continental rise and slope of the northern Gulf as topographic Rossby waves

(Oey and Lee, 2002; Oey, 2008). In examining the deeper current energy distributions in Figure 2-4, stronger currents near localized topographic spots which in Oey et al. (2009) we identified as “topocaustics” should be focused on. Examples of these localized regions are listed in Table 2-1.

Table 2-1 Localized regions of strong currents inferred from Figure 2-4.

Name	Isobaths (m)	From Lon, Lat (°W, °N)	To Lon, Lat (°W, °N)	At z-level (m)
Lower Sigsbee	2000~3000	(92, 25.6)	(91.5, 26.5)	-500
SW DeSoto Canyon	1000~3000	(90, 27.6)	(88, 26)	All
Near-1000m	800~1500	(92, 27.6)	(90.8, 27.7)	-800
		(90, 27.8)	(88, 29)	-800
Near-2000m	1000~3000	(94, 26.3)	(92, 25.8)	-1400
	1000~2000	(90.5, 27.3)	(89, 27.6)	-1400

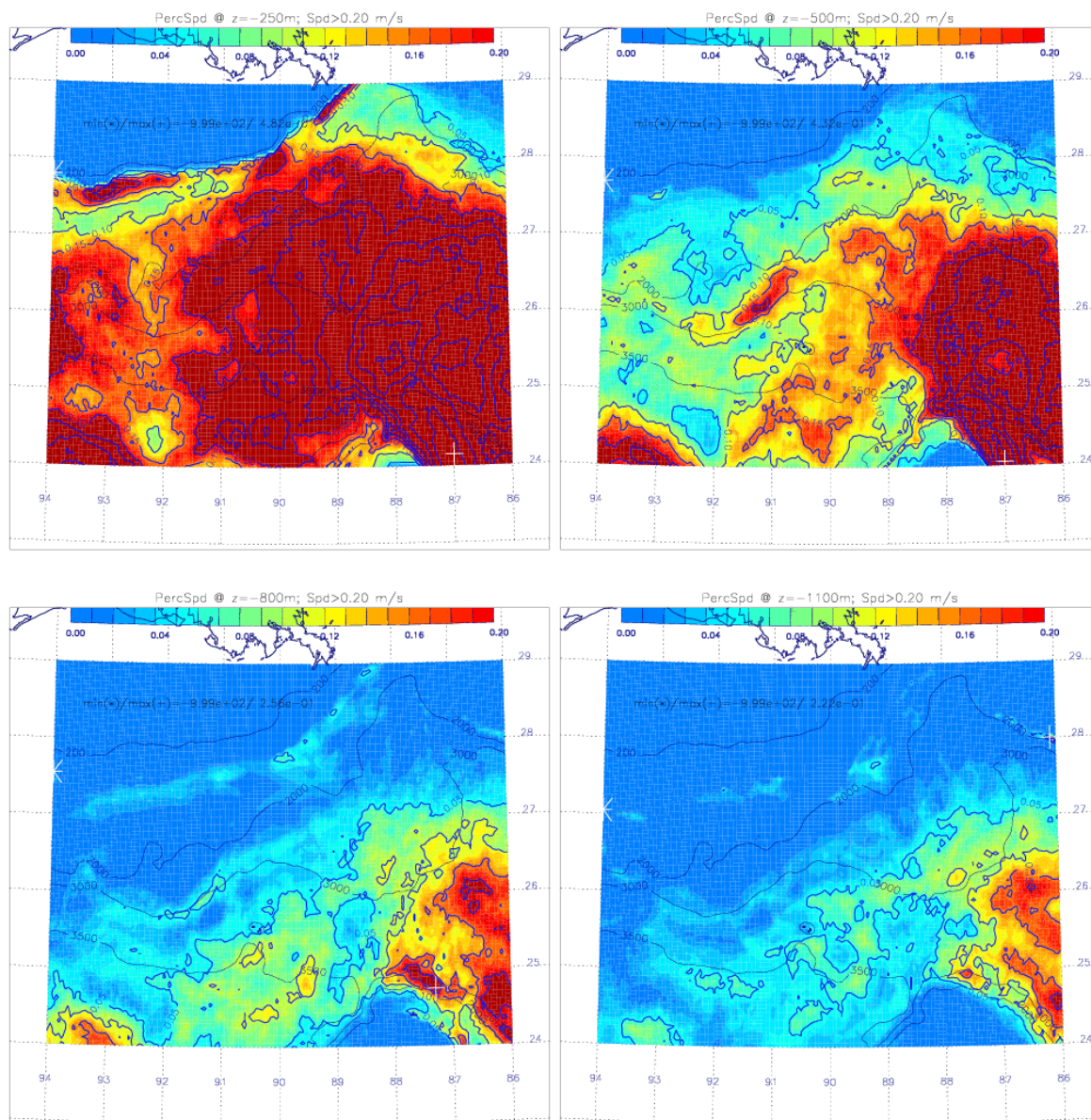


Figure 2-6 Color maps and contours of $\text{Frq}(x, \text{spd})$ = frequency of occurrences of currents that are stronger than speed $\text{Spd} = 0.2 \text{ m/s}$, at $z = -250, -500, -800$ and -1100m . Note color scale is from 0 to 0.2 (=20%) and contour (blue) interval is = 0.05 (=5%). Thin black contours show 200m, 2000m, 3000m and 3500m isobaths.

Figure 2-5 and Figure 2-6 show Frq, the frequency of occurrences of currents that are stronger than spd, for spd = 0.1 m/s (Figure 2-5) and 0.2 m/s (Figure 2-6) respectively. These confirm features listed in Table 2-1. For example, at the lower Sigsbee, Frq|0.1 is quite high, around 0.4 at z=-500m, and 0.3 at z=-800m (see Figure 2-5). Many of the features along the “Near-1000m” also have relatively high Frq|0.1, and for spd=0.2 m/s (Figure 2-6), the values decrease to less than 0.05.

2.3 Zones Selection

Based on the above analysis of current characteristics, ocean current kinetic energy distribution and observational data availability, the following four representative study Zones were selected (Figure 2-7):

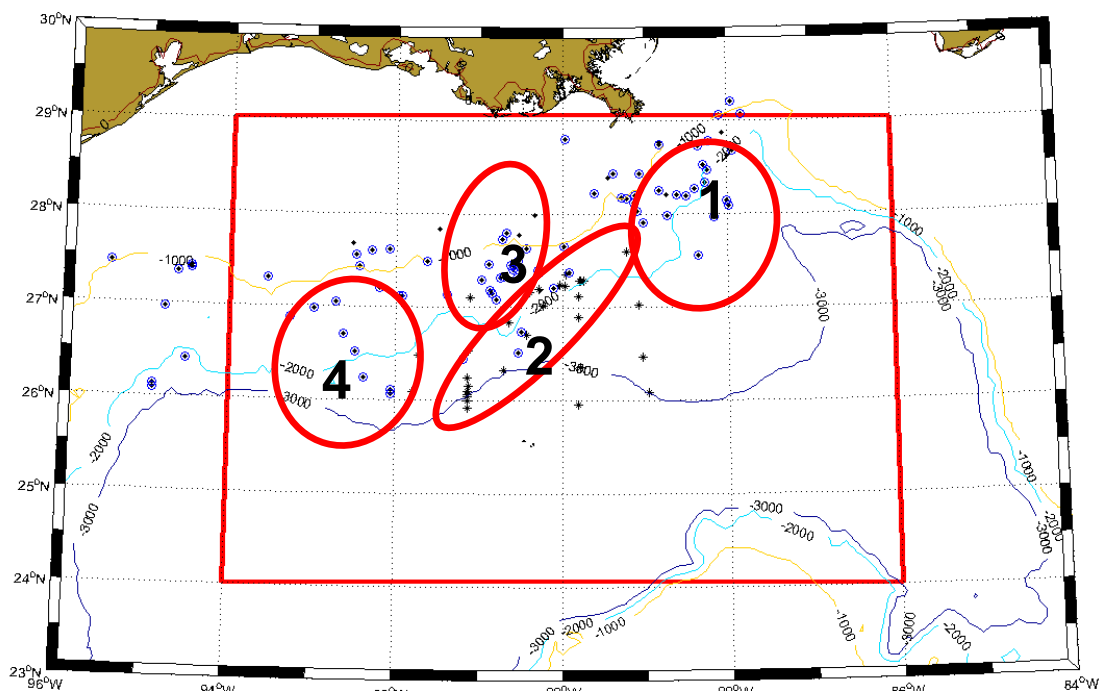


Figure 2-7 NTL ADCP stations (circled dots) and historical current mooring (+) locations. Red box is the region in Figure 2-4, Figure 2-5 and Figure 2-6. The red ellipses are proposed representative Zones.

1) Zone 1 (DeSoto Canyon area)

This zone has the following characteristics:

- Very active lease area
- The maximum northwestward LC intrusion
- Parasitic cyclones and jets can be generated when a warm eddy impinging upon continental slope.
- Two-layer jet with eastward flow at the surface and a return flow at depth
- Deep penetrations and trapping of hurricane-induced inertial energy

2) Zone 2 (base of the Sigsbee Escarpment area)

This zone has the following characteristics:

- New super-deep water oil & gas front (Petrobras' Cascade and Chinook, Chevron's Big Foot and Jack, BP's Atlantis and Shell's Stones etc.)

- Topographic Rossy Waves (TRW) and bottom intensified currents.

3) Zone 3

This zone has the following characteristics:

- Most active lease area
- On the main path of LCE
- Deep penetrations and trapping of hurricane-induced inertial energy

4) Zone 4 (Keathley Canyon area)

This zone has the following characteristics:

- The new oil & gas front (BP's Kaskida, Anadarko's Lucius etc.)
- Local kinetic energy peak from 500 to 1000m
- Possible Topographic Rossy Waves (TRW) and bottom intensified current

3. CURRENT DATA DATABASE

3.1 NTL data Acquisition and Quality Control

The long term and event current profile characterizations and subsurface elevated event screening were undertaken using all the BOEMRE NTL ADCP data available on the NDBC web site up to August 2010. A total of more than 7 million individual ensemble binary files were downloaded. Individual ensemble data were combined into a single RDI broadband binary file for each separate instrument and location within each NDBC station.

After brief review of the data, 13, 6, 17 and 8 (total 44) NTL ADCP stations were selected for further quality control and analysis for Zones 1, 2, 3 and 4, respectively. The selected stations are shown in Figure 3-1 to Figure 3-4, and Table 3-1 to Table 3-4.

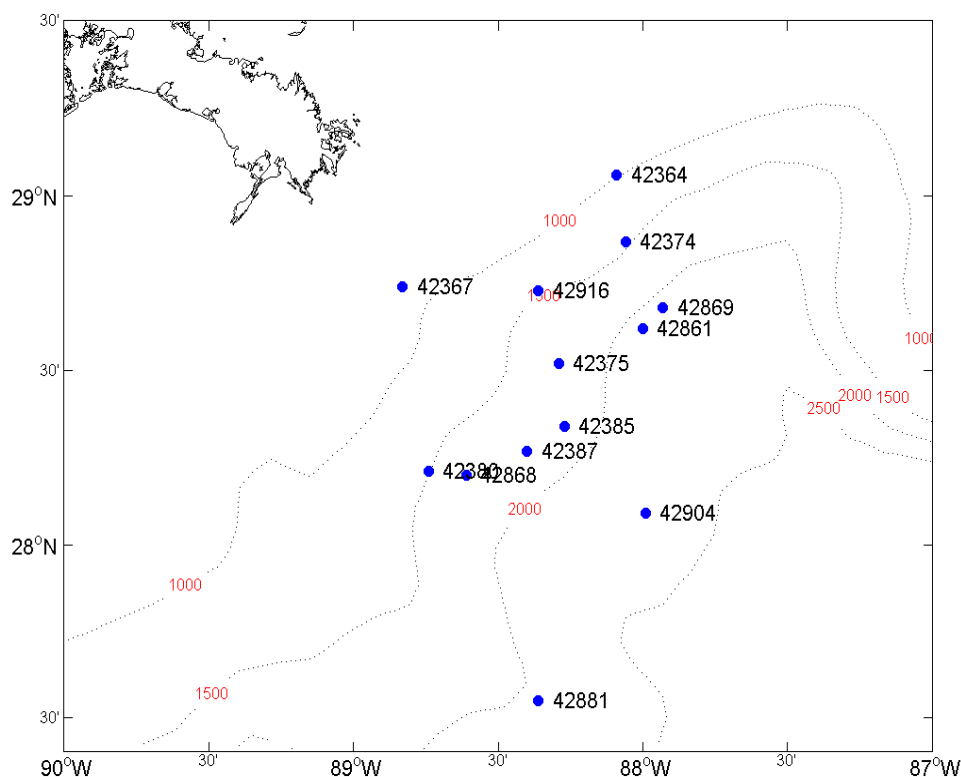


Figure 3-1 NTL ADCP stations used in this study – zone 1

Table 3-1 BOEMRE NTL ADCP Stations used in this study – zone 1

Station ID	Station Name	Longitude (°W)	Latitude (°N)	Water Depth (m)
42364	Ram-Powell - Shell International E&P	88.09	29.06	980
42367	Matterhorn - Total USA Inc.	88.83	28.74	860
42374	Horn Mountain - BP Inc.	88.06	28.87	1646
42375	Na Kika - BP Inc.	88.29	28.52	1920
42380	Devil's Tower – Williams	88.74	28.21	1710
42385	Blind Faith – Chevron	88.27	28.34	1975
42387	Thunderhawk - Murphy E&P Co.	88.40	28.27	1847
42861	Nautilus - Shell International E&P	88.00	28.62	1613
42868	Discoverer Enterprise - BP Inc.	88.61	28.20	1508
42869	Ocean Confidence - Murphy E&P Co.	87.93	28.68	2134

42881	Transocean Marianas - ENI Petroleum	88.36	27.55	2177
42904	Independence Hub - Anadarko Petro. Corp.	87.99	28.09	2438
42916	Development Driller 3 - BP Inc.	88.36	28.73	1521

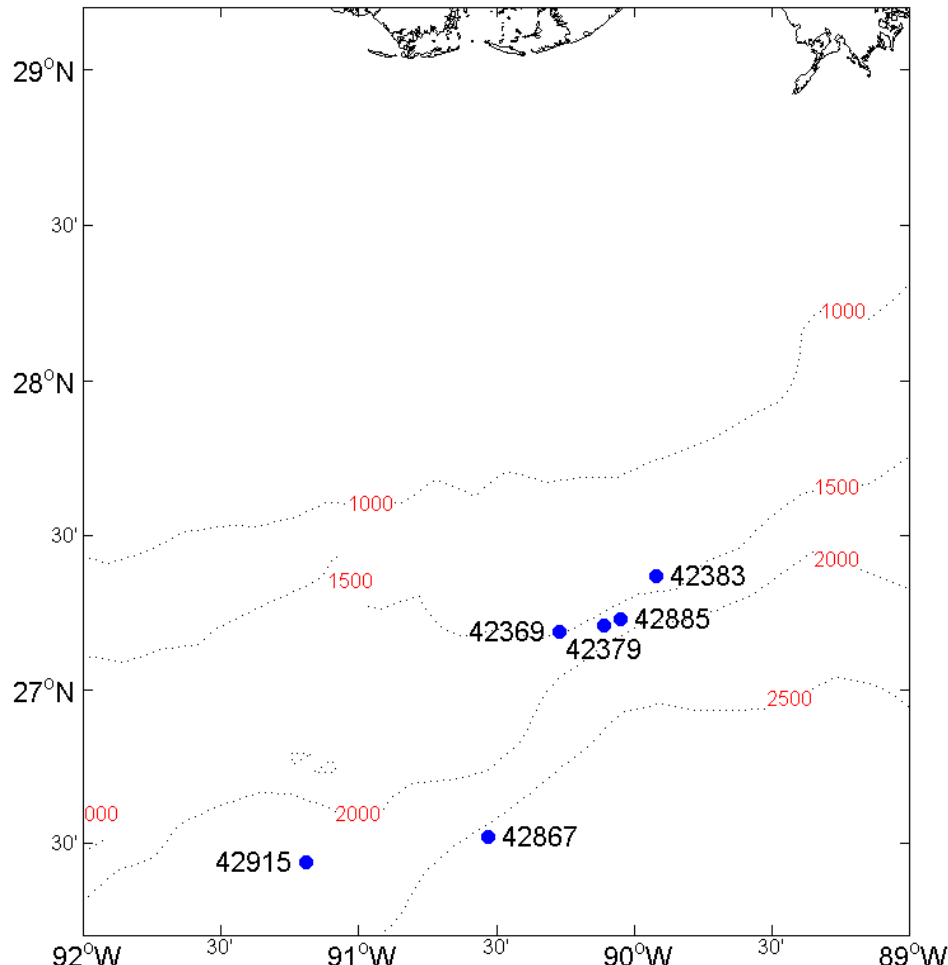


Figure 3-2 NTL ADCP stations used in this study – zone 2

Table 3-2 BOEMRE NTL ADCP Stations used in this study – zone 2

Station ID	Station Name	Longitude (°W)	Latitude (°N)	Water Depth (m)
42369	Mad Dog - BP Inc.	90.27	27.19	1372
42379	Marco Polo - Anadarko Petrol. Corp.	90.11	27.21	1286
42383	Neptune - BHP Billiton	89.92	27.37	1290
42867	DeepSeas - Petrobras USA	90.53	26.52	2691
42885	Development Driller 2 - BP Inc.	90.05	27.23	2073
42915	Maersk Developer - Maersk Drilling USA	91.19	26.44	2032

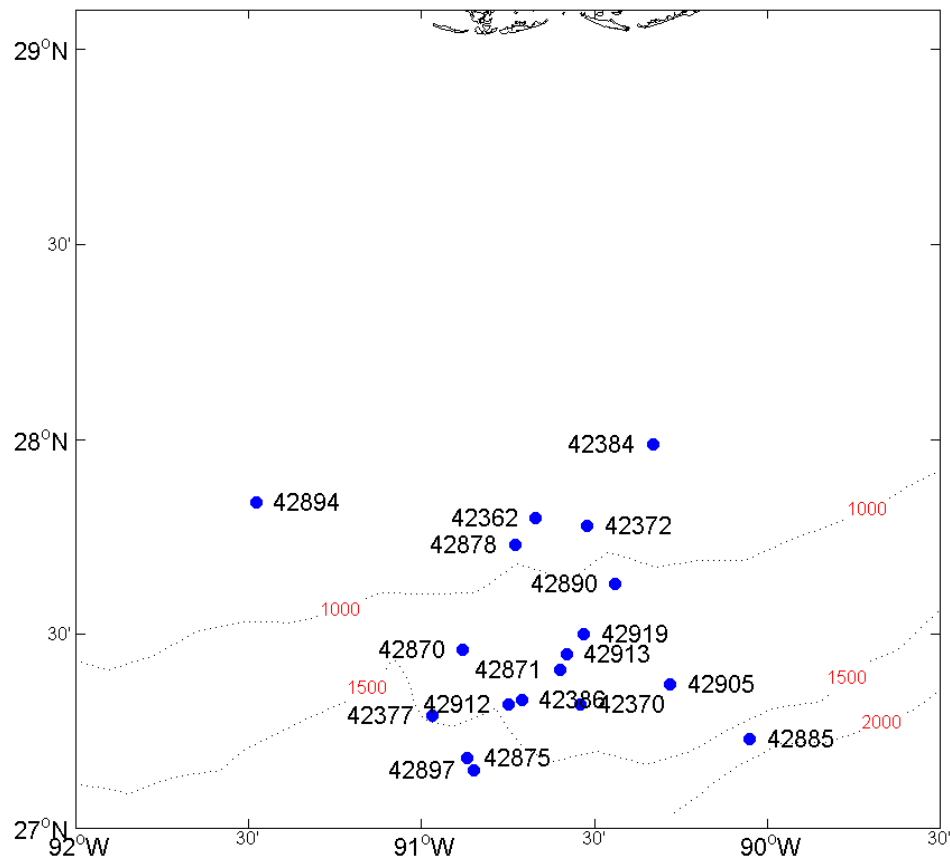


Figure 3-3 NTL ADCP stations used in this study – zone 3

Table 3-3 BOEMRE NTL ADCP stations used in this study – zone 3

Station ID	Station Name	Longitude (°W)	Latitude (°N)	Water Depth (m)
42362	Brutus - Shell International E&P	90.67	27.80	910
42370	Holstein - BP Inc.	90.54	27.32	1311
42372	Genesis - Chevron	90.52	27.78	789
42377	Constitution - Kerr-McGee Oil and Gas Corp.	90.97	27.29	1524
42384	Prince TLP - El Paso E&P Co., L.P.	90.33	27.99	455
42386	Tahiti - Chevron	90.71	27.33	1219
42870	Ocean America - Noble Energy Inc.	90.88	27.46	1295
42871	C R Luigs - BHP Billiton	90.60	27.41	1143
42875	Amos Runner - Anadarko Petrol. Corp.	90.87	27.18	805
42878	Paul Romano - Marathon Oil	90.73	27.73	899
42885	Development Driller 2 - BP Inc.	90.05	27.23	2073
42890	Front Runner - Murphy E&P Co.	90.44	27.63	1015
42894	Lorris Bouzigard - LLOG	91.48	27.84	756
42897	Development Driller 1 - BHP Billiton	90.85	27.15	1353
42905	Belford Dolphin - Anadarko Petro. Corp.	90.28	27.37	1287
42912	Discoverer Clear Leader - Chevron	90.75	27.32	2075
42913	ENSCO 8501 - Noble Energy Inc.	90.58	27.45	1986
42919	Stenna Forth - Amerada Hess Corp.	90.53	27.50	1021

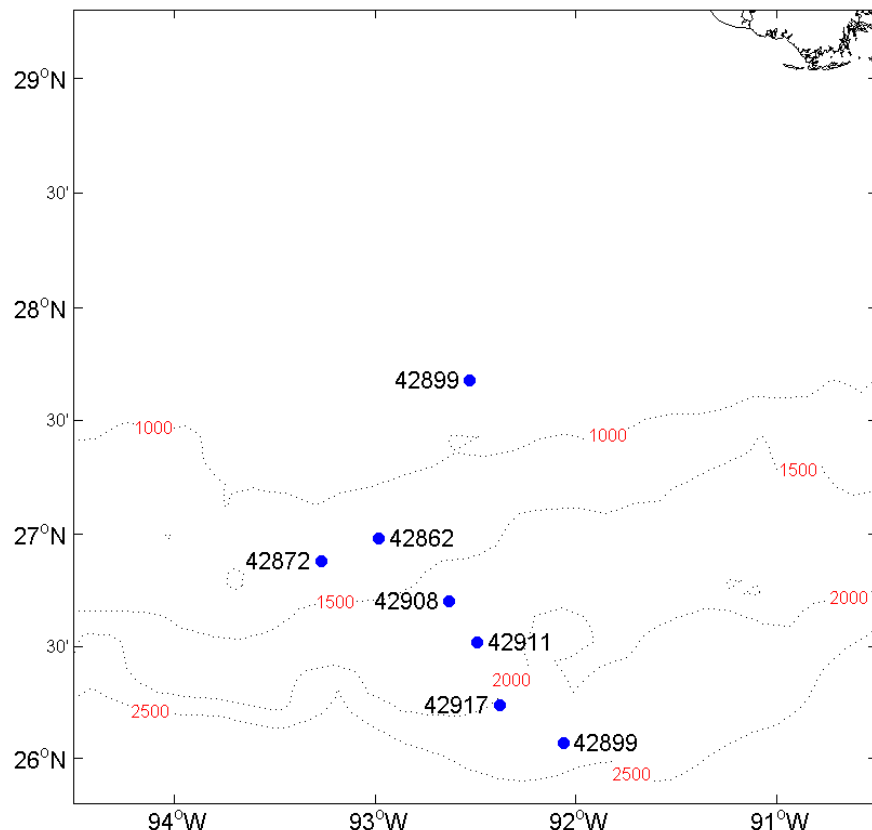


Figure 3-4 NTL ADCP stations used in this study – zone 4

Table 3-4 BOEMRE NTL ADCP stations used in this study – zone 4

Station ID	Station Name	Longitude (°W)	Latitude (°N)	Water Depth (m)
42862	Jim Thompson - Shell International E&P	92.98	26.98	
42872	Deepwater Horizon - BP Inc.	93.27	26.88	
42899	Ocean Endeavor - ExxonMobil	92.06	26.07	2249
42899	Ocean Endeavor - ExxonMobil	92.53	27.68	
42908	West Sirius - ExxonMobil	92.63	26.70	2116
42911	Ocean Monarch - Marathon Oil	92.49	26.52	
42917	Discoverer Inspiration - Chevron	92.38	26.24	

3.1.1 Data Quality Control

Fugro GEOS performed quality control procedures to verify the each ADCP data using a combination of error flagging techniques. The error flagging was based on the internal instrument controls (error bit-checks) and the following information:

- Percent Good
- Speed Spikes
- Limited Range
- Ancillary Data

All data with percent good return below 75% were error flagged. Current speeds that had a significant change in speed from one time-step to the next were considered speed spikes. These were visually identified and error flagged. The raw current speeds were also limited to the range of 0 – 3 m/s. The ancillary data (e.g. battery signal, heading, pitch and roll) were scanned in order to assess deviations in the internal power signal and any movements of the instrument.

After applying the above filters, the data were plotted and visually scanned for any extreme events and extraneous speed spikes. These are carefully analyzed in conjunction with the above mentioned parameters to determine if the current speeds are a natural event or anthropogenically induced.

MATLAB binary data is provided for each of these separate quality controlled datasets with filenames containing the NDBC station number. Each file contains a self explanatory structure with all parameters in SI units.

We have noticed that numerous errors and irregularities in the NTL header metadata are evident. Some obvious errors include the water depth variations for fixed platform, the sign convention for longitude, and incorrect ADCP type etc. The most critical deficiency in the metadata is the frequent discrepancy between two values of transducer depth from the NTL header and the RDI binary fixed leader. Both values are often set manually by the data originators but the latter value was often derived from a pressure sensor.

The frequent discrepancy between two values of transducer depth from the NTL header and the RDI binary fixed leader persisted into phase two. Both values are often set manually by the data originators with the latter sometimes derived from a pressure sensor. Following the phase one procedure, the generally more reliable transducer depth from the NTL header was used to compute a fixed depth array for all files. Note that this value was not always more reliable so both are included in the binary data provided with this report. To accommodate temporal variations in transducer depth, distance to first bin, bin length and number of bins, separate data sets were generated whenever the calculated time series of the depth to bin one or bin two varied by more than 4m from a mean value. The distinct data sets created by this process are indicated by distinct data set identification numbers.

3.2 Historical mooring data

Historical BOEMRE mooring data were also used in this study. The selected ones are shown in Table 3-5 and Figure 3-5. More detail regarding the data sets are documented in BOEMRE reports MMS 2003-049 and MMS 2006-074. The quality controlled data were provided by SAIC through BOEMRE.

Table 3-5 BOEMRE Historical Mooring Stations Used in This Study

Station ID	Longitude (°W)	Latitude (°N)	Water Depth (m)
I1	89.79	27.29	1998
I2	89.97	27.23	1998
I3	89.81	27.12	2175
I4	90.03	27.24	1957
L4	91.13	25.92	3350

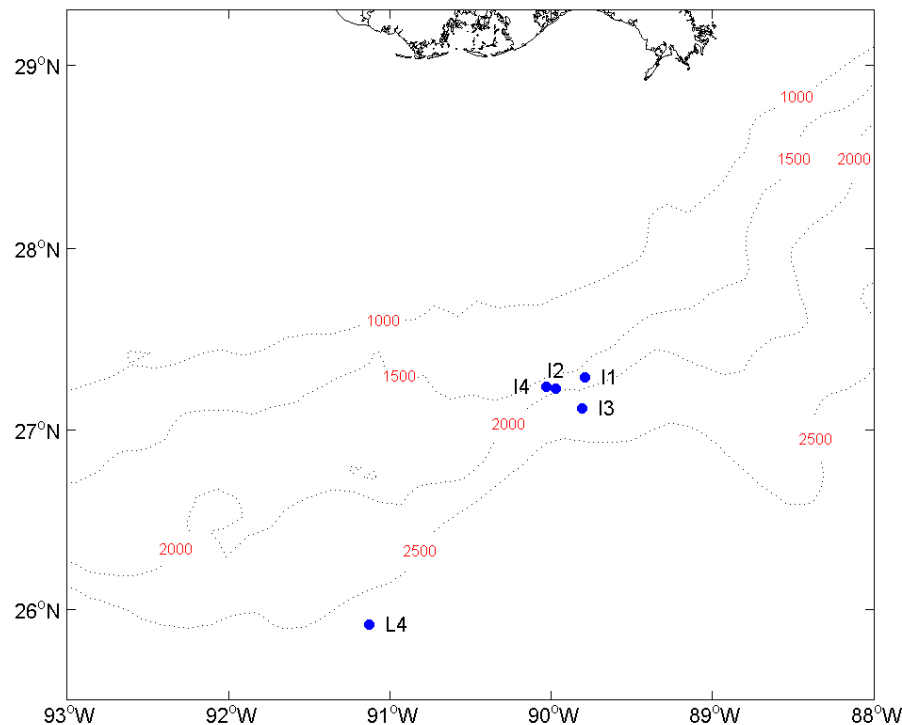


Figure 3-5 BOEMRE Historical Mooring Stations Used in this Study

3.3 PROFS model data

The following three types of PROFS model data were used in this study:

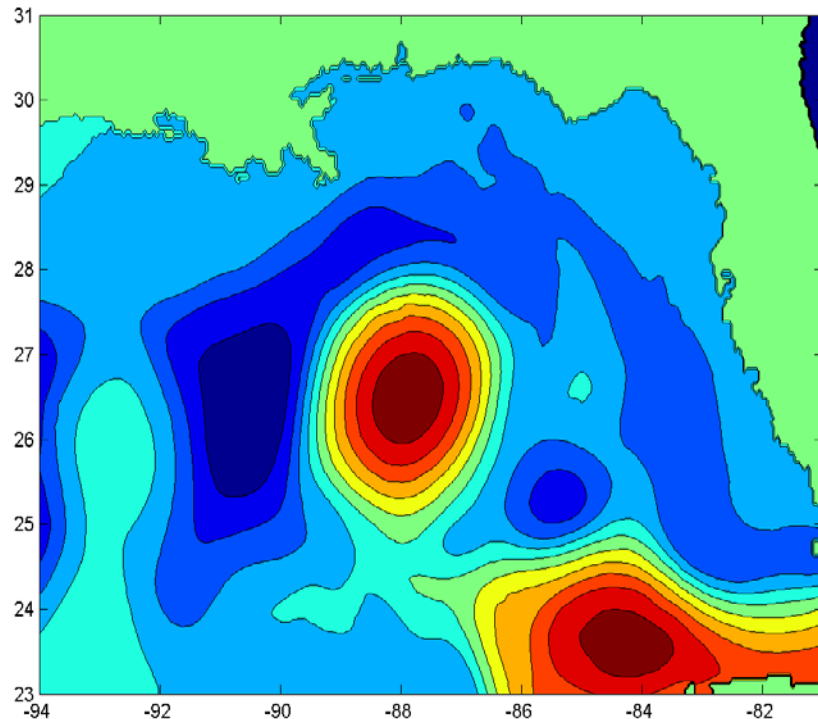


Figure 3-6 Sea surface elevation on 10 October 2007. The region is where daily data were generated for this project.

- 1) Daily three-dimensional ocean data (currents, temperature and salinity etc.) data for the northern Gulf of Mexico from 14 April 2001 to 8 November 2007. Figure 3-6 shows the domain daily data were generated. The data files are in netcdf format.
- 2) Three-hourly time series from 1993 to 2009 of the following parameters at the 464 stations (Table 3-6) were generated for this project. The data files are in IEEE binary format and matlab binary format. The following parameters are included:
 - uwn = west-east kinematic wind stress (m/s)²
 - vwn = south-north kinematic wind stress (m/s)²
 - Equation for computing wind stress from wind speed, including the functional dependence of the drag coefficient on wind speed
 - en: free-surface elevation (m)
 - uan: depth-averaged west-east vel (m/s)
 - van: depth-averaged south-north vel (m/s)
 - unz: west-east vel (m/s); i.e. z-profile of u
 - vnz: south-north vel (m/s); i.e. z-profile of v
 - tnz: potential temperature (DegC); i.e. z-profile of t
 - snz: salinity (psu); i.e. z-profile of s
 - knz: vertical eddy viscosity (m²/s); i.e. z-profile of km
 - wnz: vertical velocity (m/s); i.e. z-profile of w

Table 3-6 PROFS Model Stations

No	Station Name	Longitude (°W)	Latitude (°N)	Water Depth (m)	No	Station Name	Longitude (°W)	Latitude (°N)	Water Depth (m)
1	CBRCM	87.4070	29.3758	541	233	MOD_017E	91.9678	27.1506	1463
2	DSC-A1-1	88.4316	29.2623	131	234	MOD_018E	93.2029	26.7289	1448
3	DSC-A2-2	88.3766	29.0874	607	235	MOD_019E	93.6379	26.6293	1427
4	DSC-A3-1	88.2924	28.8111	1324	236	MOD_020E	94.7242	26.6880	1440
5	DSC-B1-2	87.8813	29.3990	146	237	MOD_021E	94.8869	26.7256	1521
6	DSC-B2-2	87.8226	29.2219	711	238	MOD_022E	95.5168	26.4753	1505
7	DSC-B3-1	87.7786	29.0838	1384	239	MOD_023E	95.4813	25.9885	1616
8	DSC-C1-2	87.3775	29.6237	185	240	MOD_024E	95.7871	25.2535	1568
9	DSC-C2-2	87.1954	29.4304	517	241	MOD_025E	96.1269	24.6476	1765
10	DSC-C3-1	87.2828	28.9975	1136	242	MOD_026E	96.4960	24.0646	1580
11	DSC-D1-2	86.8536	30.0456	103	243	MOD_027E	96.6884	23.4345	1750
12	DSC-D2-2	86.8339	29.3728	511	244	MOD_028E	96.8931	22.5617	1715
13	DSC-D9-1	86.8445	29.7200	173	245	MOD_029E	96.6853	21.8839	1815
14	DSC-E1-2	86.2725	29.6784	78	246	MOD_030E	96.2947	21.2497	1826
15	EBRCM	88.1530	29.1410	633	247	MOD_031E	96.1163	20.6818	1768
16	ESE2	83.9249	25.3595	124	248	MOD_032E	95.7756	19.9425	1953
17	F072	79.9734	28.9808	272	249	MOD_033E	95.4527	19.4068	1656
18	HR-GC-1	91.5295	27.7820	550	250	MOD_034E	94.7924	19.2303	1678
19	HR-MC-1	89.7300	28.0984	707	251	MOD_035E	94.4461	19.4805	1413
20	LSE01	96.4363	27.2661	146	252	MOD_036E	93.9362	19.8510	1434
21	LSU13	96.4390	27.3081	132	253	MOD_037E	93.4374	20.2143	1484
22	LTX-04-B	96.4241	27.0936	221	254	MOD_038E	92.6302	20.8068	1566
23	LTX-05-B	96.1040	27.4530	233	255	MOD_039E	92.6168	21.1675	1497
24	LTX-06-B	95.6320	27.6904	309	256	MOD_040E	92.2953	22.0623	1318
25	LTX-07-B	95.0183	27.8297	252	257	MOD_041E	91.5486	22.4868	1279
26	LTX-08-B	94.1066	27.8159	252	258	MOD_042E	90.6841	22.9122	1161
27	LTX-09-B	93.5163	27.8084	173	259	MOD_043E	90.2645	23.1262	1324

28	LTX-10-B	92.6766	27.9291	238	260	MOD_044E	89.4563	23.6524	1344
29	LTX-11-B	91.9696	27.9028	216	261	MOD_045E	88.8026	23.9795	887
30	LTX-12-B	90.4742	27.9099	644	262	MOD_046E	87.9449	24.6059	1487
31	LTX-13-B	90.5079	28.0558	252	263	MOD_047E	86.7715	24.2362	1488
32	LTX-45-B	96.1040	27.4530	233	264	MOD_048E	86.3208	23.3159	1989
33	LTX-46-B	96.1219	27.6505	102	265	MOD_049E	85.8929	22.1248	1536
34	LTX-47-B	96.2643	27.3184	199	266	MOD_050E	86.0020	21.4512	1637
35	LTX-48-B	91.1639	27.9890	185	267	MOD_051E	86.3923	20.2857	1181
36	LTX-49-B	95.7678	27.4365	575	268	MOD_052E	86.9409	19.5172	1624
37	M0A1	84.8689	25.7064	1934	269	MOD_053E	86.9814	19.0159	1818
38	M0C2	84.2397	25.8943	177	270	MOD_054E	87.4847	17.9926	1438
39	M0E2	84.5940	27.4606	162	271	MOD_055E	83.9035	21.9117	974
40	M0E3	84.6777	27.3648	205	272	MOD_056E	84.4664	21.7538	1205
41	M0G1	85.5339	25.6116	3255	273	MOD_057E	85.1723	22.0121	1468
42	M0H2	85.2943	28.3968	189	274	MOD_058E	84.3949	22.7036	1468
43	M0P2	95.1482	26.0077	2036	275	MOD_059E	83.7431	23.0004	1081
44	M0Q1	94.8087	25.8542	3082	276	MOD_060E	82.8059	23.4546	1878
45	M0R1	94.1381	25.4647	3476	277	MOD_061E	81.9708	23.5280	1625
46	M0S1	95.6177	25.3863	1568	278	MOD_062E	81.4450	23.4430	1180
47	M0T1	95.9408	24.5828	2440	279	MOD_001F	83.3521	23.5337	1852
48	MDD3	91.8352	27.9245	163	280	MOD_002F	84.1376	24.6071	1865
49	MEE1	92.0315	27.5059	843	281	MOD_003F	84.6803	25.2570	1934
50	MFF1	92.0444	26.7518	1775	282	MOD_004F	84.8689	25.7064	1934
51	MGG1	92.0384	25.6291	3057	283	MOD_005F	84.9863	26.3148	2009
52	MHH1	91.9359	24.5454	3713	284	MOD_006F	85.2708	27.0906	1990
53	OTEC2-1	87.9031	29.1034	1163	285	MOD_007F	85.6281	27.6243	2161
54	OTECM-1	87.5758	29.1839	1150	286	MOD_008F	86.2875	27.9725	2180
55	W.TX-02	96.0281	26.4463	747	287	MOD_009F	87.1852	28.2842	2061
56	W.TX-A1	95.8984	27.0349	800	288	MOD_010F	87.3278	28.3718	1951
57	W.TX-B1	95.9993	25.9631	673	289	MOD_011F	87.9258	28.7918	1978
58	XA22	82.1321	24.0205	865	290	MOD_012F	88.2501	28.2311	2075
59	XA31	82.2056	23.7630	1536	291	MOD_013F	89.4448	27.4263	1989
60	XB42	80.7033	24.0475	969	292	MOD_014F	90.0463	27.1488	2177
61	Z273	81.3707	24.4758	229	293	MOD_015F	90.5263	26.8353	2023
62	Z287	82.9196	24.4123	220	294	MOD_016F	91.0629	26.7612	1890
63	ZA12	82.1800	24.3800	251	295	MOD_017F	92.0098	26.5221	1954
64	ZB12	81.0719	24.5123	234	296	MOD_018F	93.1596	26.3970	1865
65	ZB22	80.9544	24.4023	324	297	MOD_019F	93.5984	26.2978	1922
66	ZB30	80.7205	24.1753	754	298	MOD_020F	94.6980	26.4273	1888
67	ZB31	80.8198	24.1641	745	299	MOD_021F	94.8468	26.3075	1921
68	ASMM01	89.6925	28.4591	560	300	MOD_022F	95.1568	26.1205	1937
69	ATW-1	89.8125	27.3054	1853	301	MOD_023F	95.3015	25.8253	2152
70	CGN02	89.0251	28.7946	433	302	MOD_024F	95.6085	25.1966	2204
71	DSTO1-1	86.7535	30.0745	82	303	MOD_025F	95.9455	24.7211	2129
72	DSTO2-1	87.1062	29.5033	436	304	MOD_026F	96.2989	23.9160	2033
73	DSTO3-1	86.8012	29.2770	493	305	MOD_027F	96.4865	23.3532	2133
74	E.BRK-M1	94.5551	27.8024	305	306	MOD_028F	96.4823	22.5619	2304
75	EB966	89.7543	28.1968	630	307	MOD_029F	96.4831	21.9836	2188
76	E.BRK-U1	94.5551	27.8024	305	308	MOD_030F	96.1027	21.3560	2115
77	G.CYN1-1	91.5393	27.8293	452	309	MOD_031F	95.9252	20.9085	2067

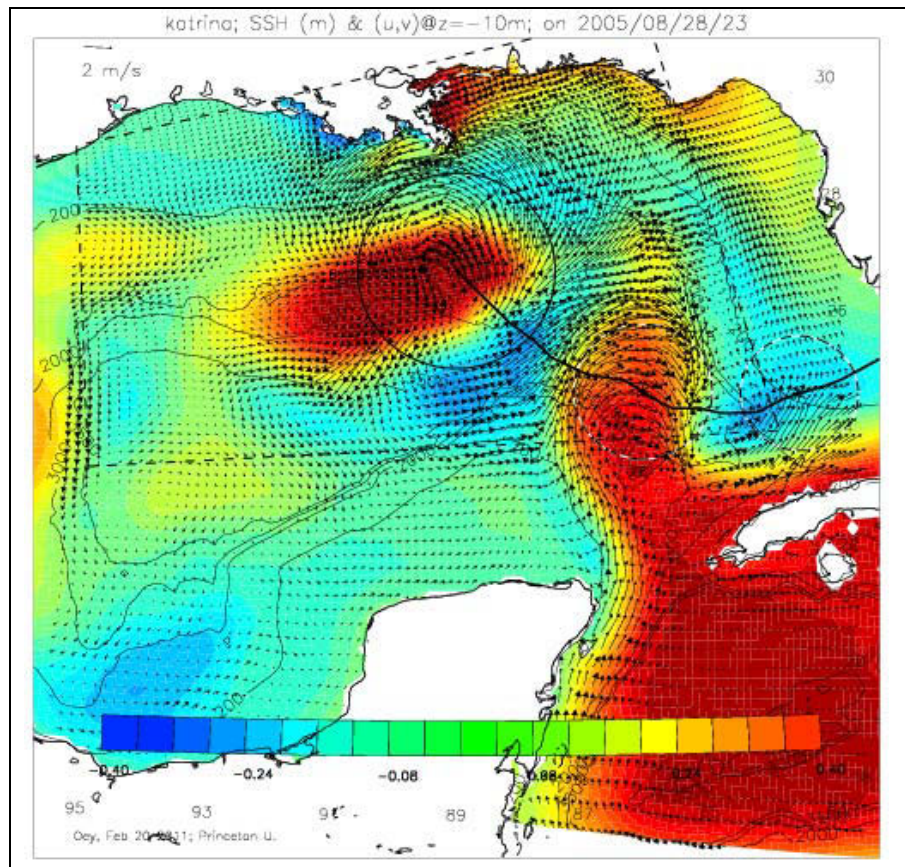
78	G.CYN2-1	91.5295	27.7820	550	310	MOD_032F	95.5929	20.0617	2302
79	GC033-1	90.2196	27.9553	584	311	MOD_033F	95.2739	19.5306	2241
80	GC474-1	90.2556	27.5194	1150	312	MOD_034F	94.9473	19.3772	2116
81	M.CYN-1	88.5757	28.9445	677	313	MOD_035F	94.5905	19.7570	1752
82	MARAT	90.8614	27.8428	596	314	MOD_036F	94.0658	20.3718	1970
83	MC01	89.6311	28.2209	825	315	MOD_037F	93.4171	20.5919	1984
84	MC010	89.3421	28.5806	344	316	MOD_038F	92.7837	20.8125	2197
85	MC217-1	87.9258	28.7918	1978	317	MOD_039F	92.7669	21.2886	2296
86	V.KNL-1	88.2785	29.1586	397	318	MOD_040F	92.2950	22.1688	1976
87	VK786-1	87.8226	29.2219	711	319	MOD_041F	91.6981	22.5879	2569
88	VK786-2	87.7636	29.0368	1525	320	MOD_042F	90.6875	23.0127	1720
89	PRE-I1	89.8008	27.2478	1998	321	MOD_043F	90.4061	23.1213	1668
90	PRE-I2	89.9173	27.1693	2108	322	MOD_044F	89.4624	23.7478	2022
91	PRE-I3	89.7771	27.1311	2203	323	MOD_045F	88.9436	24.0636	1988
92	PRE-J1	90.1986	27.2434	1539	324	MOD_046F	87.8388	24.7967	2177
93	MOD_001C	83.3413	24.3652	425	325	MOD_047F	86.5399	24.3570	2110
94	MOD_002C	83.8284	24.7505	407	326	MOD_048F	86.2081	23.4353	2769
95	MOD_003C	84.2296	25.2178	396	327	MOD_049F	85.7721	22.1281	1782
96	MOD_004C	84.4191	25.6788	407	328	MOD_050F	85.7586	21.4526	1962
97	MOD_005C	84.5943	26.5545	421	329	MOD_051F	86.2737	20.1256	2147
98	MOD_006C	85.0089	27.3757	513	330	MOD_052F	86.8136	19.5093	2153
99	MOD_007C	85.4053	28.0283	511	331	MOD_053F	86.9973	18.8440	2281
100	MOD_008C	86.0561	28.3510	490	332	MOD_054F	87.3552	17.9774	2088
101	MOD_009C	86.6682	28.8721	477	333	MOD_055F	83.8985	21.7685	1460
102	MOD_010C	87.1954	29.4304	517	334	MOD_056F	84.4630	21.6112	1789
103	MOD_011C	87.9321	29.1949	686	335	MOD_057F	85.2904	22.0090	1915
104	MOD_012C	88.6901	28.9181	608	336	MOD_058F	84.5169	22.8251	2306
105	MOD_013C	89.6804	28.4124	585	337	MOD_059F	83.8635	23.1198	1975
106	MOD_014C	90.1047	28.0280	541	338	MOD_060F	82.8189	23.5801	1691
107	MOD_015C	90.8614	27.8428	596	339	MOD_061F	81.9995	23.7828	1519
108	MOD_016C	91.3966	27.8034	551	340	MOD_062F	82.5036	23.6083	1693
109	MOD_017C	92.2134	27.7235	523	341	MOD_001G	83.3400	23.4104	2074
110	MOD_018C	93.1793	27.5393	506	342	MOD_002G	84.2467	24.5947	2561
111	MOD_019C	93.7821	27.6426	513	343	MOD_003G	84.6494	25.0630	2457
112	MOD_020C	94.8499	27.7283	509	344	MOD_004G	84.8369	25.5240	2445
113	MOD_021C	95.3065	27.6408	657	345	MOD_005G	84.9863	26.3148	2009
114	MOD_022C	96.0720	27.0691	547	346	MOD_006G	85.2708	27.0906	1990
115	MOD_023C	96.1987	26.3344	482	347	MOD_007G	85.6101	27.5553	2417
116	MOD_024C	96.1651	25.6685	552	348	MOD_008G	86.1626	27.9323	2359
117	MOD_025C	96.5147	24.9085	532	349	MOD_009G	87.1693	28.2272	2477
118	MOD_026C	96.9051	24.2077	763	350	MOD_010G	87.4233	28.2920	2518
119	MOD_027C	97.6057	23.3479	0	351	MOD_011G	87.7614	28.2196	2470
120	MOD_028C	97.6045	22.4681	507	352	MOD_012G	88.0488	27.4261	2507
121	MOD_029C	97.3455	21.7851	501	353	MOD_013G	89.3584	27.0111	2505
122	MOD_030C	96.9016	21.0361	530	354	MOD_014G	90.0007	26.9120	2521
123	MOD_031C	96.5107	20.2138	554	355	MOD_015G	90.4947	26.6538	2496
124	MOD_032C	96.1542	19.5716	474	356	MOD_016G	90.9846	26.2711	2446
125	MOD_033C	95.3217	18.8502	477	357	MOD_017G	91.9346	25.9708	2463
126	MOD_034C	94.6657	18.7992	434	358	MOD_018G	93.1318	26.1646	2278
127	MOD_035C	94.3323	18.9145	501	359	MOD_019G	93.5856	26.1826	2156

128	MOD_036C	93.3527	19.2605	624	360	MOD_020G	94.6776	26.2089	2628
129	MOD_037C	92.7035	19.6328	496	361	MOD_021G	94.6726	26.1528	2768
130	MOD_038C	92.0593	20.1376	381	362	MOD_022G	94.9800	25.9606	2691
131	MOD_039C	92.1644	21.0346	430	363	MOD_023G	95.1271	25.7161	2734
132	MOD_040C	92.1469	21.7328	428	364	MOD_024G	95.4353	25.2036	2628
133	MOD_041C	91.3992	22.2770	422	365	MOD_025G	95.7654	24.7263	2684
134	MOD_042C	90.5352	22.7106	523	366	MOD_026G	95.9220	23.8441	2637
135	MOD_043C	89.9790	23.0350	468	367	MOD_027G	96.0969	23.0144	2474
136	MOD_044C	89.4385	23.3592	395	368	MOD_028G	96.0945	22.5621	2569
137	MOD_045C	88.5298	23.9021	350	369	MOD_029G	96.0952	22.1798	2620
138	MOD_046C	88.0341	24.2266	433	370	MOD_030G	95.7316	21.4589	2491
139	MOD_047C	87.0935	23.6992	574	371	MOD_031G	95.5606	21.0147	2510
140	MOD_048C	86.7970	23.0620	521	372	MOD_032G	95.4127	20.1797	2600
141	MOD_049C	86.3823	22.1123	480	373	MOD_033G	95.2520	19.9206	2592
142	MOD_050C	86.3715	21.4494	518	374	MOD_034G	94.9214	19.7750	2552
143	MOD_051C	86.7591	20.5989	402	375	MOD_035G	94.5614	20.2690	2555
144	MOD_052C	87.2970	20.0145	475	376	MOD_036G	94.0490	20.7382	2510
145	MOD_053C	87.5133	18.8889	607	377	MOD_037G	93.5596	20.9598	2414
146	MOD_054C	87.9004	17.8580	482	378	MOD_038G	93.0840	21.0631	2588
147	MOD_055C	83.6922	22.2009	0	379	MOD_039G	92.9213	21.2925	2803
148	MOD_056C	84.4664	21.7538	1205	380	MOD_040G	92.4471	22.1691	2725
149	MOD_057C	84.7057	22.0258	578	381	MOD_041G	91.8469	22.5860	3289
150	MOD_058C	84.2739	22.5797	802	382	MOD_042G	90.8309	23.0086	2260
151	MOD_059C	83.6233	22.8787	654	383	MOD_043G	90.4102	23.2200	2265
152	MOD_060C	82.7816	23.1989	1315	384	MOD_044G	89.5994	23.7401	2326
153	MOD_061C	81.9437	23.2658	855	385	MOD_045G	88.8184	24.1655	2009
154	MOD_062C	81.4172	23.1731	552	386	MOD_046G	87.8494	24.8846	2620
155	MOD_001D	83.2977	24.0223	970	387	MOD_047G	86.5512	24.4548	2451
156	MOD_002D	83.9208	24.6322	901	388	MOD_048G	86.1064	23.6635	3275
157	MOD_003D	84.4621	25.2864	856	389	MOD_049G	85.6521	22.1315	1920
158	MOD_004D	84.6515	25.7385	856	390	MOD_050G	85.5174	21.4544	2065
159	MOD_005D	84.7714	26.3504	891	391	MOD_051G	86.4060	19.9730	2260
160	MOD_006D	85.0766	27.2064	814	392	MOD_052G	86.6869	19.5014	3001
161	MOD_007D	85.5773	27.8499	838	393	MOD_053G	86.8537	19.0059	2719
162	MOD_008D	86.2151	28.1205	893	394	MOD_054G	87.2266	17.9620	2920
163	MOD_009D	86.9980	28.4456	943	395	MOD_055G	83.8942	21.6234	2151
164	MOD_010D	87.3298	29.1431	1113	396	MOD_056G	84.4601	21.4665	2568
165	MOD_011D	88.0134	29.0769	1119	397	MOD_057G	85.4090	22.0058	2094
166	MOD_012D	88.5345	28.8062	1066	398	MOD_058G	84.6396	22.9440	2398
167	MOD_013D	89.4710	28.0954	1054	399	MOD_059G	83.9845	23.2365	2587
168	MOD_014D	90.0343	27.7225	1011	400	MOD_060G	82.8323	23.7037	1494
169	MOD_015D	90.8188	27.6429	1019	401	MOD_061G	82.0297	24.0311	855
170	MOD_016D	91.3471	27.5584	988	402	MOD_062G	82.5315	23.8565	1157
171	MOD_017D	92.0133	27.4066	988	403	MOD_001H	83.3282	23.2853	1717
172	MOD_018D	93.2692	27.1901	971	404	MOD_002H	84.3561	24.5823	3135
173	MOD_019D	93.8733	27.2654	939	405	MOD_003H	84.7747	25.1465	2983
174	MOD_020D	94.6584	27.4536	923	406	MOD_004H	84.9625	25.6000	2988
175	MOD_021D	95.2823	27.4356	1017	407	MOD_005H	85.2032	26.2791	3233
176	MOD_022D	95.7236	26.9545	1003	408	MOD_006H	85.3778	27.0703	2927
177	MOD_023D	95.8340	26.1377	1000	409	MOD_007H	85.6992	27.4638	3111

178	MOD_024D	95.9681	25.3102	1021	410	MOD_008H	86.2532	27.8454	3061
179	MOD_025D	96.3168	24.7118	1080	411	MOD_009H	87.0411	27.7498	2971
180	MOD_026D	96.6970	24.1366	1133	412	MOD_010H	87.1421	27.1879	2902
181	MOD_027D	97.1131	23.0961	1054	413	MOD_011H	87.3437	26.4236	2946
182	MOD_028D	97.1115	22.4683	1158	414	MOD_012H	87.7839	26.1286	2947
183	MOD_029D	96.8942	21.8848	1300	415	MOD_013H	89.2146	26.2260	2972
184	MOD_030D	96.4915	21.1424	1238	416	MOD_014H	89.9111	26.4081	2997
185	MOD_031D	96.3084	20.5690	1034	417	MOD_015H	90.5770	26.3213	2944
186	MOD_032D	95.9608	19.8226	1233	418	MOD_016H	90.9561	26.0771	3200
187	MOD_033D	95.4612	19.2727	1171	419	MOD_017H	91.9028	25.7096	3034
188	MOD_034D	94.6407	19.0805	970	420	MOD_018H	93.1110	25.9843	3056
189	MOD_035D	94.4675	19.2073	1128	421	MOD_019H	93.5730	26.0649	2895
190	MOD_036D	93.6401	19.5619	887	422	MOD_020H	94.6577	25.9813	3070
191	MOD_037D	92.9887	19.9256	1040	423	MOD_021H	94.5040	26.0504	2938
192	MOD_038D	92.4831	20.6767	1103	424	MOD_022H	94.8087	25.8542	3082
193	MOD_039D	92.4639	21.1633	991	425	MOD_023H	95.1117	25.4718	3217
194	MOD_040D	92.2959	21.9545	903	426	MOD_024H	95.2612	25.1459	3238
195	MOD_041D	91.6955	22.3812	1156	427	MOD_025H	95.5828	24.5926	3176
196	MOD_042D	90.6812	22.8105	801	428	MOD_026H	95.5571	23.6926	3082
197	MOD_043D	90.1234	23.1311	883	429	MOD_027H	95.5462	23.0185	3026
198	MOD_044D	89.4503	23.5559	894	430	MOD_028H	95.5438	22.5631	3045
199	MOD_045D	88.6698	23.9887	614	431	MOD_029H	95.5435	22.3729	2993
200	MOD_046D	88.0527	24.4126	933	432	MOD_030H	95.3684	21.8751	2990
201	MOD_047D	86.8640	23.9239	994	433	MOD_031H	95.2037	21.2319	3035
202	MOD_048D	86.5653	23.3007	1021	434	MOD_032H	95.0444	20.7709	3098
203	MOD_049D	86.1366	22.1185	1040	435	MOD_033H	94.8888	20.4062	3053
204	MOD_050D	86.2478	21.4500	780	436	MOD_034H	94.8888	20.4062	3053
205	MOD_051D	86.5117	20.4425	1107	437	MOD_035H	94.7157	20.5216	3081
206	MOD_052D	87.0480	19.8454	1091	438	MOD_036H	94.3704	20.8678	3032
207	MOD_053D	87.2381	19.0365	1133	439	MOD_037H	93.7049	21.4235	2996
208	MOD_054D	87.6395	17.8248	1089	440	MOD_038H	93.3846	21.5288	2992
209	MOD_055D	83.7974	22.0567	772	441	MOD_039H	93.2274	21.5259	2944
210	MOD_056D	84.4664	21.7538	1205	442	MOD_040H	92.4471	22.2736	3245
211	MOD_057D	84.9379	22.0191	781	443	MOD_041H	91.8484	22.6872	3685
212	MOD_058D	84.3799	22.4428	687	444	MOD_042H	90.8344	23.1075	3147
213	MOD_059D	83.7332	22.8718	720	445	MOD_043H	90.5566	23.3120	3423
214	MOD_060D	82.7935	23.3275	1797	446	MOD_044H	89.6057	23.8340	3234
215	MOD_061D	81.9570	23.3978	1260	447	MOD_045H	88.8268	24.2571	2826
216	MOD_062D	81.4310	23.3090	823	448	MOD_046H	87.6102	24.9978	3092
217	MOD_001E	83.2575	23.6653	1603	449	MOD_047H	86.4428	24.5631	3305
218	MOD_002E	84.0289	24.6197	1349	450	MOD_048H	85.9869	23.6724	3478
219	MOD_003E	84.5709	25.2717	1287	451	MOD_049H	85.5325	22.1350	2017
220	MOD_004E	84.7599	25.7224	1287	452	MOD_050H	85.2787	21.4565	2541
221	MOD_005E	84.8786	26.3325	1341	453	MOD_051H	86.1496	20.1208	3052
222	MOD_006E	85.1641	27.1108	1327	454	MOD_052H	86.7120	19.1667	3619
223	MOD_007E	85.5406	27.7150	1197	455	MOD_053H	86.9058	18.4800	3094
224	MOD_008E	86.1976	28.0583	1161	456	MOD_054H	86.9714	17.9316	3883
225	MOD_009E	87.0911	28.3650	1269	457	MOD_055H	83.8907	21.4762	2557
226	MOD_010E	87.2333	28.4514	1290	458	MOD_056H	84.4580	21.3198	3180
227	MOD_011E	87.9698	28.9368	1593	459	MOD_057H	85.5282	22.0027	2081

228	MOD_012E	88.3781	28.6892	1592	460	MOD_058H	84.8865	23.1742	2062
229	MOD_013E	89.4822	27.5951	1577	461	MOD_059H	84.4121	24.1410	2958
230	MOD_014E	90.0694	27.2639	1649	462	MOD_060H	82.8459	23.8256	1253
231	MOD_015E	90.7334	27.2178	1400	463	MOD_061H	82.0615	24.2731	376
232	MOD_016E	91.1733	27.3730	1492	464	MOD_062H	82.5608	24.0977	583

- 3) Hourly three-dimensional ocean data (currents, temperature and salinity etc.) for the northern Gulf of Mexico region during hurricanes Katrina and Rita (see Figure 3-7 and Figure 3-8). The data files are in netcdf format



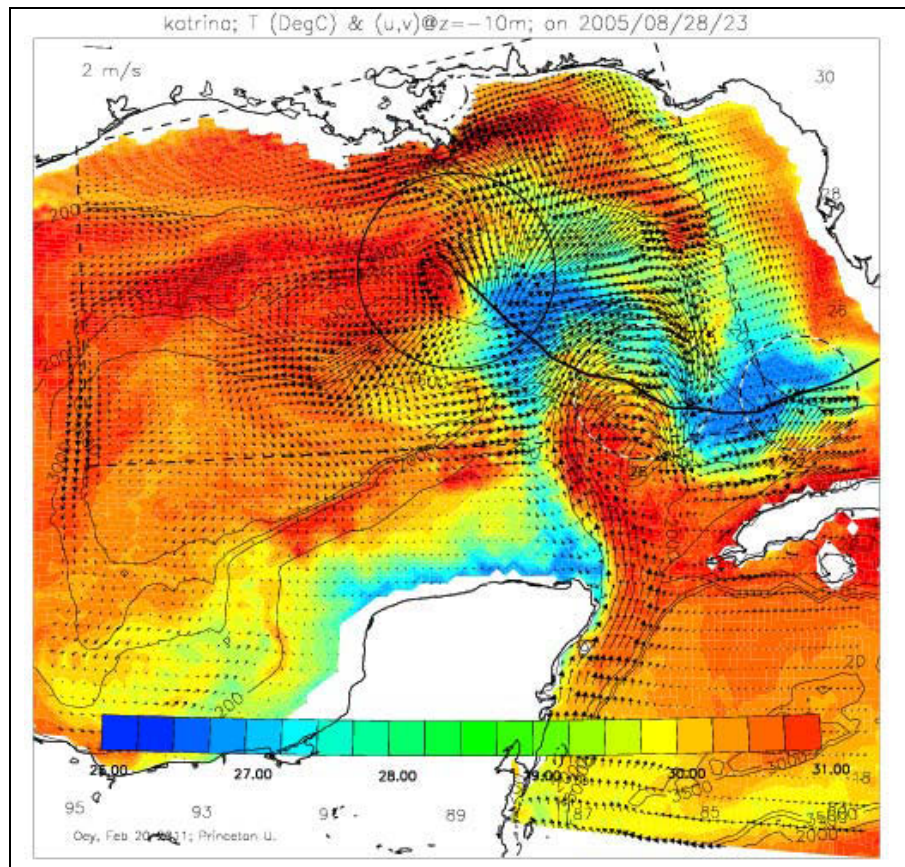
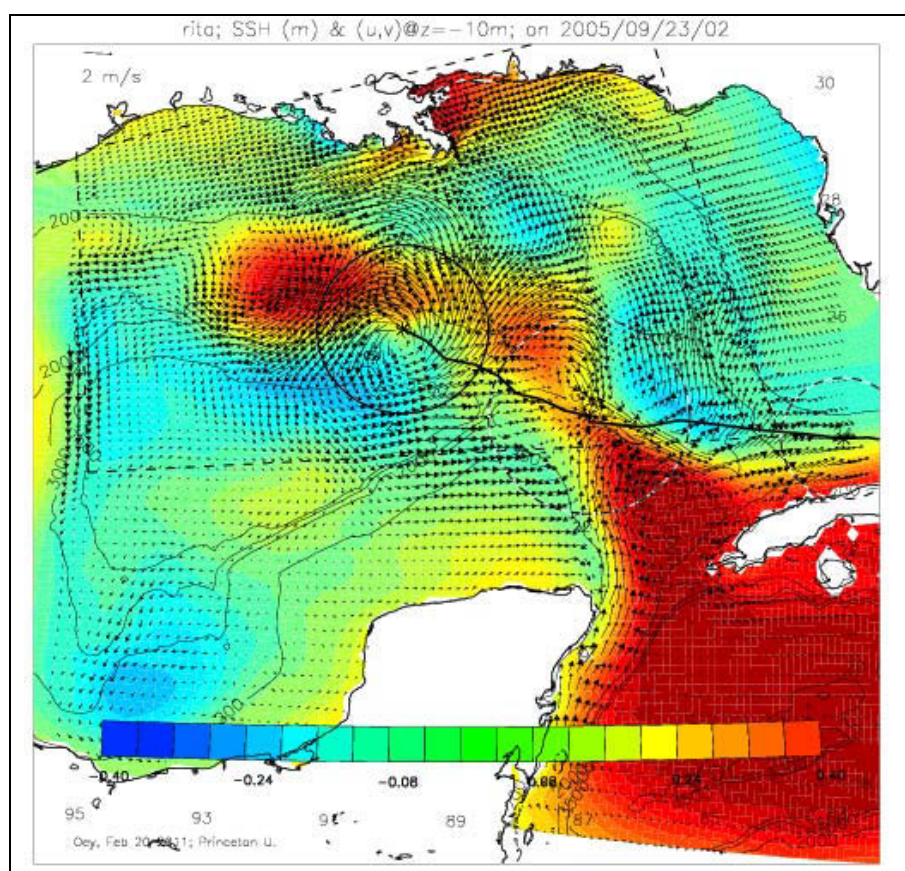


Figure 3-7 SSH + currents at surface (top) and temperature and currents at $z=-10m$ below the surface for Hurricane Katrina on Aug/28/2005. Dashed region is where data were generated for this project.



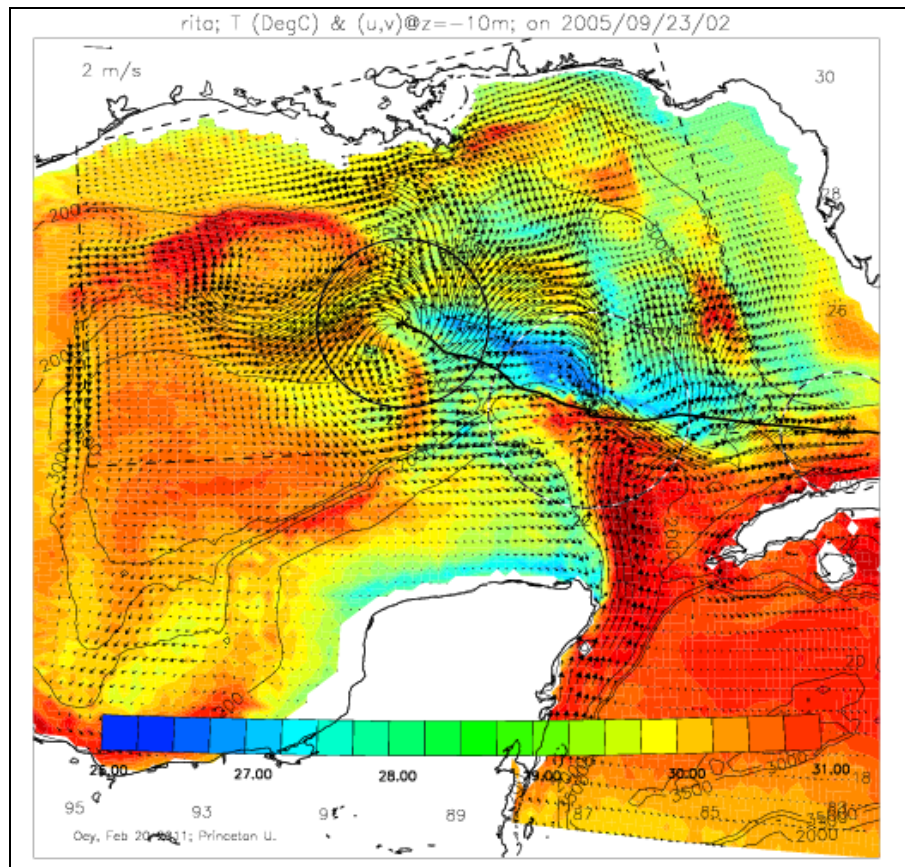


Figure 3-8 SSH + currents at surface (top) and temperature and currents at $z=-10m$ below the surface for Hurricane Katrina on Sep/23/2005. Dashed region is where data were generated for this project.

4. SUBSURFACE ELEVATED CURRENT EVENTS

4.1 Subsurface Elevated Current Events Screening

We have done extensive subsurface, high-speed current jets screening study in the deepwater region of the Gulf of Mexico using NTL data up to April 2006 (Jeans and Fan, 2007). We have concluded that automated screening procedure based on predefined criteria is not suitable. The predefined automated criteria resulted in a large number of clearly erroneous jet events and allowed the potential for missing submerged events at times of simultaneous strong surface flows. Instead, manual event selection based on examination of colour contour plots of current speed through depth and time was used. In this study, the same approach was adopted. Subsurface elevated current events screening was conducted by visual inspection of the colour flooded contour plots. Only data sets with data in upper 1000m were plotted and examined. As examples, Figure 4-1 to Figure 4-120 are the monthly speed contour for NTL stations 42364 and 42370, which have been used to derive long term and event current profile characteristics for Zone 1 and 2.

The screening study further confirmed the conclusions drawn by (Jeans and Fan, 2007) and Fan et al. (2007) that two modes of subsurface elevated current events exist in the Gulf of Mexico: (1) submerged speed peaks with inertial period and (2) events isolated in time with no clear periodicity. The latter can be divided further as shallow jet events (between 150m to 600m) and deep jet events (deeper than 600m). **Most of the events are within the top 500m, only a few weak deep (deeper than 500m) events have been identified.**

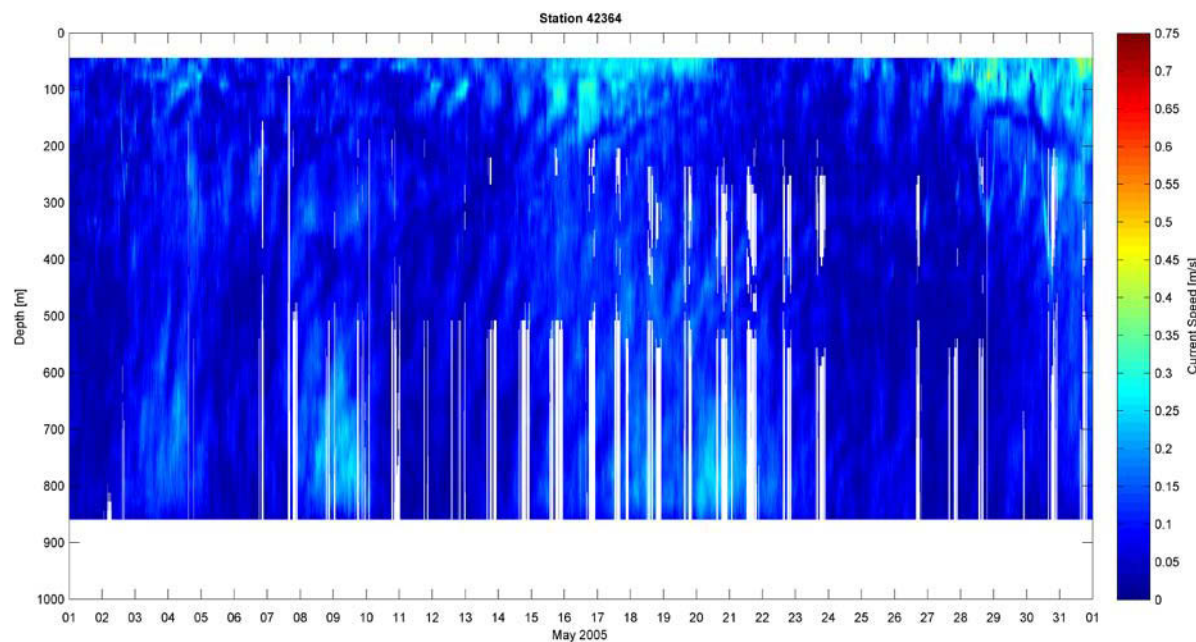


Figure 4-1 Current Speed Contour at NTL Station 42364 – May 2005

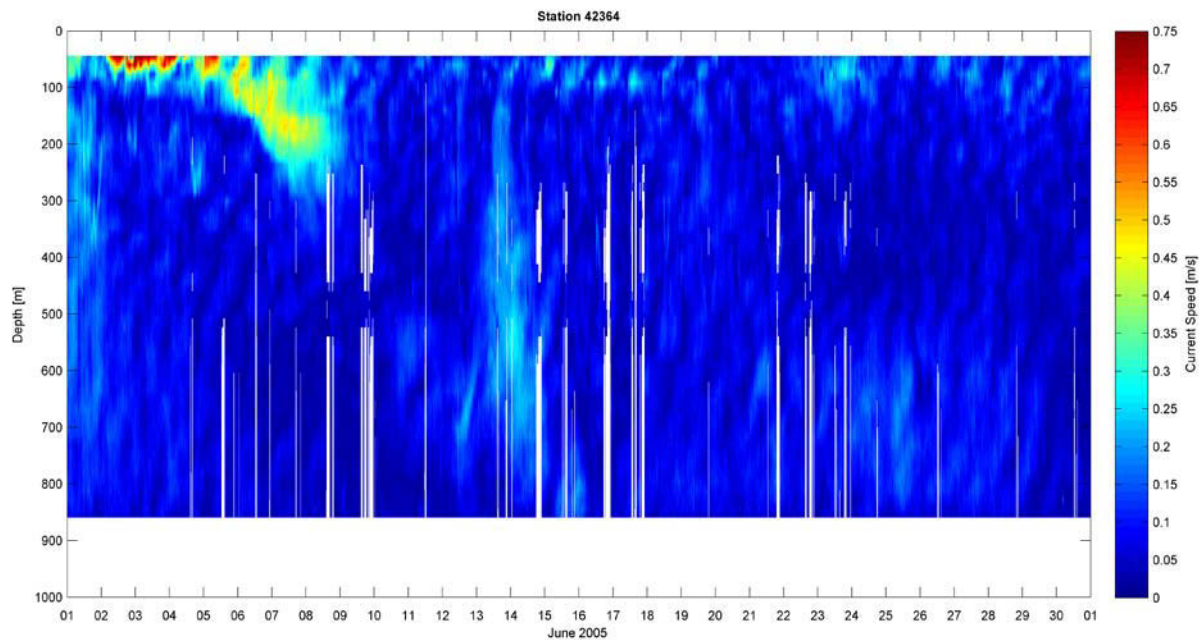


Figure 4-2 Current Speed Contour at NTL Station 42364 – June 2005

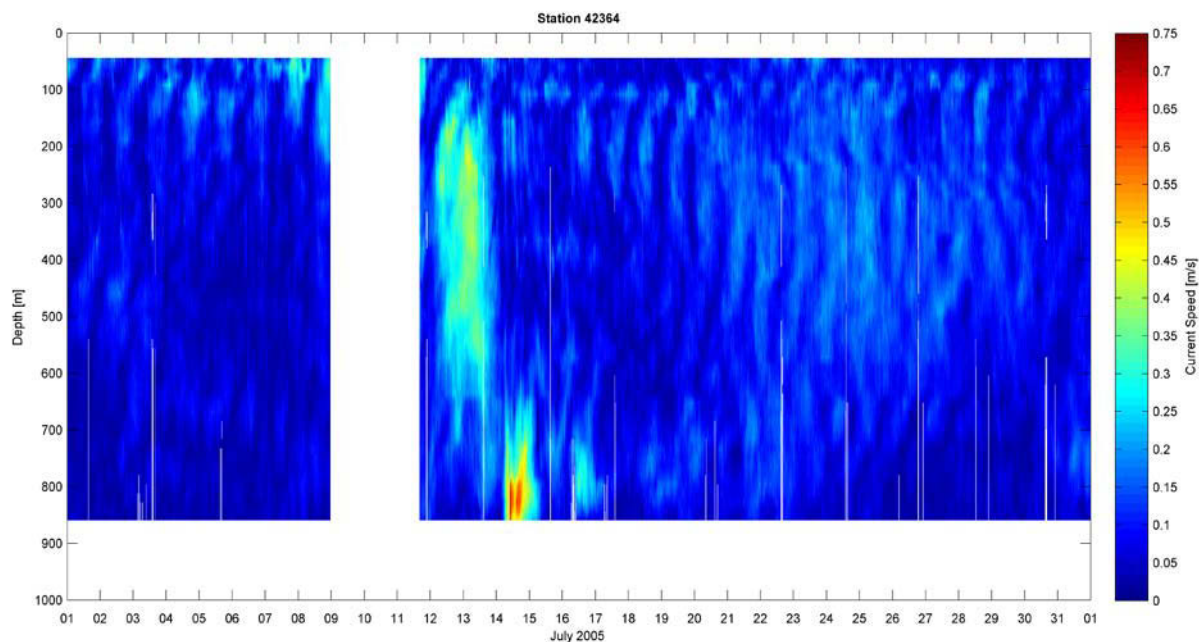


Figure 4-3 Current Speed Contour at NTL Station 42364 – July 2005

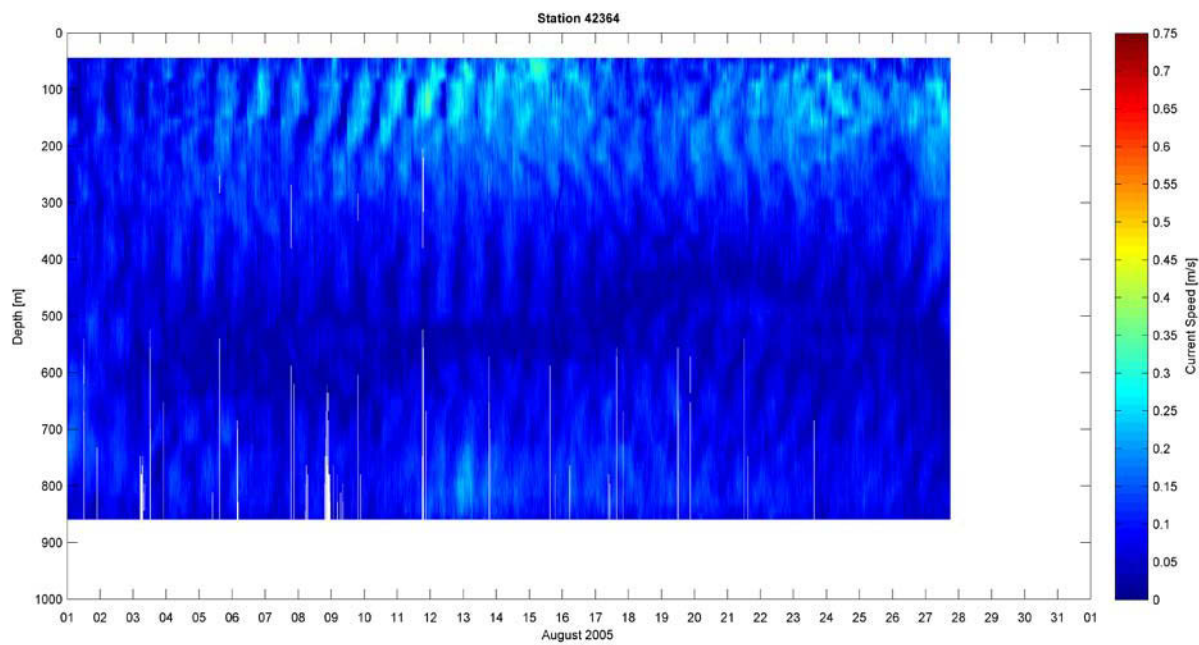


Figure 4-4 Current Speed Contour at NTL Station 42364 – August 2005

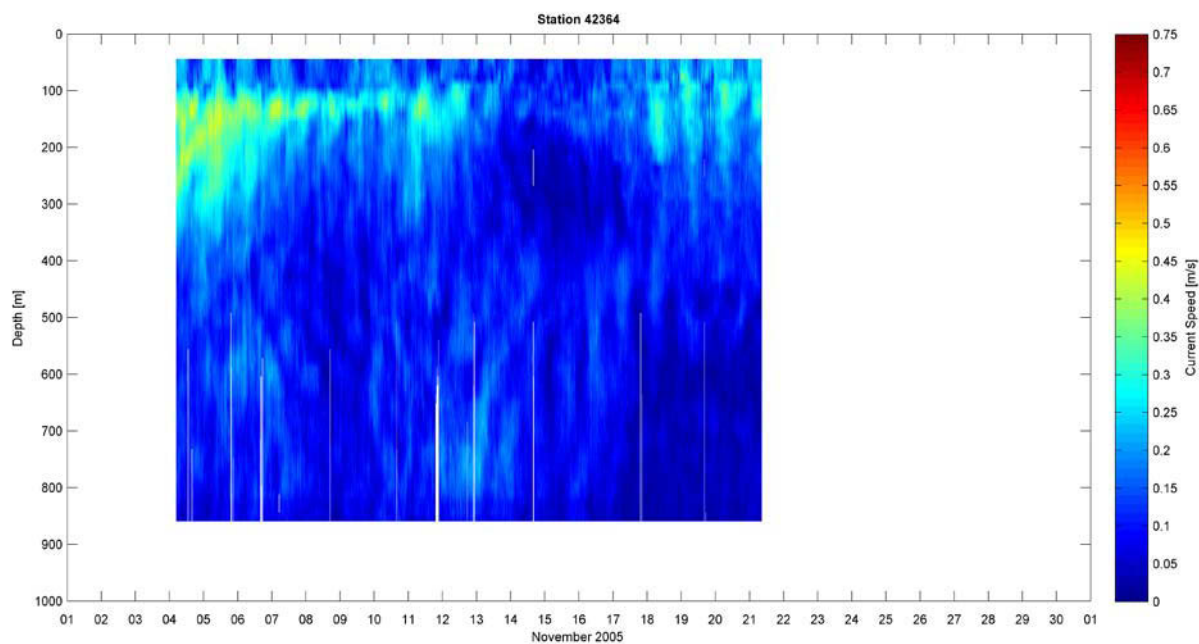


Figure 4-5 Current Speed Contour at NTL Station 42364 – November 2005

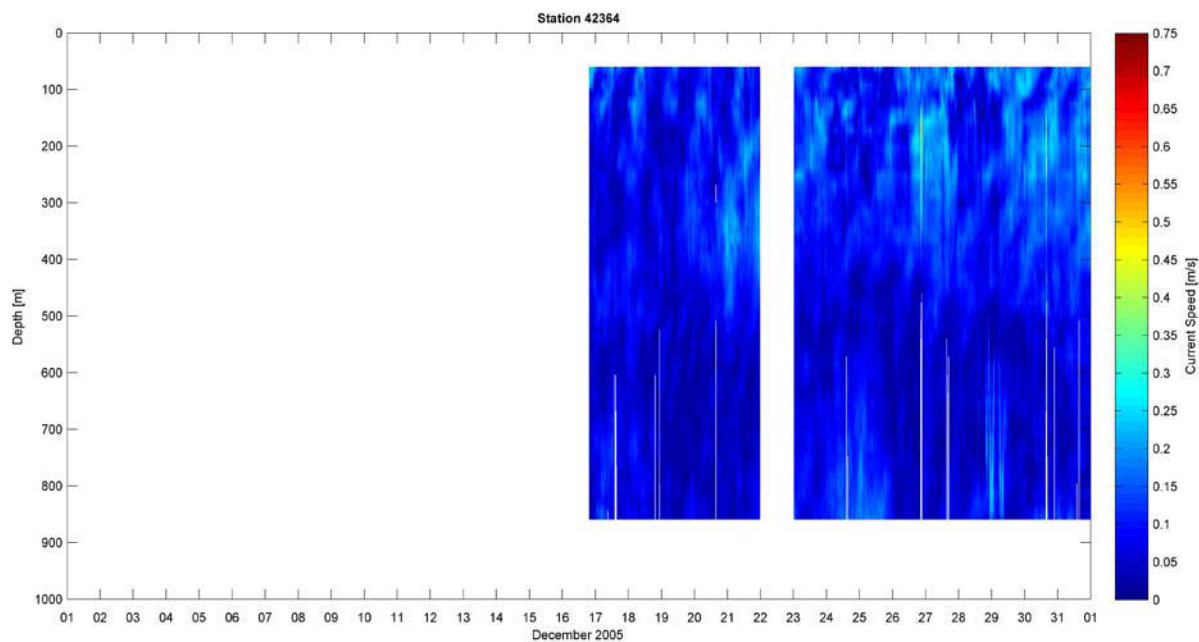


Figure 4-6 Current Speed Contour at NTL Station 42364 – December 2005

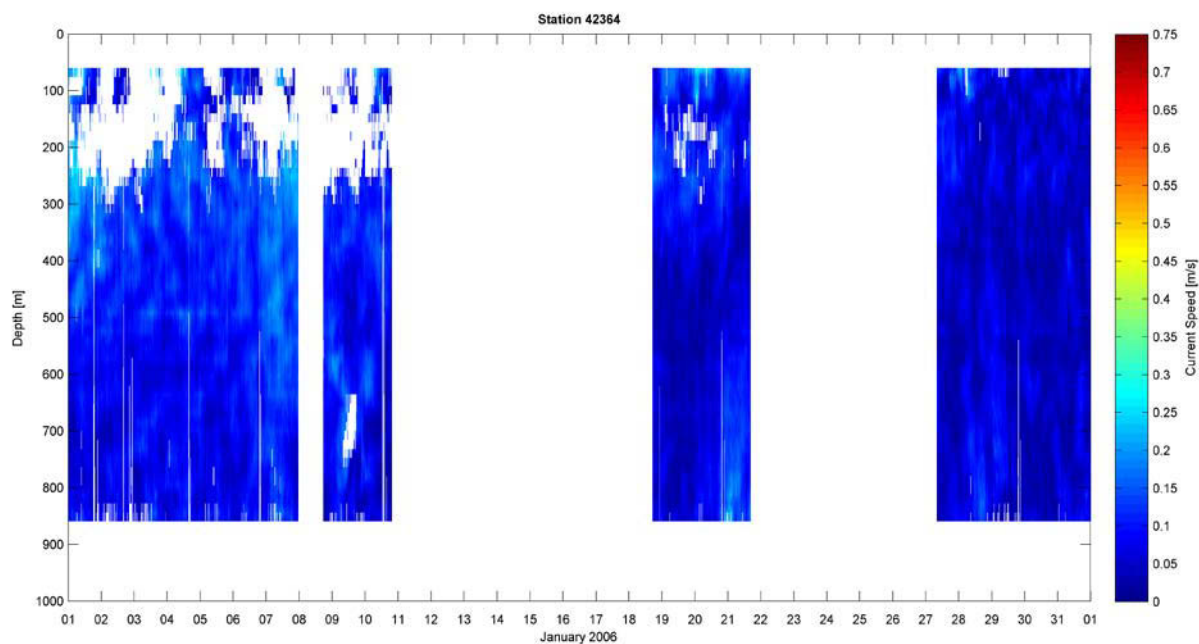


Figure 4-7 Current Speed Contour at NTL Station 42364 – January 2006

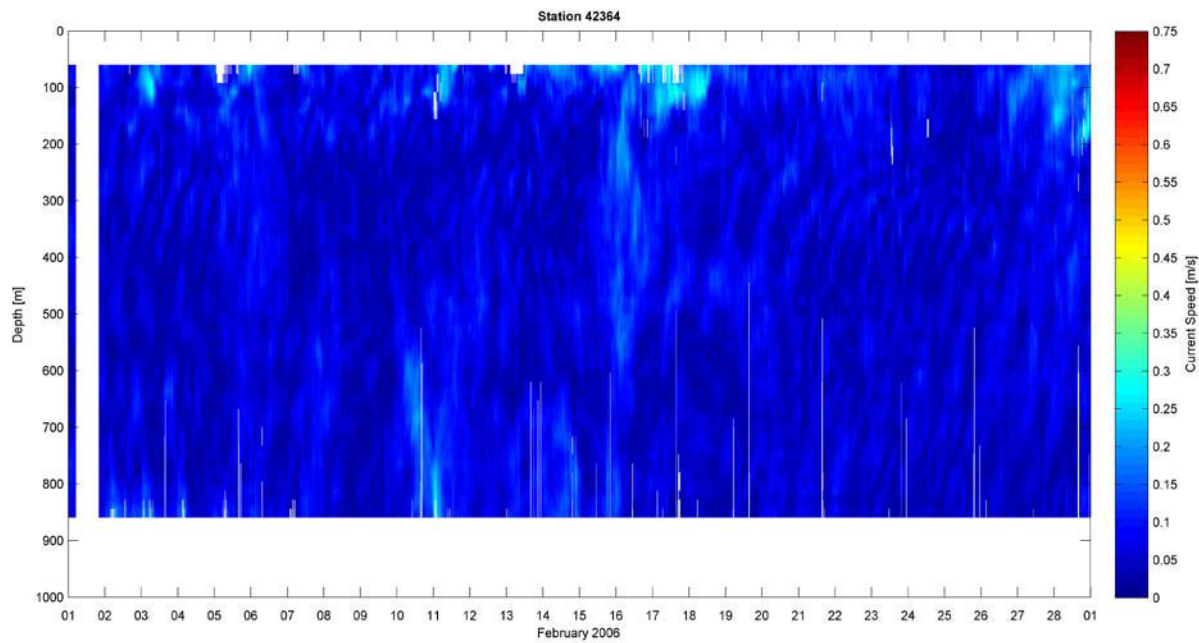


Figure 4-8 Current Speed Contour at NTL Station 42364 – February 2006

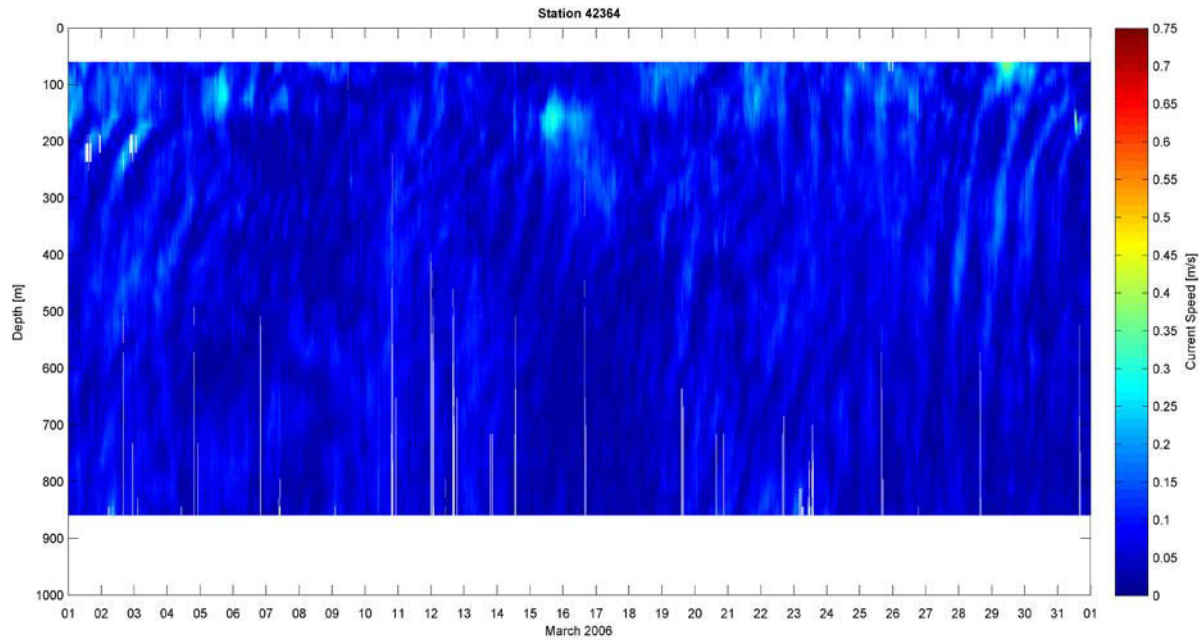


Figure 4-9 Current Speed Contour at NTL Station 42364 – March 2006

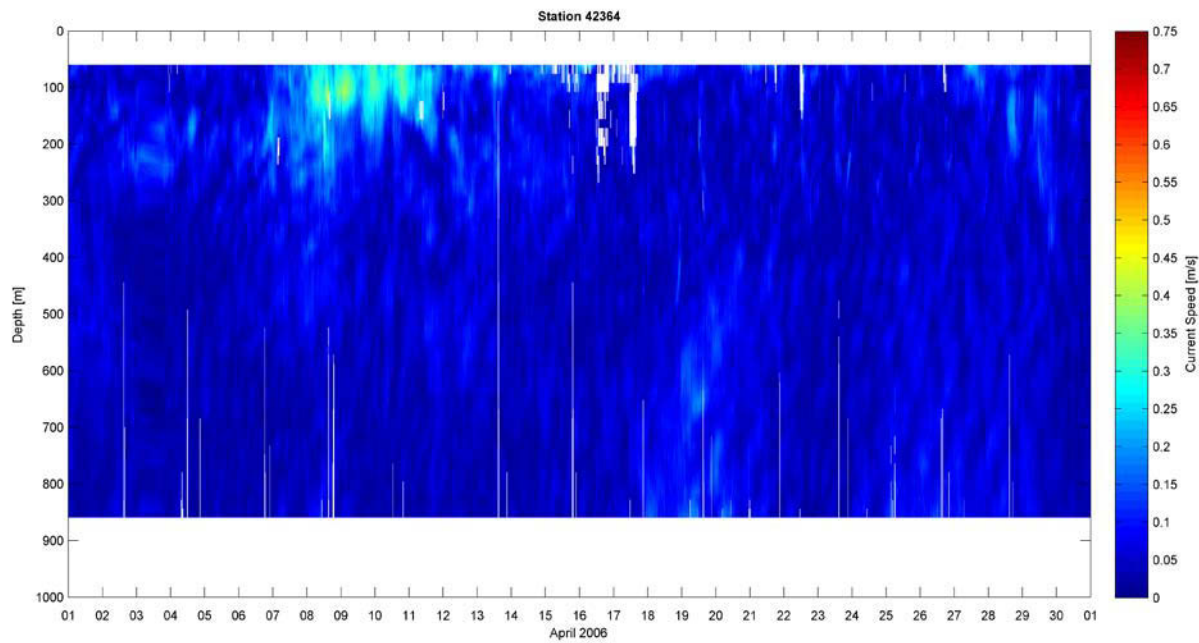


Figure 4-10 Current Speed Contour at NTL Station 42364 – April 2006

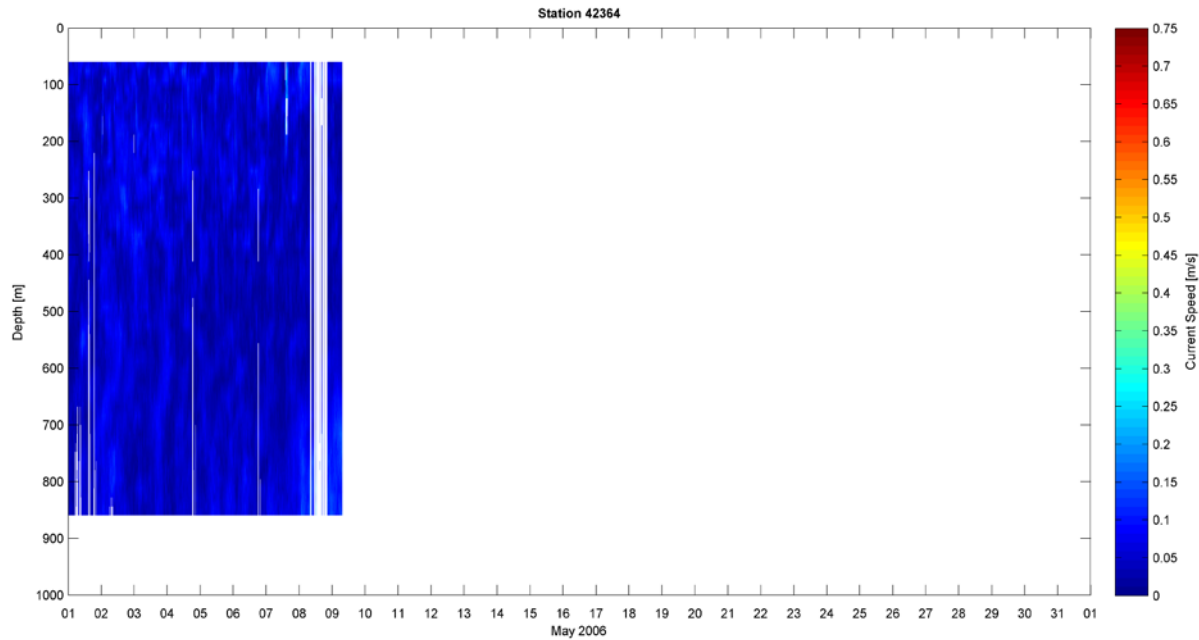


Figure 4-11 Current Speed Contour at NTL Station 42364 – May 2006

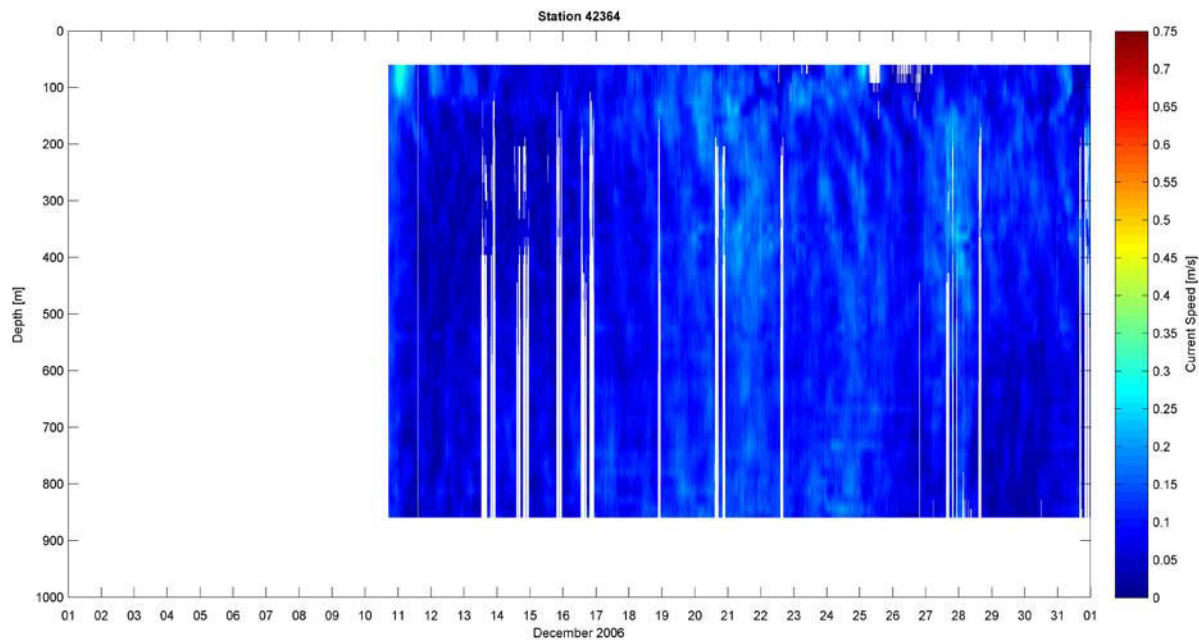


Figure 4-12 Current Speed Contour at NTL Station 42364 – December 2006

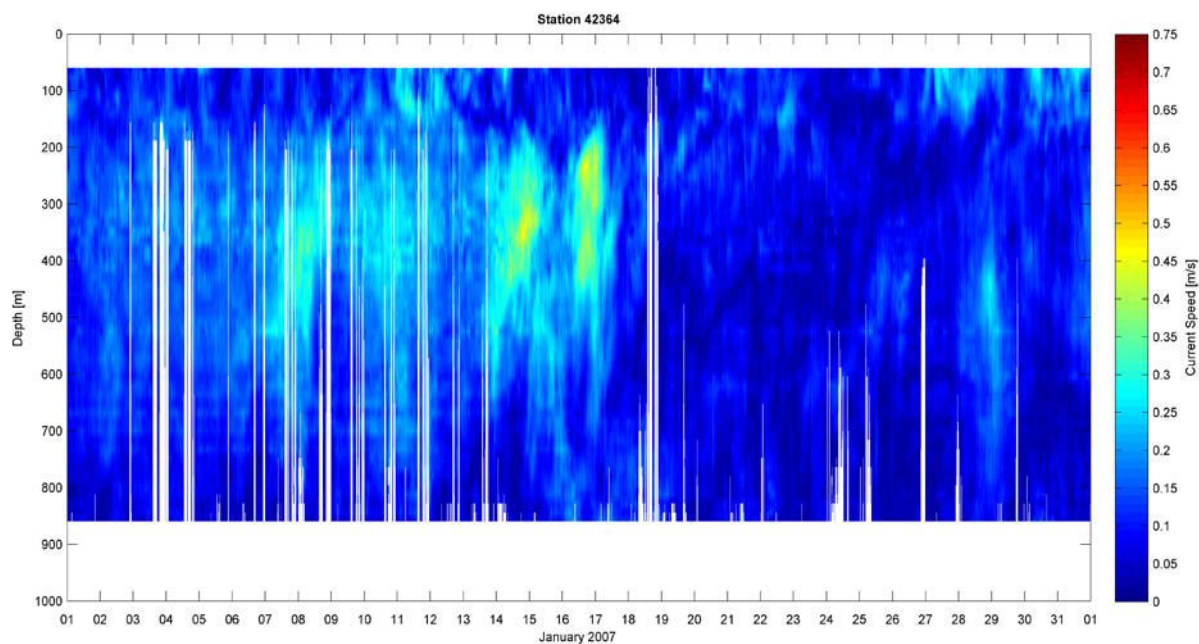


Figure 4-13 Current Speed Contour at NTL Station 42364 – January 2007

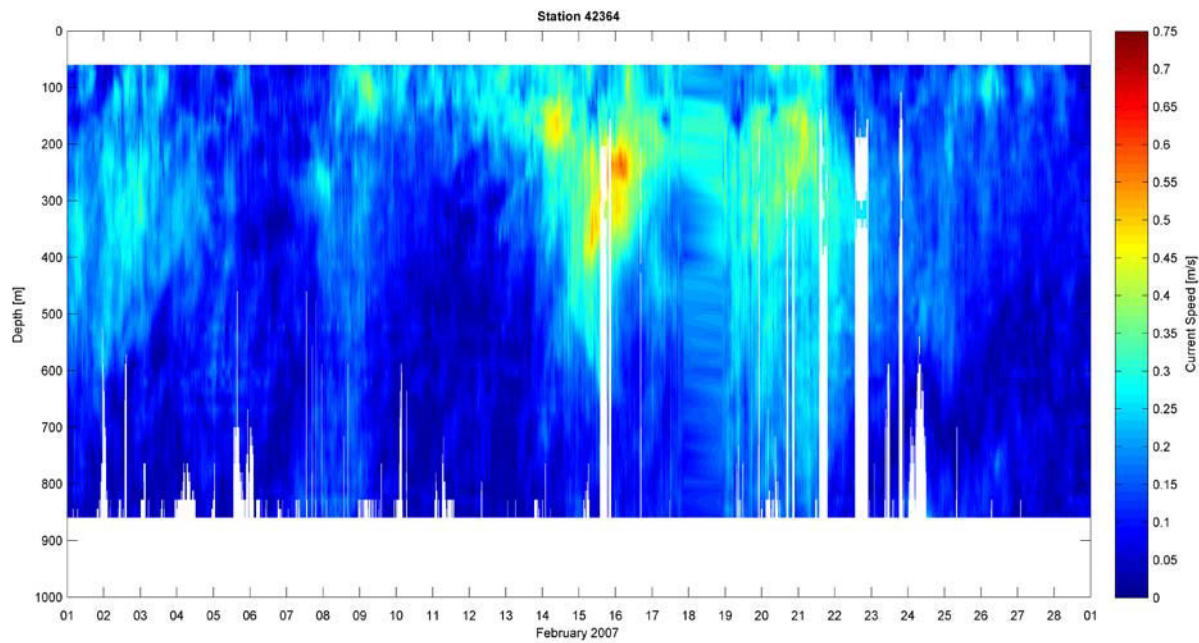


Figure 4-14 Current Speed Contour at NTL Station 42364 – February 2007

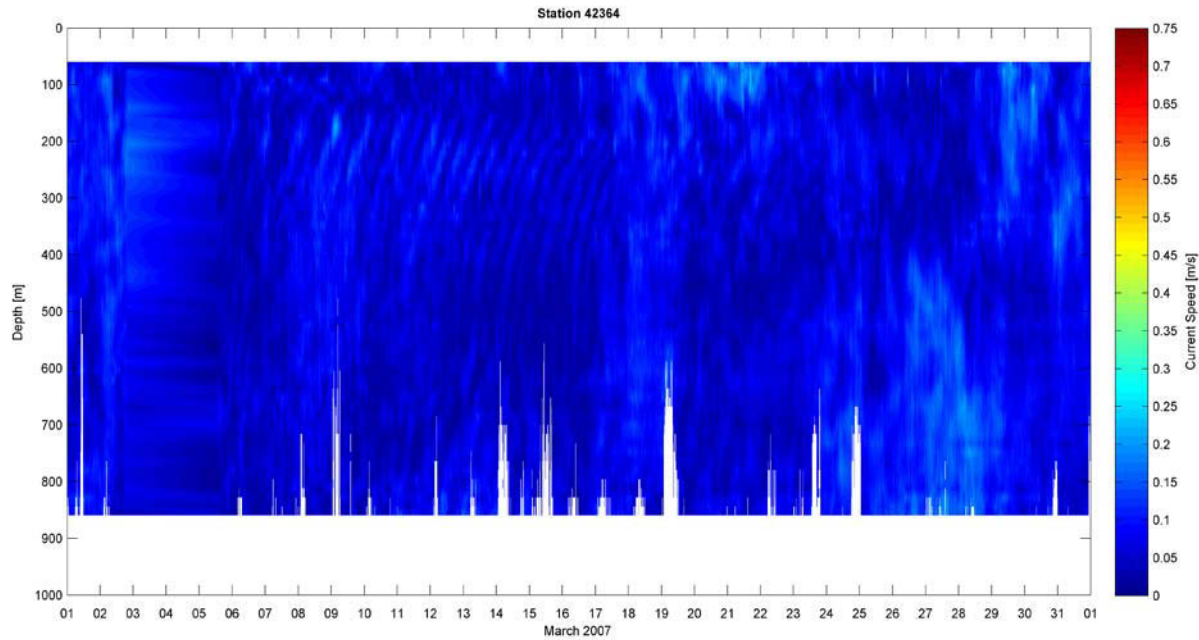


Figure 4-15 Current Speed Contour at NTL Station 42364 – March 2007

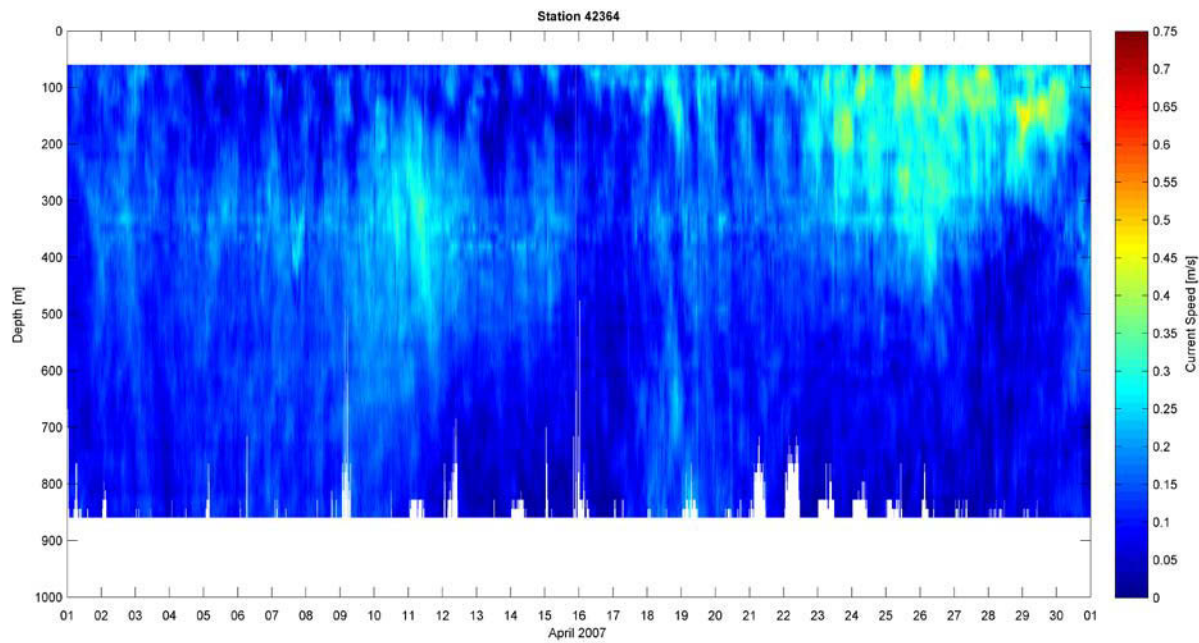


Figure 4-16 Current Speed Contour at NTL Station 42364 – April 2007

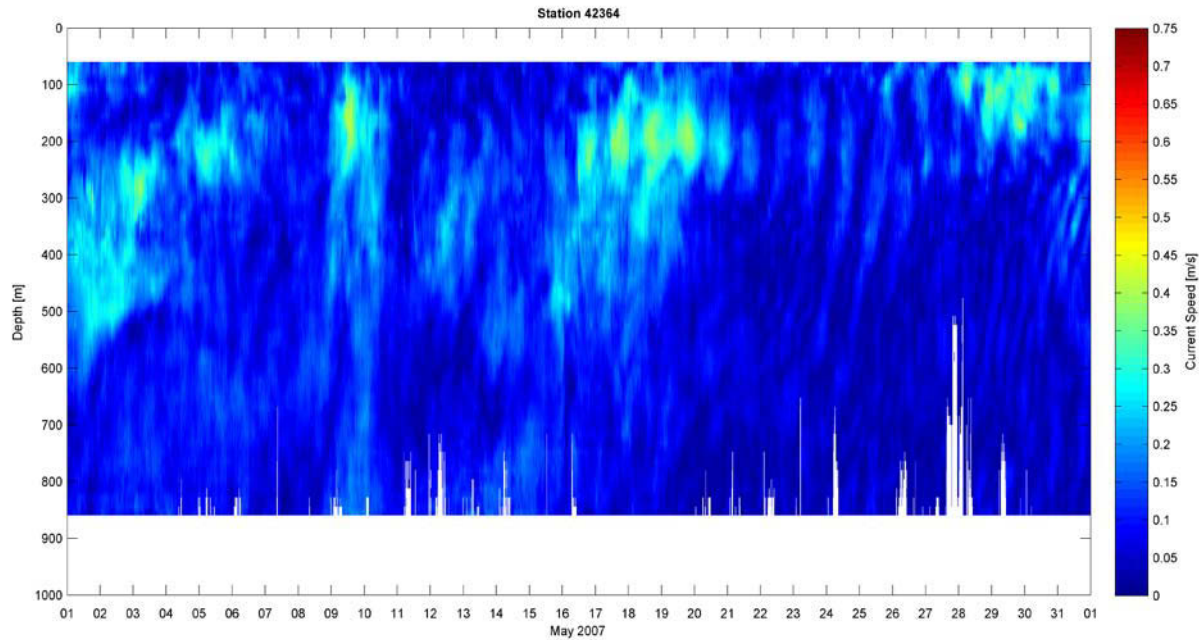


Figure 4-17 Current Speed Contour at NTL Station 42364 – May 2007

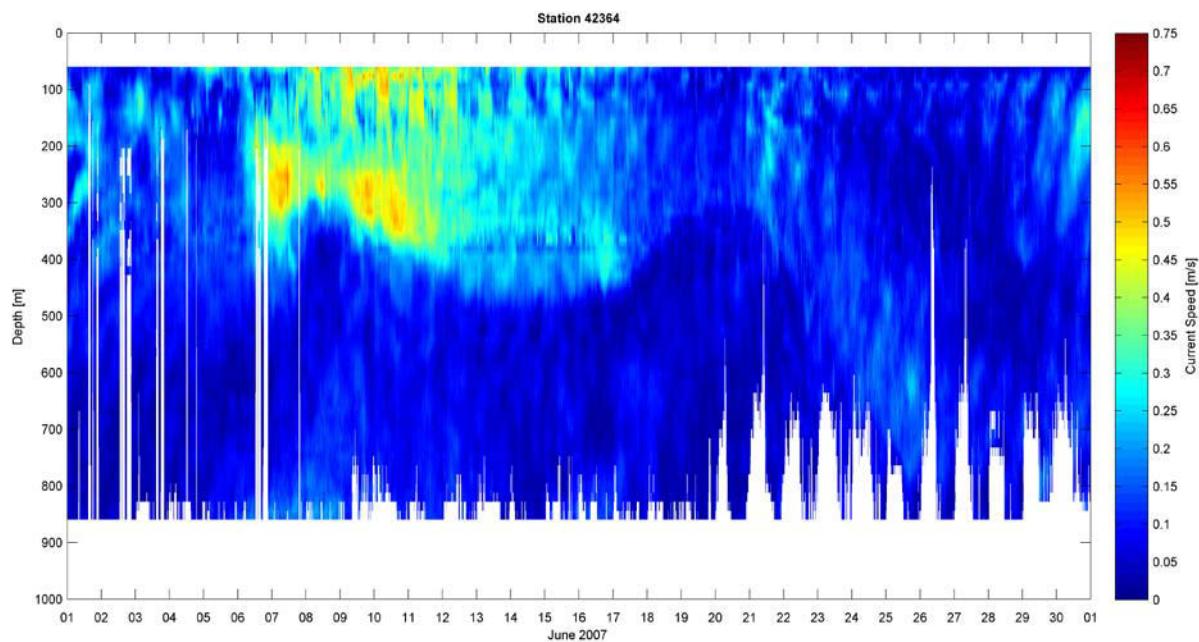


Figure 4-18 Current Speed Contour at NTL Station 42364 – June 2007

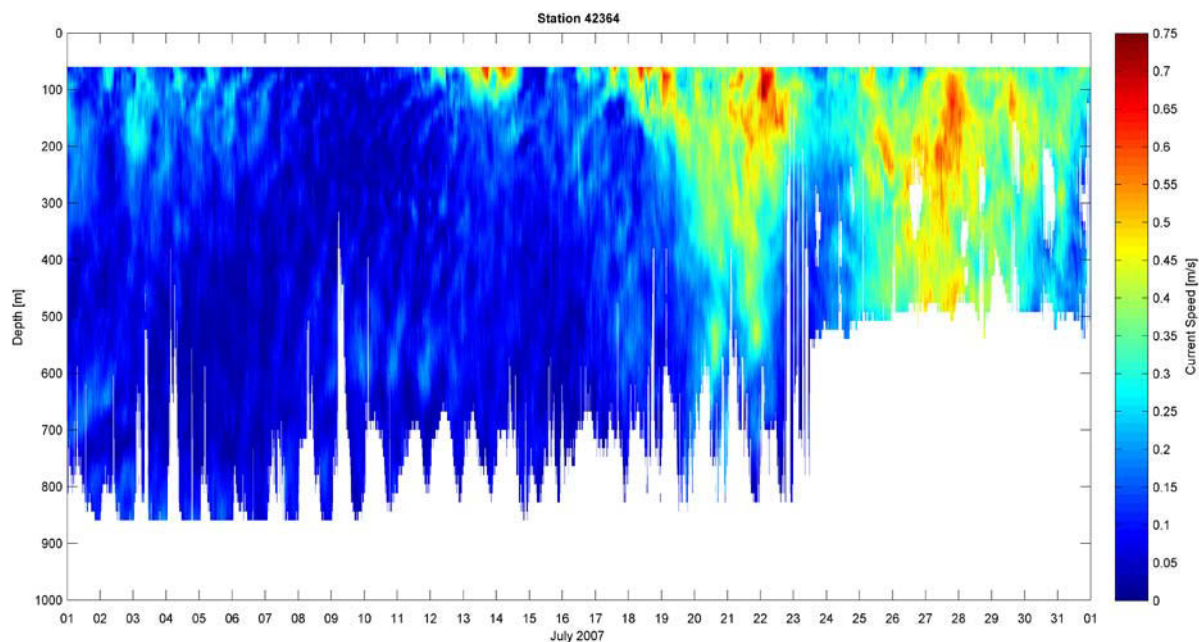


Figure 4-19 Current Speed Contour at NTL Station 42364 – July 2007

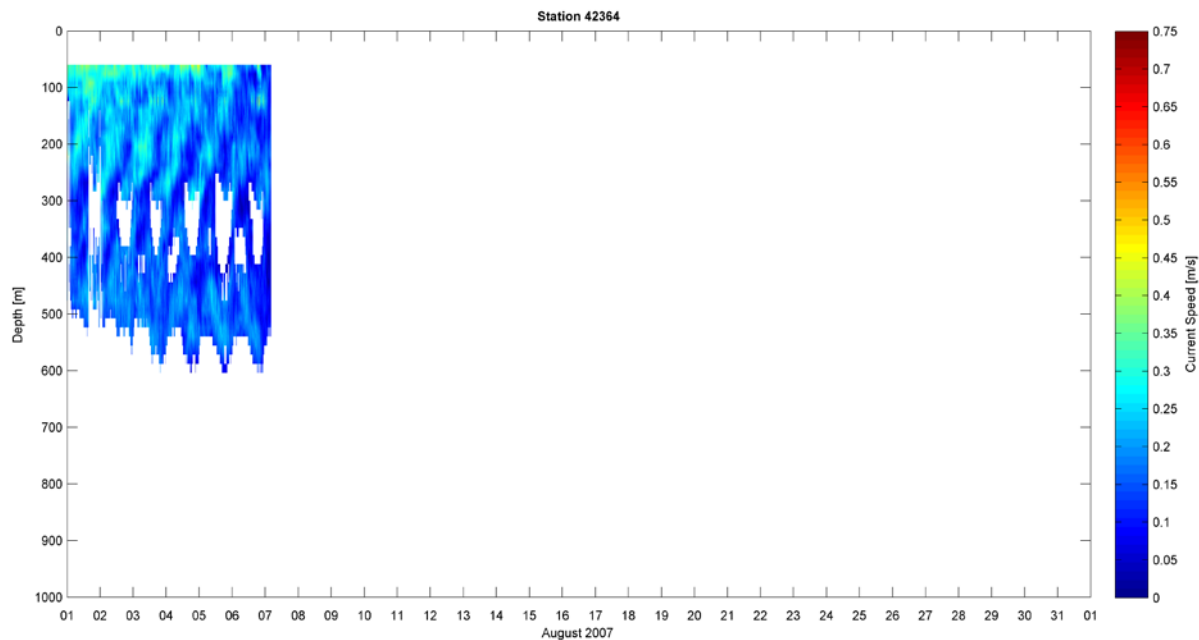


Figure 4-20 Current Speed Contour at NTL Station 42364 – Agust 2007

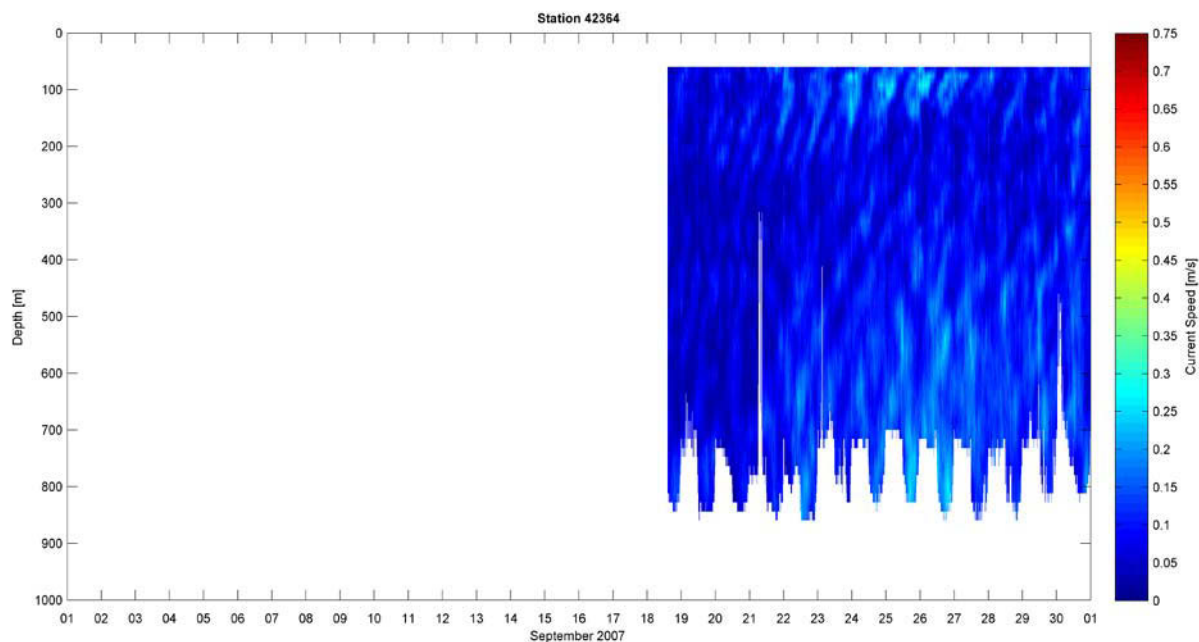


Figure 4-21 Current Speed Contour at NTL Station 42364 – September 2007

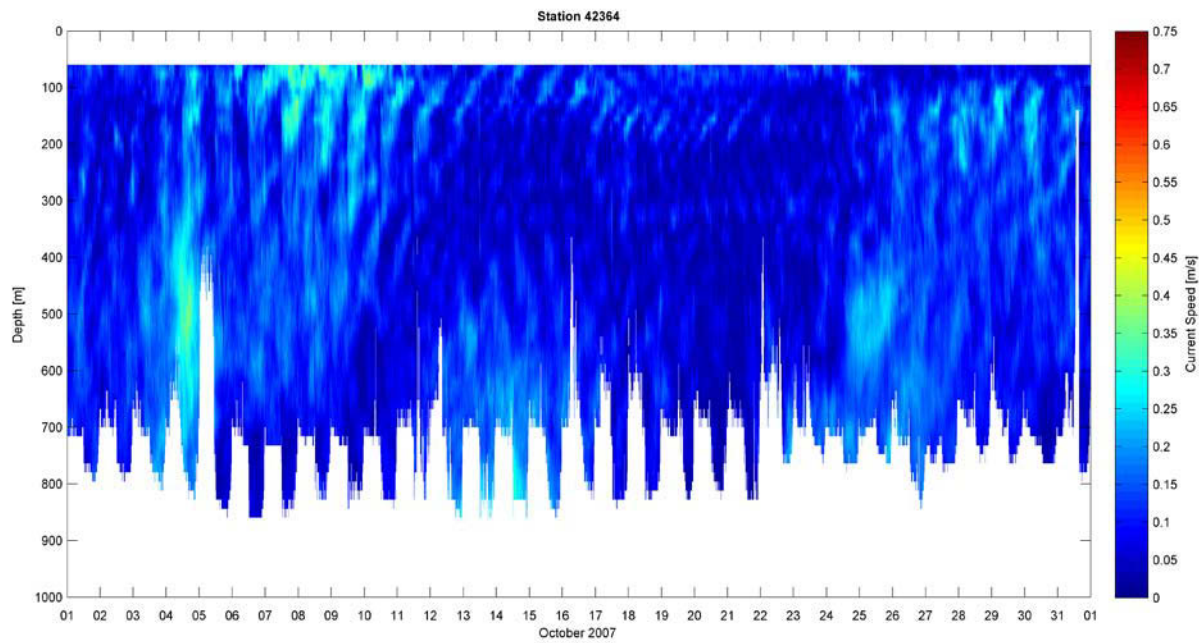


Figure 4-22 Current Speed Contour at NTL Station 42364 – October 2007

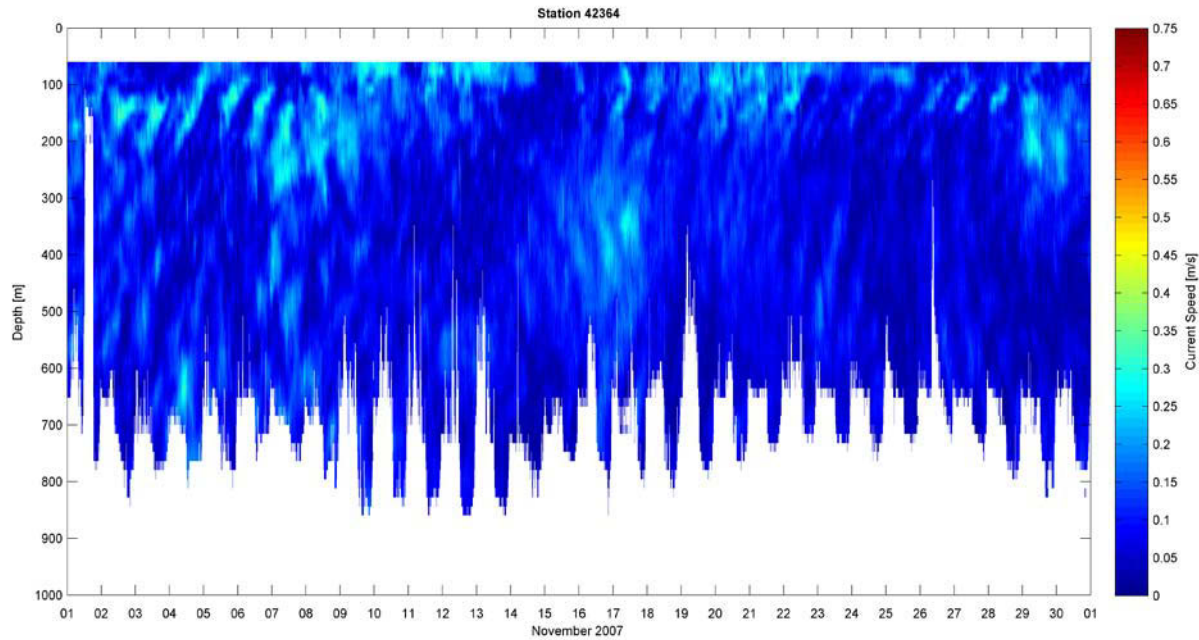


Figure 4-23 Current Speed Contour at NTL Station 42364 – November 2007

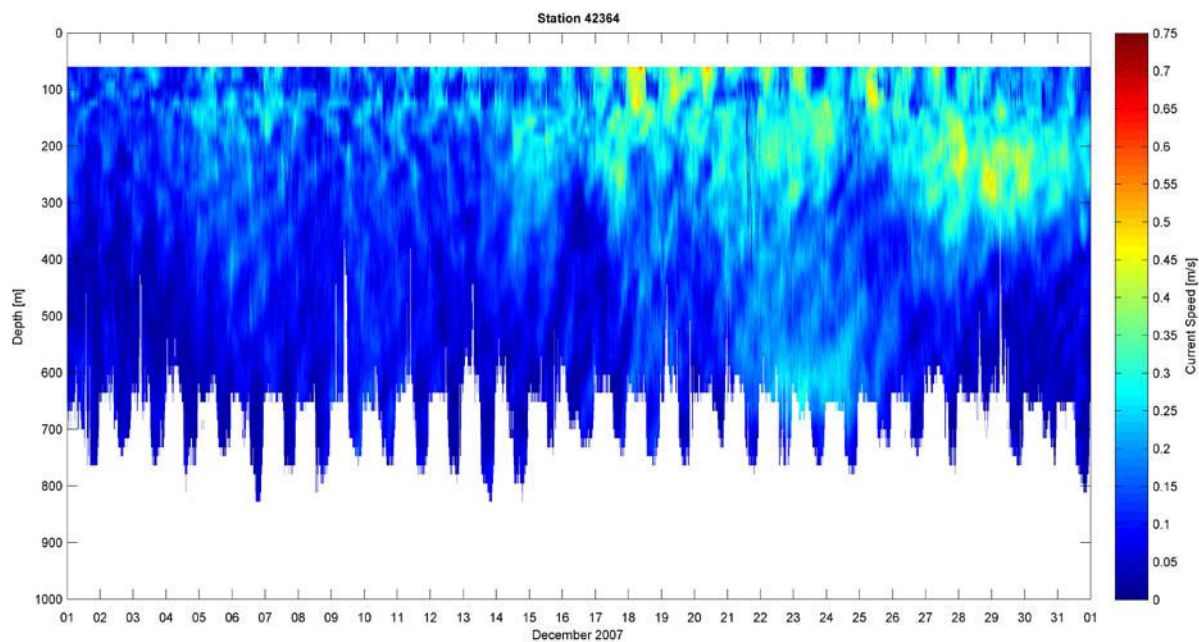


Figure 4-24 Current Speed Contour at NTL Station 42364 – December 2007

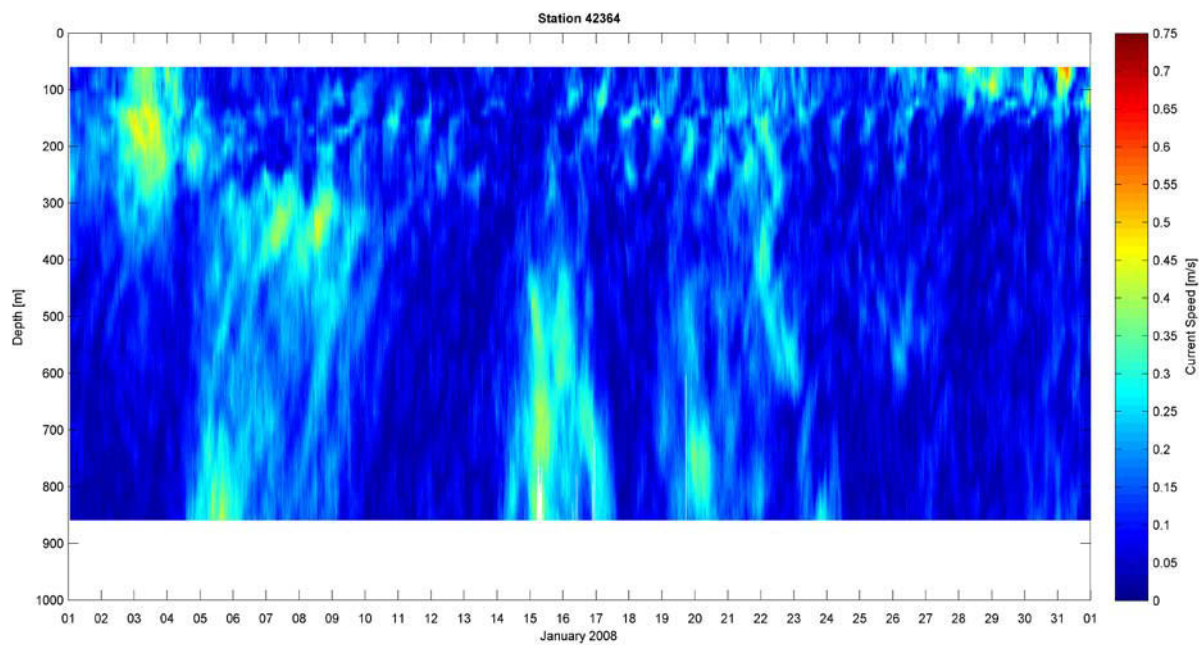


Figure 4-25 Current Speed Contour at NTL Station 42364 – January 2008

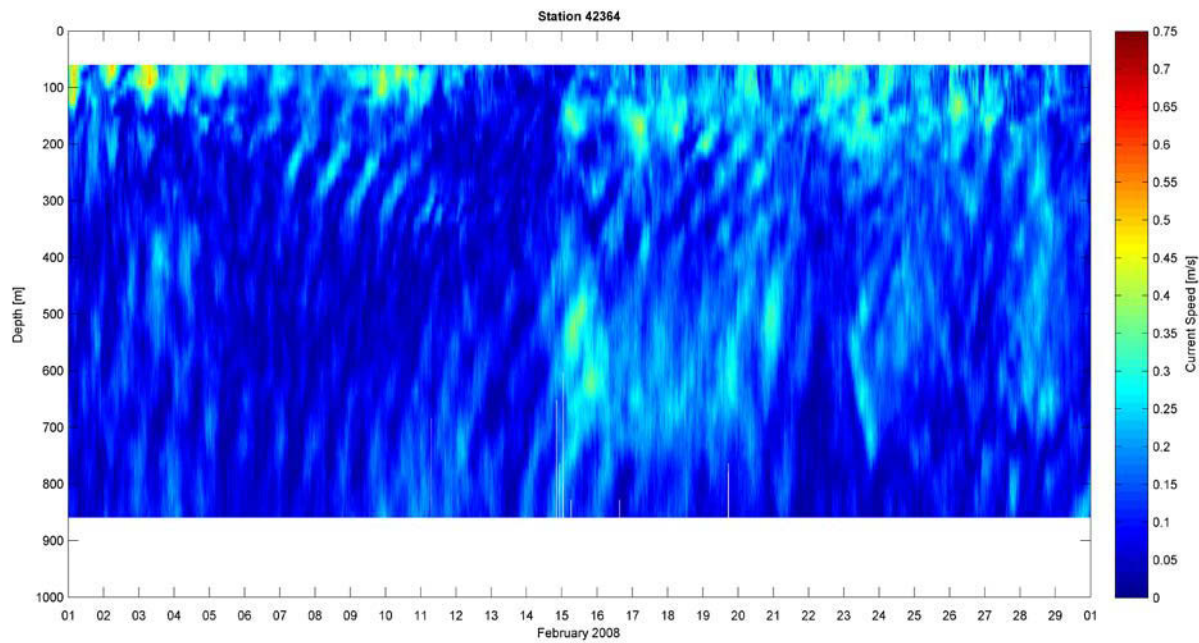


Figure 4-26 Current Speed Contour at NTL Station 42364 – February 2008

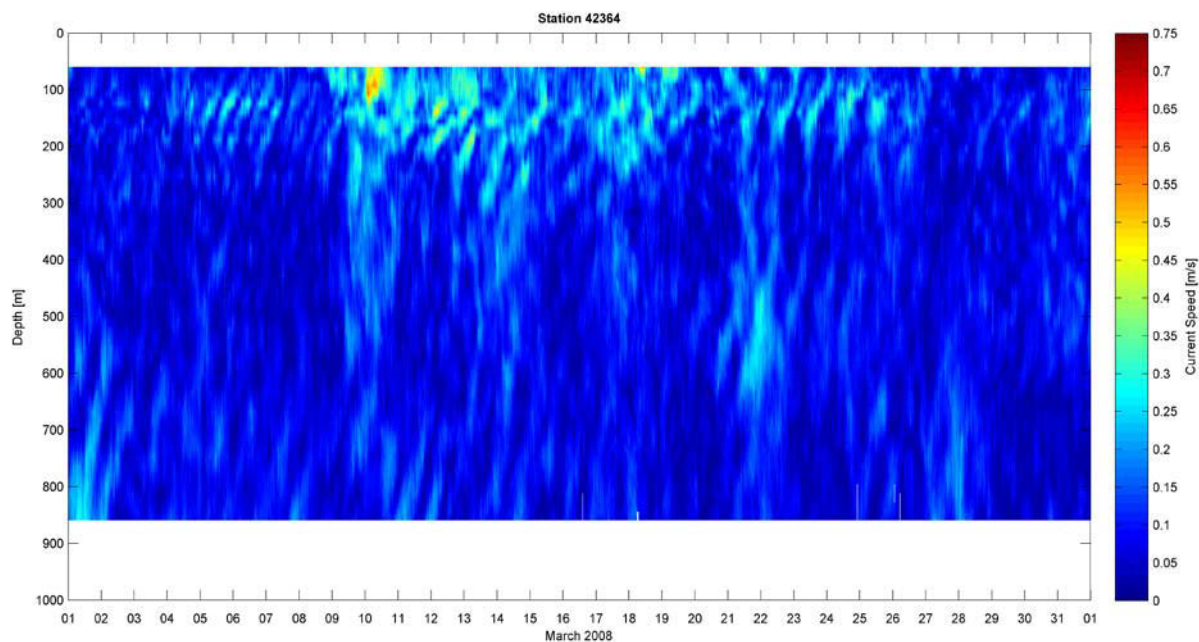


Figure 4-27 Current Speed Contour at NTL Station 42364 – March 2008

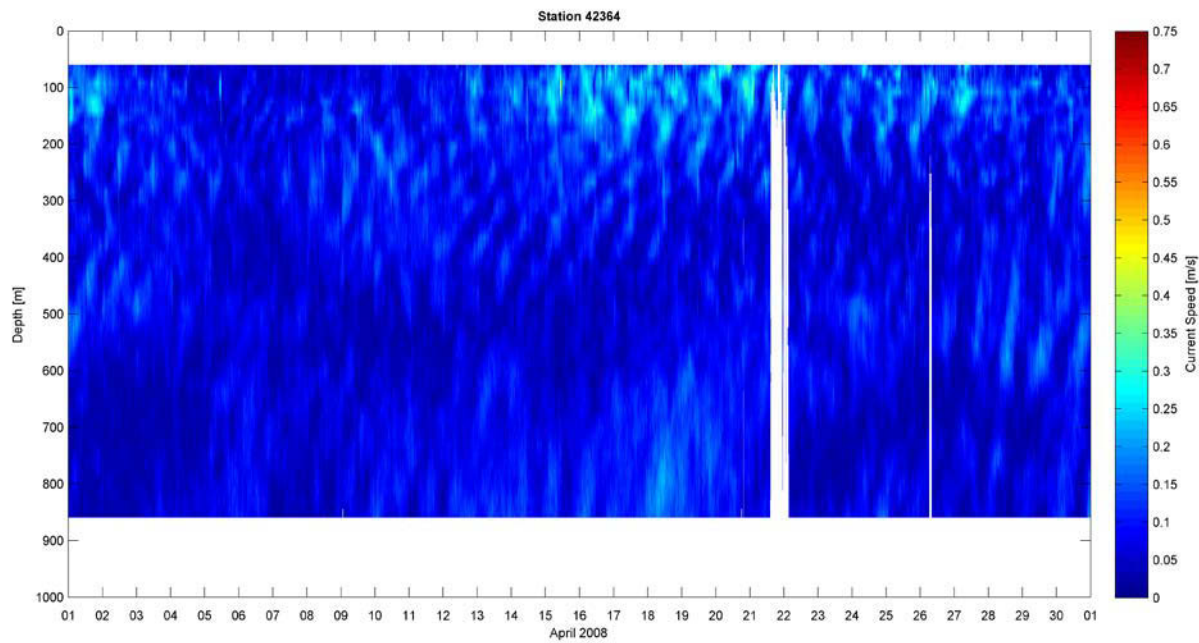


Figure 4-28 Current Speed Contour at NTL Station 42364 – April 2008

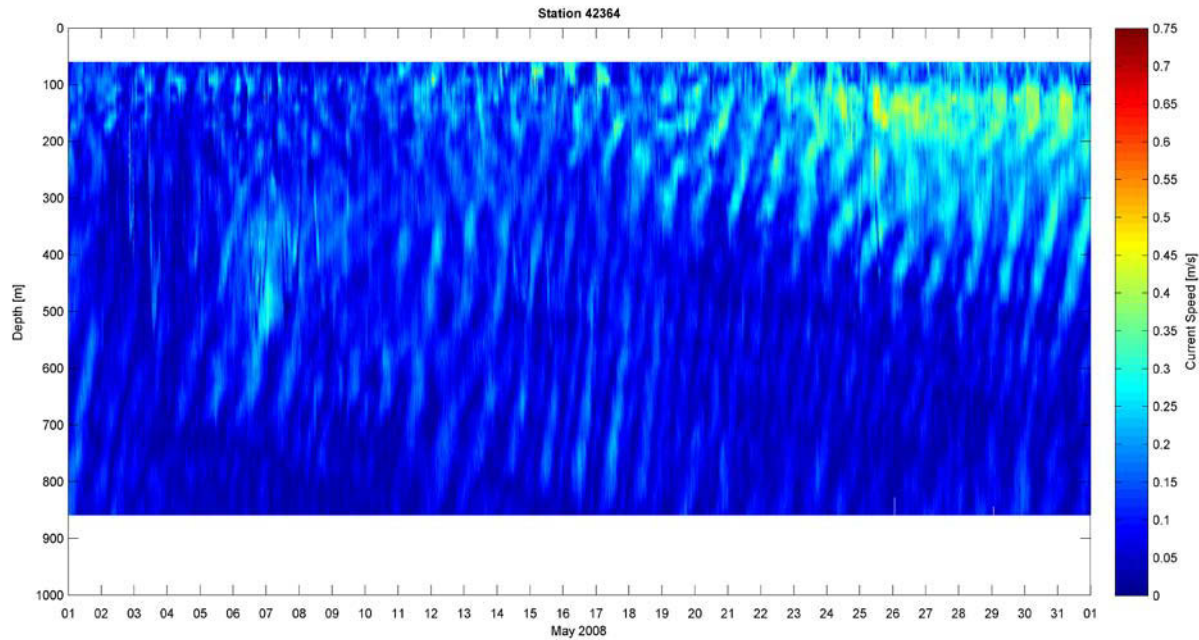


Figure 4-29 Current Speed Contour at NTL Station 42364 – May 2008

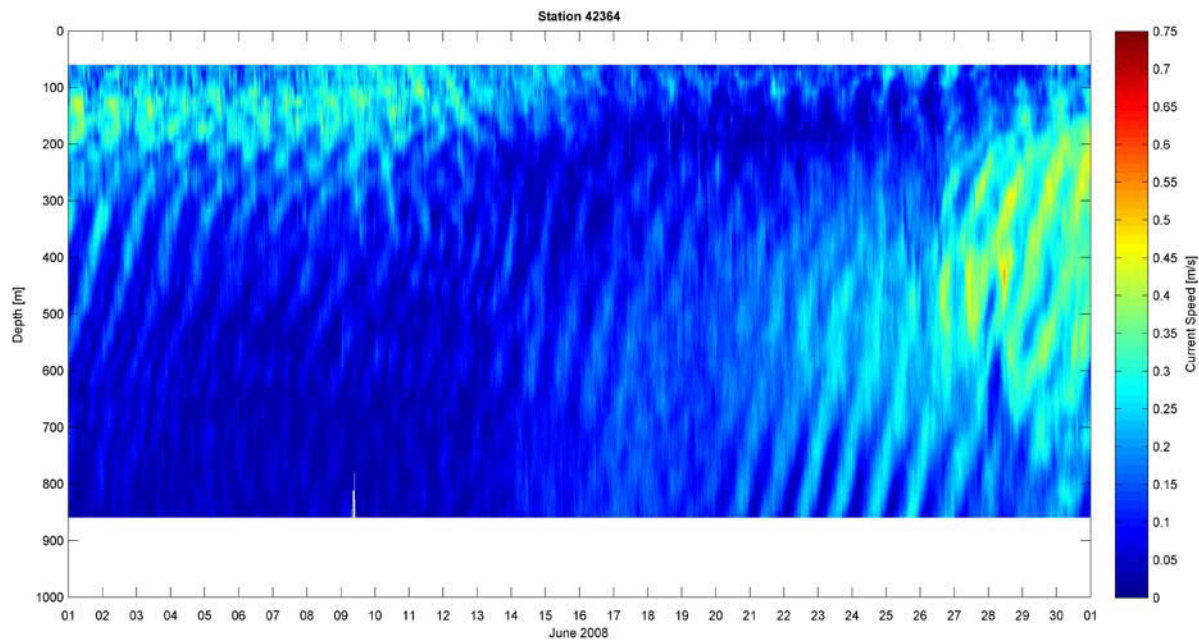


Figure 4-30 Current Speed Contour at NTL Station 42364 – June 2008

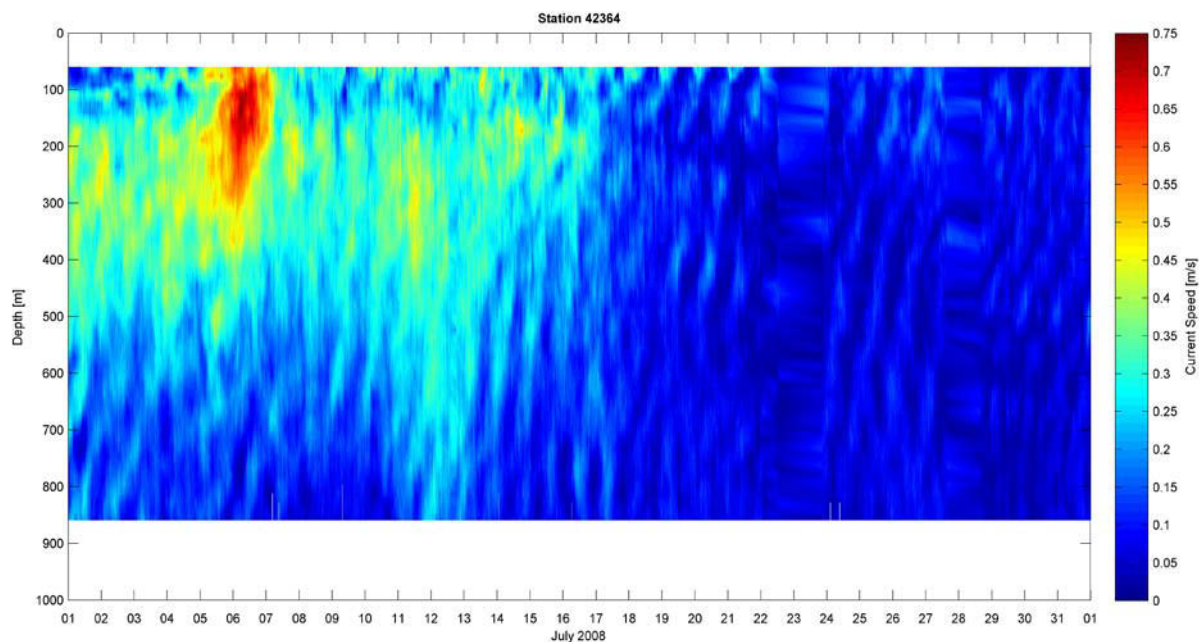


Figure 4-31 Current Speed Contour at NTL Station 42364 – July 2008

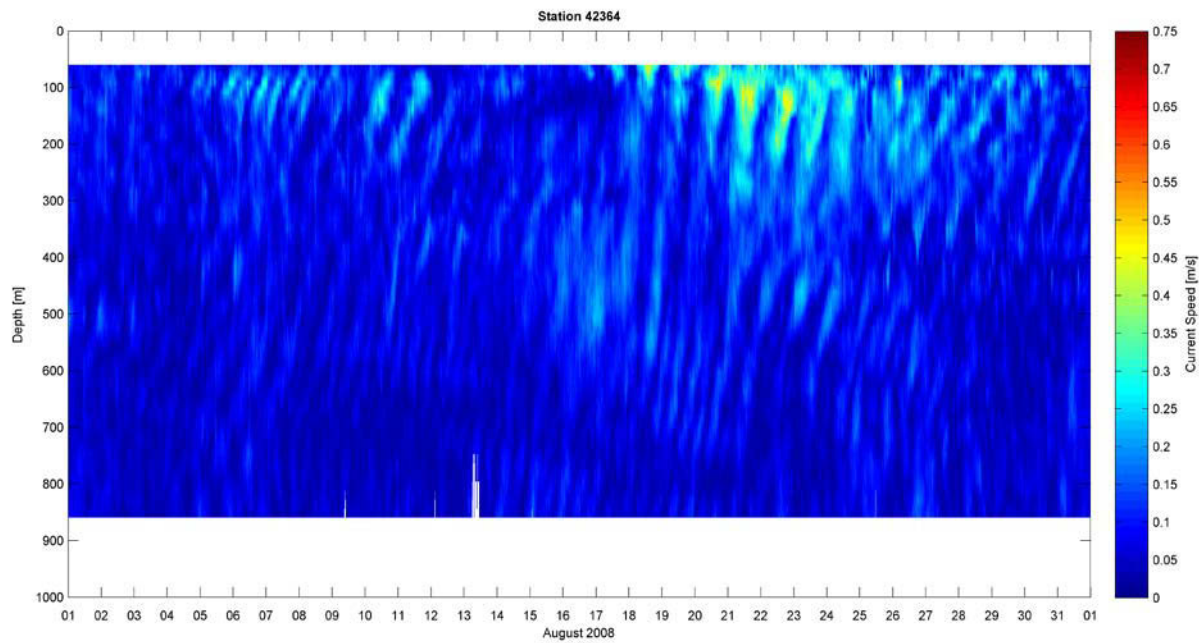


Figure 4-32 Current Speed Contour at NTL Station 42364 – Agust 2008

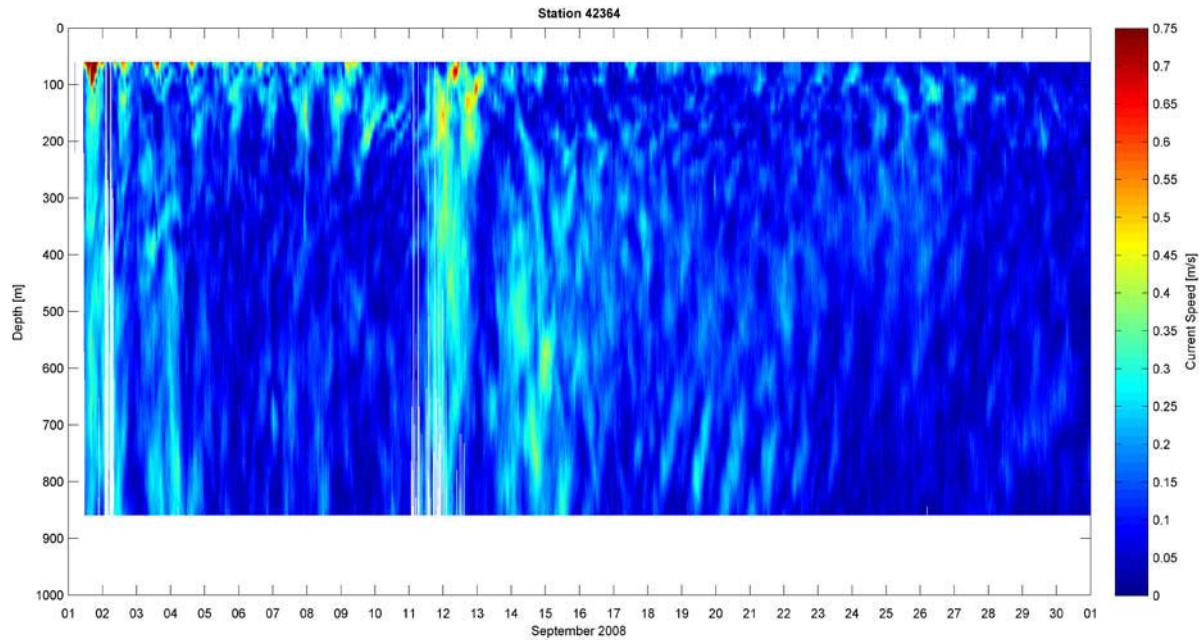


Figure 4-33 Current Speed Contour at NTL Station 42364 – September 2008

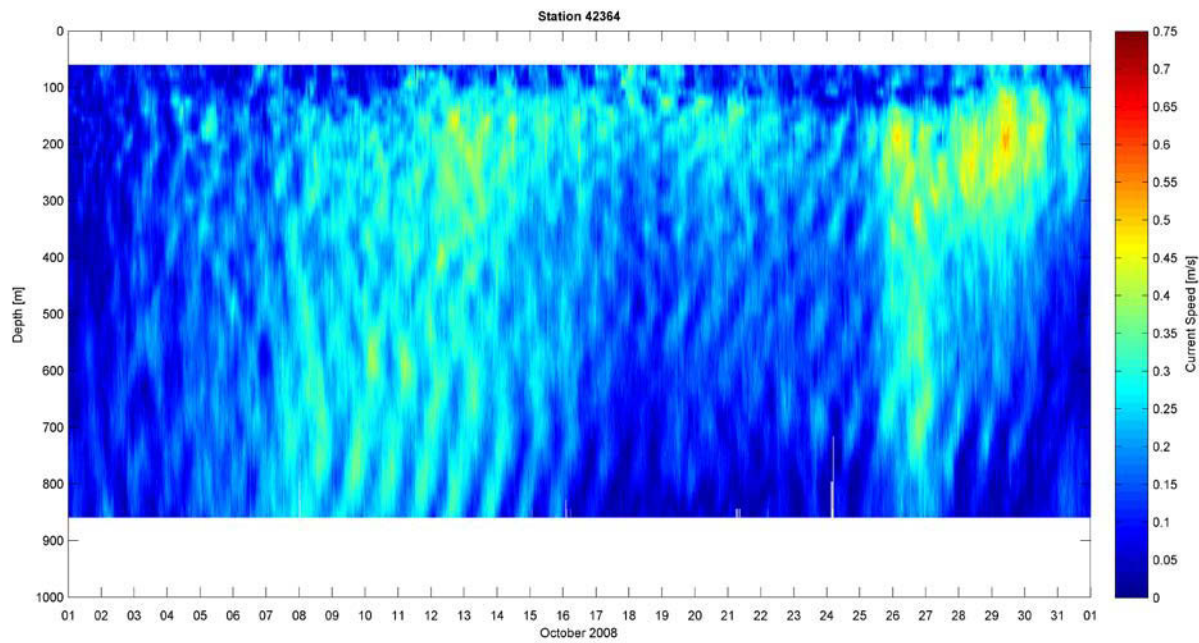


Figure 4-34 Current Speed Contour at NTL Station 42364 – October 2008

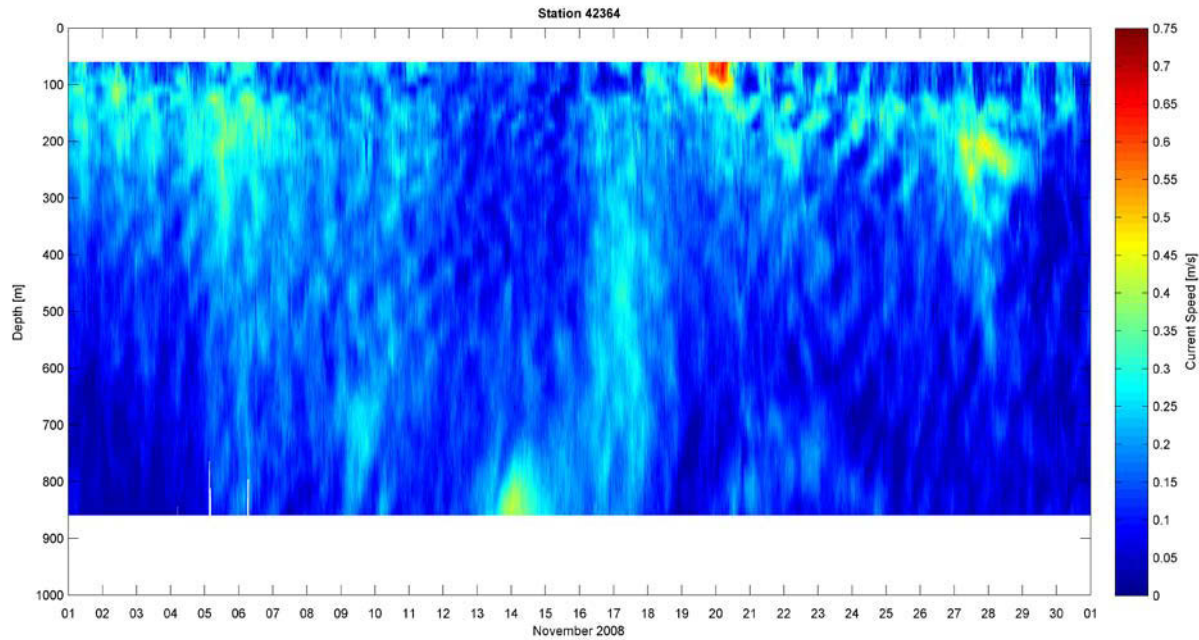


Figure 4-35 Current Speed Contour at NTL Station 42364 – November 2008

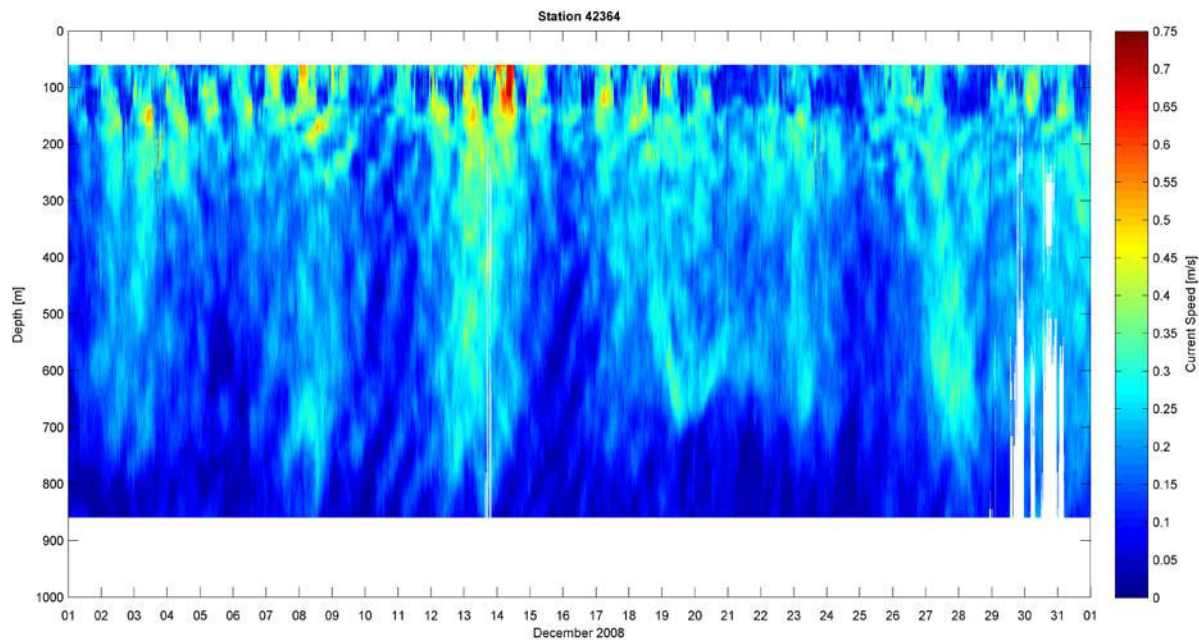


Figure 4-36 Current Speed Contour at NTL Station 42364 – December 2008

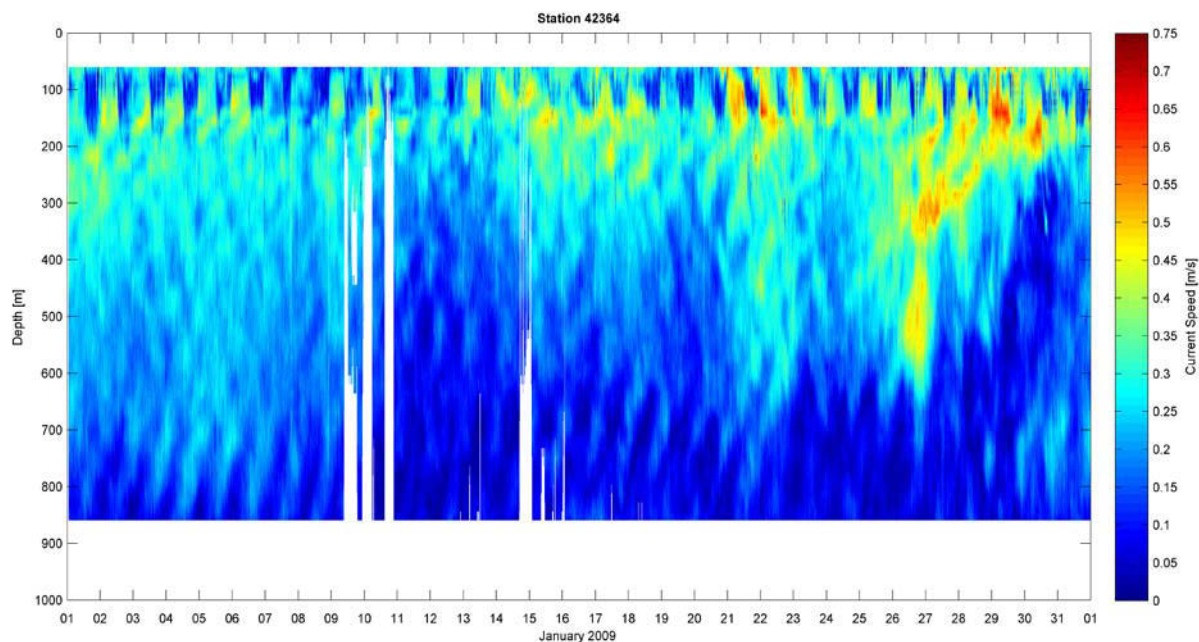


Figure 4-37 Current Speed Contour at NTL Station 42364 – January 2009

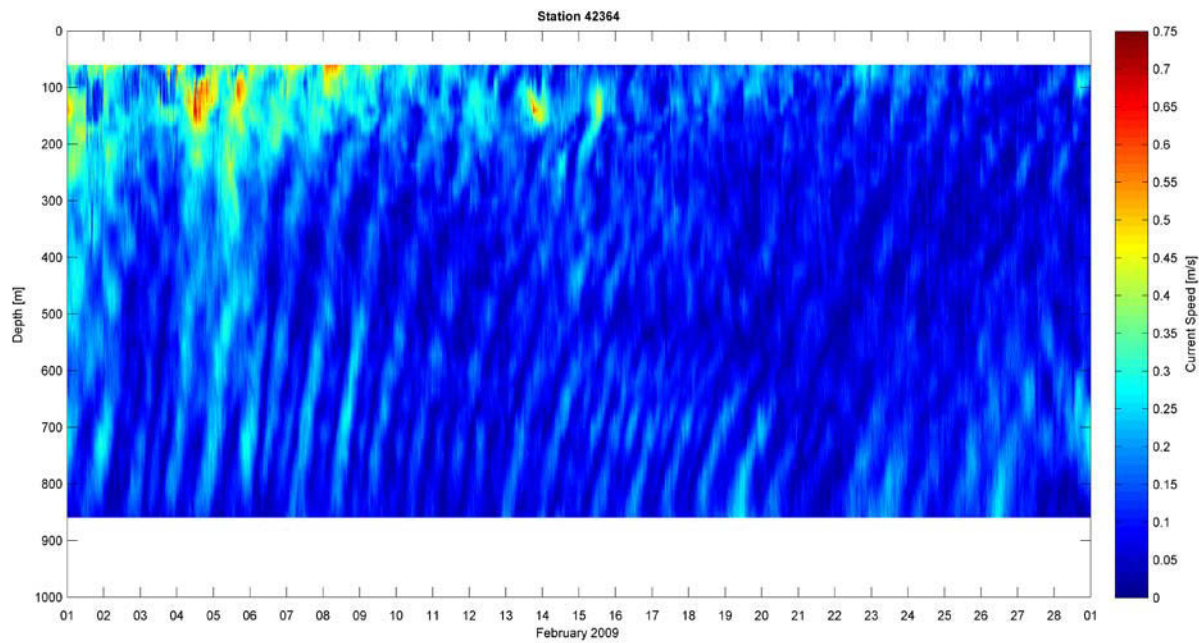


Figure 4-38 Current Speed Contour at NTL Station 42364 – February 2009

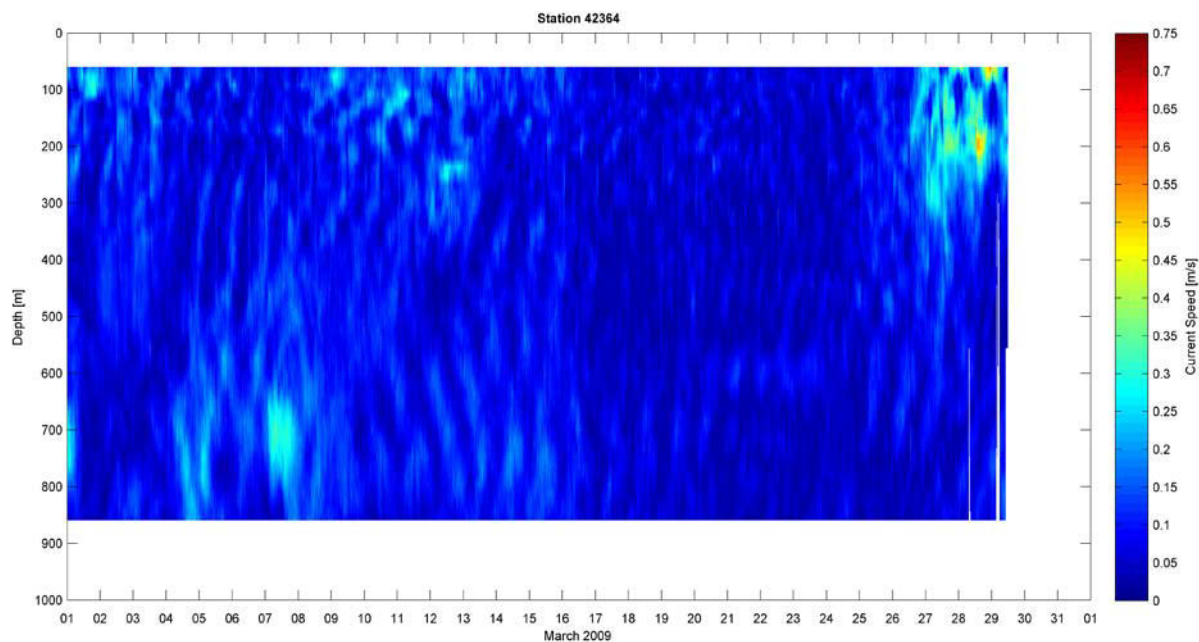


Figure 4-39 Current Speed Contour at NTL Station 42364 – March 2009

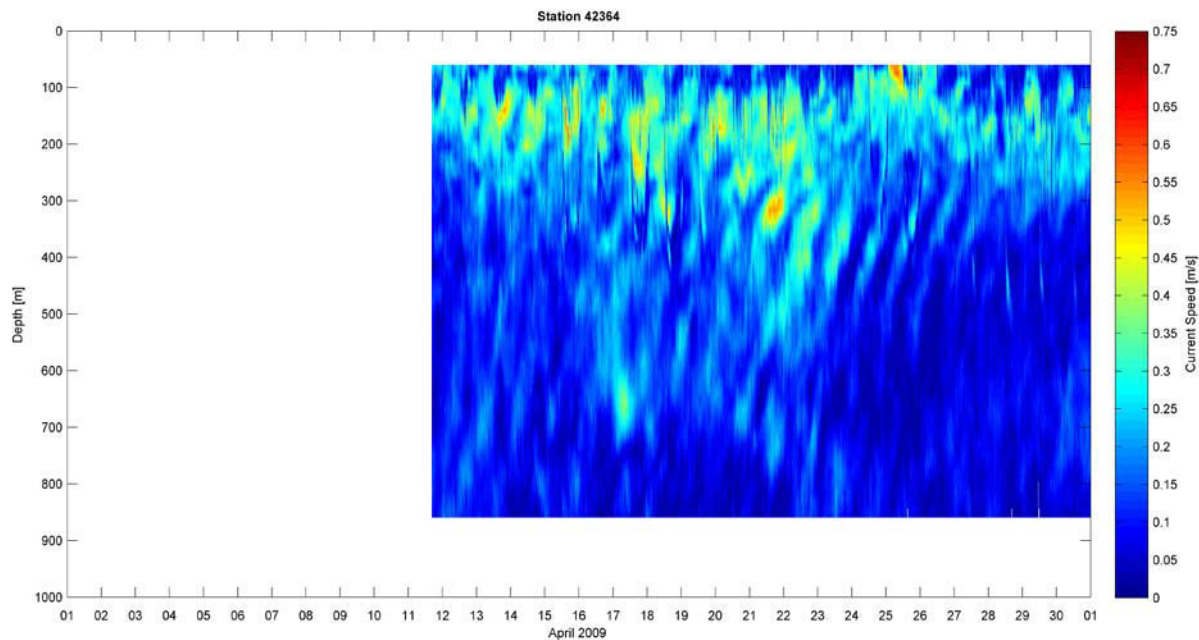


Figure 4-40 Current Speed Contour at NTL Station 42364 – April 2009

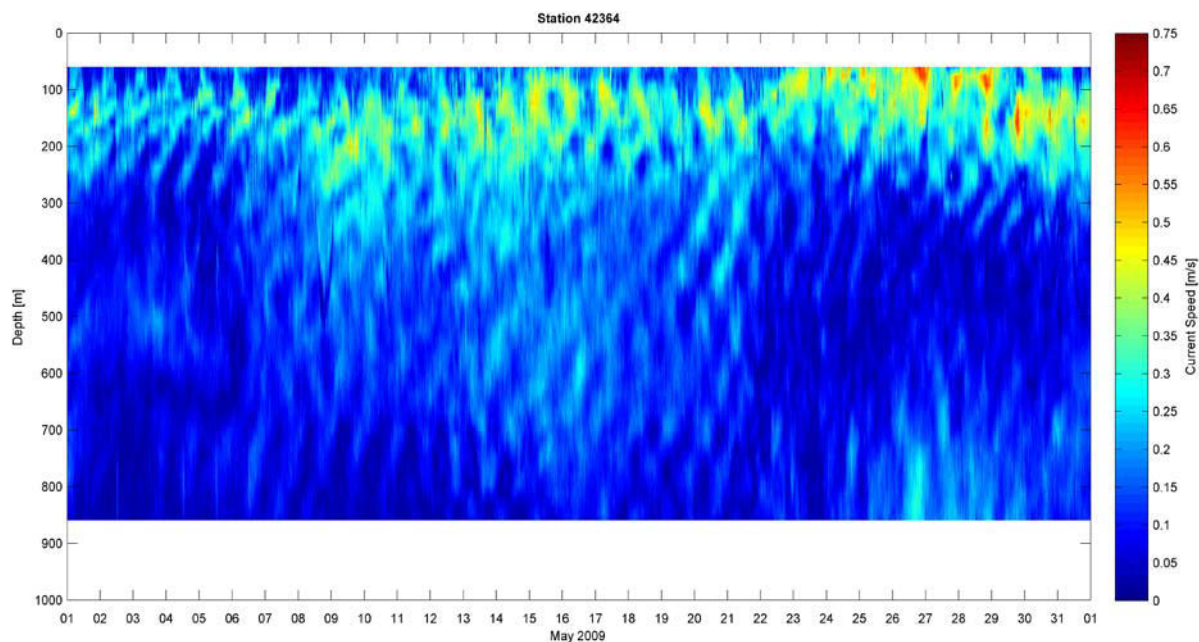


Figure 4-41 Current Speed Contour at NTL Station 42364 – May 2009

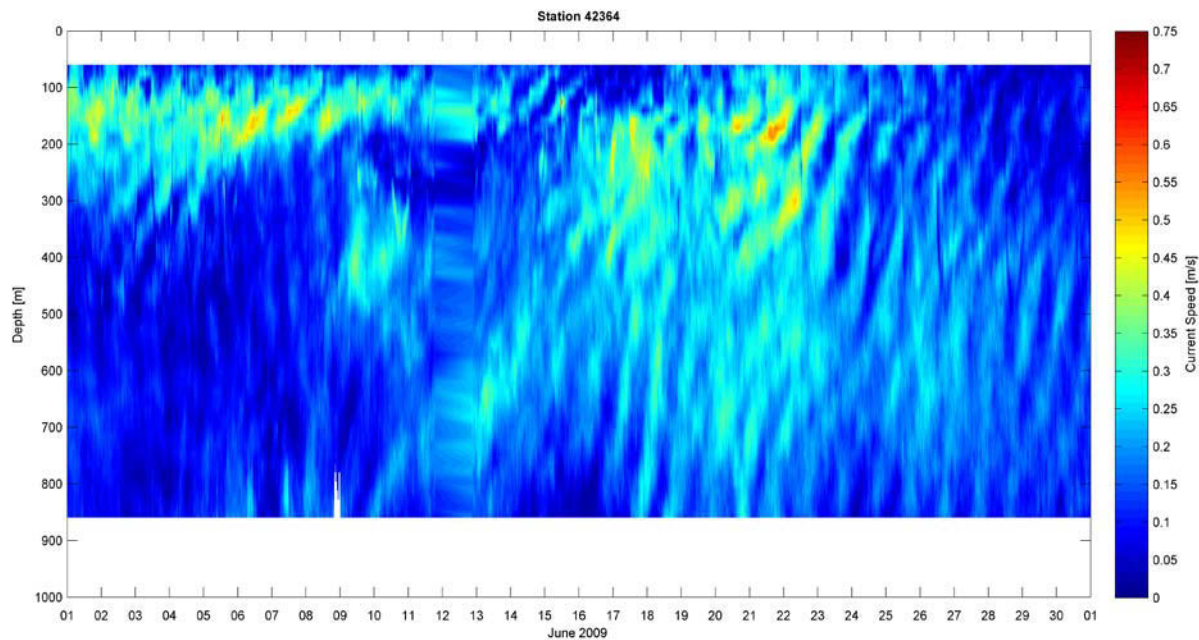


Figure 4-42 Current Speed Contour at NTL Station 42364 – June 2009

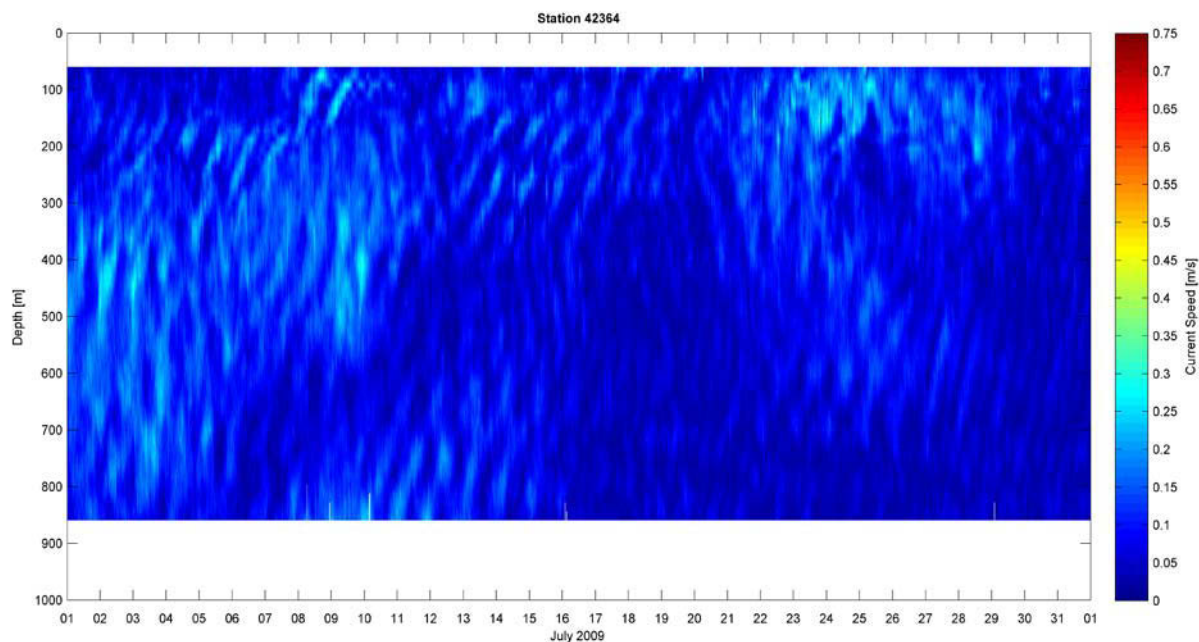


Figure 4-43 Current Speed Contour at NTL Station 42364 – July 2009

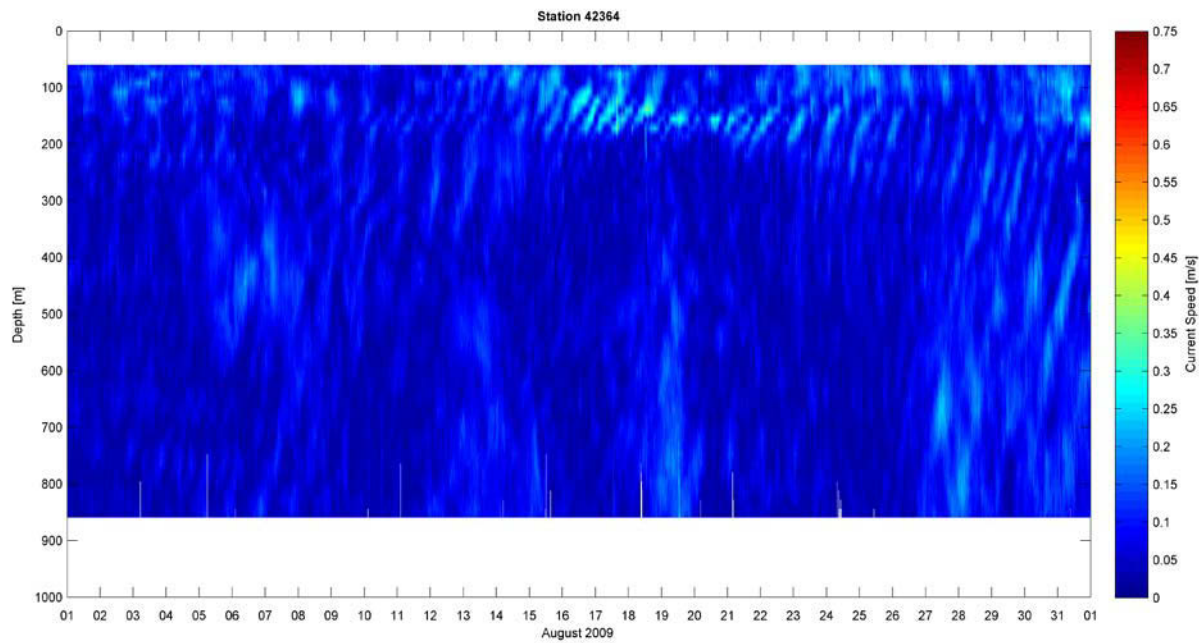


Figure 4-44 Current Speed Contour at NTL Station 42364 – August 2009

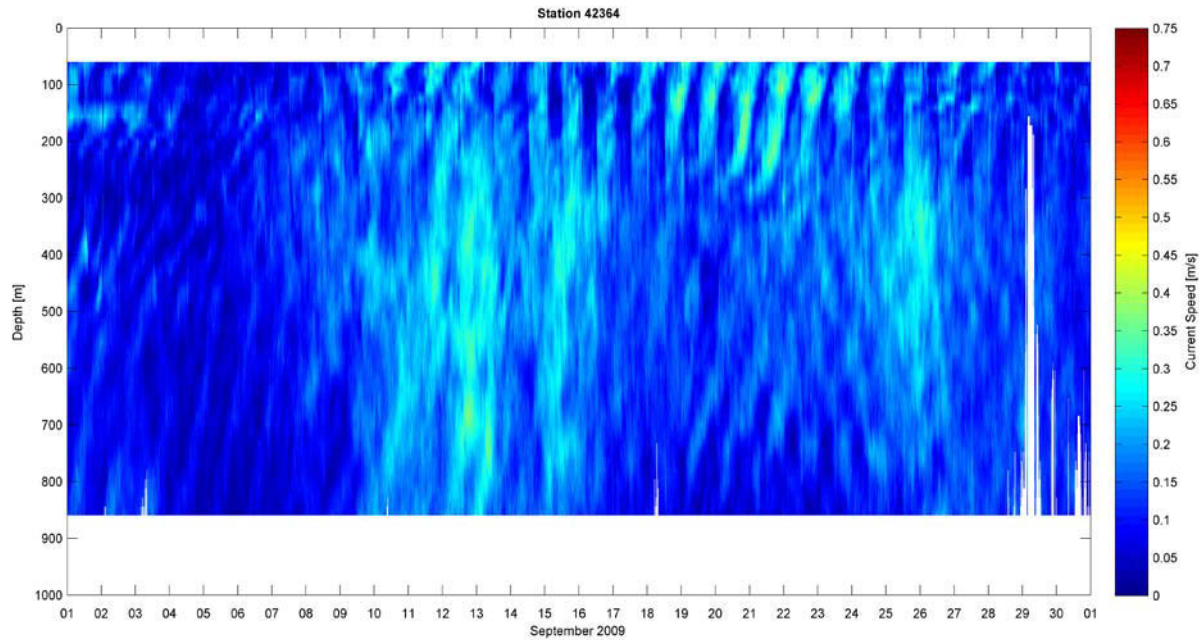


Figure 4-45 Current Speed Contour at NTL Station 42364 – September 2009

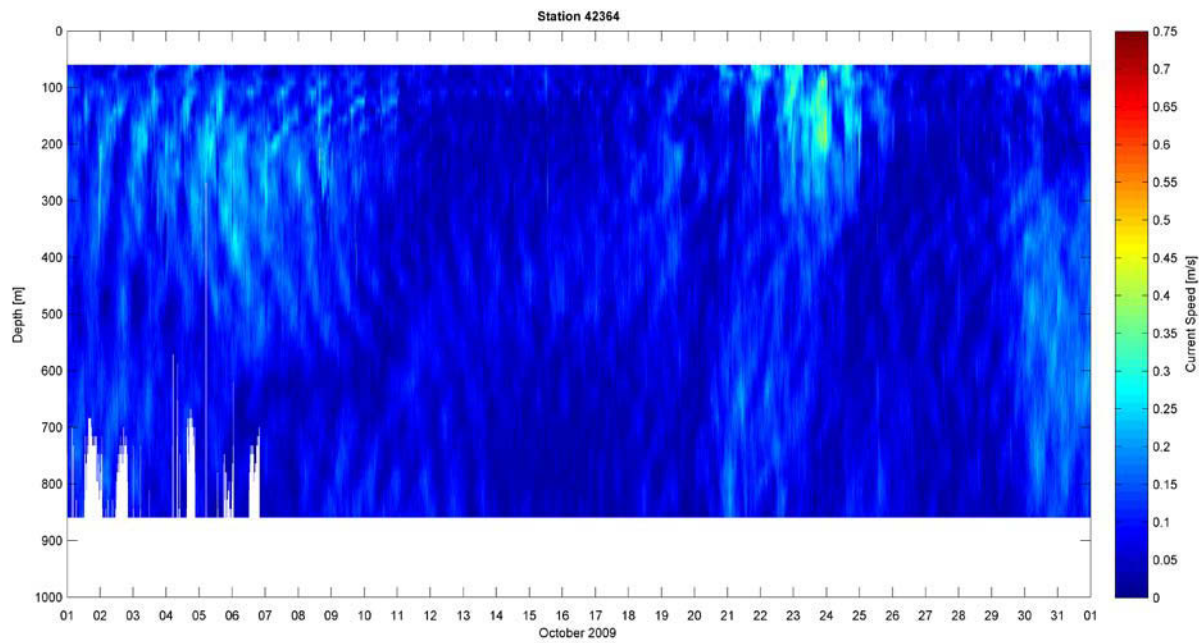


Figure 4-46 Current Speed Contour at NTL Station 42364 – October 2009

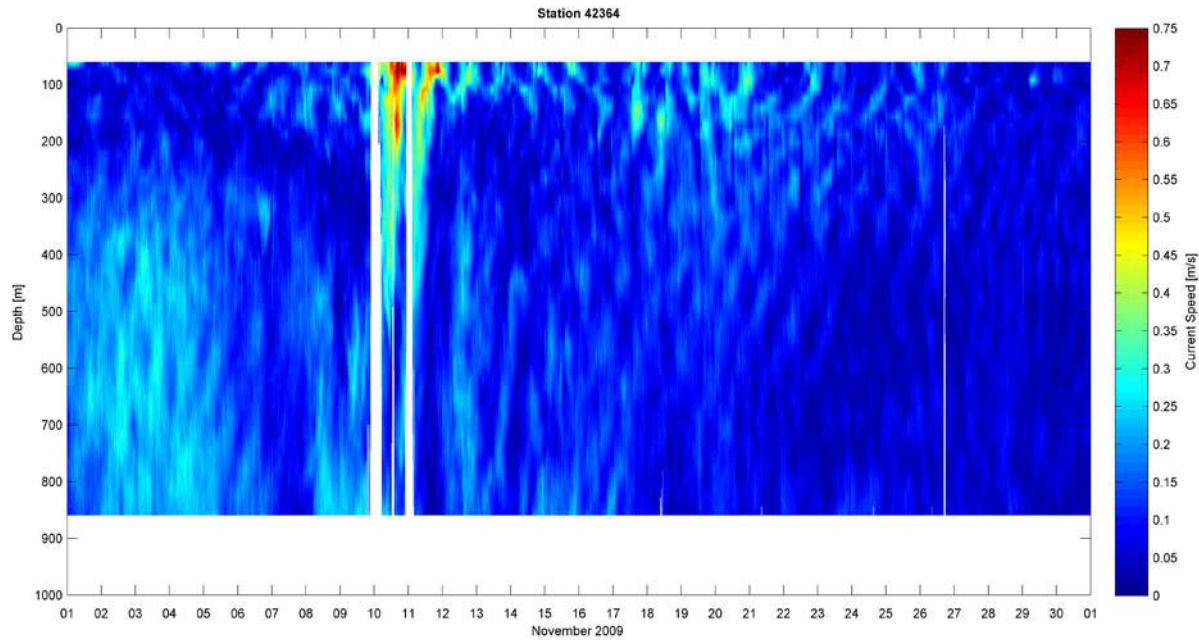


Figure 4-47 Current Speed Contour at NTL Station 42364 – November 2009

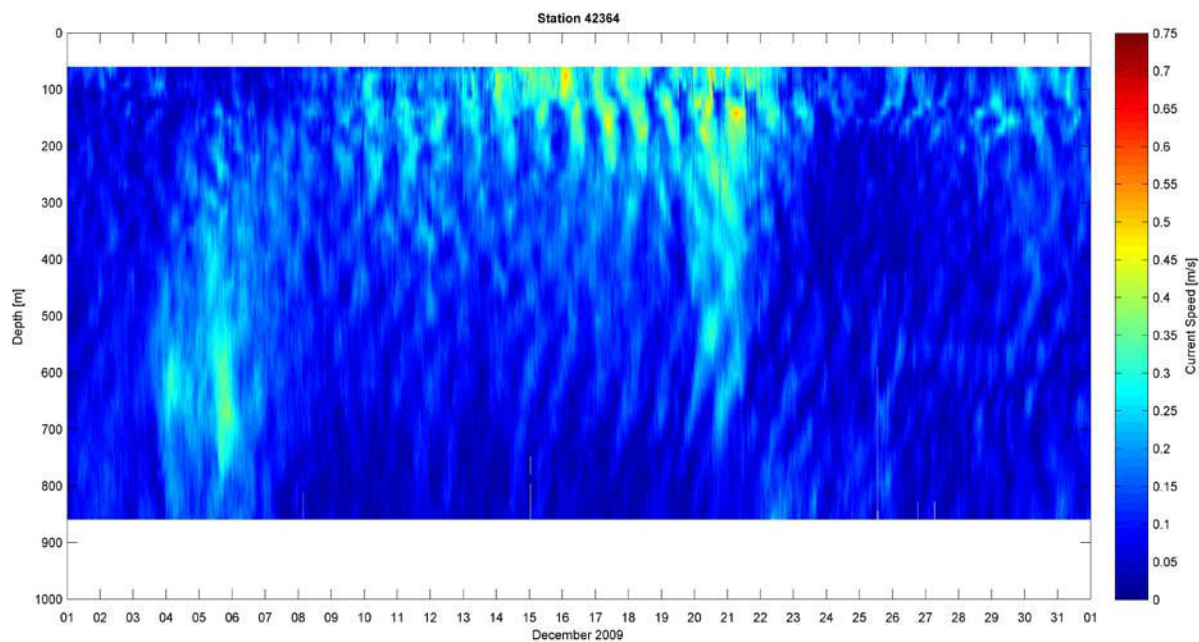


Figure 4-48 Current Speed Contour at NTL Station 42364 – December 2009

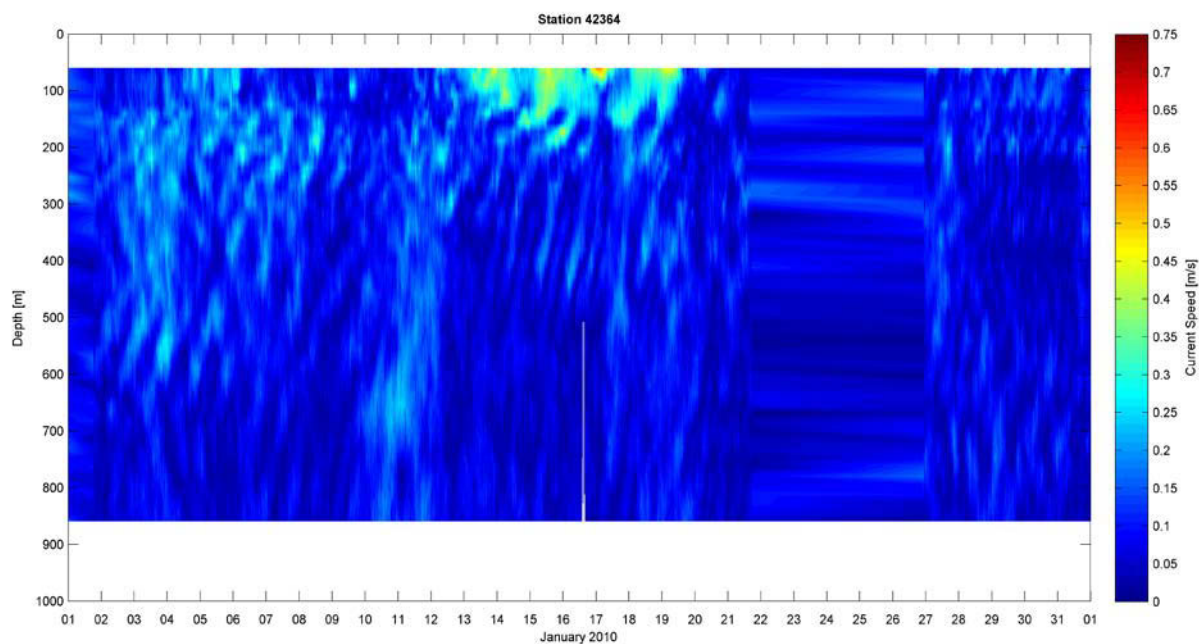


Figure 4-49 Current Speed Contour at NTL Station 42364 – January 2010

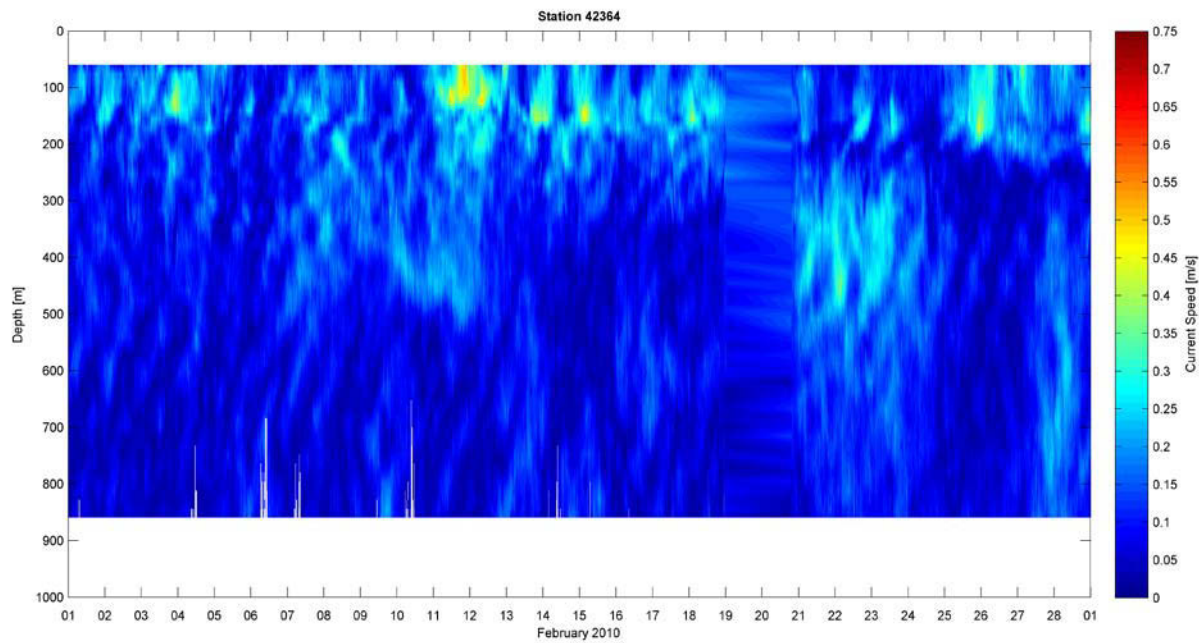


Figure 4-50 Current Speed Contour at NTL Station 42364 – February 2010

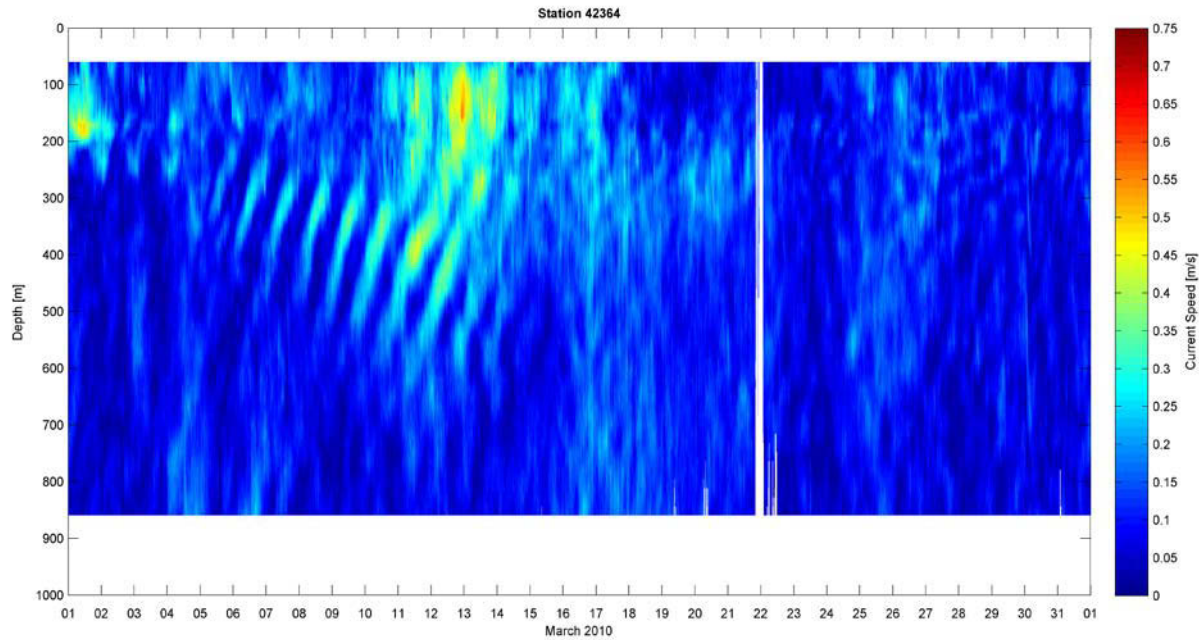


Figure 4-51 Current Speed Contour at NTL Station 42364 – March 2010

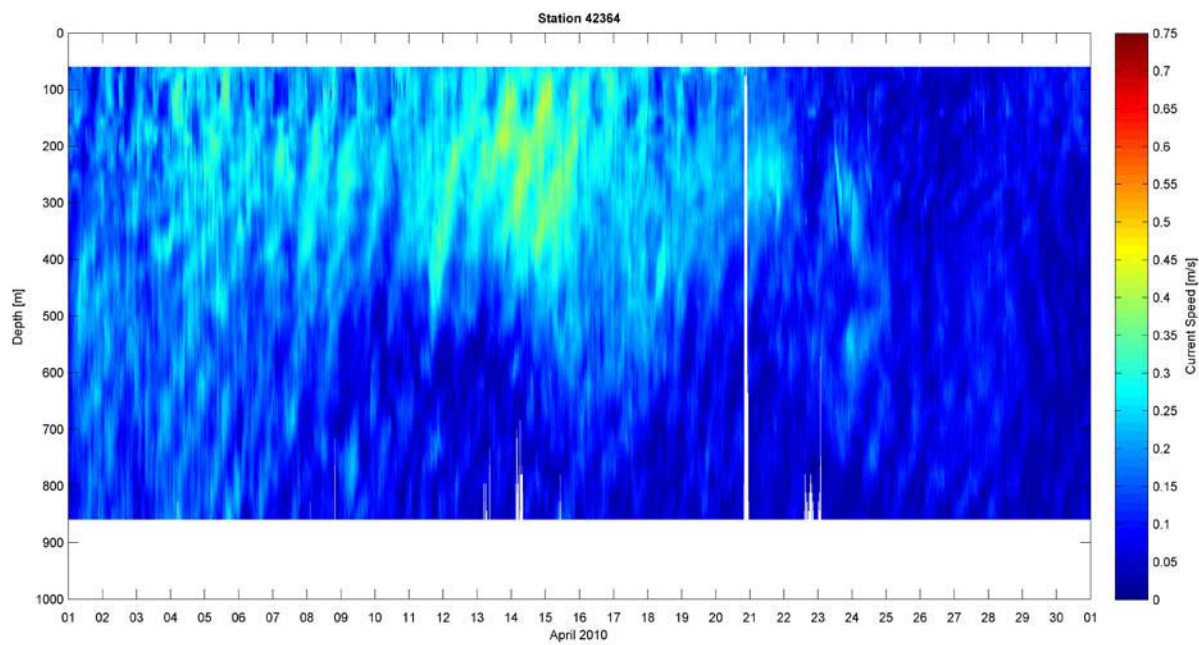


Figure 4-52 Current Speed Contour at NTL Station 42364 – April 2010

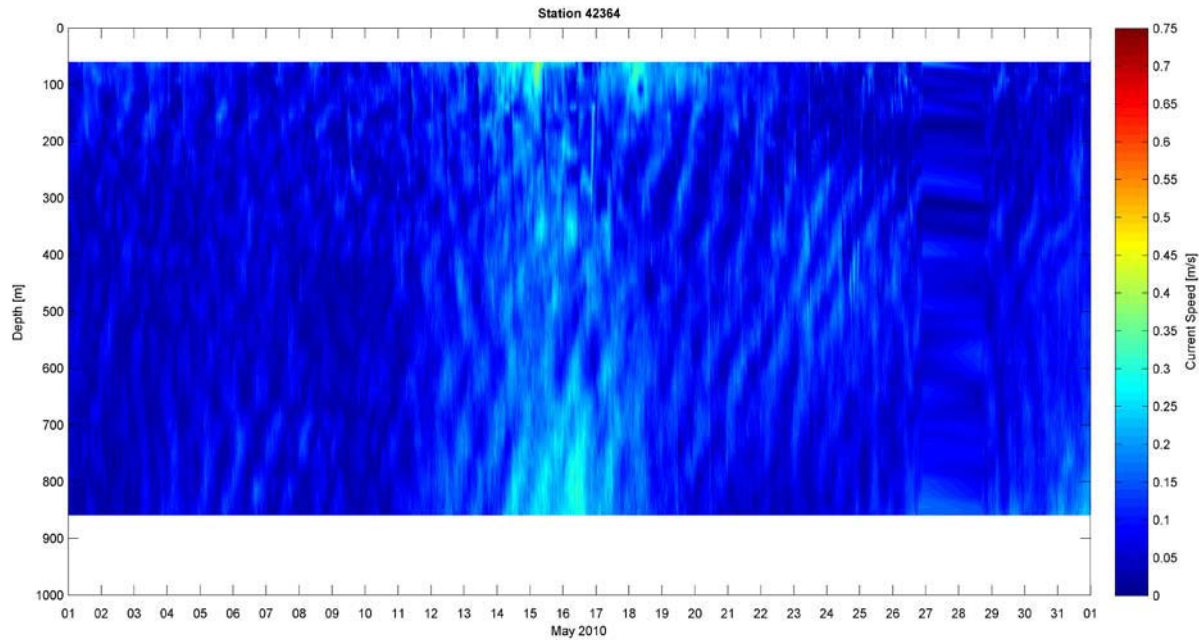


Figure 4-53 Current Speed Contour at NTL Station 42364 – May 2010

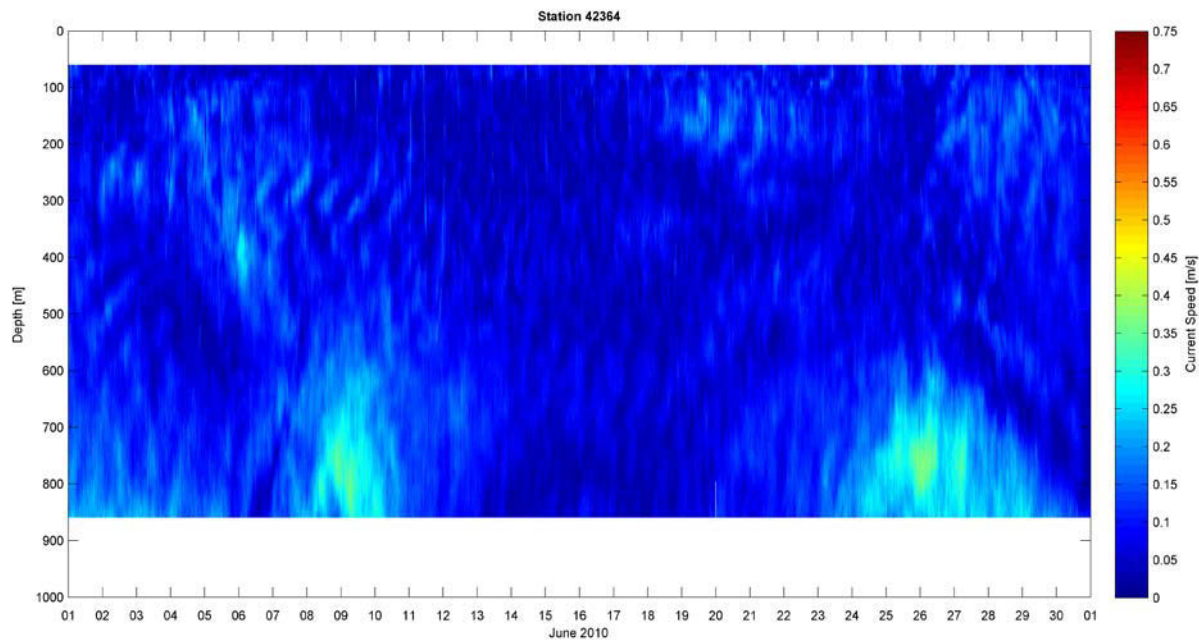


Figure 4-54 Current Speed Contour at NTL Station 42364 – June 2010

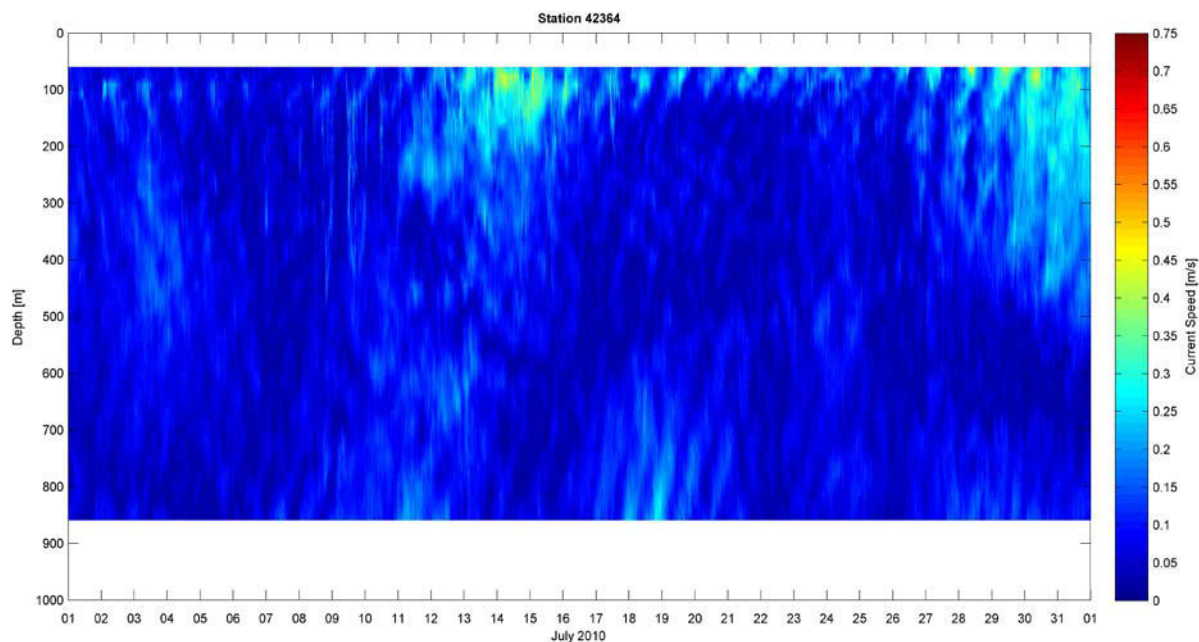


Figure 4-55 Current Speed Contour at NTL Station 42364 – July 2010

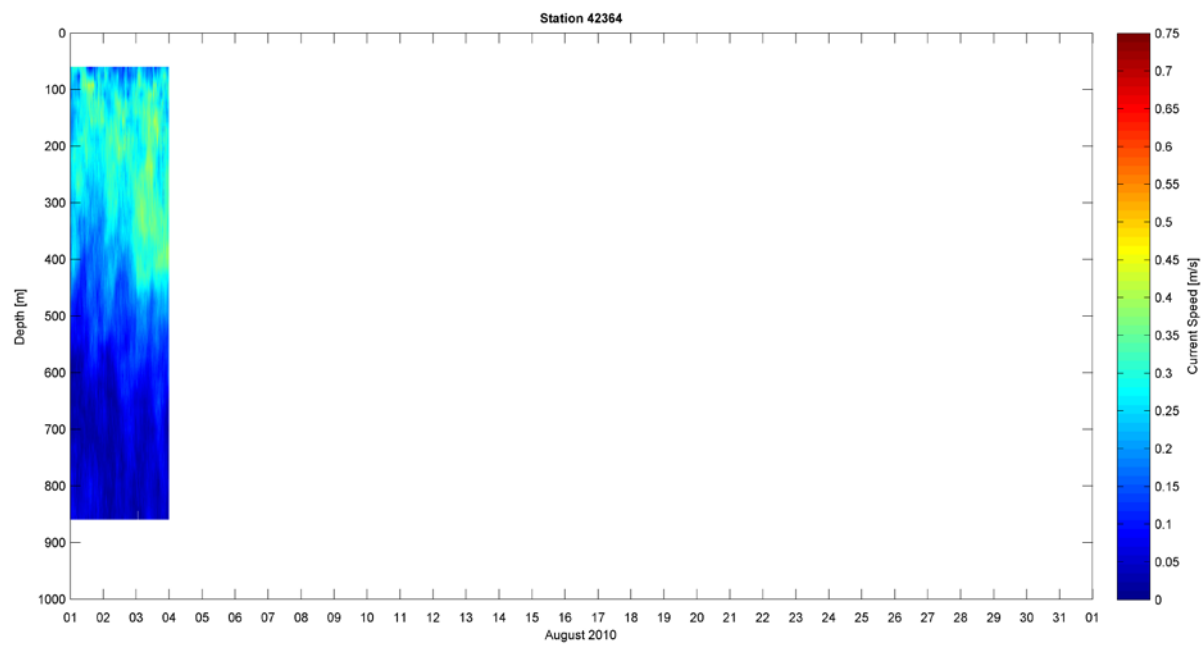


Figure 4-56 Current Speed Contour at NTL Station 42364 – August 2010

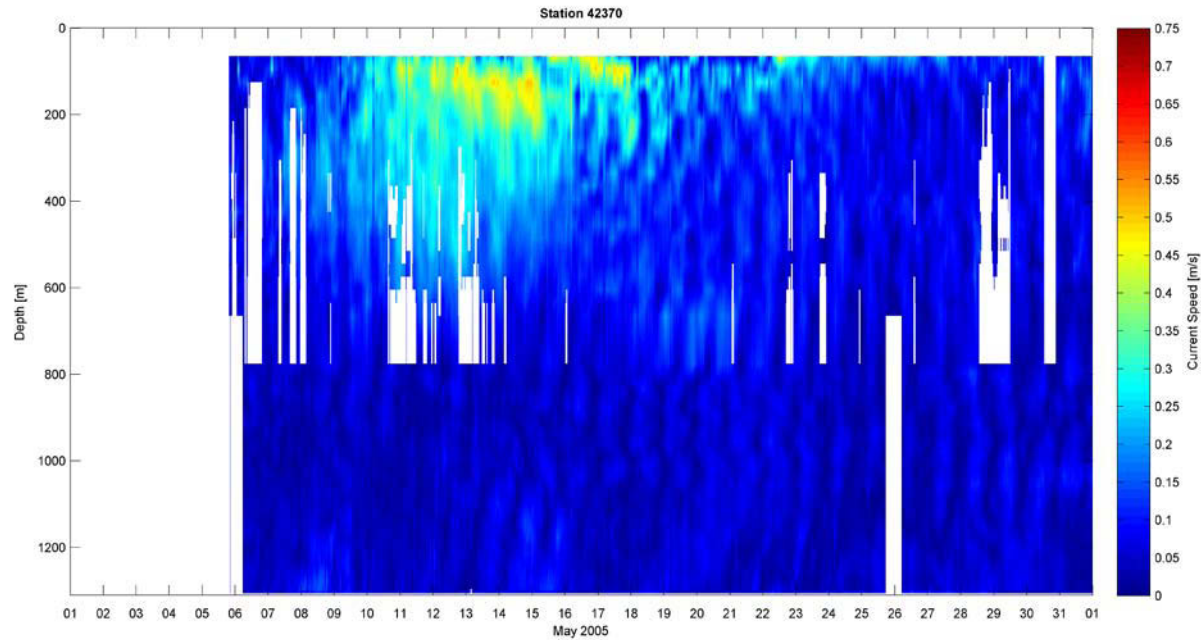


Figure 4-57 Current Speed Contour at NTL Station 42370 – May 2005

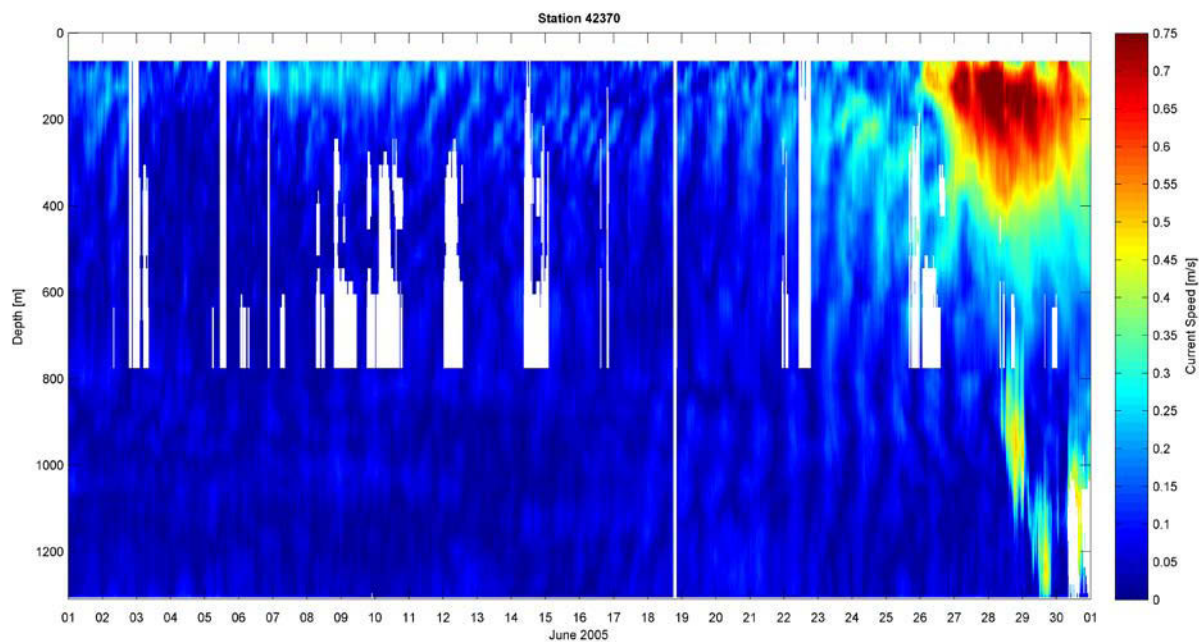


Figure 4-58 Current Speed Contour at NTL Station 42370 – June 2005

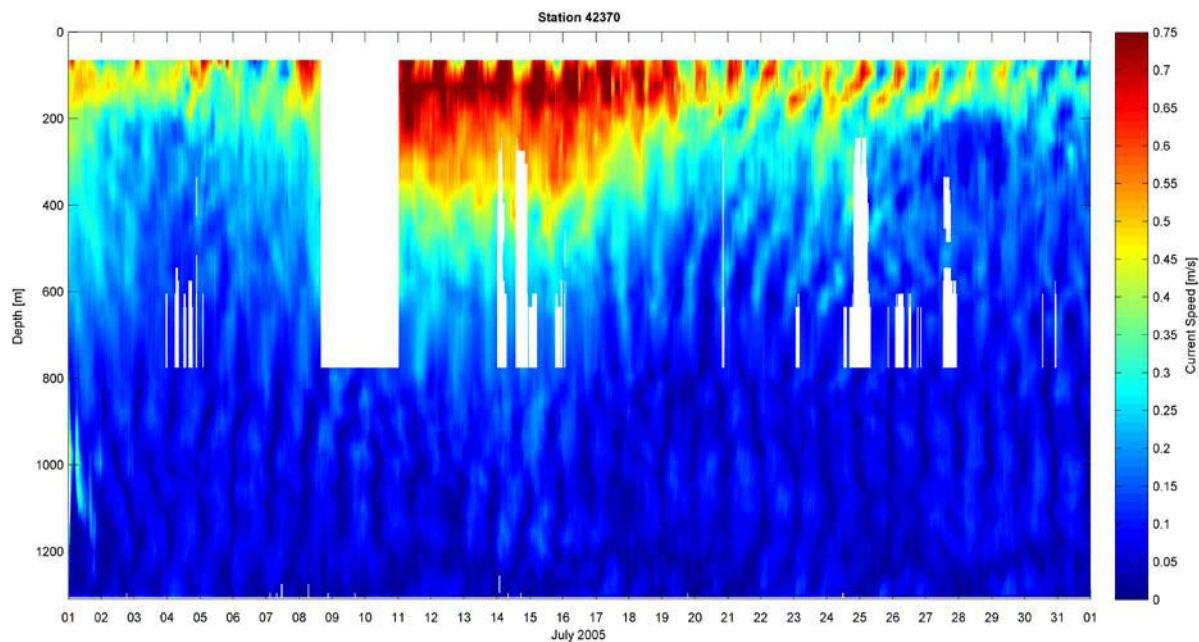


Figure 4-59 Current Speed Contour at NTL Station 42370 – July 2005

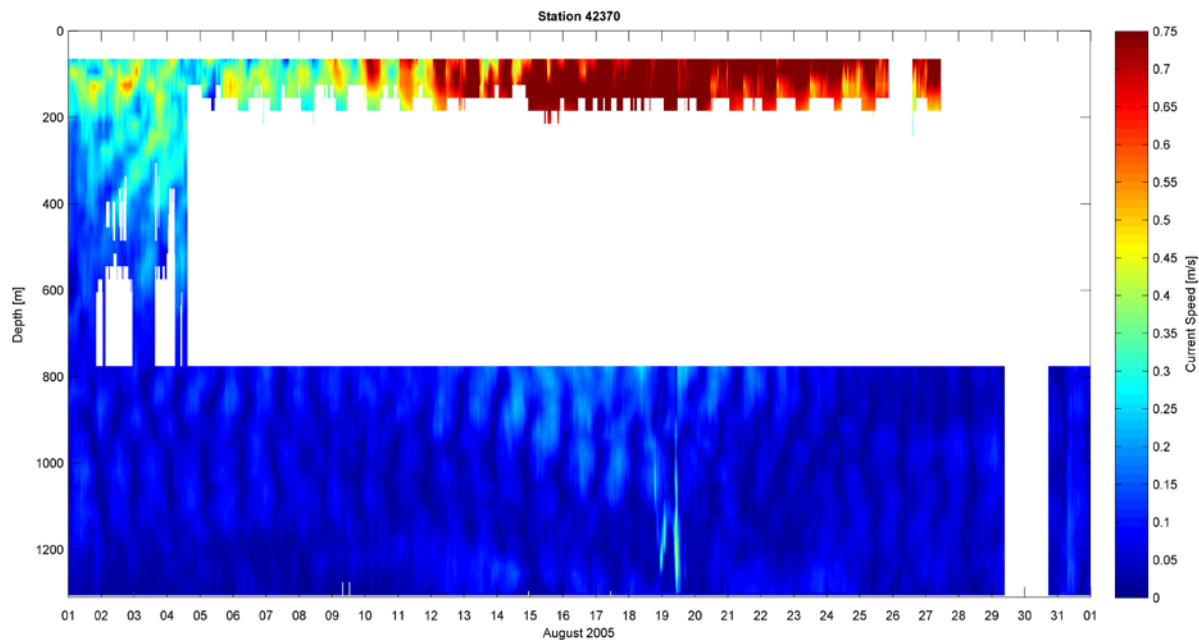


Figure 4-60 Current Speed Contour at NTL Station 42370 – August 2005

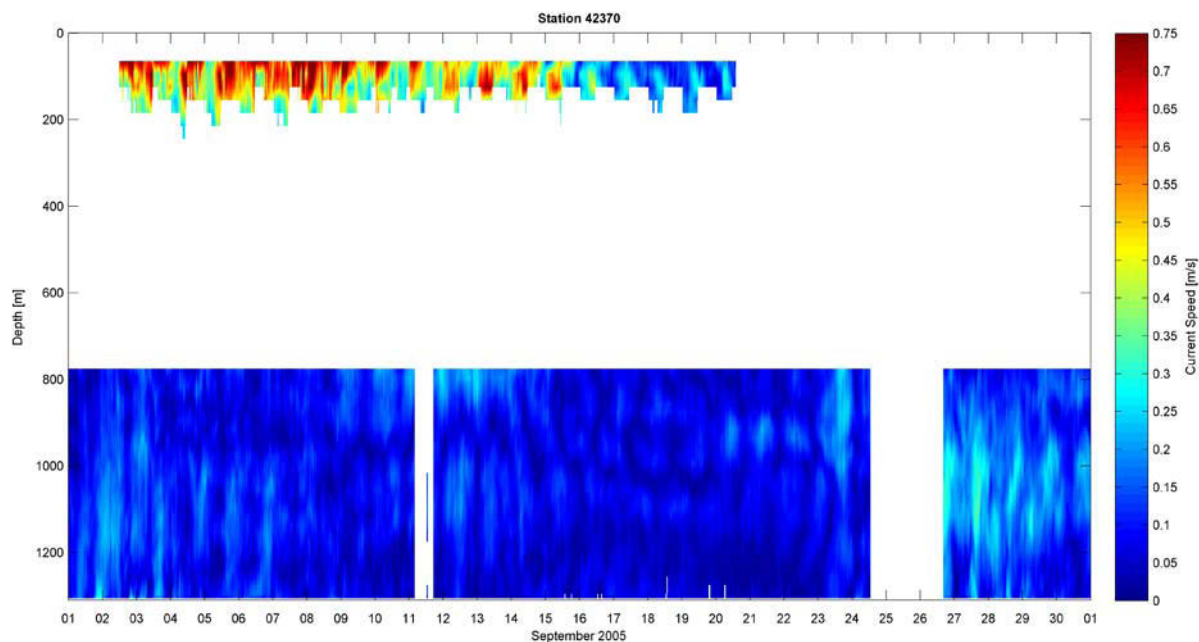


Figure 4-61 Current Speed Contour at NTL Station 42370 – September 2005

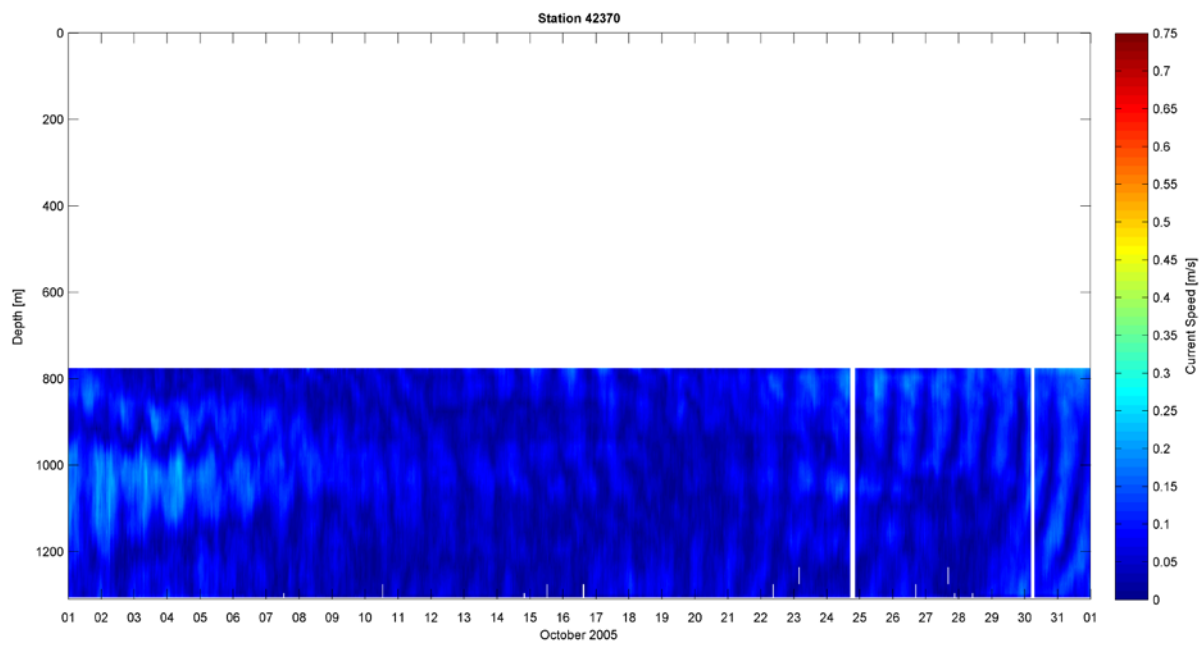


Figure 4-62 Current Speed Contour at NTL Station 42370 – October 2005

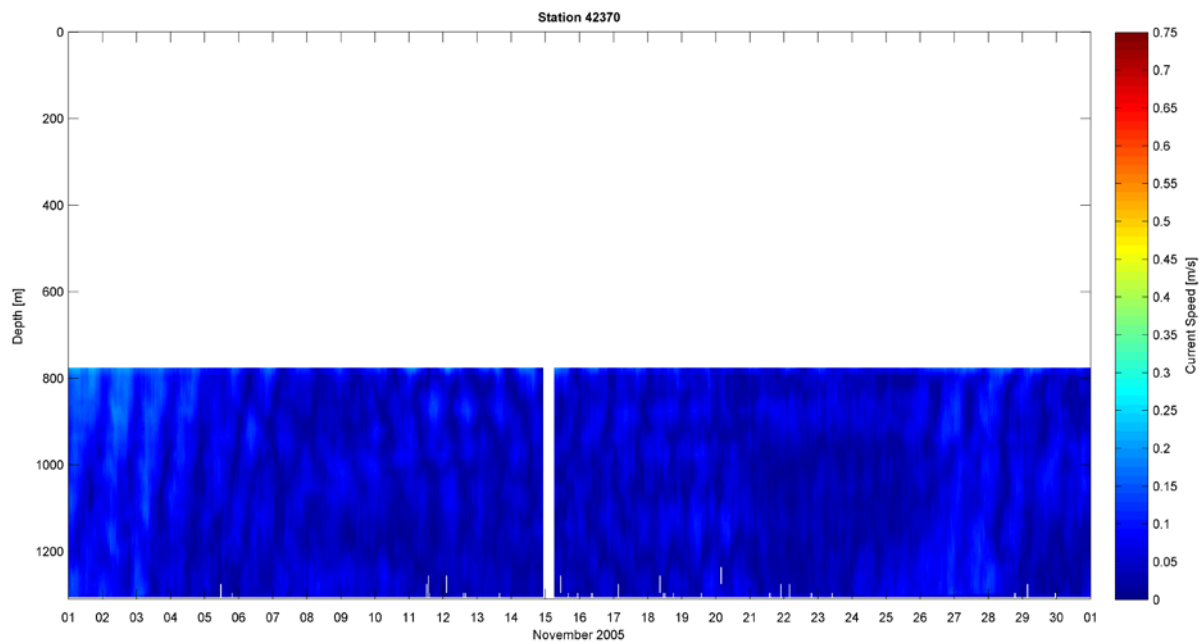


Figure 4-63 Current Speed Contour at NTL Station 42370 – November 2005

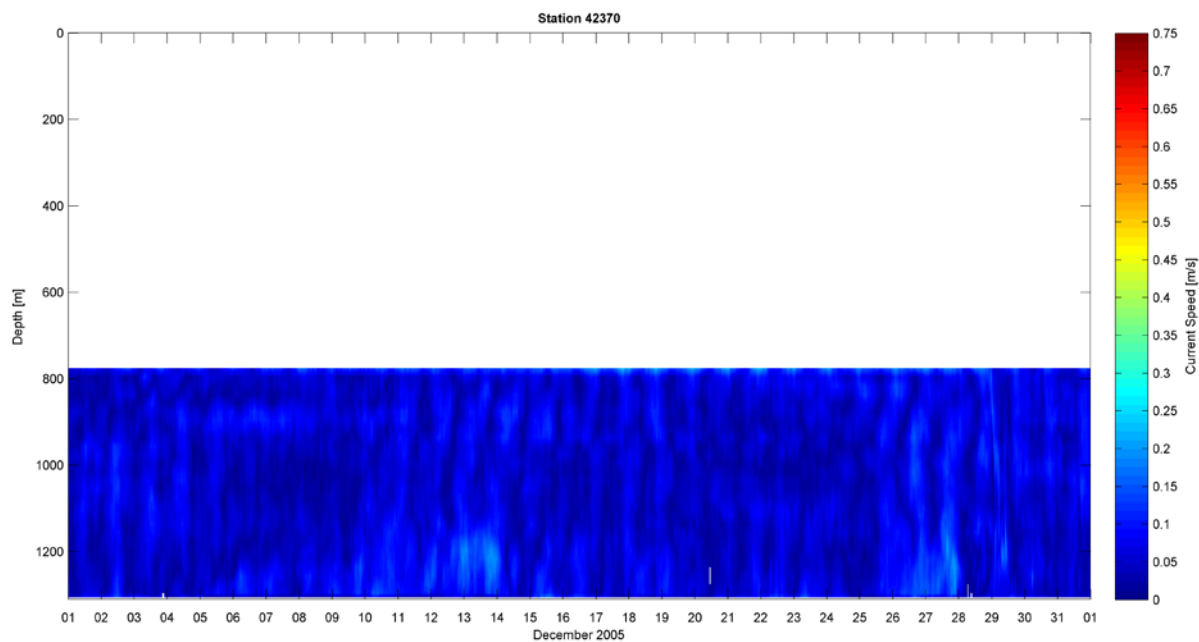


Figure 4-64 Current Speed Contour at NTL Station 42370 – December 2005

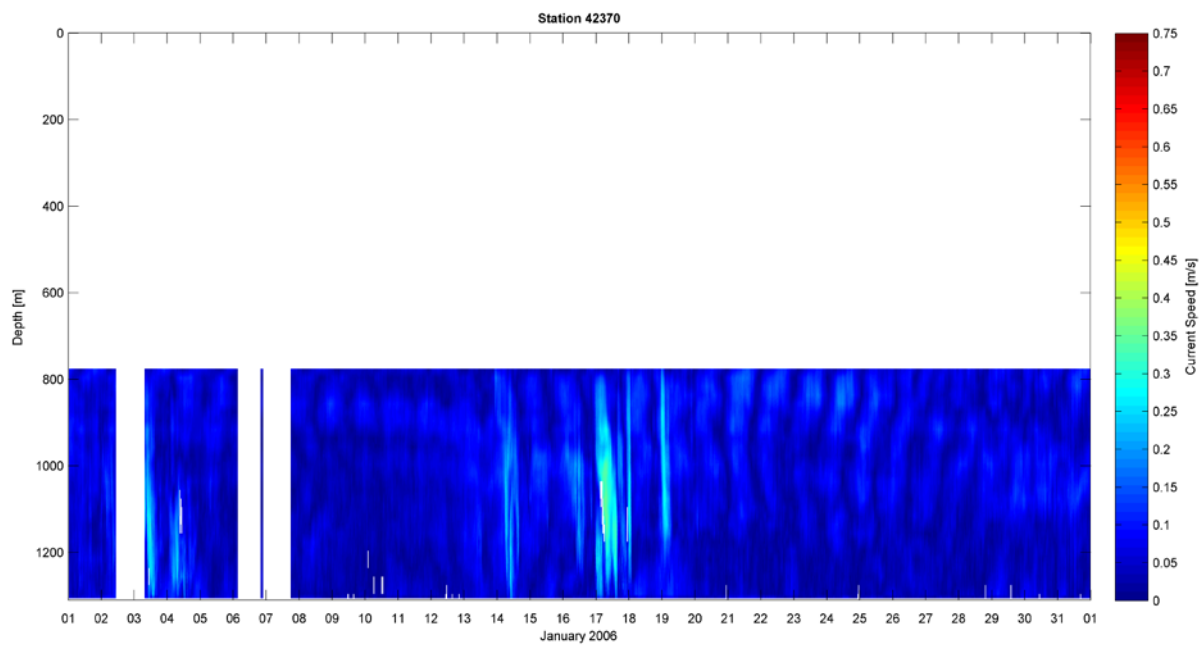


Figure 4-65 Current Speed Contour at NTL Station 42370 – January 2006

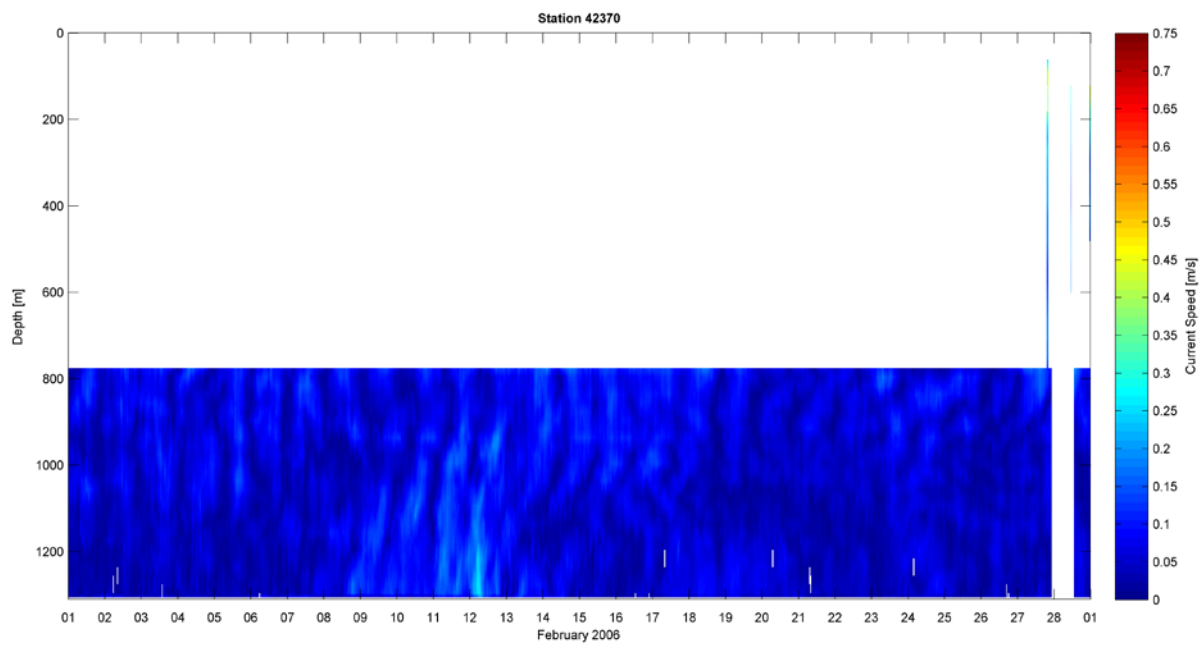


Figure 4-66 Current Speed Contour at NTL Station 42370 – February 2006

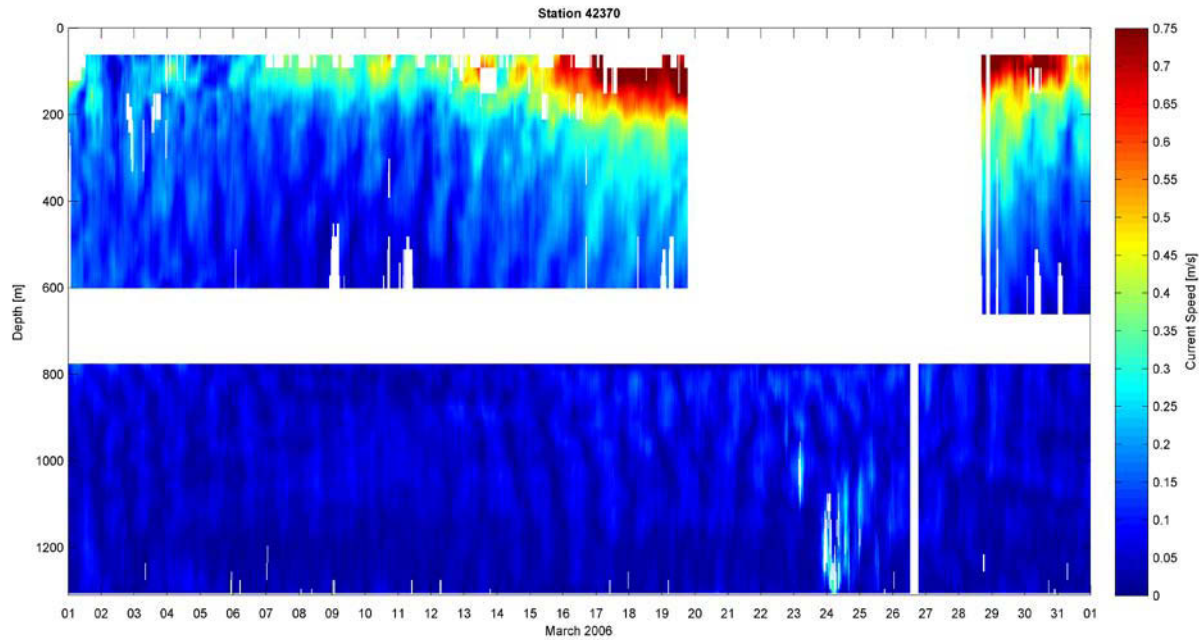


Figure 4-67 Current Speed Contour at NTL Station 42370 – March 2006

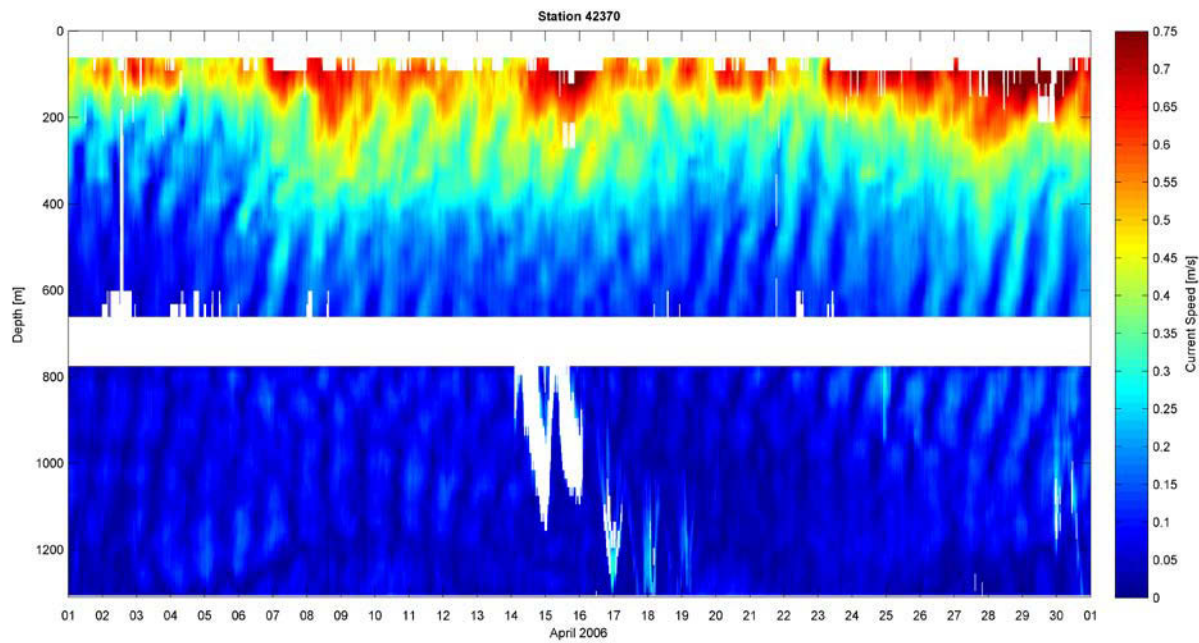


Figure 4-68 Current Speed Contour at NTL Station 42370 – April 2006

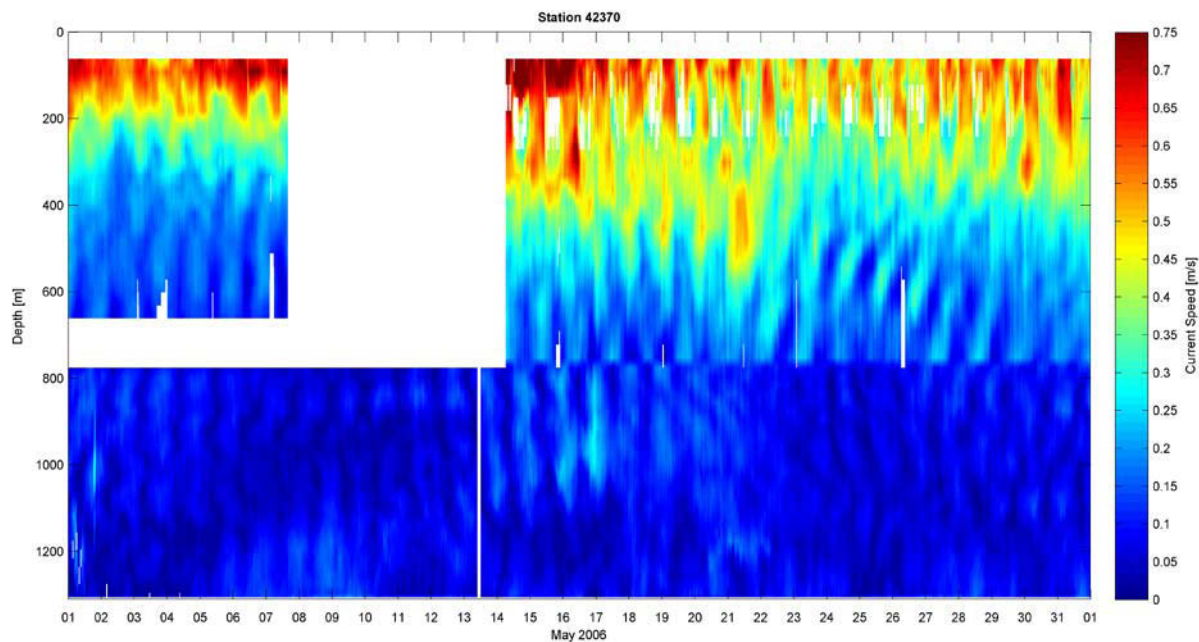


Figure 4-69 Current Speed Contour at NTL Station 42370 – May 2006

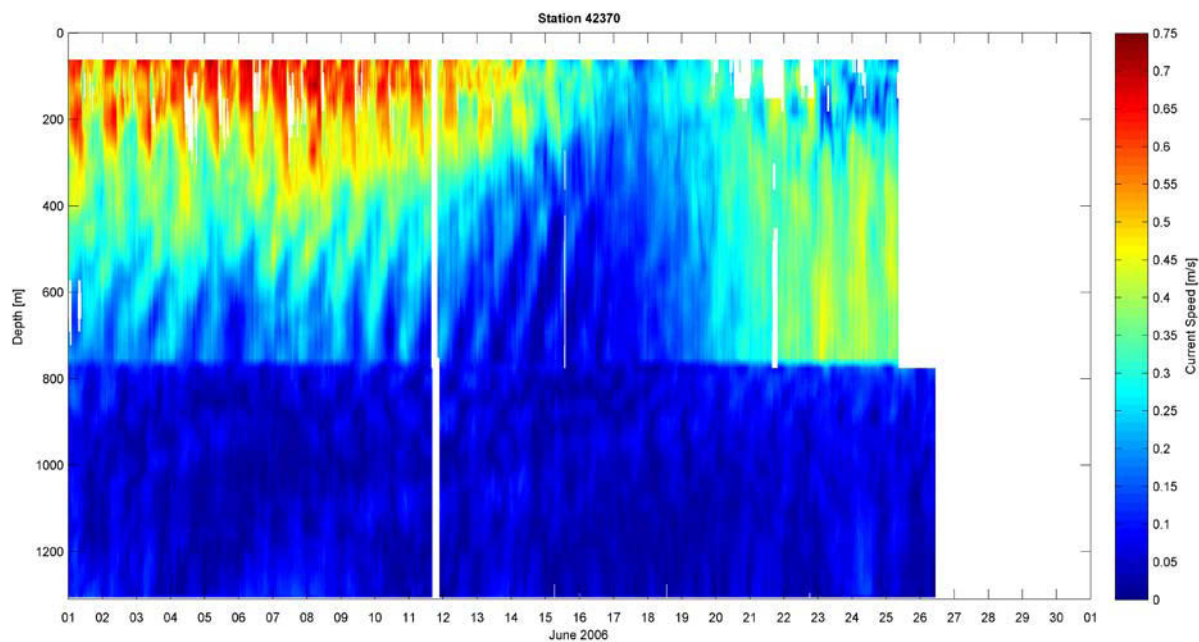


Figure 4-70 Current Speed Contour at NTL Station 42370 – June 2006

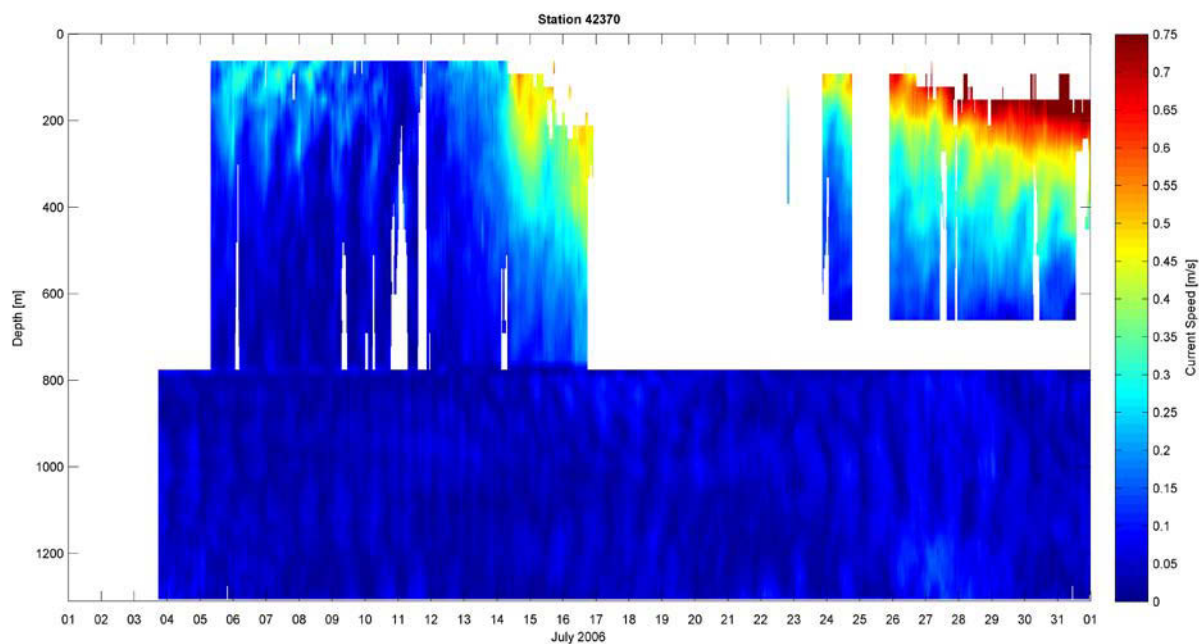


Figure 4-71 Current Speed Contour at NTL Station 42370 – July 2006

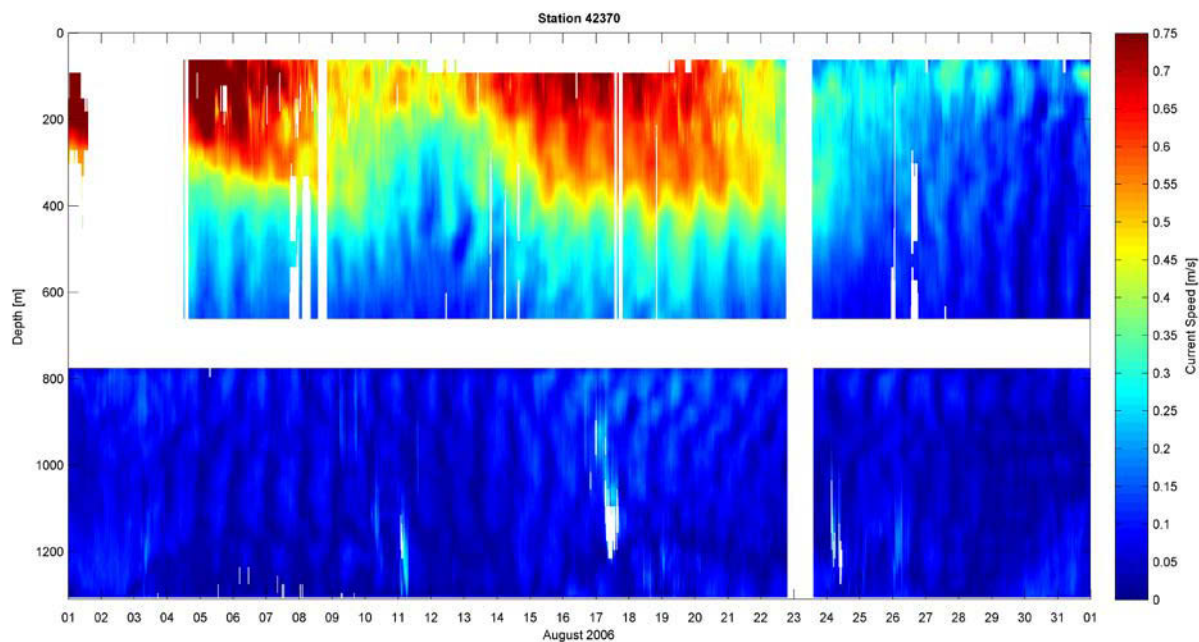


Figure 4-72 Current Speed Contour at NTL Station 42370 – August 2006

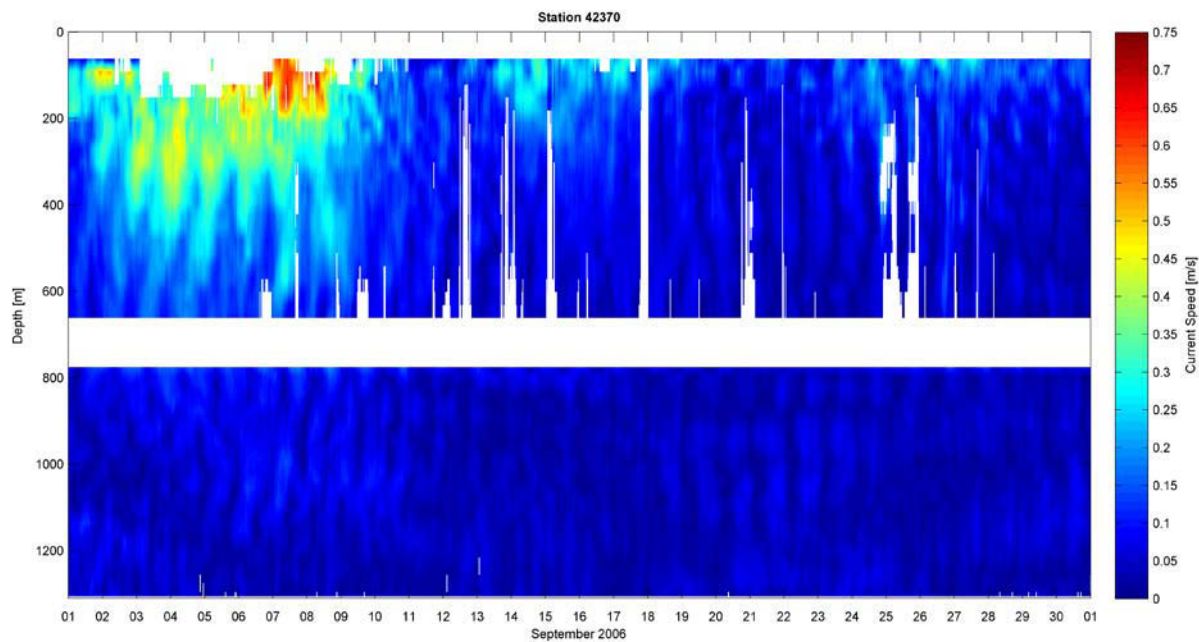


Figure 4-73 Current Speed Contour at NTL Station 42370 – September 2006

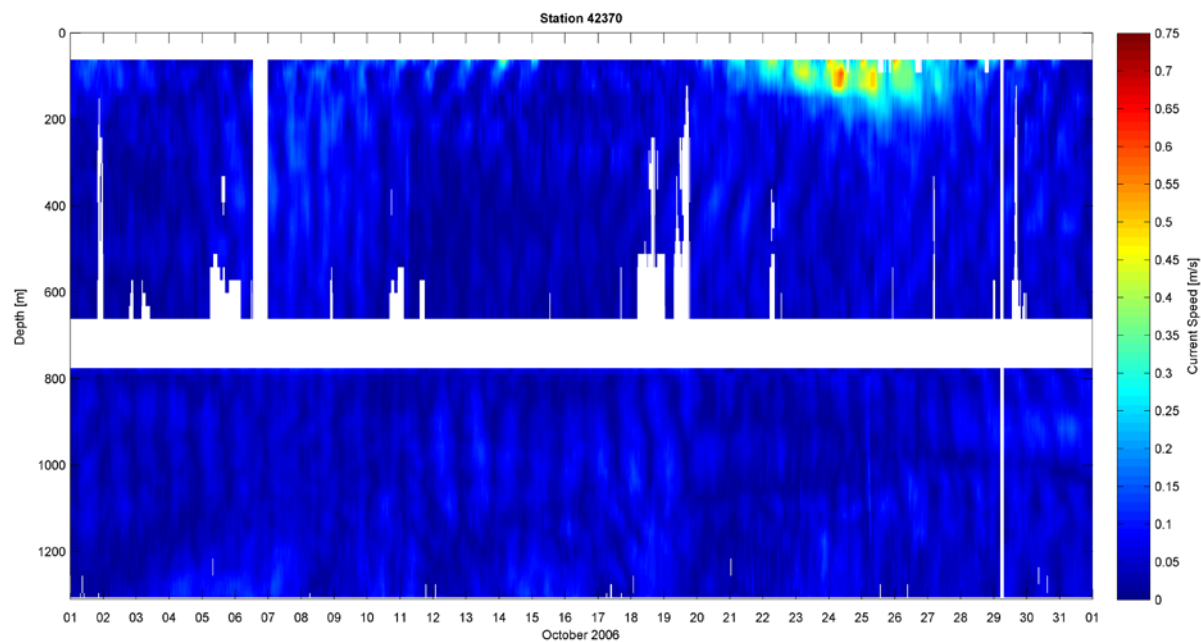


Figure 4-74 Current Speed Contour at NTL Station 42370 – October 2006

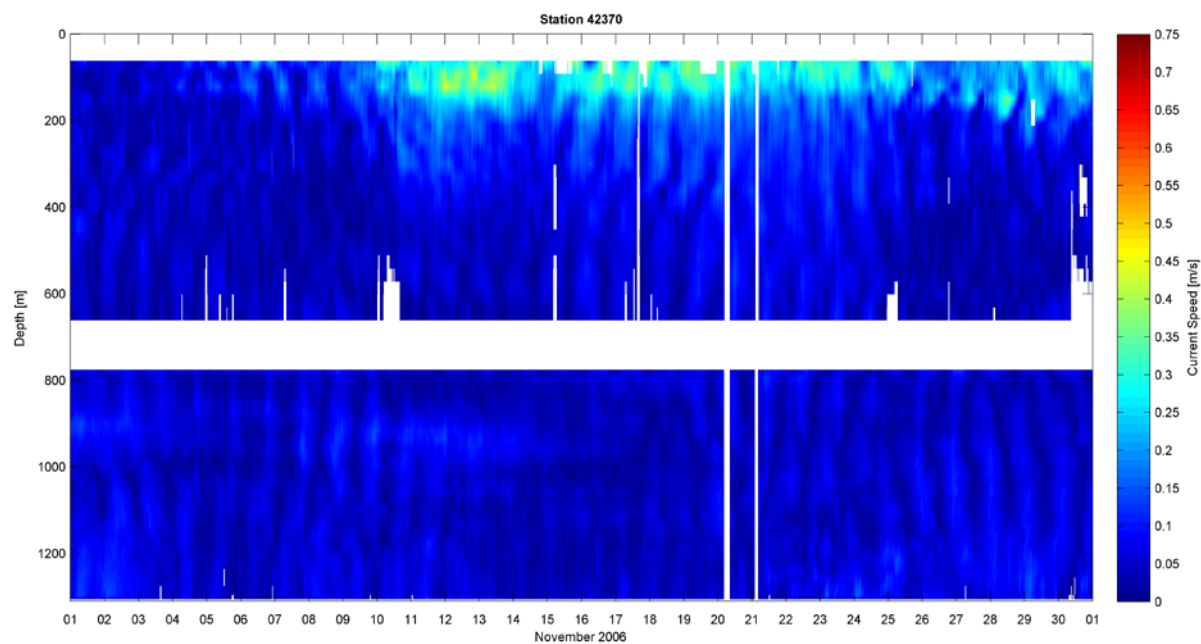


Figure 4-75 Current Speed Contour at NTL Station 42370 – November 2006

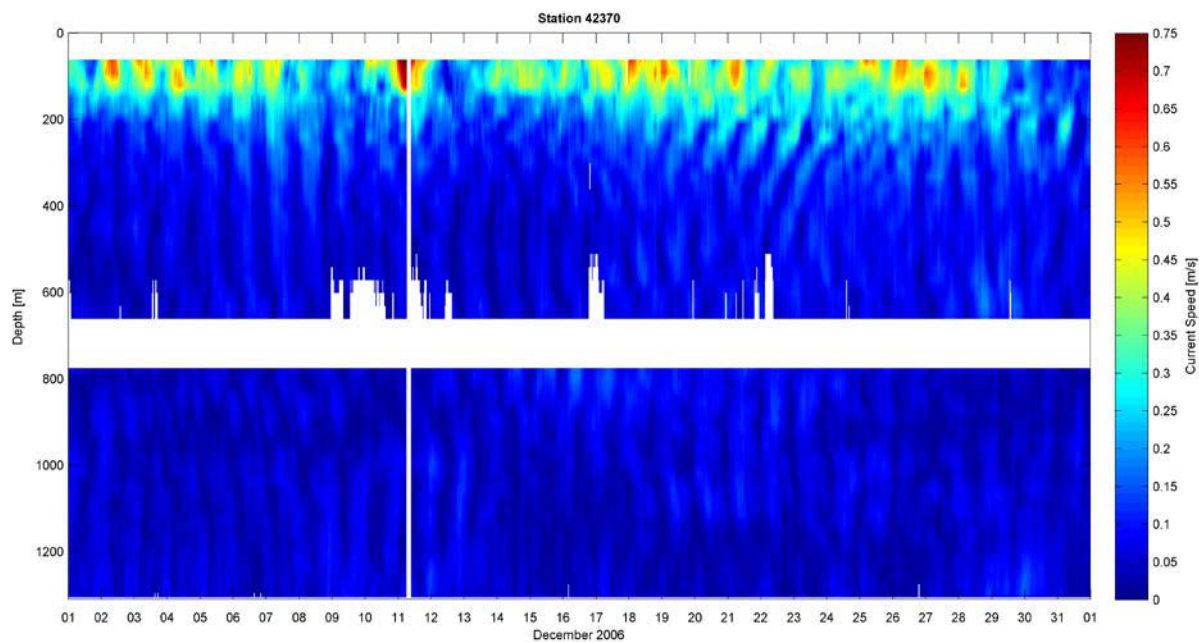


Figure 4-76 Current Speed Contour at NTL Station 42370 – December 2006

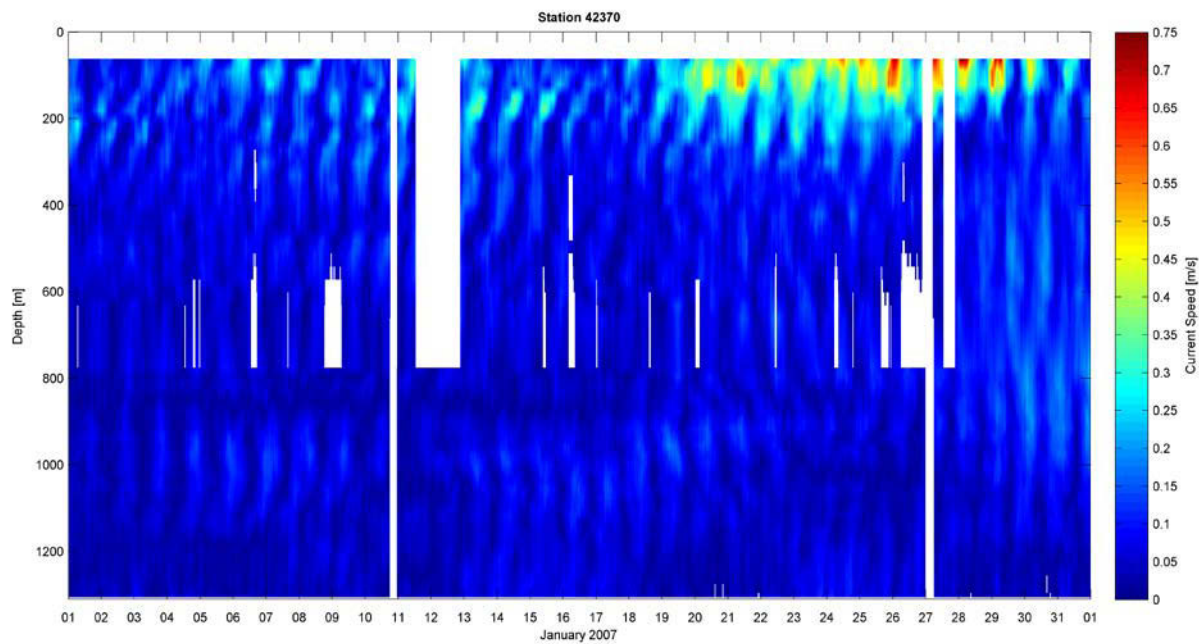


Figure 4-77 Current Speed Contour at NTL Station 42370 – January 2007

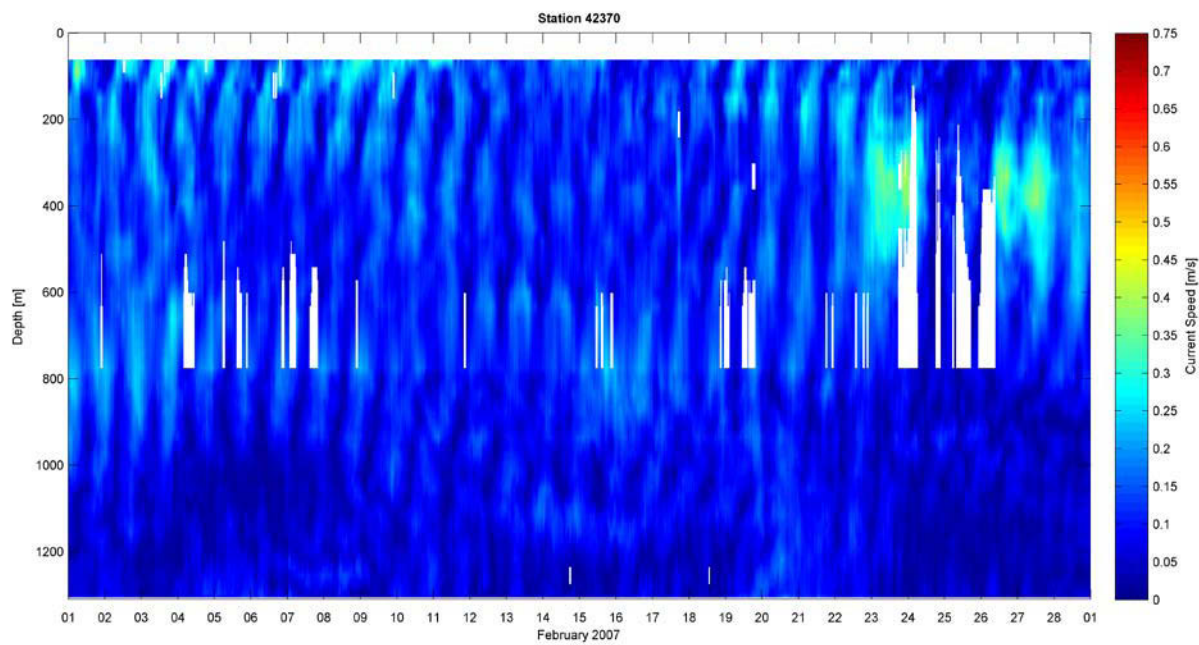


Figure 4-78 Current Speed Contour at NTL Station 42370 – February 2007

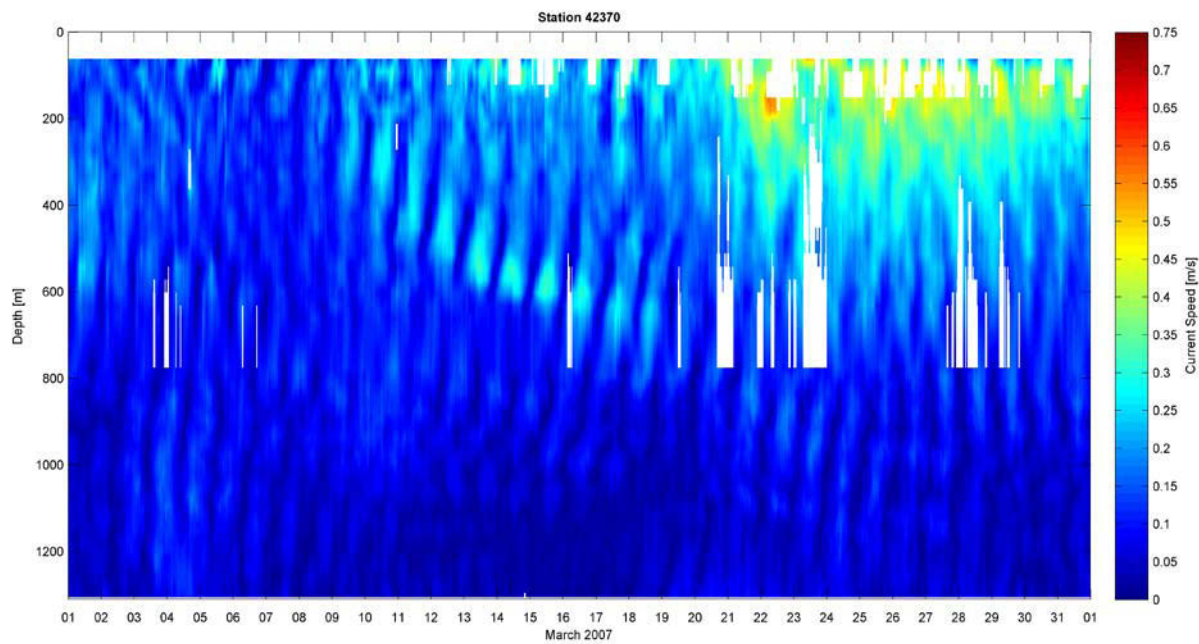


Figure 4-79 Current Speed Contour at NTL Station 42370 – March 2007

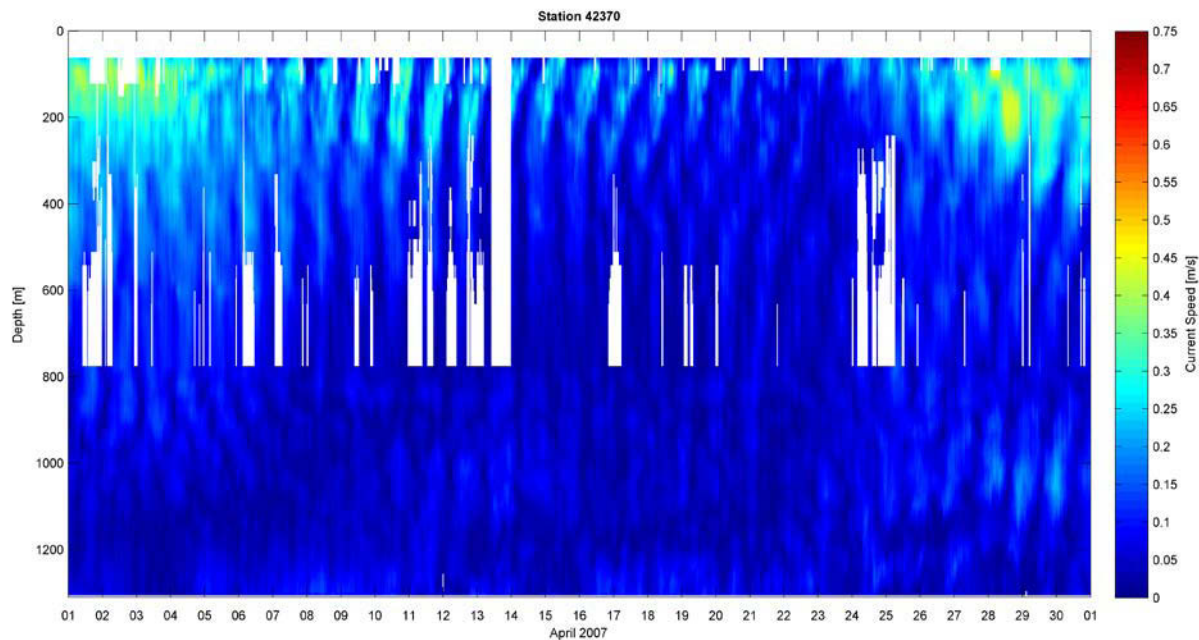


Figure 4-80 Current Speed Contour at NTL Station 42370 – April 2007

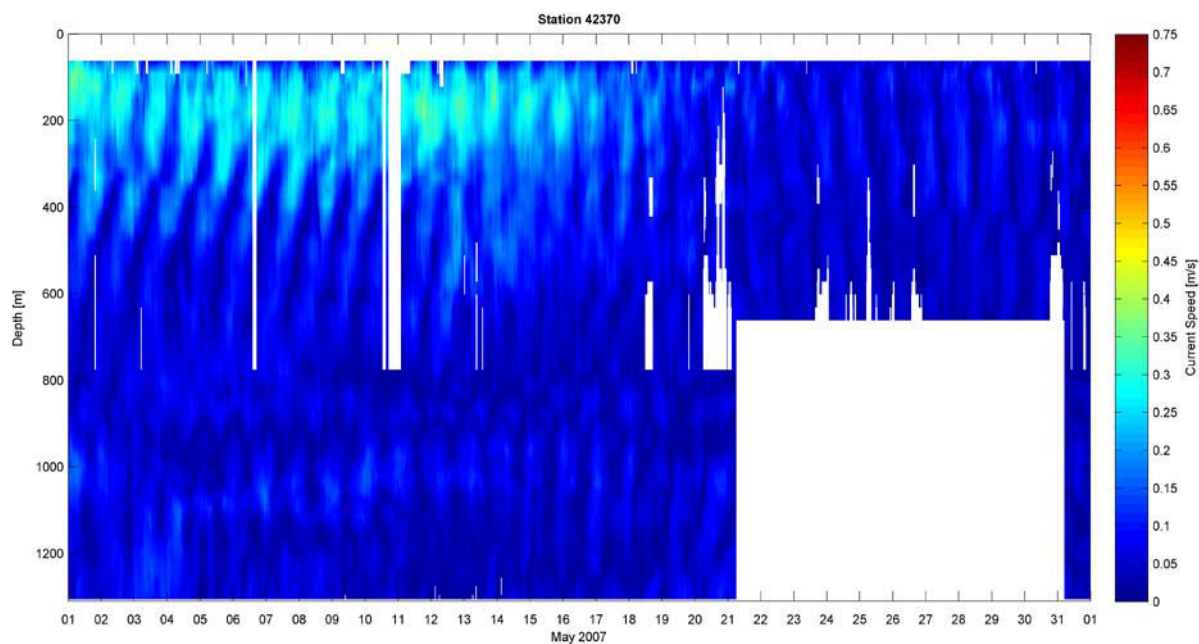


Figure 4-81 Current Speed Contour at NTL Station 42370 – May 2007

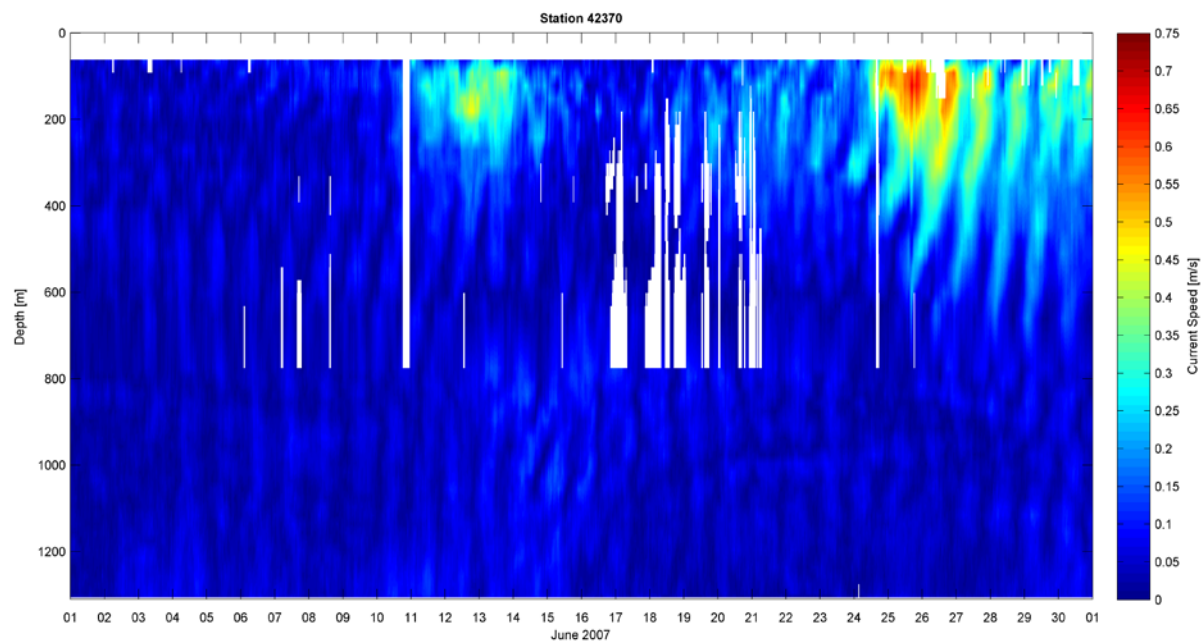


Figure 4-82 Current Speed Contour at NTL Station 42370 – June 2007

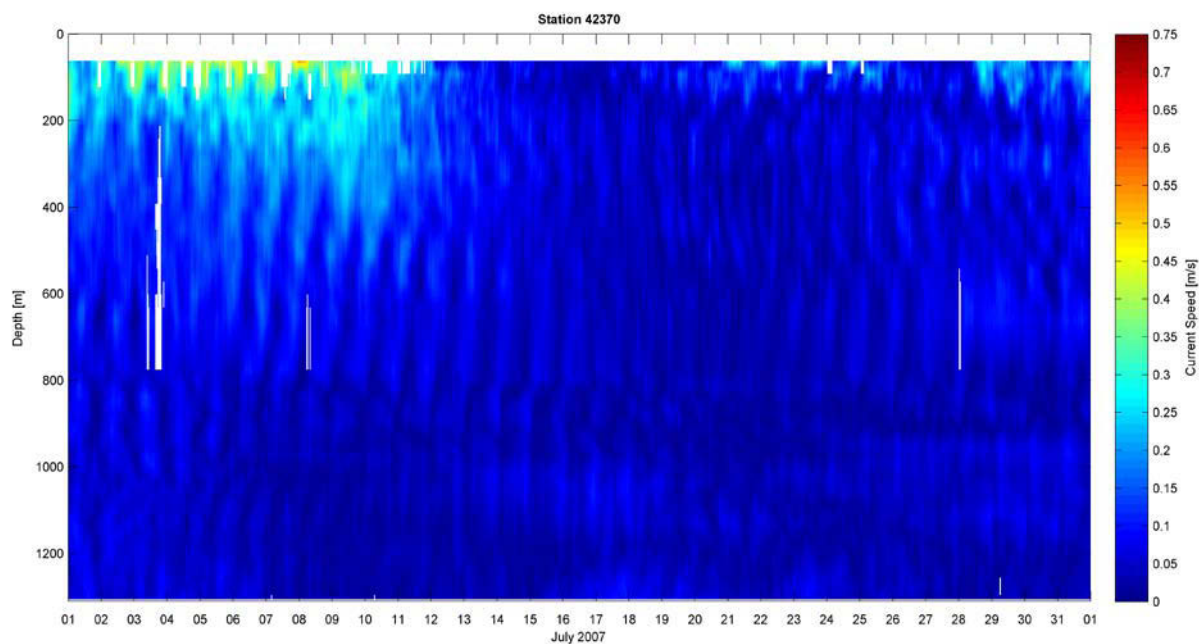


Figure 4-83 Current Speed Contour at NTL Station 42370 – July 2007

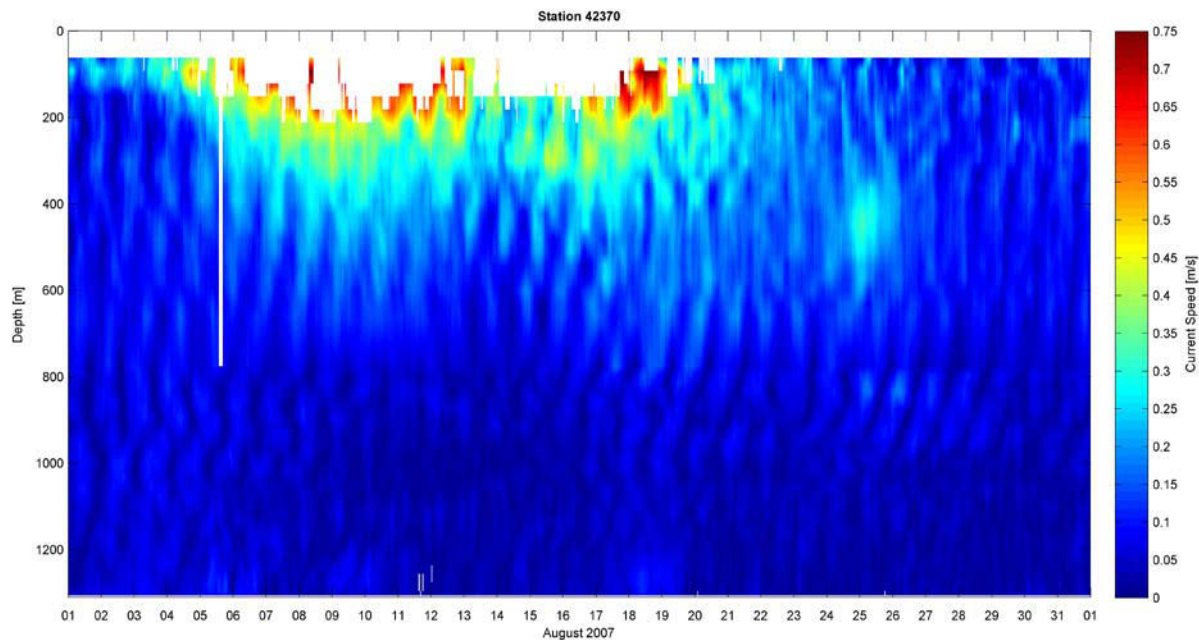


Figure 4-84 Current Speed Contour at NTL Station 42370 – Agust 2007

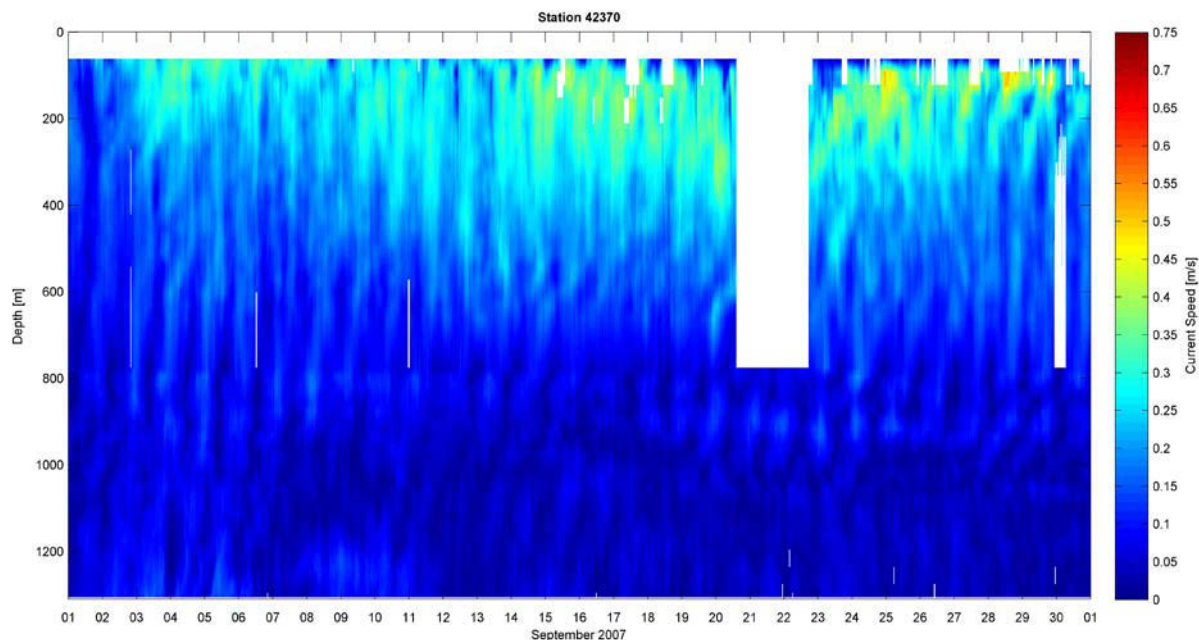


Figure 4-85 Current Speed Contour at NTL Station 42370 – September 2007

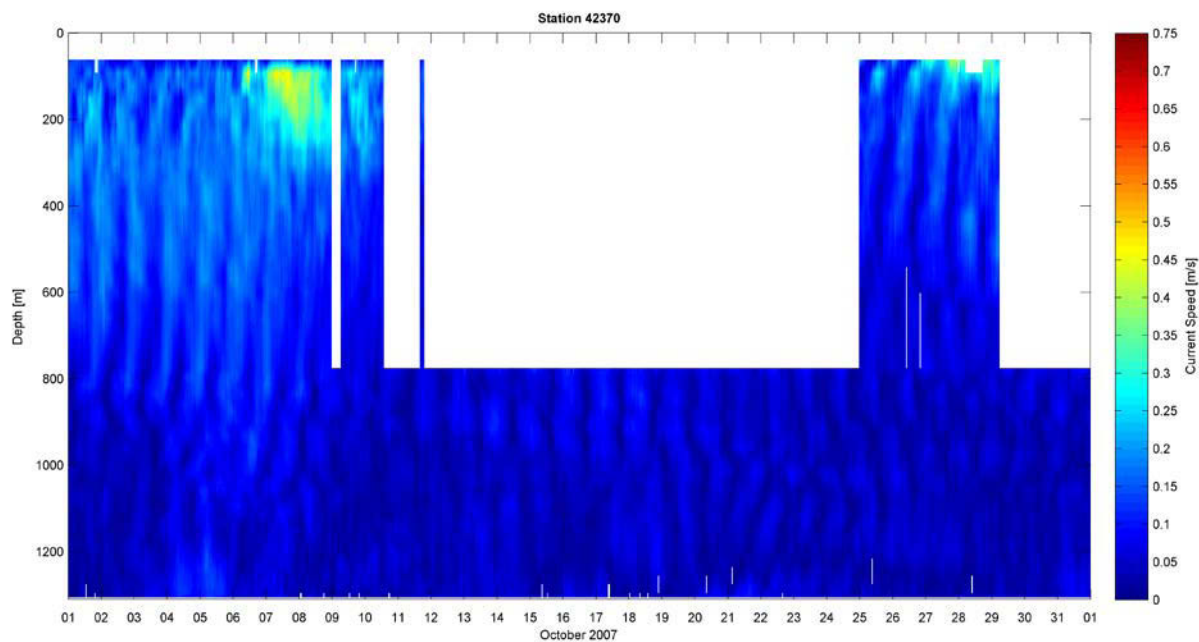


Figure 4-86 Current Speed Contour at NTL Station 42370 – October 2007

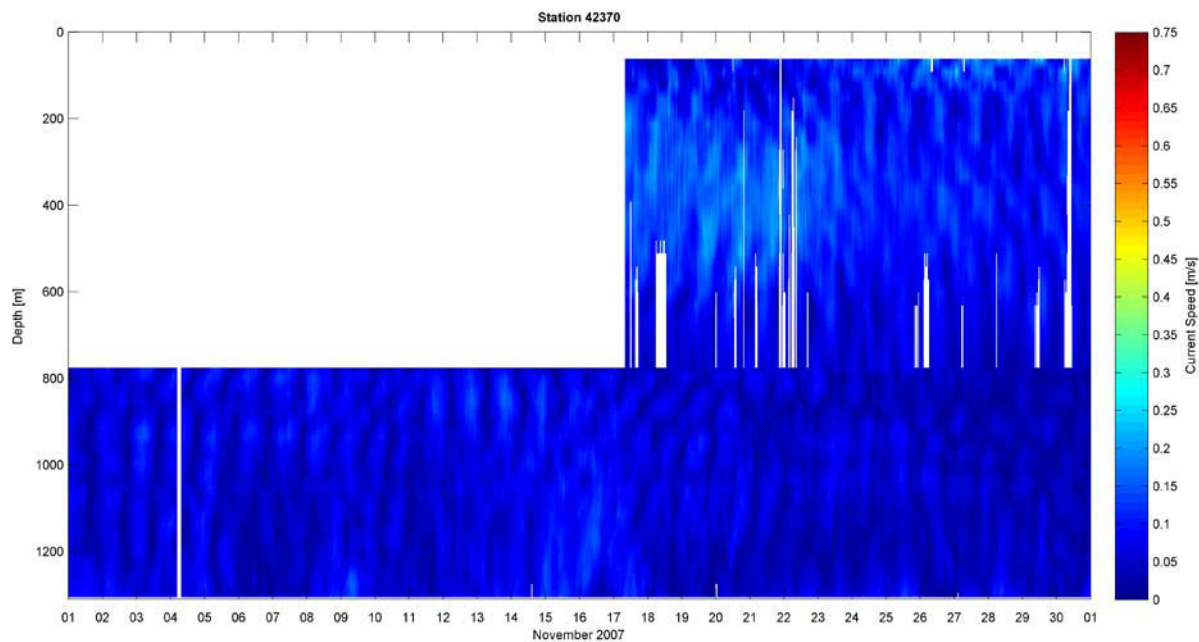


Figure 4-87 Current Speed Contour at NTL Station 42370 – November 2007

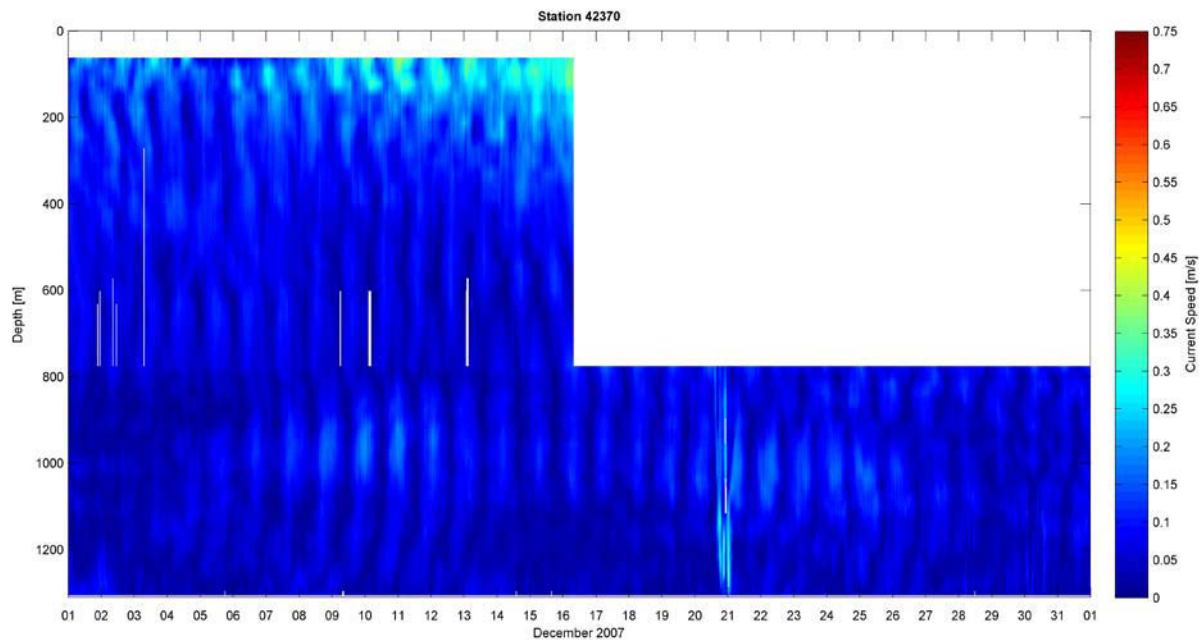


Figure 4-88 Current Speed Contour at NTL Station 42370 – December 2007

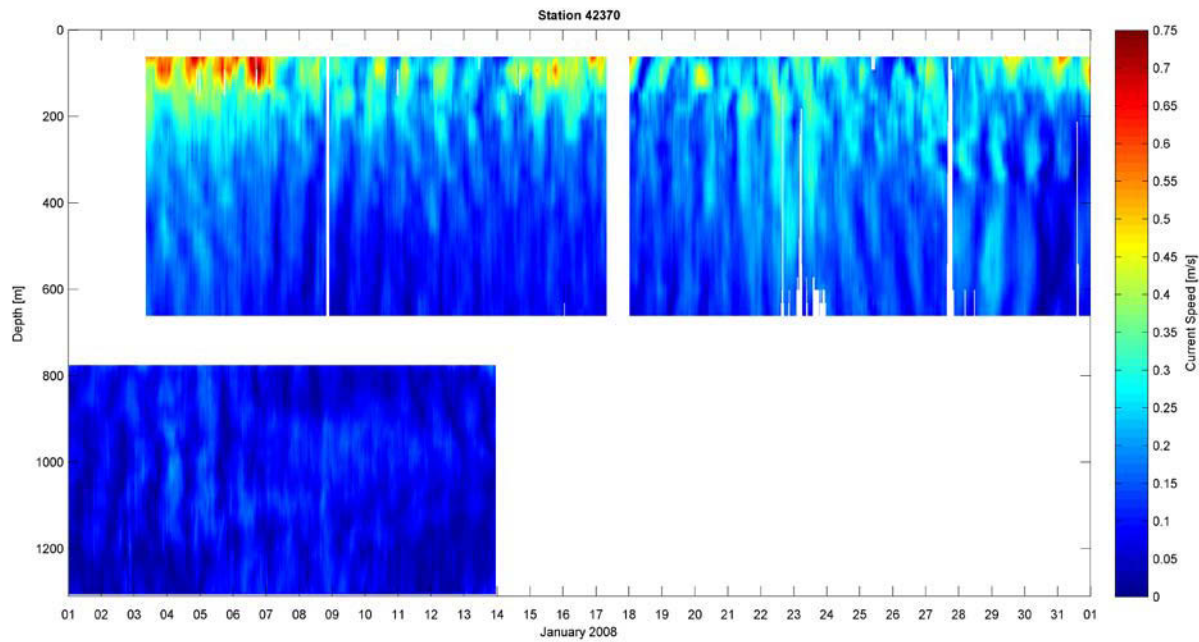


Figure 4-89 Current Speed Contour at NTL Station 42370 – January 2008

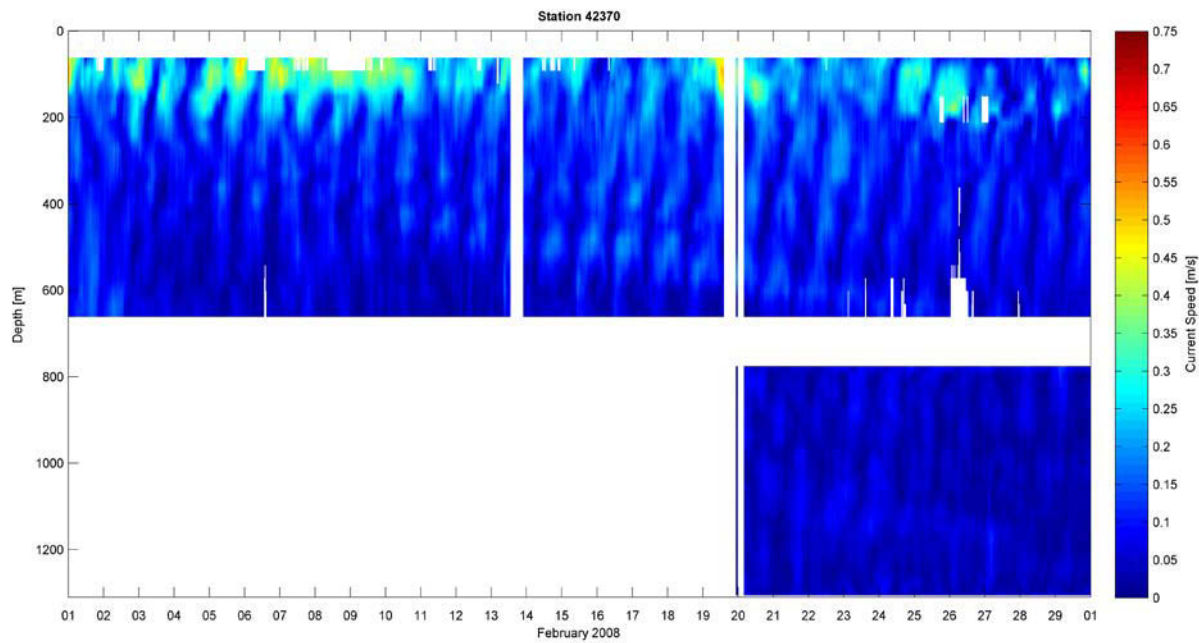


Figure 4-90 Current Speed Contour at NTL Station 42370 – February 2008

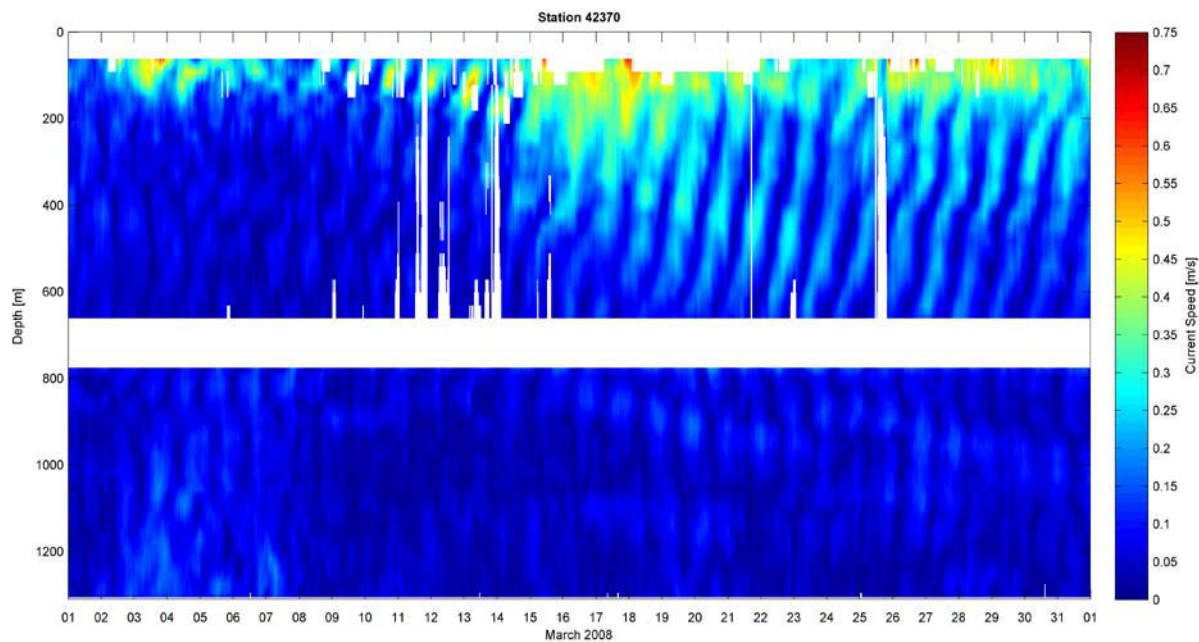


Figure 4-91 Current Speed Contour at NTL Station 42370 – March 2008

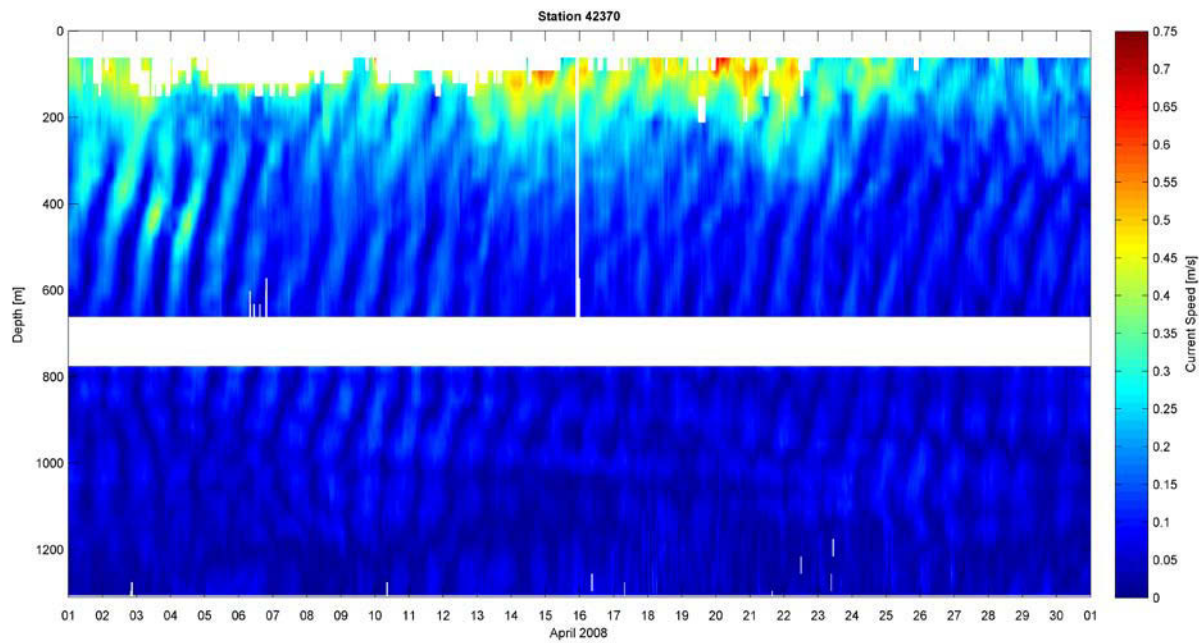


Figure 4-92 Current Speed Contour at NTL Station 42370 – April 2008

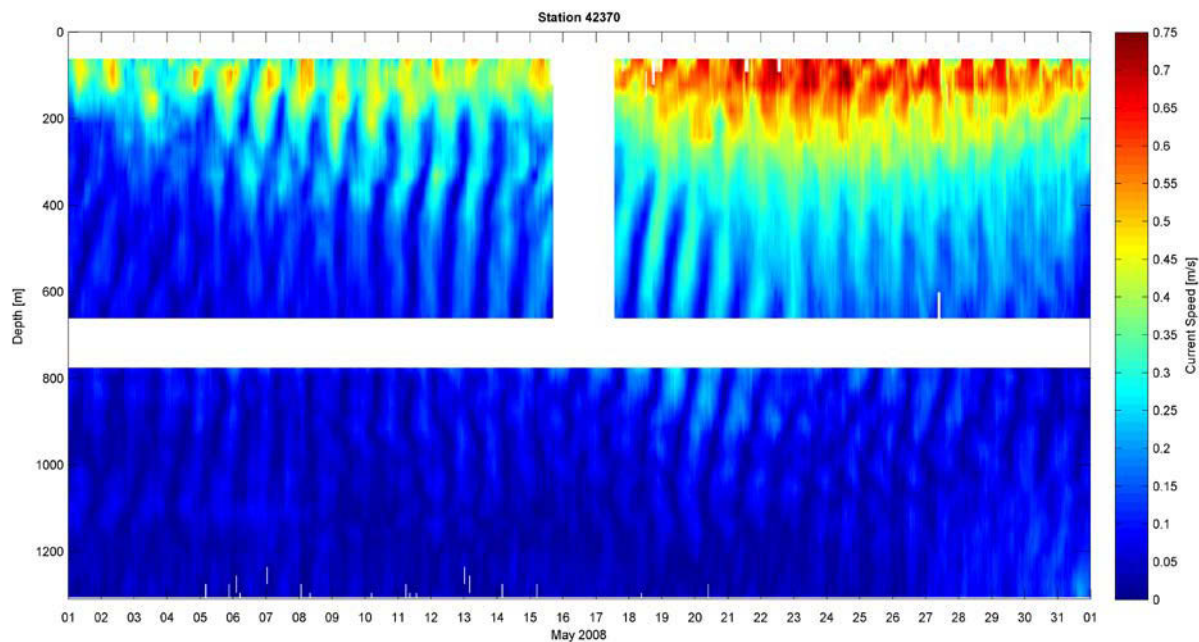


Figure 4-93 Current Speed Contour at NTL Station 42370 – May 2008

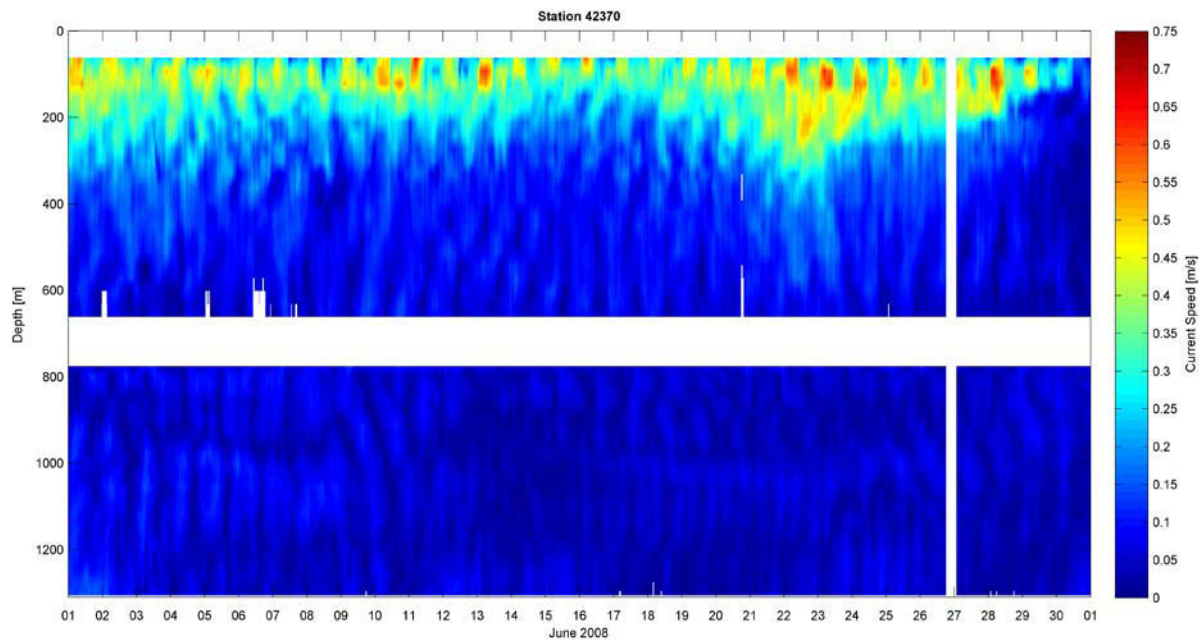


Figure 4-94 Current Speed Contour at NTL Station 42370 – June 2008

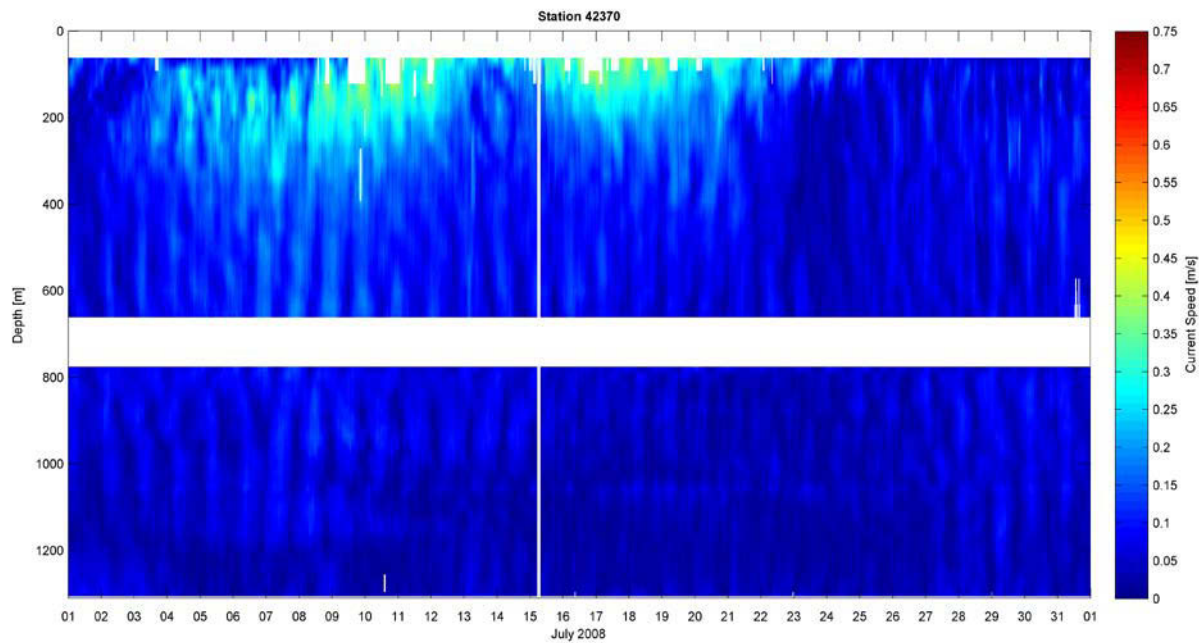


Figure 4-95 Current Speed Contour at NTL Station 42370 – July 2008

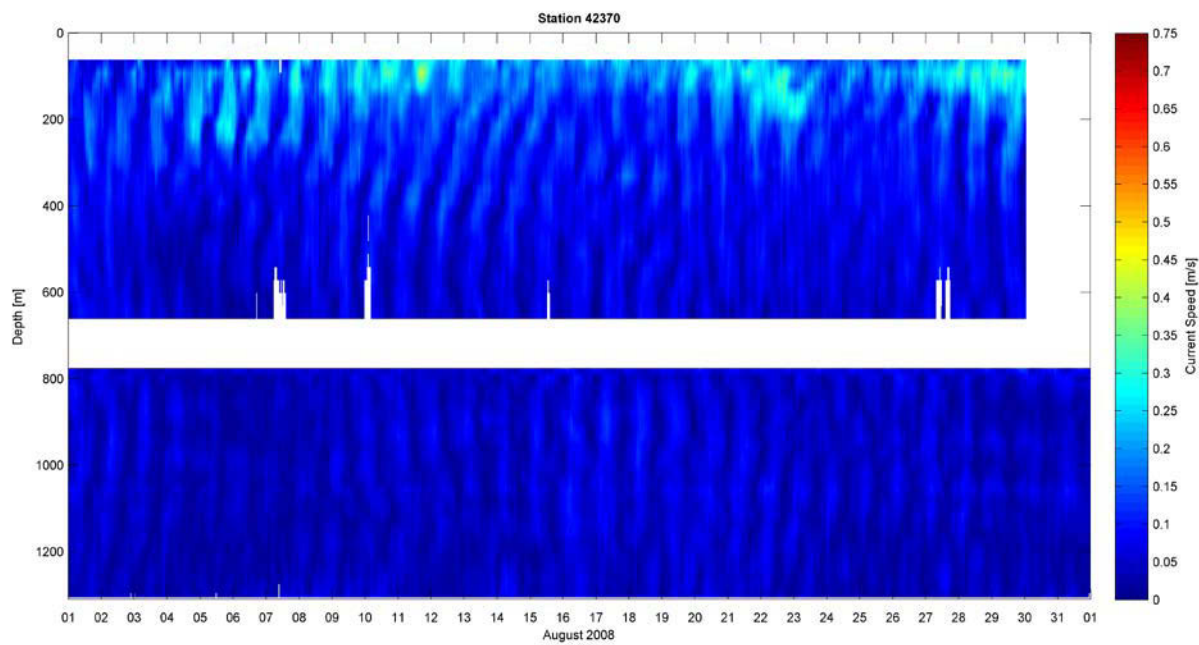


Figure 4-96 Current Speed Contour at NTL Station 42370 – Agust 2008

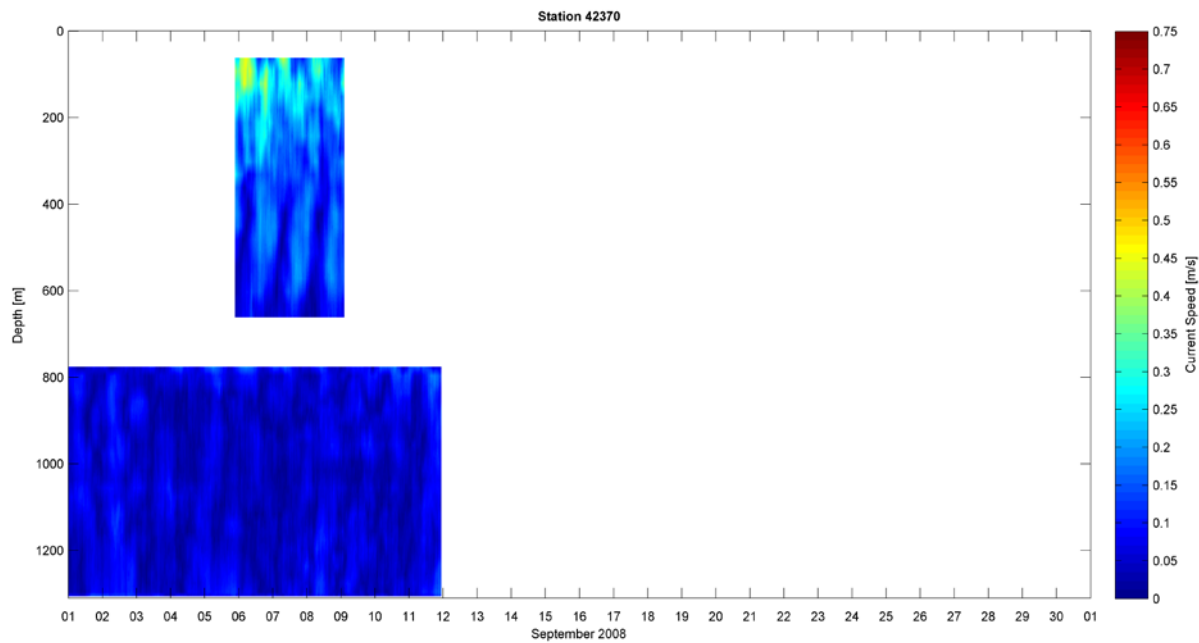


Figure 4-97 Current Speed Contour at NTL Station 42370 – September 2008

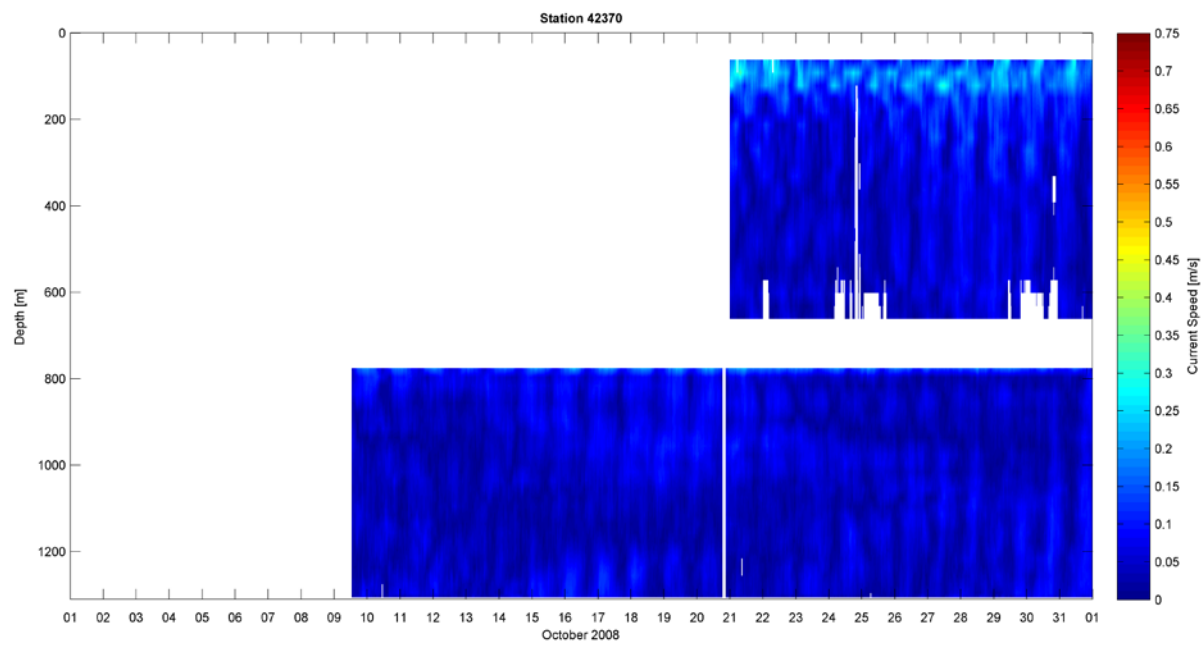


Figure 4-98 Current Speed Contour at NTL Station 42370 – October 2008

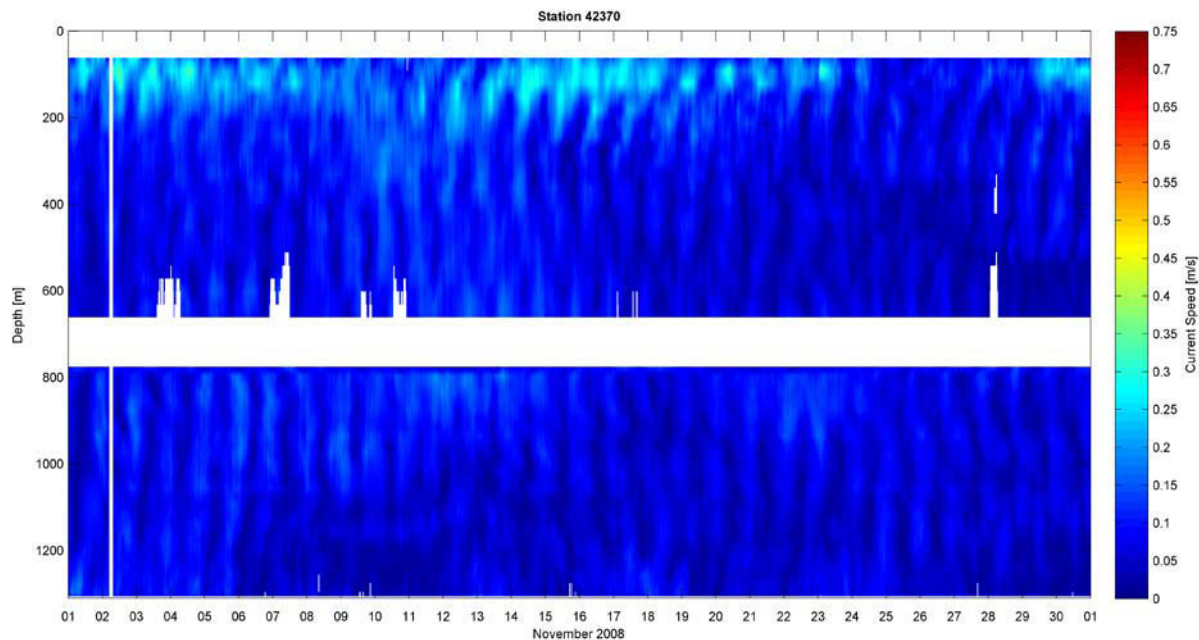


Figure 4-99 Current Speed Contour at NTL Station 42370 – November 2008

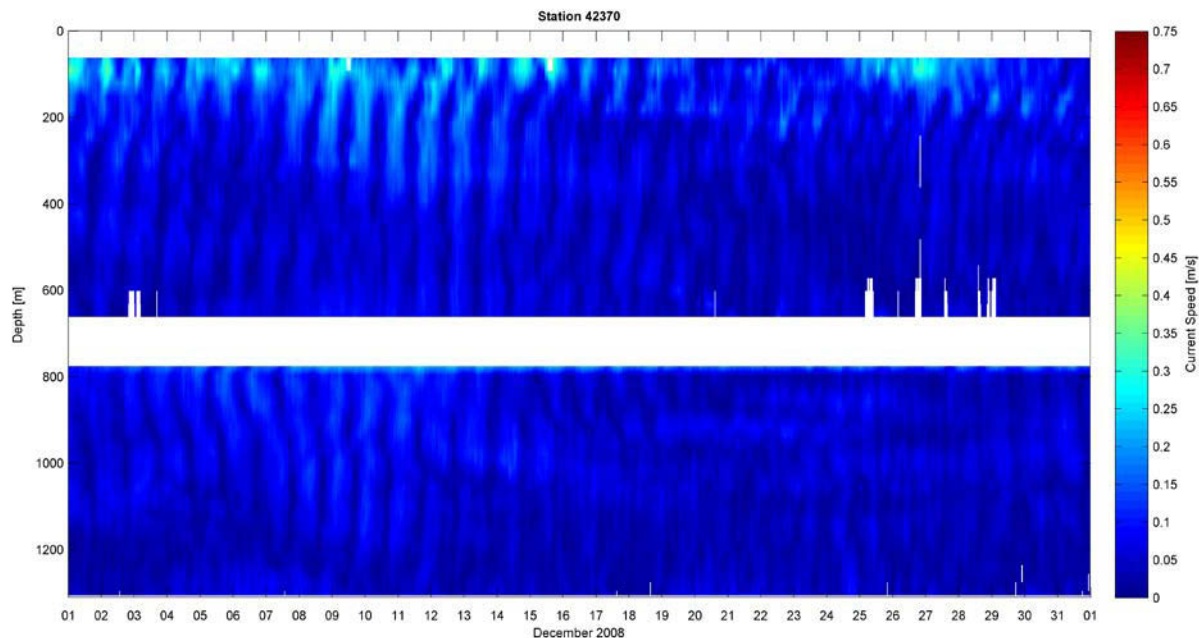


Figure 4-100 Current Speed Contour at NTL Station 42370 – December 2008

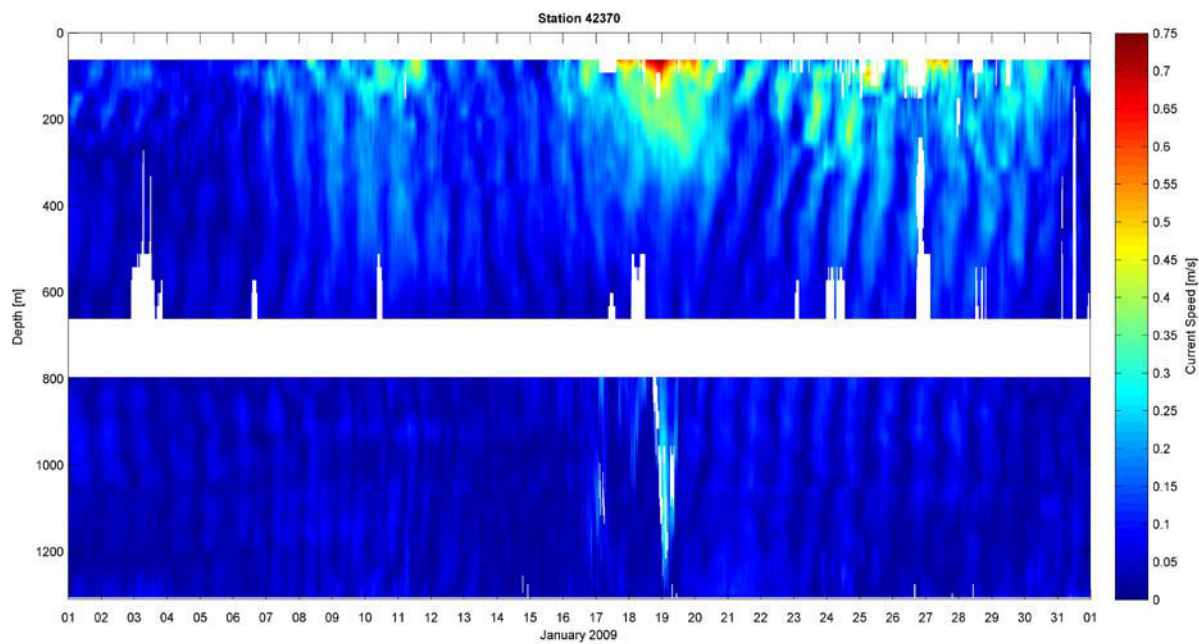


Figure 4-101 Current Speed Contour at NTL Station 42370 – January 2009

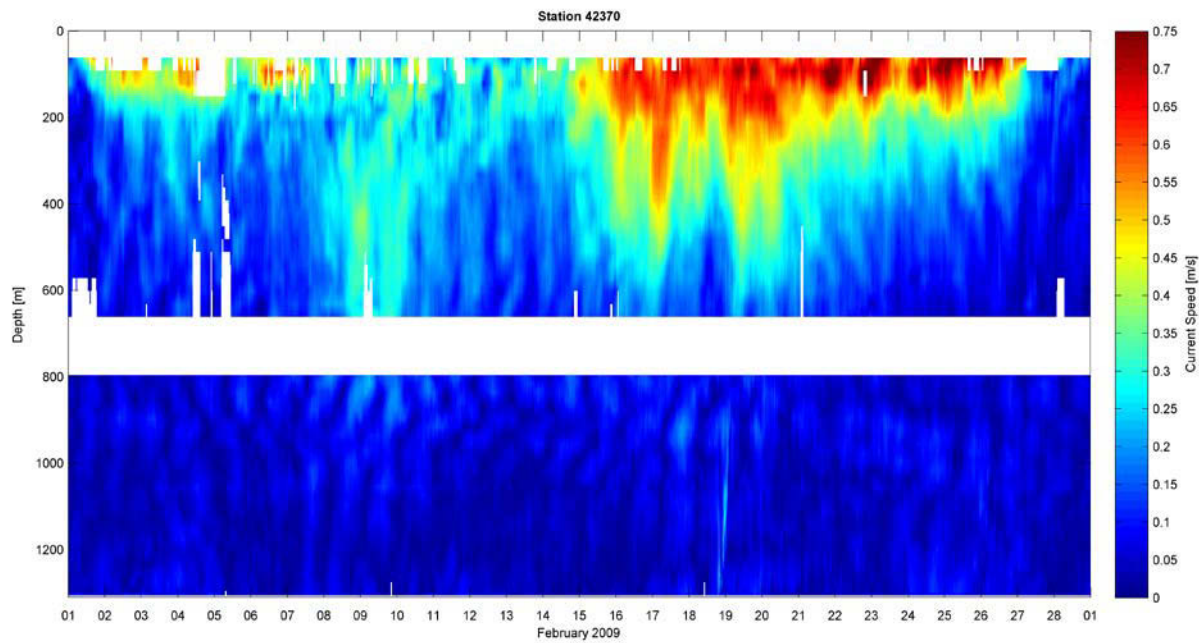


Figure 4-102 Current Speed Contour at NTL Station 42370 – February 2009

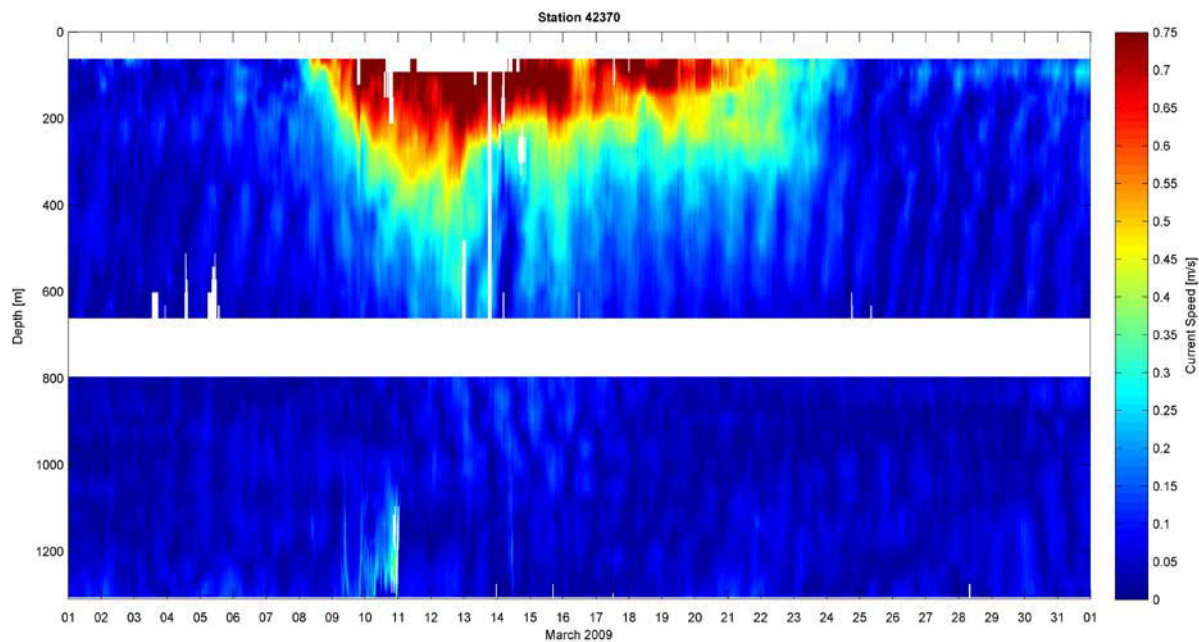


Figure 4-103 Current Speed Contour at NTL Station 42370 – March 2009

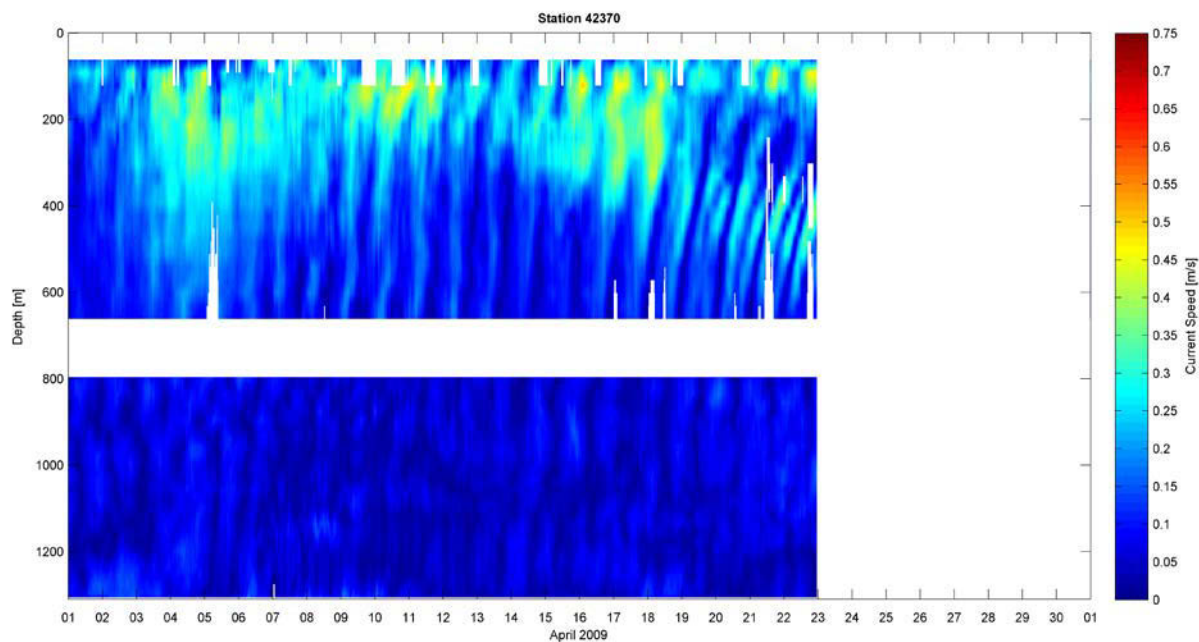


Figure 4-104 Current Speed Contour at NTL Station 42370 – April 2009

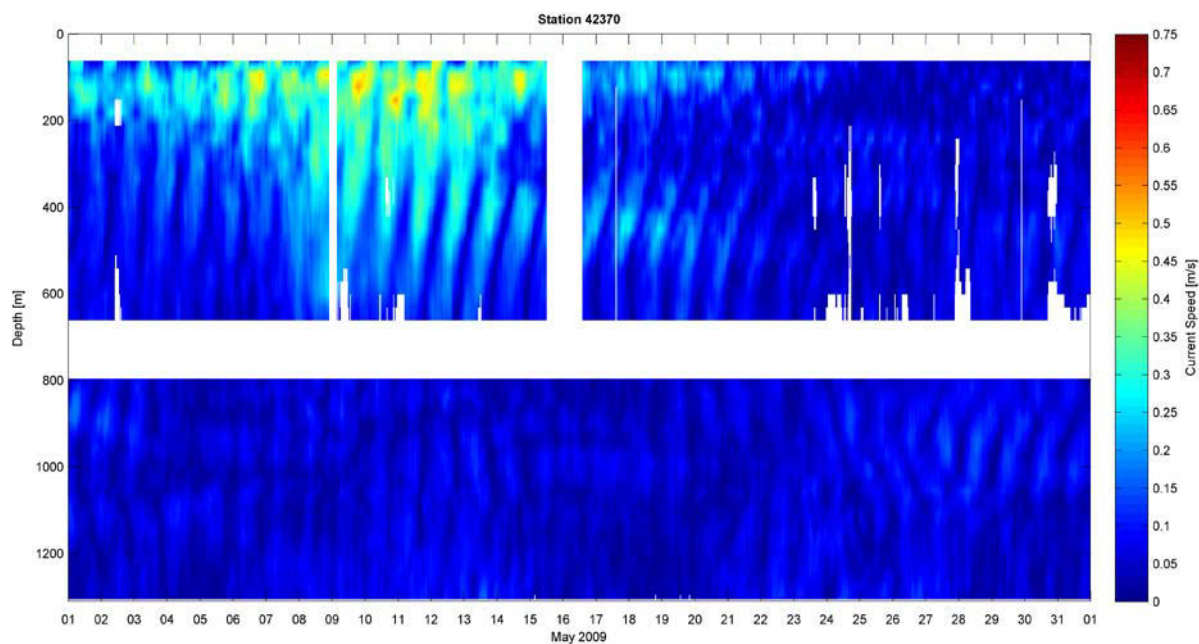


Figure 4-105 Current Speed Contour at NTL Station 42370 – May 2009

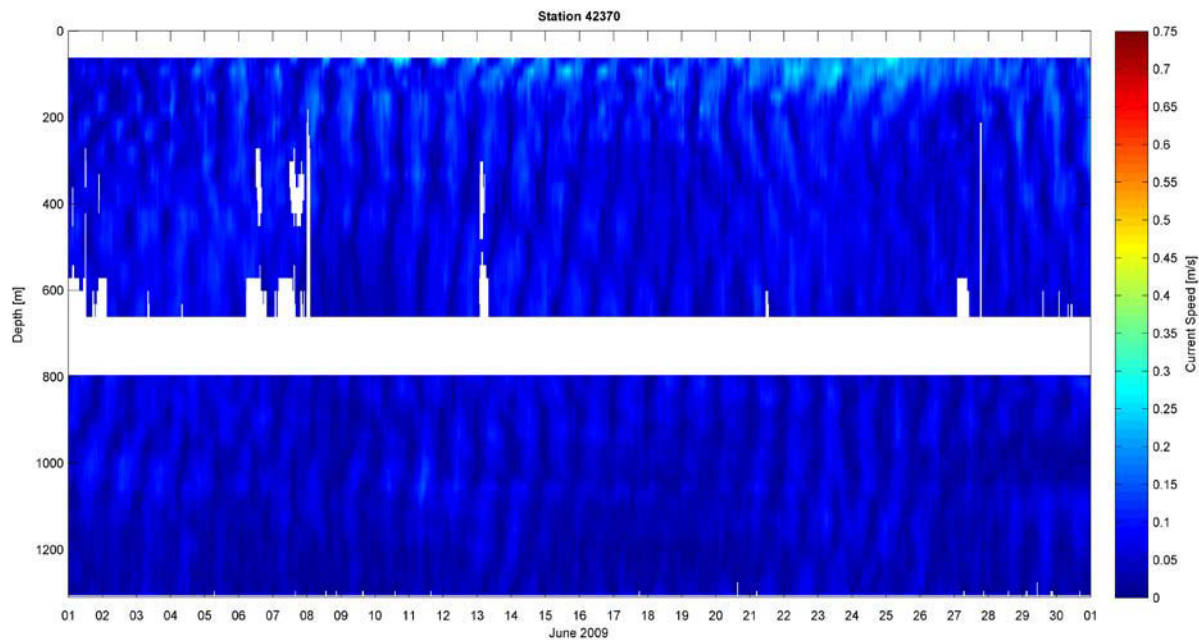


Figure 4-106 Current Speed Contour at NTL Station 42370 – June 2009

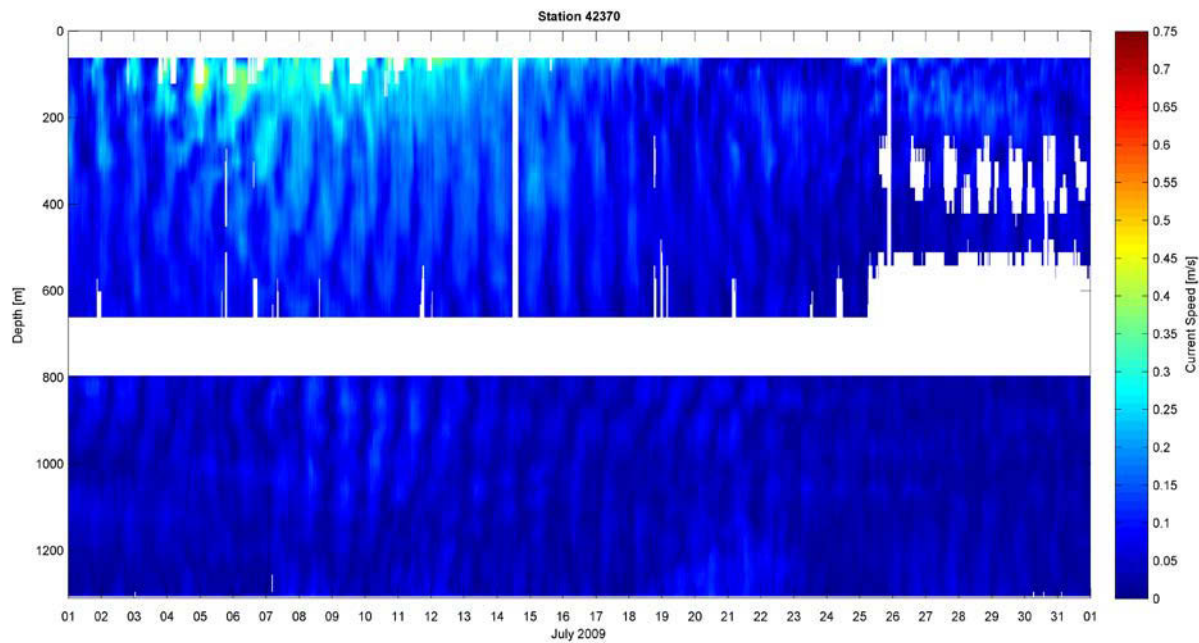


Figure 4-107 Current Speed Contour at NTL Station 42370 – July 2009

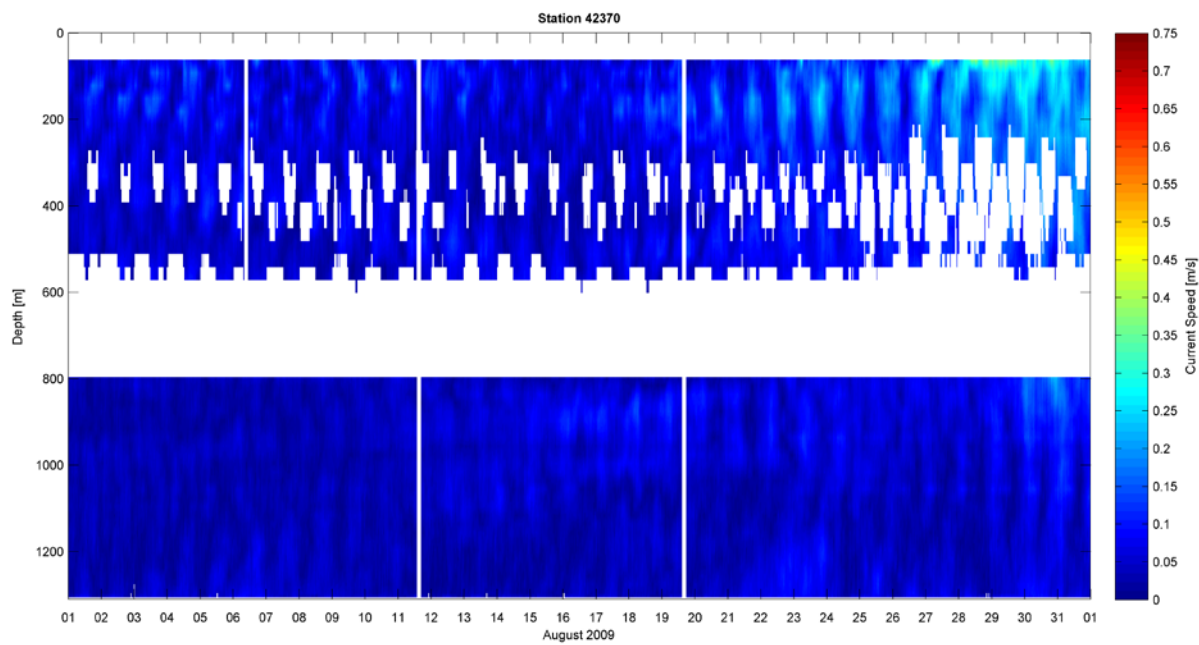


Figure 4-108 Current Speed Contour at NTL Station 42370 – August 2009

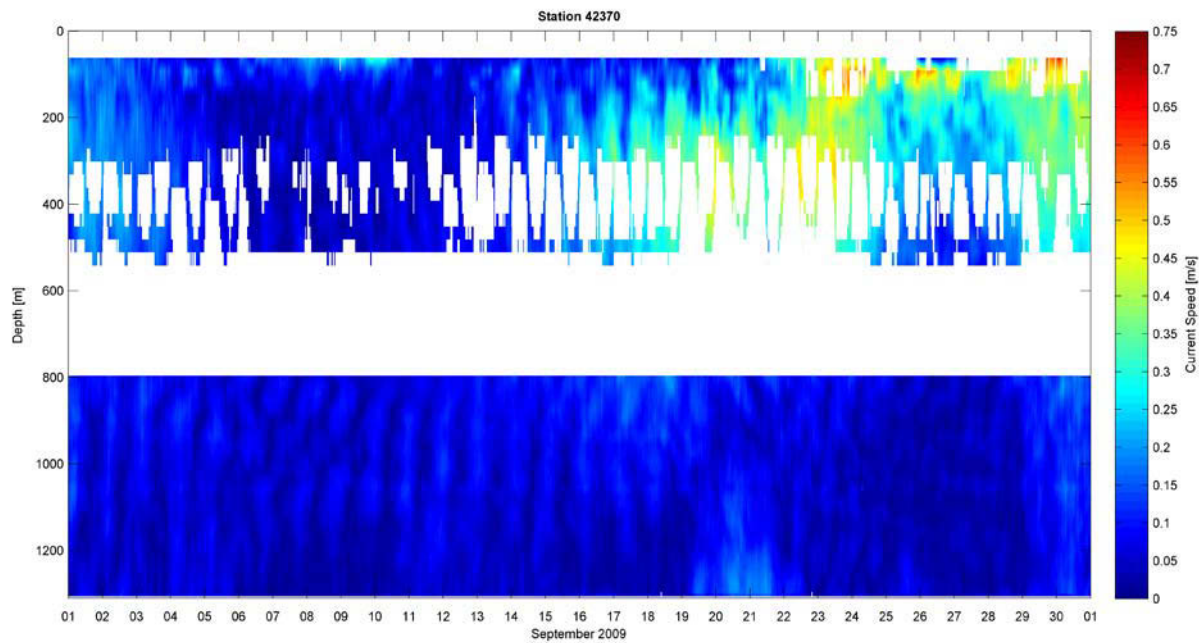


Figure 4-109 Current Speed Contour at NTL Station 42370 – September 2009

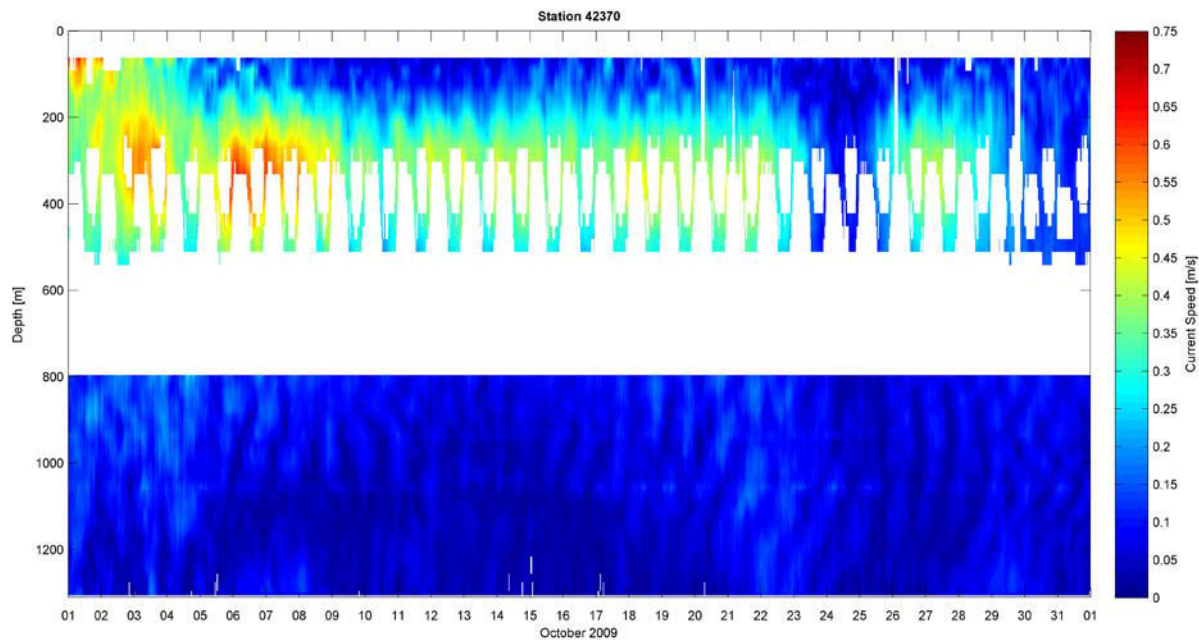


Figure 4-110 Current Speed Contour at NTL Station 42370 – October 2009

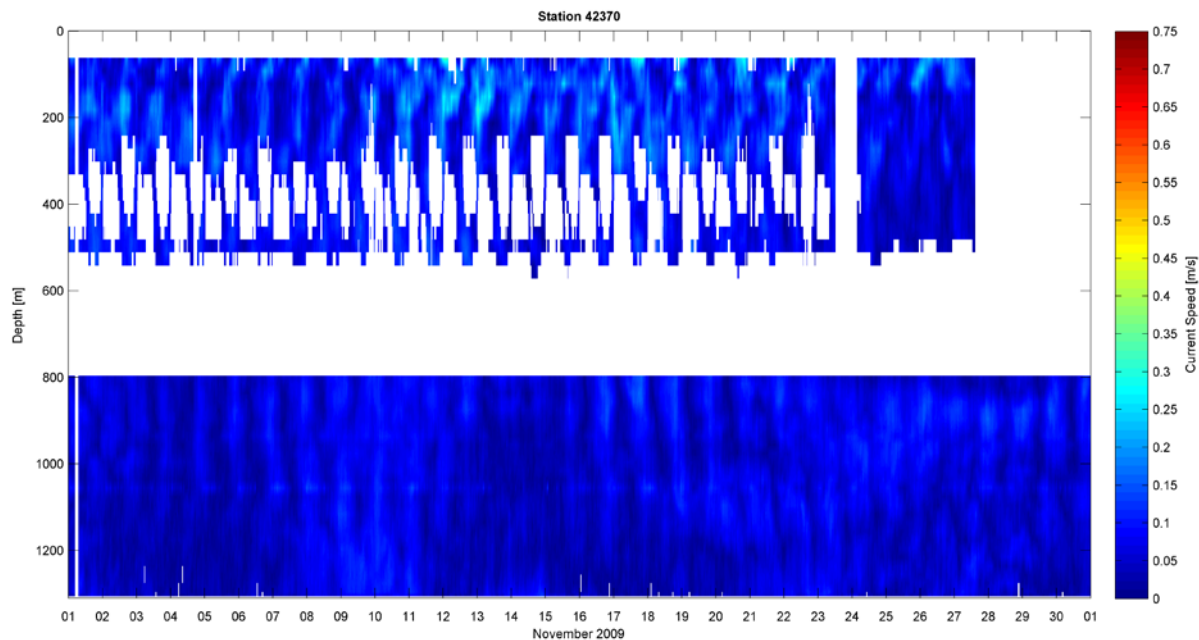


Figure 4-111 Current Speed Contour at NTL Station 42370 – November 2009

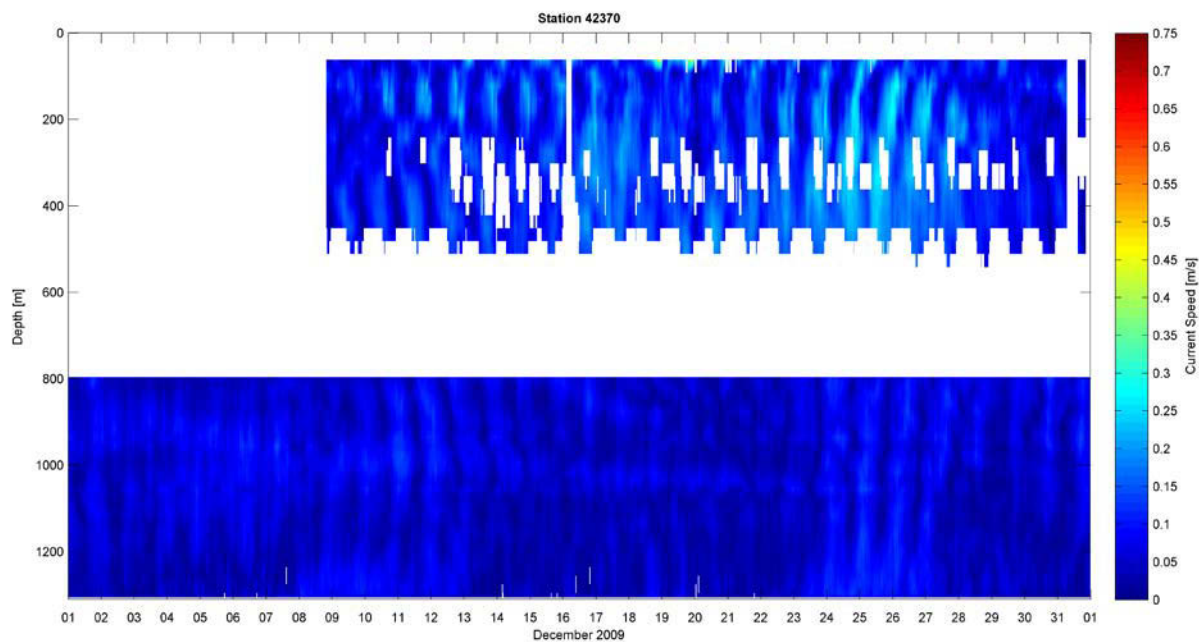


Figure 4-112 Current Speed Contour at NTL Station 42370 – December 2009

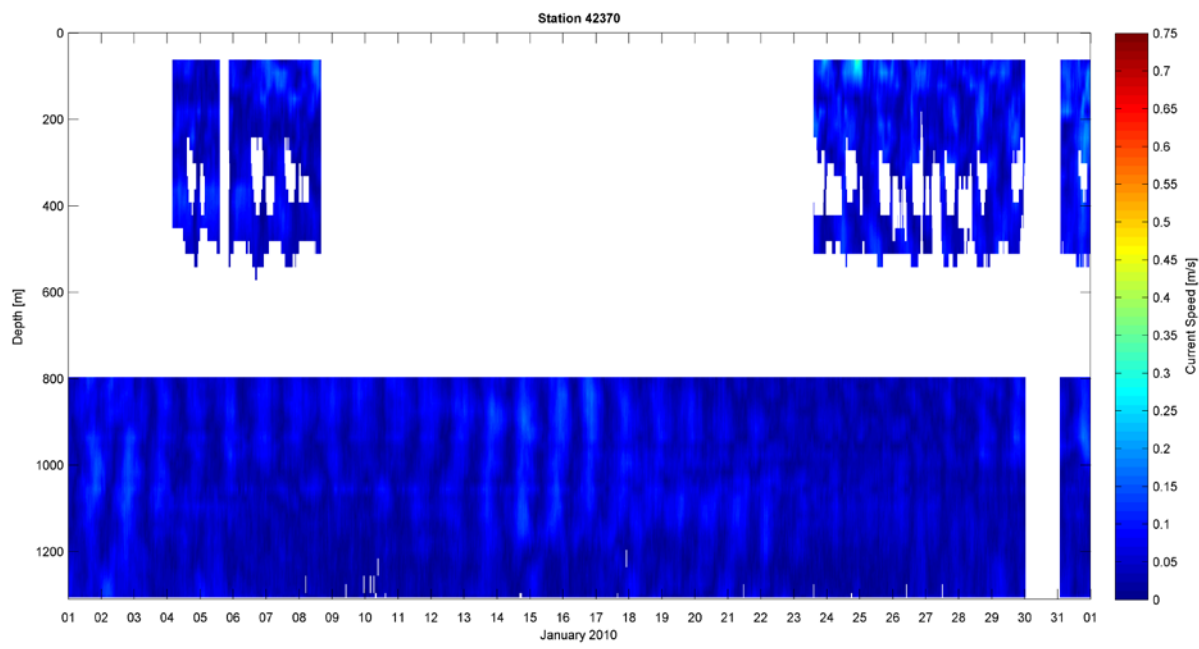


Figure 4-113 Current Speed Contour at NTL Station 42370 – January 2010

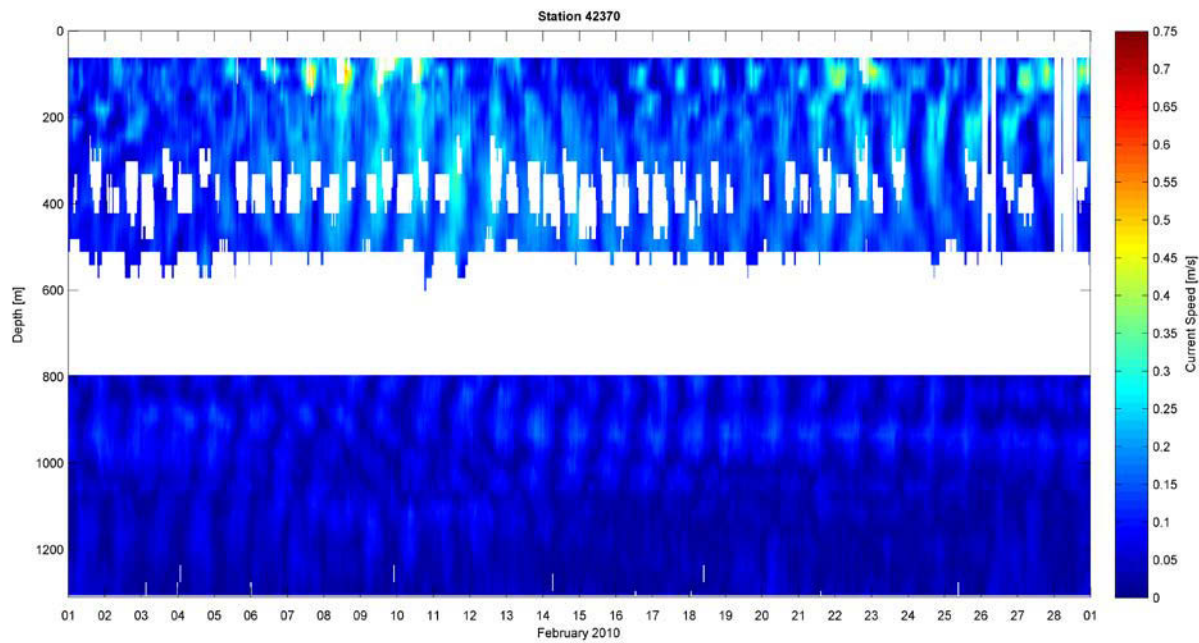


Figure 4-114 Current Speed Contour at NTL Station 42370 – February 2010

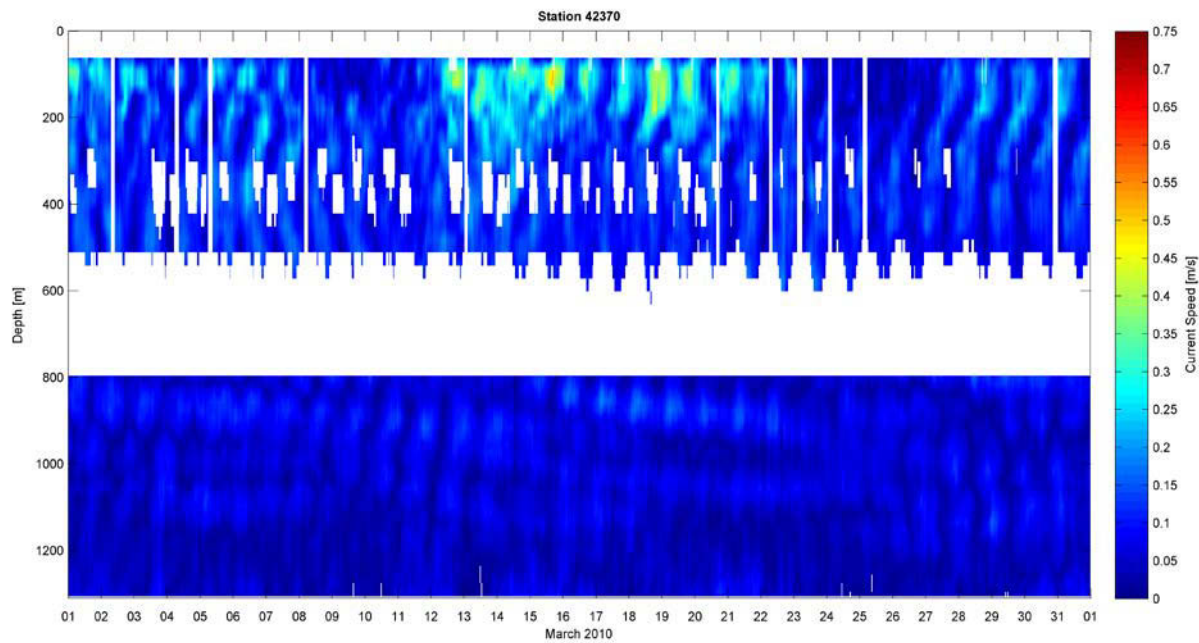


Figure 4-115 Current Speed Contour at NTL Station 42370 – March 2010

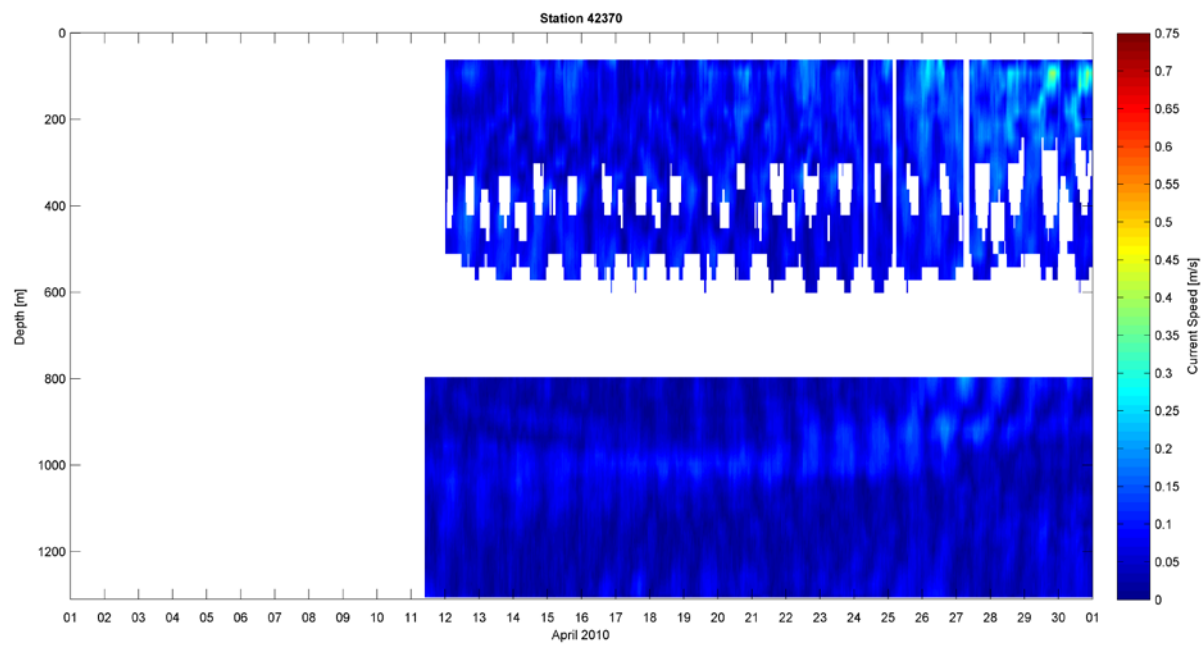


Figure 4-116 Current Speed Contour at NTL Station 42370 – April 2010

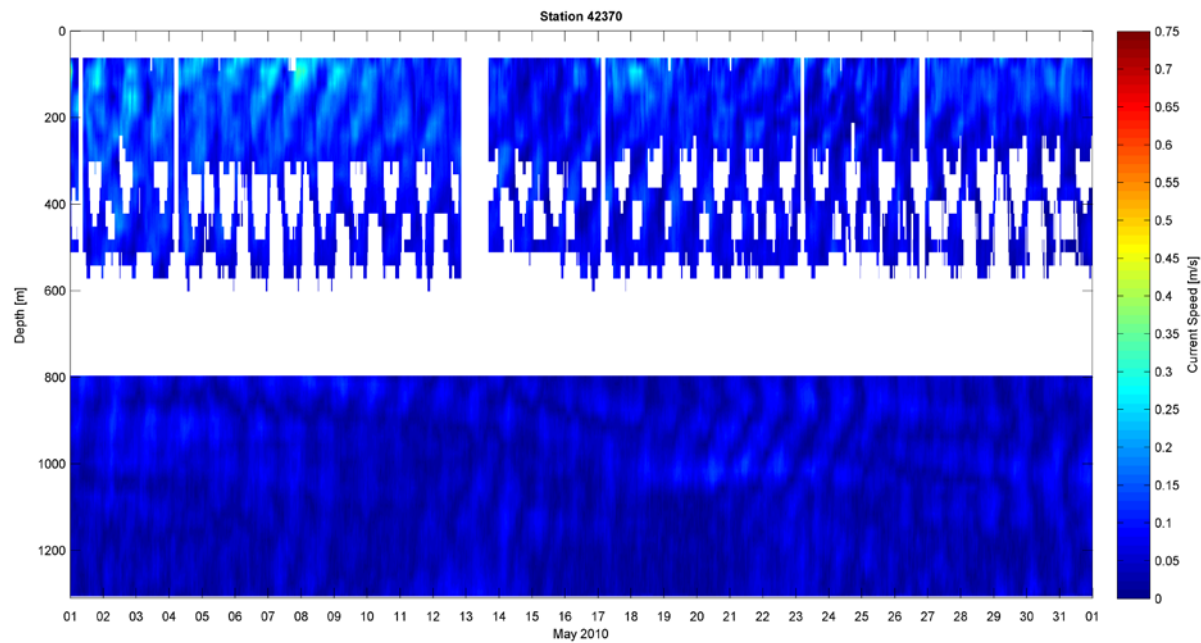


Figure 4-117 Current Speed Contour at NTL Station 42370 – May 2010

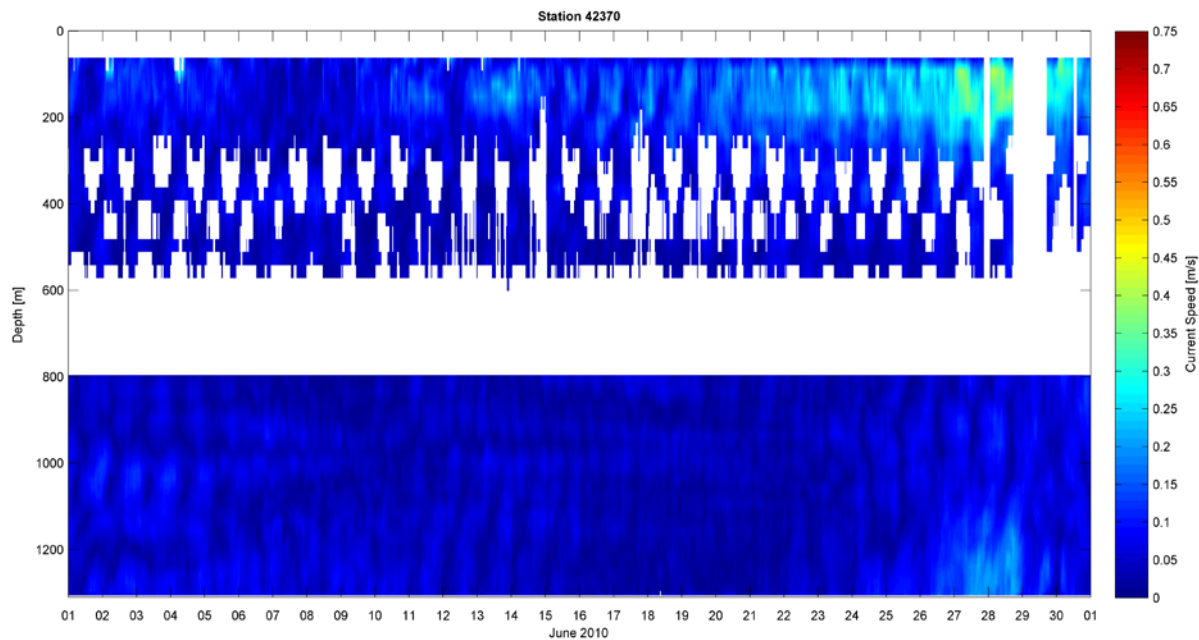


Figure 4-118 Current Speed Contour at NTL Station 42370 – June 2010

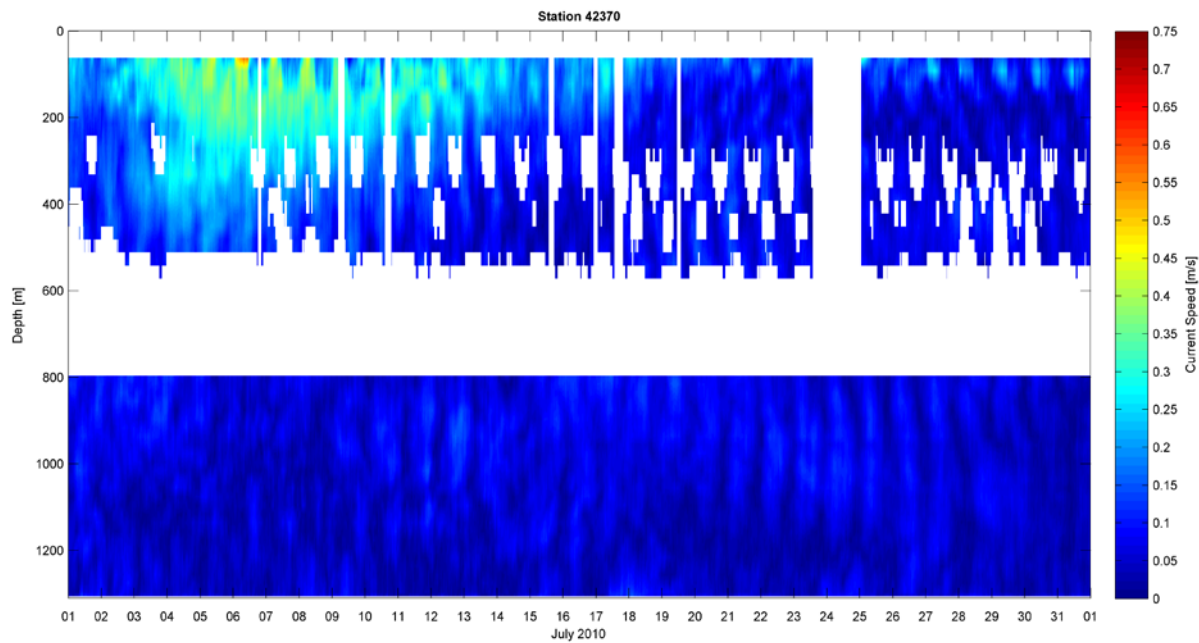


Figure 4-119 Current Speed Contour at NTL Station 42370 – July 2010

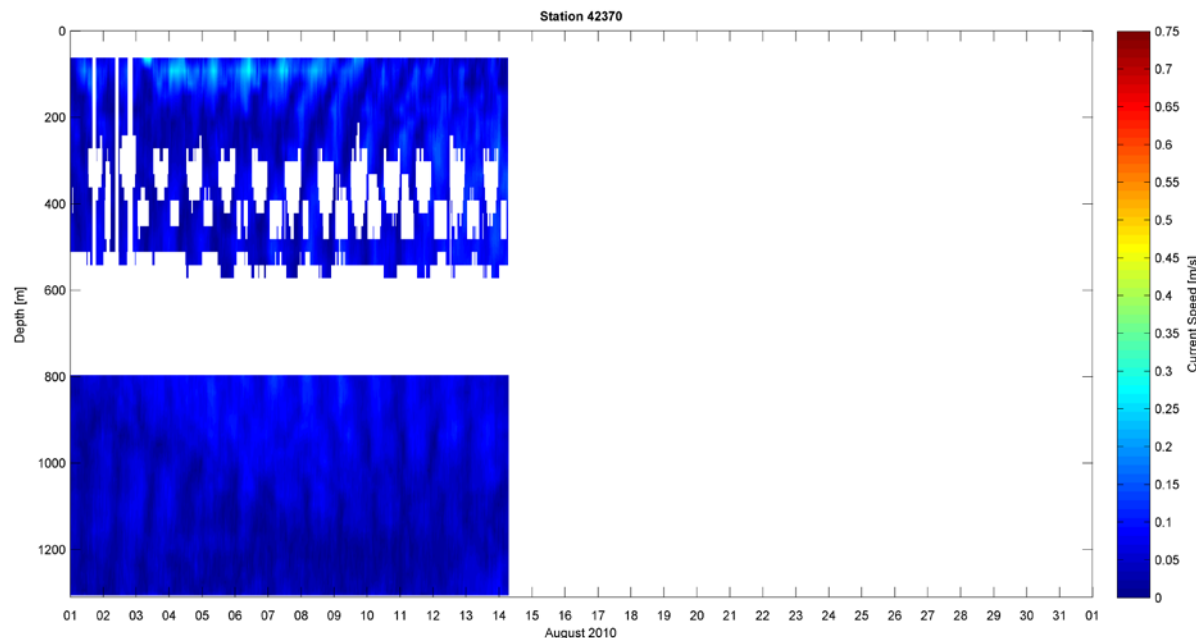


Figure 4-120 Current Speed Contour at NTL Station 42370 – August 2010

4.2 Subsurface Elevated Current Events Interpretation

We are using several identified events listed in Table 4-1 to explain the possible mechanism of the subsurface elevated current events.

Table 4-1 Selected Subsurface Elevated Current Events

NTL ID	Location	Time Period	Mode
42868	28.164°N 88.484°W	Sep 02, 05 – Sep 08, 05	Inertial
		Mar 02, 07 – Mar 11, 07	Shallow
42863	28.257°N 88.467°W	Mar 01, 07 – Mar 08, 07	Shallow
42364	29.060°N 88.090°W	Jul 14, 05 – Jul 14, 05	Deep
42873	28.840°N 88.560°W	Jul 15, 05 – Jul 15, 05	Deep

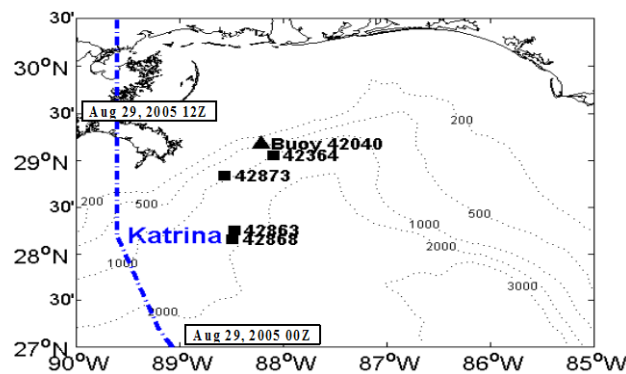


Figure 4-121 Hurricane Katrina track, NDBC buoy 42040 and selected NTL ADCP measurement locations

4.2.1 Submerged Speed Peaks with Inertial Period

Near inertial oscillations with a period of approximately 24 hours are known to exist in the Gulf of Mexico with the passage of a hurricane. Figure 4-122 is an example of such a feature in the wake of hurricane Katrina. On August 29, 2005, hurricane Katrina passed NTL station 42868 and made an initial landfall in coastal Louisiana (Figure 4-121). The left and right panels of Figure 4-122 are observed ADCP and PROFS horizontal current velocity at NTL Station 42868 for Hurricane Katrina, respectively. Unfortunately, the ADCP site was not operational due to hurricane Katrina; only data 4 days after Katrina is available and presented here. The PROFS data cover the entire history of hurricane Katrina within the Gulf and following landfall.

The PROFS data show that inertial oscillations were generated immediately after hurricane Katrina passed (on Aug 29, 2005 12Z). Currents were enhanced at the surface and rotated clockwise. The maximum current speed was larger than 2m/s at station 42868. The surface near-inertial motion decreased with the energy propagating eastward and downward.

On September 5, 2005, nearly a week after the landfall of Katrina, observations (left panel of Figure 4-122) show that the near surface inertial motions were still strong with amplitudes larger than 0.5 m/s, which indicated a persistence of oscillations over several inertial cycles.

The observations also show the line of constant phase propagated toward the surface, confirming the suggested downward energy flux within PROFS. This was likely due to the strong anticyclonic loop current eddy Vortex (Figure 4-123), following on from theory proposed by Wang (1991). Similar vertical inertial oscillations within the region were observed by Hamilton et al. (2000) after the passage of hurricane Georges on September 27, 1998.

4.2.2 Events Isolated in Time with No Clear Periodicity – Deep Jet Events

Two very deep jet events were identified at station 42364 (left panel of Figure 4-124) and 42873 (left panel of Figure 4-126) within 24 hours on July 14, 2005 to July 15, 2005, respectively. The peak currents at both stations flowed southwestward along with the bathymetry. The lag between the two events suggested that energy propagated southwestward which is consistent with the characteristics of Topographic Rossby Waves (TRWs) (Hamilton, 1990). But TRWs in the Gulf of Mexico are usually driven by Loop Current (LC) pulsation, Loop Current Eddy (LCE) shedding, and perhaps LCE itself, with a group speed of about 2 – 3 km/day (Oey and Lee, 2002). During these particular events the LC and LCE Vortex were located well south and southwest of the sites and the energy propagation speed is much higher, so it is thought that other processes forced the events. On July 8, 2005, Hurricane Dennis passed over the eastern Gulf of Mexico and made landfall on July 11, 2005 in Mississippi and western Florida. The 10-day PROFS forecast from July 6, 2005 showed that downward propagating inertial currents in the wake of Dennis offshore the western coast of Florida fed the energy to bottom currents which then moved along the 1000 and 2000m isobaths (Figure 4-125 and Figure 4-127). The bottom trapped waves propagated along these isobaths toward stations 42364 and 42873. The right panels of Figure 4-124 and Figure 4-126 are current velocity stick plots at the two stations from the PROFS forecast. The model captures the jet events but they are weaker than the observed values, a general tendency of ocean models (Oey, 1998).

4.2.3 Events Isolated in Time with No Clear Periodicity –Shallow Jet Events

From March 1-10, 2007, two subsurface intensified current events were observed at two adjacent NTL stations 42863 and 42868 (Figure 4-128). The peaks of the jets are about 0.5m/s near 500m for both stations. The roughly half day lag between the two peaks indicates the down slope propagation of the jets. Figure 4-129 shows the satellite sea surface height anomaly + model mean superimposed over

sea surface temperature from the Colorado Center for Astrodynamics Research, University of Colorado (<http://argo.colorado.edu/~realtime/welcome/>). Eddy Zorro, only slightly attached to the Loop Current during this time, rotated clockwise as it progressed northward and impacted the slope southeast of the Mississippi Delta, including the respective NTL ADCP stations. Local SSH maxima both northwest and southeast of the stations forced downwelling near the surface while the propagating warm eddy Zorro forced bottom upwelling. This resulted in the formation of a strong upwelling and downwelling cell. The on-slope portion of eddy Zorro then “peeled-off” and formed a bottom boundary layer which “lifted” the strong along-slope (southward) current or jet away from the bottom layer. This is consistent with the subsurface jet generation mechanism originally proposed by Oey and Zhang (2004).

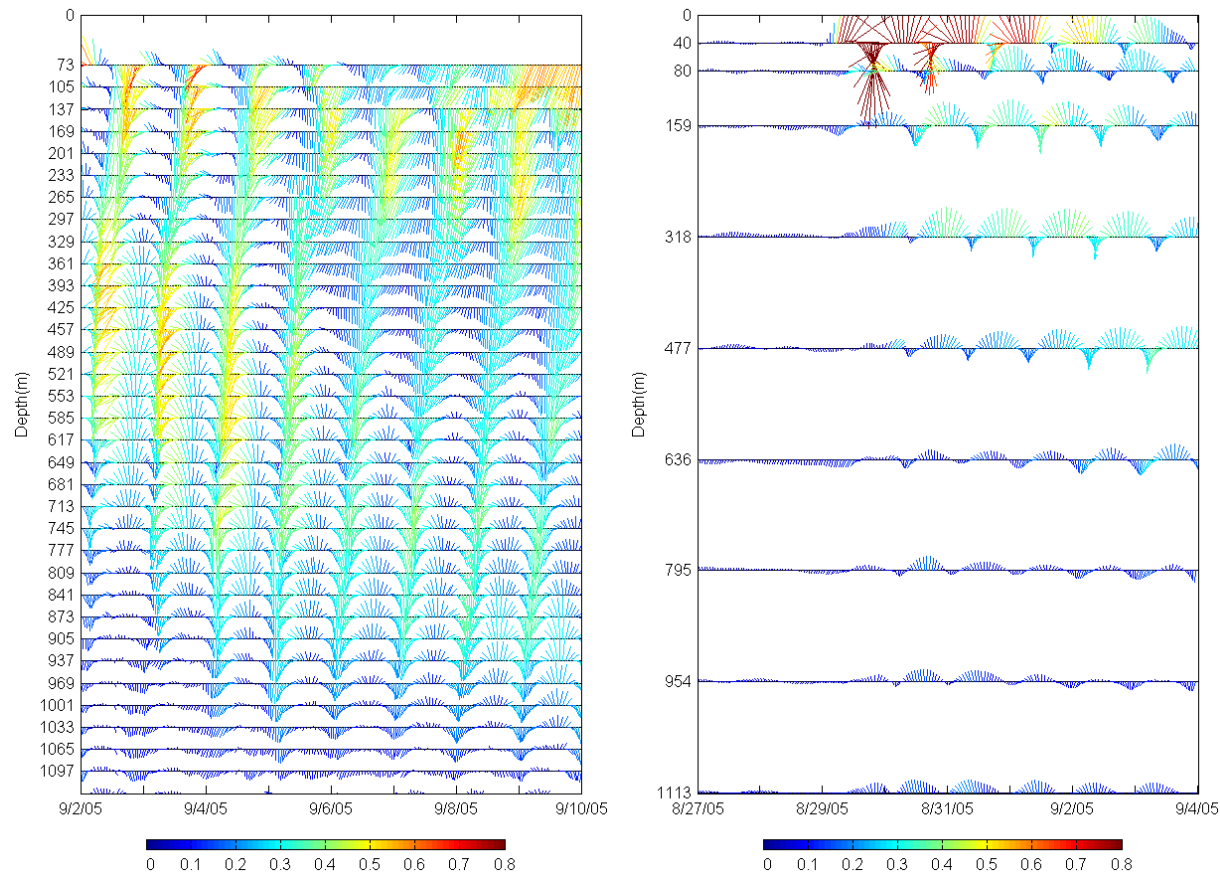


Figure 4-122 Observed (left) and PROFS (right) horizontal current velocity at NTL Station 42868 during and following Hurricane Katrina. Upward is North. Speed unit is m/s.

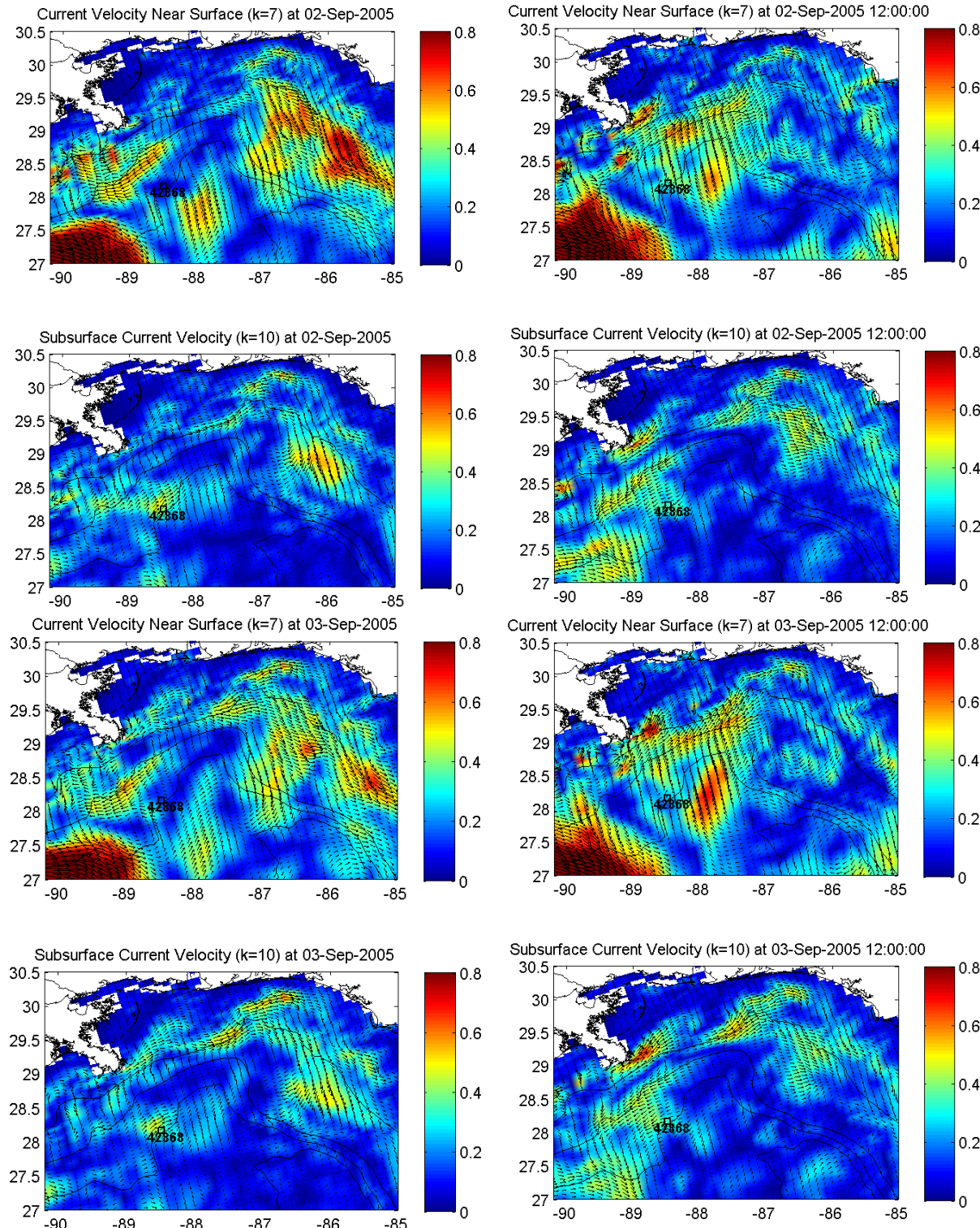


Figure 4-123 Near surface (80m at station 42868) and subsurface (477m at station 42868) PROFS model current velocity. Speed unit is m/s.

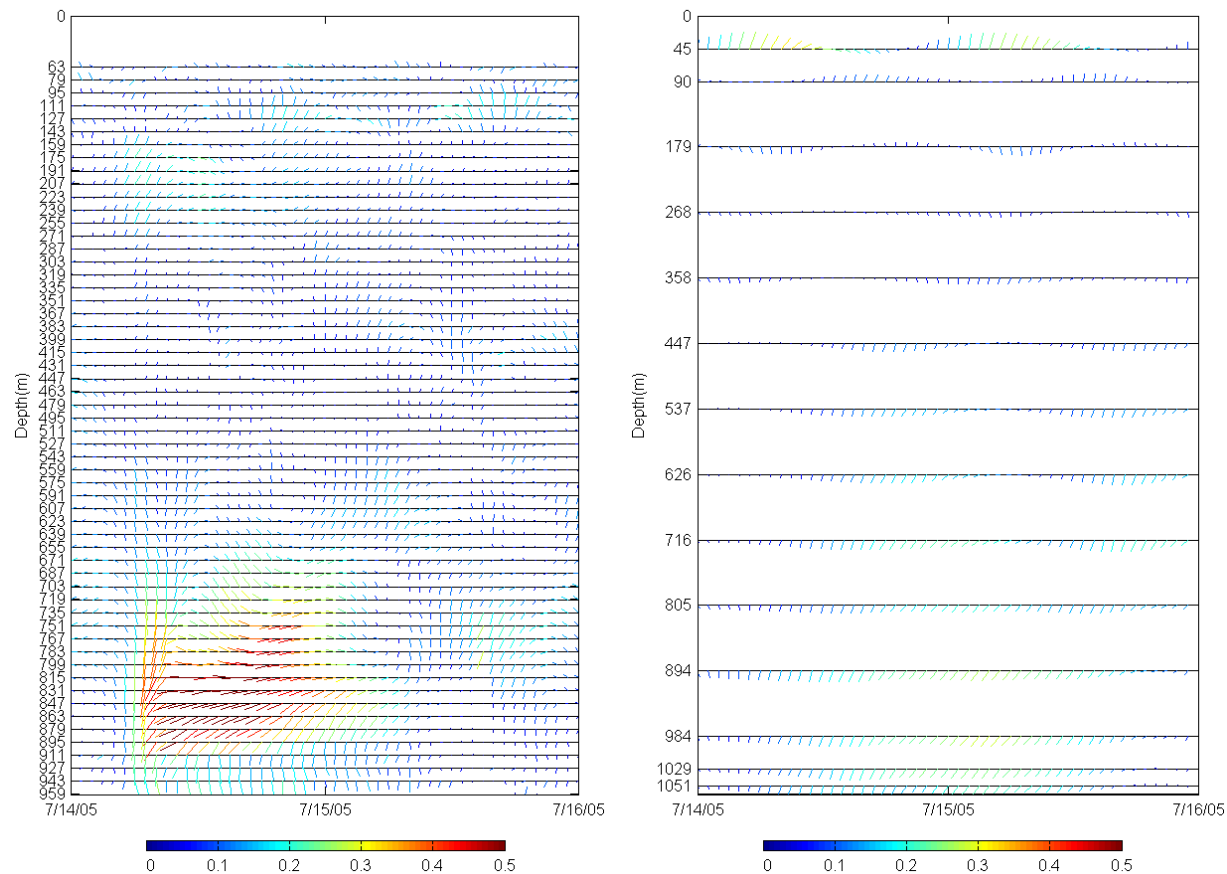


Figure 4-124. Observed (left) and PROFS (right) horizontal current velocity at NTL Station 42364. Upward is North. Speed unit is m/s.

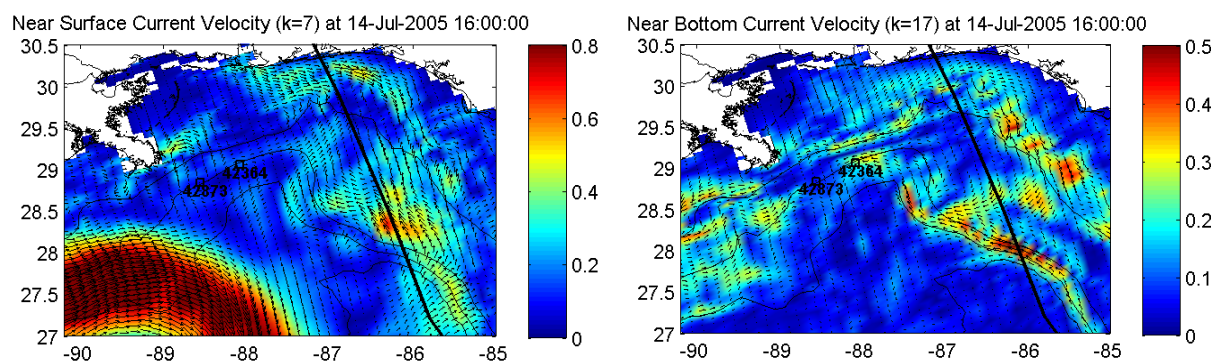


Figure 4-125 Near surface (45m at station 42364) and near bottom (894m at station 42364) PROFS horizontal current velocity. Speed unit is m/s. The solid line is Hurricane Dennis track.

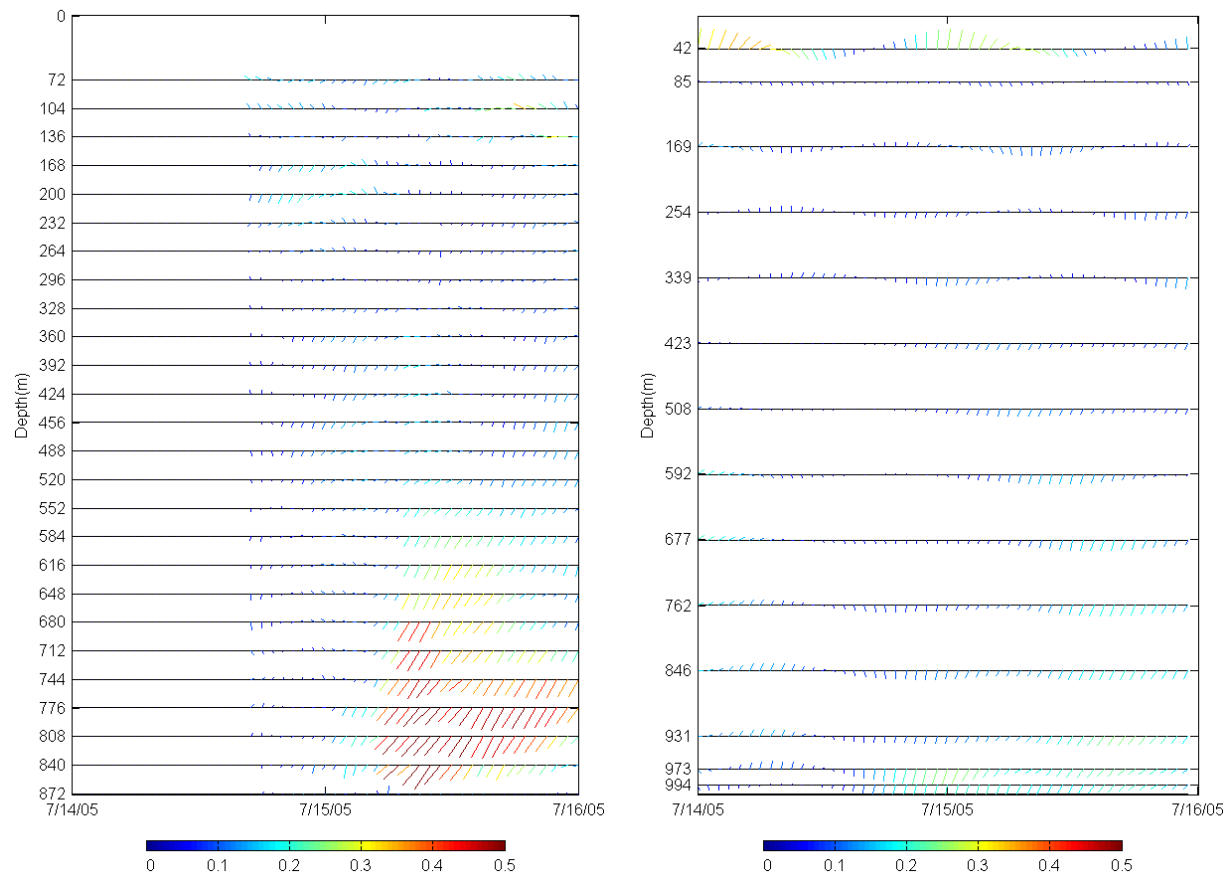


Figure 4-126 Observed (left) and PROFS (right) horizontal current velocity at NTL Station 42873. Upward is North. Speed unit is m/s.

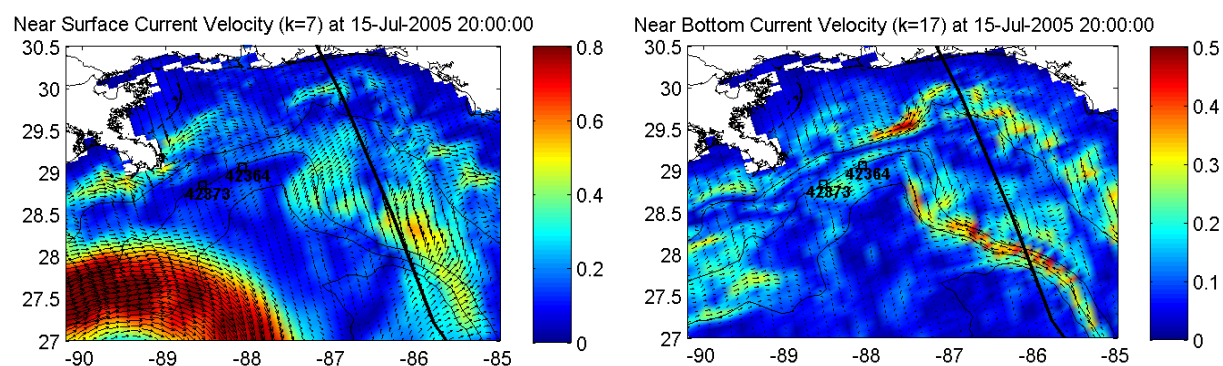


Figure 4-127 Near surface (42m at station 42873) and near bottom (846m at station 42873) PROFS horizontal current velocity. Speed unit is m/s. The solid line is Hurricane Dennis track.

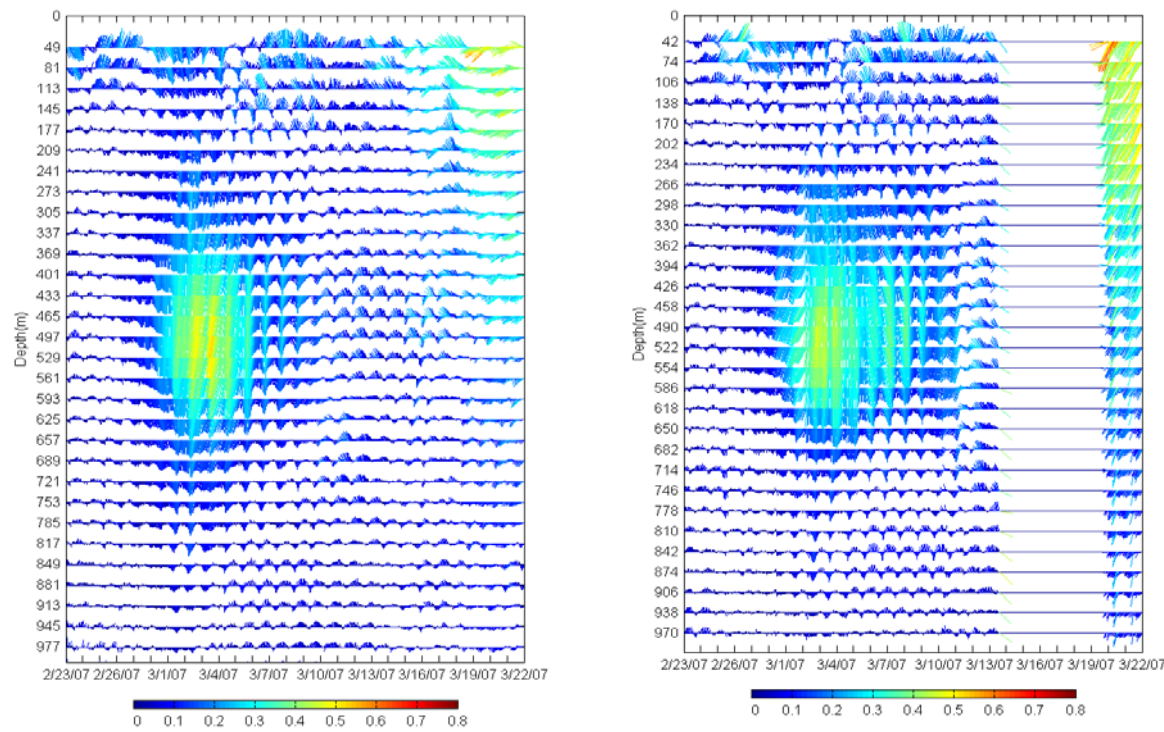


Figure 4-128 Observed horizontal current velocity at NTL Station 42863 and 42868. Upward is North. Speed unit is m/s.

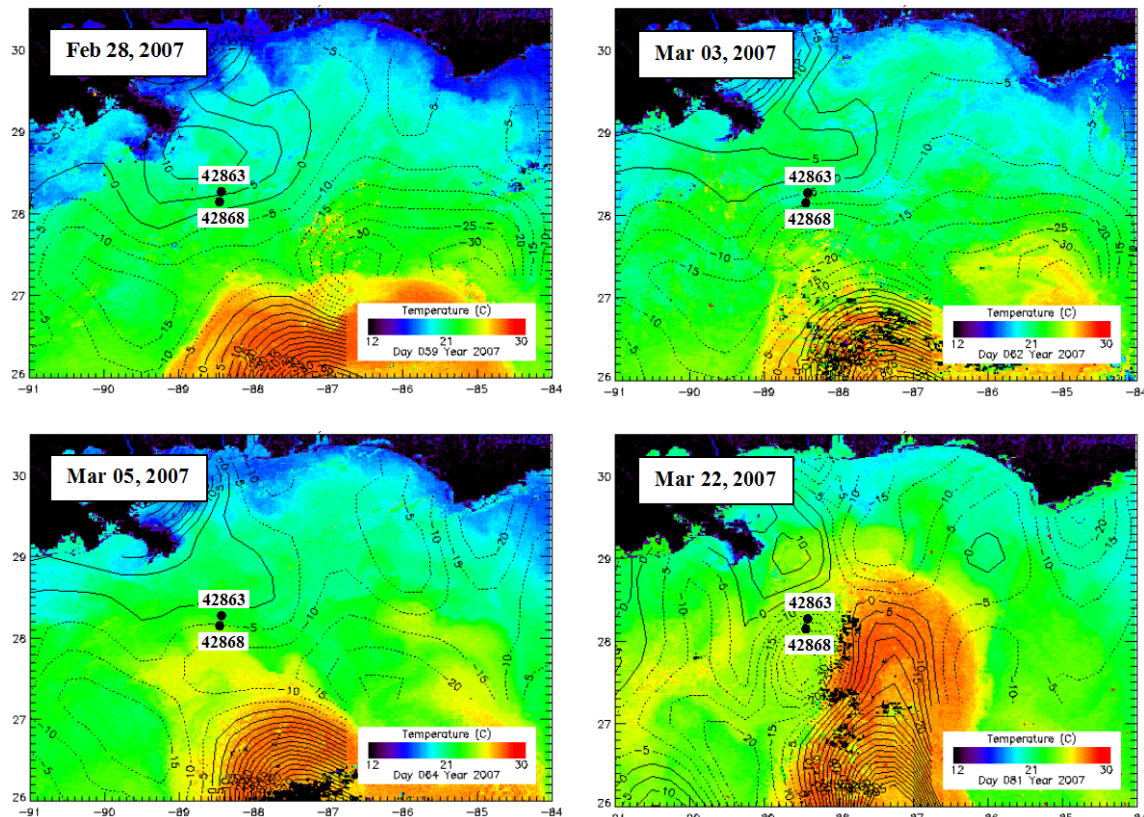


Figure 4-129 Satellite sea surface height and sea surface temperature. The black dots are the locations of NTL stations 42863 and 42868.

5. CURRENT PROFILE CHARACTERIZATIONS

Current Profile Characterization (CPC) is a type of data reduction in which a large number of measured (or modelled) profiles is reduced to small number for a particular engineering application. It can provide a valuable insight into the flow regime. The CPC current profile criteria consist of a discrete number of characteristic profiles, each of which has an associated percentage frequency of occurrence. These criteria are appropriate for riser fatigue calculations (including Vortex Induced Vibration modeling) and operability assessments.

Current Profile Characterization can be conducted via EOF analysis or the direct method (Jeans et al., 2002). Event screenings studies have shown that inertial currents are an important component of the current regime, and current speed peaks are not confined to fixed depth levels. The suitability of EOF analysis for riser fatigue applications can be uncertain, because the objective is to provide an accurate representation of every measured profile. The design implications of simplifying the more complex profiles are unknown. Well established methods of direct characterisation by Fugro (Jeans et al., 2002; Jeans et al., 2005) therefore were applied in this study to derive fatigue profiles.

5.1 Zone 1

5.1.1 Long Term Current Profile Characterizations

The representative long term current profile characterizations for Zone 1 were derived from NTL ADCP data from April 2005 to August 2010 at station 42364. The mean, minimum and maximum current speeds at each depth level associated with each characteristic profile are in the associated file c56323_long_term_cpc_zone_1.xls in MS Excel format.

5.1.2 Short Term Current Profile Characterizations

5.1.2.1 Event 1

The short term representative current profile characterizations were derived from the post hurricane Katrina current data from 2 September 2005 to 16 September 2005 at NTL station 42868. The mean, minimum and maximum current speeds at each depth level associated with each characteristic profile are in the associated file c56323_short_term_cpc_zone_1_event_1.xls in MS Excel format.

5.1.2.2 Event 2

The short term representative current profile characterizations were derived from a Subsurface elevated event current data from 27 February 2007 to 13 March 2007 at NTL station 42868. The mean, minimum and maximum current speeds at each depth level associated with each characteristic profile are the associated file c56323_short_term_cpc_zone_1_event_2.xls in MS Excel format.

5.1.2.3 Event 3

The short term representative current profile characterizations were derived from a Subsurface elevated event current data from from 14 July 2005 to 16 July 2005 at NTL station 42364. The mean, minimum and maximum current speeds at each depth level associated with each characteristic profile are in the associated file c56323_short_term_cpc_zone_1_event_3.xls in MS Excel format.

5.2 Zone 2

5.2.1 Long Term Current Profile Characterizations

5.2.1.1 Deep Area (near 2,000m)

The representative long term current profile characterizations for the deep part (about 2,000m) of the Zone 2 were derived from BOEMRE Deepwater Observations Current Mooring Data (Moorings: I1, I2, I3, and I4) from August 1999 to September 2001. The mean, minimum and maximum current speeds at each depth level associated with each characteristic profile are in the associated file c56323_long_term_cpc_zone_2_deep.xls in MS Excel format.

5.2.1.2 Shallow Area (near 1,300m)

The representative long term current profile characterizations for the shallow part (about 1,300m) of the Zone 2 were derived from representative current data from April 2005 to August 2010 at NTL station 42370. The mean, minimum and maximum current speeds at each depth level associated with each characteristic profile are in the associated file c56323_long_term_cpc_zone_2_shallow.xls in MS Excel format.

5.2.2 Short Term Current Profile Characterizations

5.2.2.1 Deep Area - Event 1

The short term representative current profile characterizations were derived from a Subsurface elevated event current data from 2 September 2005 to 16 September 2005 (post hurricane Katrina) at NTL station 42867. Normalized current profile derived from PROFS data at station 355 and 317 were used to extend NTL data from 754m to 2300m (bottom). The mean, minimum and maximum current speeds at each depth level associated with each characteristic profile are in the associated file c56323_short_term_cpc_zone_2_deep_event_1.xls in MS Excel format.

5.2.2.2 Shallow Area - Event 1

The short term representative current profile characterizations were derived from a Subsurface elevated event current data from from 7 April 2007 to 14 April 2007 at NTL station 42885. The mean, minimum and maximum current speeds at each depth level associated with each characteristic profile are in the associated file c56323_short_term_cpc_zone_2_shallow_event_1.xls in MS Excel format.

5.2.2.3 Shallow Area - Event 2

The short term representative current profile characterizations were derived from a Subsurface elevated event current data from from 7 March 2007 to 15 March 2007 at NTL station 42379. The mean, minimum and maximum current speeds at each depth level associated with each characteristic profile are in the associated file c56323_short_term_cpc_zone_2_shallow_event_2.xls in MS Excel format.

5.3 Zone 3

5.3.1 Long Term Current Profile Characterizations

The representative long term current profile characterizations for Zone 3 were derived from January 2006 to May 2010 at NTL station 42377. The mean, minimum and maximum current speeds at each depth level associated with each characteristic profile are in the associated file c56323_long_term_cpc_zone_3.xls in MS Excel format.

5.3.2 Short Term Current Profile Characterizations

5.3.2.1 Event 1

The short term representative current profile characterizations were derived from the post hurricane Katrina current data from 26 January 2006 to 5 February 2006 at NTL station 42377. The mean, minimum and maximum current speeds at each depth level associated with each characteristic profile are in the associated file c56323_short_term_cpc_zone_3_event_1.xls in MS Excel format.

5.3.2.2 Event 2

The short term representative current profile characterizations were derived from a Subsurface elevated event current data from 20 June 2006 to 27 June 2006 at NTL station 42377. The mean, minimum and maximum current speeds at each depth level associated with each characteristic profile are the associated file c56323_short_term_cpc_zone_3_event_2.xls in MS Excel format.

5.4 Zone 4

5.4.1 Long Term Current Profile Characterizations

The representative long term current profile characterizations for Zone 4 were derived from BOEMRE Deepwater Observations Current Mooring Data (Moorings: L4) from February 2003 to April 2004. The mean, minimum and maximum current speeds at each depth level associated with each characteristic profile are in the associated file c56323_long_term_cpc_zone_4.xls in MS Excel format.

5.4.2 Short Term Current Profile Characterizations

No elevated current event was found from the data in this zone.

6. REFERENCE

- Berntsen, J. and L.-Y. Oey, 2010. Estimation of the internal pressure gradient in σ -coordinate ocean models: comparison of second-, fourth-, and sixth-order schemes. *Ocean Dyn.* 60, 317-330. DOI 10.1007/s10236-009-0245-y.
- Brooks, D., 1983. "The wake of Hurricane Allen in the western Gulf of Mexico," *Journal of Physical Oceanography*, 13, 117-129, 1983.
- Chang, Y.-L. and L.-Y. Oey, 2010. Why can wind delay the shedding of Loop Current eddies? *J. Phys. Oceanogr.*, in press.
- Craig, P. D., and M. L. Banner, 1994. Modeling wave-enhanced turbulence in the ocean surface layer. *J. Phys. Oceanogr.*, 24, 2546–2559.
- DiMarco, S.F., M.K. Howard, W.D. Nowlin Jr., and R.O. Reid, 2004. "Subsurface, high-speed current jets in the deepwater region of the Gulf of Mexico," *U.S. Dept. of the Interior, Minerals Management Service, Gulf of Mexico OCS Region, New Orleans, LA. OCS Study MMS 2004-022*, 98pp.
- Donohue, K., P. Hamilton, K. Leaman, R. Leben, M. Prater, D.R. Watts, and E. Waddell. 2006. Exploratory study of deepwater currents in the Gulf of Mexico. Volume II: Technical report. U.S. Dept. of the Interior, Minerals Management Service, Gulf of Mexico OCS Region, New Orleans, LA. OCS Study MMS 2006-074. 430 pp.
- Driver, D., G. Jeans, C. Harragin, and A. Moore, 2005. "The validity of apparent subsurface jet currents in the Gulf of Mexico," *IEEE 8th Current Measurement Technology Conference, Southampton Oceanography Center, UK*.
- Ezer, T., L-Y. Oey, H-C. Lee, and W. Sturges, 2003. The variability of currents in the Yucatan Channel: Analysis of results from a numerical ocean model. *Journal of Geophysical Research*, 108(C1), 3012, 10.1029/2002JC001509.
- Fan, S., Oey, L.-Y., and Hamilton, P., 2004. Assimilation of Drifter and Satellite Data in a Model of the Northeastern Gulf of Mexico. *Continental Shelf Research*, 24(9), 1001-1013.
- Fan, S., K. Dupuis, L. Harrington-Missin, M. Calverley, A. Watson and G. Jeans, 2010. Validation of HYCOM current profiles using MMS NTL observations. Houston, USA. OTC Paper 20797.
- Fan, S., G. Jeans, C. Yetko and L.-Y. Oey, 2007. Submerged Jet Currents in the Gulf of Mexico. *Proceedings of MTS/IEEE OCEANS 2007*. October 2007. Vancouver, Canada.
- Forristall, G.Z., Cooper, C.K., 1997. "Design current profiles using empirical orthogonal functions and inverse FORM methods", Proc. Offshore Technology Conf., no. OTC 8267, pp. 11-21.
- Gianfelici, F., Venturi, M., 2005. "The Statistical Analysis of Deep Water Current Profiles", Proc. Offshore Mediterranean Conference, no. 028, p. 11.
- Guiavarch, C., Treguier, A.M., Vangriesheim, A., 2008. "Remotely forced biweekly deep oscillations on the continental slope of the Gulf of Guinea", *Journal of Geophysical Research*, vol. 113, no. C06002, p. 12.
- Hamilton, P., 1990. "Deep currents in the Gulf of Mexico," *J. Phys. Oceanogr.*, 20:1087-1104, 1990.
- Hamilton, P., T.J. Berger, J.J. Singer, E. Waddell, J.H. Churchill, R.R. Leben, T.N. Lee and W. Sturges, 2000. "DeSoto Canyon eddy intrusion study final report, Volume II: technical report," *OCS Study MMS 2000-080*. U.S. Dept. of the Interior, Minerals Management Service, Gulf of Mexico OCS Region, New Orleans, LA. 275 pp.
- Hamilton, P., J.J. Singer, E. Waddell, and K. Donohue. 2003. Deepwater Observations in the Northern Gulf of Mexico from In-Situ Current Meters and PIES. Final Report. Volume II: Technical Report. U.S. Dept. of the Interior, Minerals Management Service, Gulf of Mexico OCS Region, New Orleans, LA. OCS Study MMS 2003-049. 95 pp.
- Jeans, G., Cooper, C., 2005. "Characterisation of Subsurface Jet Currents Offshore West Africa", Proc. ISOPE Conf., vol. III, pp. 688-693.
- Jeans G. and S. Fan, 2007. Gulf of Mexico Subsurface jet screening. Proceedings of OMAE2007, 26th International Conference on Offshore Mechanics and Arctic Engineering, June, 2007, San Diego, California.

- Jeans, G., Grant, C., Feld, G., 2002. "Improved Current Profile Criteria For Deepwater Riser Design", Proc. OMAE Conf., no. OMAE2002-28153, p. 5.
- Jeans, G., Moore, A.N., 1999. "Practical Considerations for the use of ADCPs in Offshore Engineering", Proc. IEEE Working Conference On Current Measurement, p. 5.
- Keen, T.R. and S.E. Allen, 2000. "The generation of internal waves on the continental shelf by Hurricane Andrew," *Journal of Geophysical Research*, 105(C11), 26,203-26,224, 2000.
- Lin, X.-H., L.-Y. Oey and D.-P. Wang, 2007. Altimetry and drifter data assimilations of Loop Current and eddies. *J. Geophys. Res.* 112, C05046, doi:10.1029/2006JC 003779, 2007.
- Lambrakos, K.F., D.E. Sidarta, H.M. Thompson, A. Steen, 2005, "Methods for Reducing a Large Number of Current Profiles to a Small Subset for Riser VIV Analysis", Proc. OMAE Conf., no. OMAE2005-67279, p. 10.
- Meling, T.S., Eik, K.J., Nygård, E., 2002, "An assessment of EOF current scatter diagrams with respect to riser VIV fatigue damage", Proc. OMAE Conf., no. OMAE2002-28062, p. 9.
- Mellor, G. L., and T. Yamada, 1982. Development of a turbulence closure model for geophysical fluid problems, *Rev. Geophys.*, 20, 851– 875.
- Mellor, G. L., 2002. User Guide for a Three-Dimensional, Primitive Equation, Numerical Ocean Model (Jul/2002 Version), 42 pp., Atmos. & Oceanic Sci. Prog., Princeton Univ. NJ, USA. (<http://www.aos.princeton.edu/WWWPUBLIC/htdocs.pom/PubOnLine/POL.html>).
- Mellor, G. L., M. A. Donelan, and L-Y. Oey, 2008. A surface wave model for coupling with numerical ocean circulation models. *J. Atmos. Oceanic Tech.*, 25, 1785-1807.
- Mendoume Minko, I.D., Prevosto, M., Damy, G., 2008, "Statistical Modelling of Current Profiles for a Riser Reliability Design", Proc. OMAE Conf., no. OMAE2008-57933, p. 8.
- Oey, L.-Y., 2008. Loop Current and Deep Eddies. *J. Phys. Oceanogr.* 38, 1426-1449.
- Oey, L.-Y. and Lee, H.-C, 2002. Deep Eddy Energy and Topographic Rossby Waves in the Gulf of Mexico. *J. Phys. Oceanogr.*, 32(12):3499-3527.
- Oey, L.-Y. and H.-C. Zhang, 2004. A mechanism for the generation of subsurface cyclones and jets. *Cont. Shelf Res.*, 24, 2109-2131.
- Oey, L.-Y., H.-C. Lee and W. J. Schmitz Jr., 2003. Effects of Winds and Caribbean Eddies on the Frequency of Loop Current Eddy Shedding: A Numerical Model Study, *JGR*, 108 (C10), 3324, doi:10.1029/2002JC001698, 2003.
- Oey L.-Y., T. Ezer and H.J. Lee, 2005a. Loop Current, Rings and Related Circulation in the Gulf of Mexico: A Review of Numerical Models and Future Challenges. In "Circulation in the Gulf of Mexico: Observations and Models," W. Sturges, A. Lugo-Fernandez, Eds, Geophysical Monograph Series, Vol.161, 360pp, 2005.
- Oey L.-Y., T. Ezer, G. Forristall, C. Cooper, S. DiMarco, S. Fan, 2005b. An exercise in forecasting loop current and eddy frontal positions in the Gulf of Mexico, *Geophys. Res. Lett.*, 32, L12611, doi:10.1029/2005GL023253.
- Oey L.-Y., T. Ezer, D.-P. Wang, S. Fan and X.-Q. Yin, 2006. Loop Current warming by Hurricane Wilma, *Geophys. Res. Lett.* 33, L08613, doi:10.1029, 2006GL025873.
- Oey, L.-Y., T. Ezer, D.-P. Wang, X.-Q. Yin and S.-J. Fan, 2007. Hurricane-induced motions and interaction with ocean currents. *Cont. Shelf Res.* 27, 1249-1263.
- Oey, L.-Y., M. Inoue, R. Lai, X.-H. Lin, S. Welsh and L. Rouse Jr. 2008. Stalling of near-inertial waves in a cyclone. *Geophys. Res. Lett.*, 35, L12604, doi:10.1029/2008GL034273.
- Oey, L.-Y., Y.-L. Chang, Z.-B. Sun & X.-H. Lin, 2009. Topocaustics. *Ocean Modelling*, 29, 277-286.
- Wang, D.P., 1991. "Generation and propagation of inertial waves in the subtropical front," *J. Marine Research* 49:619-633.
- Wang D. and Oey L.-Y, 2008. Hindcast of Waves and Currents in Hurricane Katrina. *Bulletin of the American Meteorological Society (BAMS)*. DOI:10.1175/BAMS-89-4-487.
- Wang, D-P., L-Y. Oey, T. Ezer, and P. Hamilton, 2003. Near-surface currents in DeSoto Canyon (1997–99): Comparison of current meters, satellite observation, and model simulation. *J. Phys. Oceanogr.*, 33(1), 313-326.

Yin, X.-Q. and L.-Y. Oey, 2007. Bred-ensemble ocean forecast of Loop Current and rings, *Ocean Modelling*, doi.10.1016/j.ocemod.2007.02.005.